

April, 1958

published monthly by The Institute of Radio Engineers, Inc.

Proceedings of the IRE®

contents

	Poles and Zeros	689
	John D. Ryder, Editor, 1958	690
	Scanning the Issue	691
	A Short Survey of Radio and Electronics in Colombia, T. J. Meek	692
PAPERS	A Transistorized 150-MC FM Receiver, Winfield J. Giguere	693
	A Traveling-Wave Ferromagnetic Amplifier, P. K. Tien and H. Suhl	700
	Parametric Amplification of Space Charge Waves, W. H. Louisell and C. F. Quate	707
	A Gallium Arsenide Microwave Diode, D. A. Jenny	717
	Some Applications of Ferrites to Microwave Switches, Phasers, and Isolators, <i>A. C. Brown, R. S. Cole, and W. N. Honeyman</i>	722
	Theory of Stronger-Signal Capture in FM Reception, Elie J. Baghdady	728
	Exact Ladder Network Design Using Low-Q Coils, Louis Weinberg	739
	Minimum Energy Triggering Signals, L. A. Beattie	751
	Some Studies on Delayed Feedback Circuits, Hideo Seki	758
	IRE Standards on Piezoelectric Crystals: Determination of the Elastic, Piezoelectric, and Dielectric Constants—The Electromechanical Coupling Factor, 1958	764
	Correction to "Radio Interferometry of Discrete Sources" and "Restoration in the Presence of Errors," <i>R. N. Bracewell</i>	778
CORRESPONDENCE	Bridge Method of Measuring Noise in Low-Noise Devices at Radio Frequencies, Keith S. Champlin ..	779
	A Reactance Theorem for Antennas, L. Solymar	779
	Extension of Boolean Algebra for Analysis of Mixed-Switch Diode Circuits, B. Beizer	779
	The Switching Time of the Cryotron, A. Aharoni, E. H. Frei, and S. Shtrikman	780
	A History of Some Foundations of Modern Radio-Electronic Technology, S. M. Aisenstein	780
	Aperture Correction for Instrumentation Systems, Joseph Otterman	781
	Transistor Cutoff Frequency Measurement, L. G. Cripps	781
	Spectral Analysis, Robert C. Moody	782
	Satellite Doppler Measurements, M. Bernstein, G. H. Gougoulis, <i>O. P. Layden, W. T. Scott, and H. D. Tanzman</i>	782
	Invention and Insight, Robert E. Mueller	783
	Germanium N-P-I-N Junction Transistor Triodes, D. M. Unger and A. Avakian	783
	High-Frequency Magnetic Permeability Measurements Using Toroidal Coils, <i>R. D. Harrington and R. C. Powell</i>	784
	Passive Repeater Using Double Flat Reflectors, F. Cappuccini and F. Gasparini	784
	Observations of Magneto-Ionic Duct Propagation Using Man-Made Signals of Very Low Frequency, <i>R. A. Hellwvll and E. Gehrels</i>	785
	Tuning a Probe in a Slotted Line, Jose I. Caicoya	787
	Cutoff Phenomena in Transversely Magnetized Ferrites, Ronald F. Soohoo	788
REVIEWS	Scanning the TRANSACTIONS	792
	Books:	
	"Stereophonic Sound," by N. H. Crowhurst, Reviewed by B. B. Bauer	794
	"Progress in Semiconductors, Volume Two," ed. by A. F. Gibson, P. Aigrain, and R. E. Burgess, Reviewed by L. T. DeVore	794

published monthly by The Institute of Radio Engineers, Inc.

Proceedings of the IRE®

continued

	"The Ionosphere," by Karl Rawer, <i>Reviewed by Wolfgang Pfister</i>	795
	"Digital Computer Components and Circuits," by R. K. Richards, <i>Reviewed by W. B. Cagle</i>	796
	"Elektronenröhren," by M. J. O. Strutt, <i>Reviewed by W. H. von Aulock</i>	796
	"Notes on Analog-Digital Conversion Techniques," ed. by A. K. Susskind, <i>Reviewed by C. T. Leondes</i>	796
	"Scientific and Technical Translating and Other Aspects of the Language Problem," by UNESCO, <i>Reviewed by W. N. Locke</i>	797
	Recent Books	797
ABSTRACTS	Abstracts of IRE TRANSACTIONS	798
	Abstracts and References	806
INDEX	1957 IRE TRANSACTIONS Index	818
Follows page	
IRE NEWS AND NOTES	IRE Awards, 1958	14A
	WESCON Papers Deadline Set for May 1	34A
	Calendar of Coming Events and Authors' Deadlines	34A
	Obituaries	38A
	Symposium on Electronic Waveguides	40A
	Tenth Southwestern IRE Conference and Electronics Show	40A
	1958 PGMTT National Symposium	42A
	1958 IRE NATIONAL CONVENTION RECORD	46A
DEPARTMENTS	Contributors	790
	Meetings with Exhibits	8A
	News—New Products	48A
	IRE People	50A
	Industrial Engineering Notes	62A
	Professional Group Meetings	68A
	Section Meetings	70A
	Membership	90A
	Positions Open	114A
	Positions Wanted	122A
	Advertising Index	149A

COVER: A piezoelectric crystal plate, when excited by an electric field, may exhibit one of several modes of motion. These modes may be used to determine important electric and strain properties of crystals as described in the IRE Standards on page 764.

BOARD OF DIRECTORS, 1958

*D. G. Fink, *President*
 C. E. Granqvist, *Vice-President*
 *W. R. G. Baker, *Treasurer*
 *Haraden Pratt, *Secretary*
 *J. D. Ryder, *Editor*
 A. V. Loughren, *Senior Past-President*
 *J. T. Henderson, *Junior Past President*

1958

A. N. Goldsmith
 H. R. Hegbar (R4)
 E. W. Herold
 K. V. Newton (R6)
 A. B. Oxley (R8)

F. A. Polkinghorn (R2)

D. B. Sinclair
 *Ernst Weber
 J. R. Whinnery

1958-1959

R. I. Cole (R3)
 G. A. Fowler (R7)
 *R. L. McFarlan (R1)
 D. E. Noble
 E. H. Schulz (R5)
 Samuel Seely

1958-1960

G. S. Brown
 W. H. Doherty

*Members of Executive Committee

EXECUTIVE SECRETARY

George W. Bailey
 Evelyn Benson, *Assistant to the Executive Secretary*

John B. Buckley, *Chief Accountant*

Laurence G. Cumming, *Technical Secretary*

Emily Sirjane, *Office Manager*

ADVERTISING DEPARTMENT

William C. Copp, *Advertising Manager*
 Lillian Petranek, *Assistant Advertising Manager*

EDITORIAL DEPARTMENT

Alfred N. Goldsmith, *Editor Emeritus*
 J. D. Ryder, *Editor*
 E. K. Gannett, *Managing Editor*
 Helene Frischauer, *Associate Editor*

EDITORIAL BOARD

J. D. Ryder, *Chairman*
 F. Hamburger, Jr., *Vice-Chairman*
 E. K. Gannett
 Keith Henney
 E. W. Herold
 T. A. Hunter
 G. K. Teal
 W. N. Tuttle



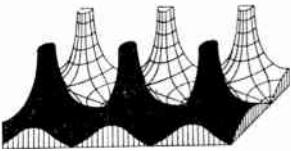
PROCEEDINGS OF THE IRE, published monthly by The Institute of Radio Engineers, Inc., at 1 East 79 Street, New York 21, N. Y. Manuscripts should be submitted in triplicate to the Editorial Department. Responsibility for contents of papers published rests upon the authors, and not the IRE or its members. All republication rights, including translations, are reserved by the IRE and granted only on request. Abstracting is permitted with mention of source.

Fifteen days advance notice is required for change of address. Price per copy: members of the Institute of Radio Engineers, one additional copy \$1.25; non-members \$2.25. Yearly subscription price: to members \$9.00, one additional subscription \$13.50; to non-members in United States, Canada, and U. S. Possessions \$18.00; to non-members in foreign countries \$19.00. Entered as second class matter, October 26, 1927, at the post office at Menasha, Wisconsin, under the act of March 3, 1879. Acceptance for mailing at a special rate of postage is provided for in the act of February 28, 1925, embodied in Paragraph 4, Section 412, P. L. and R., authorized October 26, 1927. Copyright © 1958 by The Institute of Radio Engineers, Inc.

Proceedings of the IRE



Poles and Zeros



New Format. Readers will notice that the table of contents has been expanded and moved to the first two pages of

the magazine so that it may be found more easily. In addition, we have moved the nontechnical portion of IRE News and Radio Notes, covering general news matters of no permanent reference value, to the front portion of the advertising section. These changes will be discussed in further detail next month.

Travel Is Broadening. As this is written in Hong Kong we are reminded that the world is indeed small, and that travel to far-off places is now almost routine to many—although not to us.

The airplane and electronics have made such travel possible, and the coming of the jet transport will further reduce the time involved. Have many yet considered the management economics involved in a ten-hour crossing of the Pacific? What changes in business and engineering procedures will become feasible? What will this mean in terms of information exchange?

Some indication of what more rapid transportation will mean can be found in the present-day Japanese electronic industry. The large electrical manufacturing companies of that country were largely built in the old days upon technical information received from foreign cooperators and affiliates. This transfer of information by sea-mail of drawings and infrequent exchange of engineers was slow and far from efficient. As a result, much equipment so built before World War II was thought to be of uncertain quality, and Japanese electronic equipment did not find a U. S. market.

Speedy travel and rapid transfer of information has already changed this situation, and the electronic equipment seen in Japan within the last fortnight was absolutely first class. The U. S. ancestry of much is still apparent, but now and then there is evidence of original thinking. One example is a really portable analogue computer, in which switching of coefficient resistors and integrating capacitors is by push button. Another example is that of the high-frequency network analyzer or power-system analogue computer, with the U. S. birth of which the editor aided in 1944-46. This has been recognized as an instrument well adapted to the abilities of Japanese labor, and engineered into a beautiful instrument of capabilities beyond those of the lower-frequency U. S. counterparts. This computer certainly has market

possibilities for foreign areas where such computers are yet rarities, markets which U. S. equipment cannot touch because of the high cost of the low-frequency designs.

The Japanese have also recognized the transistor as a device particularly suited to production by their numerous and hard-working female labor force. The transistor is, of course, a high-value low-weight item, well suited to export, and ambitious plans are obviously under way for large-scale production. One need not spend much time in thought to name the major export market on which their sights are set.

Japan and other eastern countries have a large and able supply of workers who are really willing to work. No four or five-day week for them; competition is such that one must work six or six and one-half days a week to exist. Such a labor supply and attitude we do not have; our automatic machines must indeed be efficient and fast to match such numerous and nimble fingers.

Our thanks to Dr. Yasujiro Niwa, IRE vice-president in 1957, and the Tokyo IRE Section, for a broadening and stimulating view of Japanese electronics and education. Of the latter—more later.

Student Awards. At this season of the year the annual college crop of engineers is sifting job offers, balancing salary against opportunity, palm trees against four seasons, and reflecting upon how little they have really learned in their four or more years. It is fitting at this time for a professional society to point out and honor those students who have done exceedingly well, both within and without the books, and the IRE has made provision for so honoring outstanding students with the IRE Student Award.

One such award, consisting of a certificate from Headquarters and a year as Member or Associate, is available for presentation to the outstanding senior EE student at each school having an IRE Student Branch or Joint Branch. Frequently the local Section stages the presentation before its members, and sweetens the prize. Both scholarship and all-around activity for the benefit of the school and the Student Branch are to be considered in selection of the student to be rewarded.

The rules provide that the initiative for selection lies with the Section Chairman or his Education chairman, but the IRE Representative on each school's faculty may be excused if he politely or vigorously, as the need may arise, nudges such gentlemen into action when action is needed. Is more than a word to the wise required?—J.D.R.

John D. Ryder

Editor, 1958



John D. Ryder was born on May 8, 1907, in Columbus, Ohio. He received the Bachelor's degree in Electrical Engineering in 1928 and the Master of Science degree in 1929 from Ohio State University. He won his Ph.D. degree in electrical engineering in 1944 from Iowa State University.

From 1929 to 1933 he was employed by the General Electric Company on vacuum tube development. In 1931 he became supervisor of the electrical and electronic section of the Research Laboratory, Bailey Meter Company, Cleveland, Ohio. As a result of this work he obtained twenty-four patents covering temperature recording and automatic control applications of electronics.

In 1941 he joined Iowa State College as Assistant Professor in Electrical Engineering. He rose to Professor in 1944, and in 1947 he assumed the Assistant Directorship of the Iowa Engineering Experiment Station. In September, 1949, he was named Head of the Department of Electrical Engineering at the University of Illinois. He left this post in July, 1954 to take up his present position as Dean of the College of Engineering at Michigan State University, East Lansing, Michigan.

Dr. Ryder has been active in the development and construction of two electronic-type 10,000-cycle network an-

alyzers for power transmission studies, one at Iowa State College and the other at the University of Illinois.

He is the author of four textbooks, *Electronic Engineering Principles, Networks, Lines and Fields*, *Electronic Fundamentals and Applications*, and *Engineering Electronics with Industrial Applications and Control*, in addition to numerous technical papers.

He was president of Eta Kappa Nu in 1956-57, and president of the National Electronics Conference for 1953. He is a fellow of the American Institute of Electrical Engineers, and the American Association for the Advancement of Science. He also holds membership in Tau Beta Pi, Eta Kappa Nu, Sigma Xi, Phi Kappa Phi, and Pi Mu Epsilon.

Dr. Ryder served as IRE President in 1955, and as an IRE Director since 1952. He joined the IRE in 1929 as an Associate, became a Senior Member in 1945, and a Fellow in 1952. He headed the following IRE committees: Appointments, 1957; Education, 1953-54; Policy Advisory, 1953; Nominations, 1957. He also was a member of the following committees: Editorial Review, Finance, Membership Relations Coordinator, Papers Review, Editorial Board, and Professional Groups. He was Vice-Chairman of the Des Moines-Ames Section in 1948.

Scanning the Issue

A Transistorized 150-MC Receiver (Giguere, p. 693)—Thanks to the development of the diffused base transistor two years ago, important advances are now being made in the application of transistors at frequencies well above 100 megacycles. An especially noteworthy example is provided by this all-transistor receiver, designed to operate as part of a two-way mobile radio system in the 152 to 174 mc band. Its principal asset is the low amount of power it draws, only 130 milliwatts as compared to the several watts required by vacuum tube receivers. This is an especially important consideration in two-way mobile units, which must operate from batteries and be turned on nearly all the time for incoming calls.

A Traveling-Wave Ferromagnetic Amplifier (Tien and Suhl, p. 700)—One of the major developments of 1957 was Suhl's proposal for an entirely new kind of solid-state microwave amplifier involving ferromagnetic materials. This proposal has since stimulated a great deal of interest in a general class of amplifier, called "parametric," which has been the subject of theoretical speculation for more than two decades. In its simplest form a parametric amplifier consists of a resonant circuit tuned to the signal to be amplified, a local source of power (called the pump) at twice the signal frequency, and a mechanism that varies the reactance of the tuned circuit at a rate equal to the pump frequency. The power supplied by the pump can be utilized, by means of the nonlinear effects produced by the variations in reactance, to amplify the signal.

The ferromagnetic amplifier mentioned above used a resonant cavity containing a ferrite sample. Ferromagnetic resonance effects in the ferrite provided the necessary mechanism for varying the reactance of the cavity. Two months ago it was shown in a letter to the editor that an electron beam can be used instead of a ferrite to vary the reactance of a cavity.

This paper and the one that follows present important new proposals of fundamental significance to the art of parametric amplification of microwave signals, in which the resonant cavity is thrown away altogether and replaced by a distributed transmission line, or its equivalent, along which traveling waves are propagated. In this first paper a circular waveguide is filled with a ferromagnetic material (in this case yttrium garnet), in which transmission lines are embedded. Here the ferromagnetic medium, instead of producing a varying reactance in a resonant cavity, provides a time-varying coupling between the transmission lines when energized by a travelling wave supplied to the waveguide by the pump. The signal is fed to one of the transmission lines, and proceeds to grow as it travels down the line as a result of this varying-coupling effect. The result is an important new type of low-noise amplifier that, because it employs traveling waves, will likely provide greater bandwidth than earlier proposals mentioned above.

Parametric Amplification of Space Charge Waves (Louisell and Quate, p. 707)—In this paper we are again concerned with parametric amplification and traveling waves. Here, however, we are dealing with an electron beam and the "fast" and "slow" space charge waves normally associated with it. If the beam is modulated with a pumping frequency equal to twice the signal frequency, the slow and fast space charge waves at the signal frequency can each be made to grow exponentially with distance. Thus, either the slow wave or fast wave can be amplified. In conventional microwave amplifiers, only the slow wave is amplified. These amplifiers have been built with noise figures less than 4 db, as reported here last month. However, the noise theorems pertaining to slow wave amplifiers do not apply for fast waves. Now a way has been found to amplify fast waves, and this may open up an important new class of microwave beam tubes in which the noise figure is even further reduced.

A Gallium Arsenide Microwave Diode (Jenny, p. 717)—

Gallium arsenide, one of the new compound semiconductor materials, has been found to be superior to the old standbys, germanium and silicon, in point contact diodes. Not only does the new compound show a lower mixer conversion loss, but promises to be operable at appreciably higher temperatures. In addition to important applications as a microwave mixer, the new device can be used to good advantage as a fast-switching diode.

Some Applications of Ferrites to Microwave Switches, Phasers, and Isolators (Brown, *et al.*, p. 722)—This paper presents an account of a number of interesting ferrite devices, the nature of which are indicated by the title. While these developments are of primary interest to microwave engineers, the highly descriptive, yet brief, form of the paper recommends it as a very readable summary for others.

Theory of Stronger-Signal Capture in FM Reception (Baghdady, p. 728)—Earlier studies have indicated that when an FM signal is disturbed by a lesser interfering signal, both should be demodulated as faithfully as possible, and only then should steps be taken to minimize the interference. This would call for a broad-band demodulator. The present study indicates a radically different approach would be better. The author finds the amplitude limiter of an FM receiver performs the added function of spreading out the spectrum of the interfering signal so that substantial portions can be filtered without disturbing the wanted signal significantly. Further interference reduction can be achieved by cascading a number of limiter-filter combinations. Thus the disturbance can be minimized before detecting it rather than after, and narrow-band, instead of broad-band, circuitry is called for.

Exact Ladder Network Design Using Low-Q Coils (Weinberg, p. 739)—Tables of circuit element values are presented which give the designer a simple and exact way of designing various dissipative ladder networks so as to take into account the usually neglected resistance associated with the reactive components (especially the coils) of the filter, thus avoiding previous discrepancies between the desired and the actual characteristics of the network. These tables will be very useful, especially to those engineers who are not circuit theorists but do need filter networks.

Minimum Energy Triggering Signals (Beattie, p. 751)—We usually worry about designing a system to give an optimum output from a given input. In this paper the tables are turned by considering what form of input signal will produce at the output a given voltage at a predetermined instant with a minimum of input energy. This analysis gives a novel and previously overlooked approach for designing a wide variety of triggering and switching systems to operate more efficiently. The theory may also be useful in the field of signal detection by defining, for example, the optimum shaped radar pulse that would produce the greatest deflection on the viewing screen.

Some Studies of Delayed-Feedback Circuits (Seki, p. 758)—An attractively simple method for improving the signal-to-noise ratio of a periodic signal is achieved by means of a delayed feedback circuit that superimposes one signal on a following signal. This reinforces the signal more than the noise because one is periodic and the other is random. The scheme is applicable to any system that uses a repetitive signal, such as radar or some types of telegraphy, and in addition suggests a method of producing artificial reverberation.

IRE Standards on Piezoelectric Crystals (p. 764)—This Standard specifies a method for determining the basic elastic, piezoelectric, and dielectric constants of crystals, and their relation to the electromechanical coupling factor.

1957 Index to IRE TRANSACTIONS (follows p. 818)—The 796 papers produced by 24 IRE Groups in their TRANSACTIONS in 1957 are indexed by subject and author.

Scanning the Transactions appears on page 792.

A Short Survey of Radio and Electronics in Colombia

T. J. MEEK†, SENIOR MEMBER, IRE

This year the IRE established a new IRE Section in Colombia, making the third Section to be formed in South America and the sixth outside the U. S. and Canada. The following survey was prepared by the organizer of the Colombia Section.—*The Editor.*

Colombia, at the northern tip of South America just west of Venezuela, is perhaps not as well known as it should be. Bordering on both the Atlantic and Pacific Oceans, it covers an area roughly twice that of Texas. For the most part the main industrial cities are located inland in the high altiplanos where the climate is forever spring. Before the advent of the airplane the chief means of communications was the burro, but with air travel, the cities of Bogota, Medellin, and Cali are in the mainstream of progress and their growth in the last thirty years can be equaled by few North American cities.

Since 1847, when the first concession was granted for a Morse telegraph line, all the governments of Colombia have realized the importance of up-to-date communication facilities. Long-distance public telephone and telegraph services are operated by the government. Because of the mountainous terrain the country is ideal for the application of very long radio links, and surveys indicated that the most economical method of providing the main trunk routes would be by vhf radio in the three-hundred megacycle range. Contracts were therefore placed which will provide a semiautomatic telephone system linking all the principal cities of the republic. This will be expanded into a fully automatic system within a few years. Giant parabolic antennas are now a common sight and many of the paths are well over a hundred miles long with unobstructed line-of-sight conditions applying.

An automatic Telex system has been installed within the last year and now connects Barranquilla on the Caribbean to the port of Buenaventura on the Pacific, in addition to many more cities. An international Telex service is planned in the near future.

Broadcasting, both of television and sound, has been accepted as a way of life by all Colombians. Bogota, the capital, has eighteen private broadcasting stations and it is a rare station that cannot boast of a short-wave or FM transmitter. A total of some one hundred and twenty radio broadcasting stations are operating throughout Colombia with some providing exclusively cultural and educational programs. It has been claimed that this was the first country in the world to use radio for educational purposes.

Television broadcasting was started in 1954 as a govern-

ment monopoly and there are now seven transmitters in operation in the principal areas of population with about nine others planned. All are linked together in a national network. Recently it has been suggested that private stations will shortly be allowed to enter this field.

While coffee represents the principal export, oil is also very important: Colombian production is third in Latin America. Because of the remoteness of the oil fields many radio networks have been established to provide communications. For the location of petroleum some of the most modern electronic apparatus is in use. Most of the eleven oil pipe lines in the country are served by communications provided by the Colombian and international companies operating them.

Until the arrival of the airplane it required eight to twelve days to travel from the coast to Bogota. In proportion to its territory and population it appears that Colombia is a world leader in civil aviation, carrying over a million passengers a year or about 10 per cent of the population. Modern facilities have been established at Barranquilla and Bogota for maintenance of the increasingly complicated electronic equipment of the airlines.

Up to now, most of the radio and electronic equipment has been imported, but the development of manufacturing facilities is progressing at an increasing rate. At present, assembly plants have been established and projected for processing many consumer items such as radio sets, phonographs, and other similar equipment.

There are many universities with excellent engineering faculties. The National University in Bogota has some four hundred students enrolled in engineering courses. The number of engineers specializing in radio and electronics is limited, but with many universities starting electronic engineering courses, it will only be a matter of time before creative engineering can be firmly established in Colombia. Some universities have an arrangement with certain American universities for students to complete the final two years of their course in the United States. Financial assistance is provided. Many other students who can afford it have studied abroad.

The outlook for the future development of radio and electronics is excellent. For a country so dependent on its means of communications it cannot fail to give full support to all these endeavors. We, who form part of the new IRE Section, all share in this feeling of optimism.

† Telephone Transmission Consultant, Empresa Nacional de Telecomunicaciones, Bogota, Colombia.



A Transistorized 150-MC FM Receiver*

WINFIELD J. GIGUERE†, MEMBER, IRE

Summary—A completely transistorized experimental 150-mc FM communication receiver utilizing diffused base transistors is described. It is a crystal controlled double conversion receiver designed for 60-kc adjacent channel spacing at any channel frequency between 152 and 174 mc. Performance curves for the receiver are provided. For experimental evaluation, the experimental receiver is used with a vacuum tube transmitter to provide a complete transceiver unit.

INTRODUCTION

OPERATION of portable two-way communication equipment requires the receiver to monitor continuously the channel for efficient usage. It is, therefore, important that the receiver draw as little power as possible if the portable battery supply is to have a long life. Portable vhf vacuum tube receivers draw several watts of power, whereas the transistorized receiver described in this paper draws 130 mw. This power saving is a result of the elimination of the power loss required by the cathode heaters and the decreased power consumption caused by the inherent low current, low voltage operation of the transistors.

The vacuum tube receiver suffers from the additional disadvantage of operating from the same power supply as the transmitter. This type of operation does not allow the battery to depolarize between heavy current transmit periods and, therefore, reduces its life.¹ Since the power supply requirements of a transistorized receiver and a vacuum tube transmitter are very different, it is natural to use two different power supplies to achieve the full advantage of transmitter battery depolarization.

Additional power saving could be accomplished by complete or partial transistorizing of the transmitter. At present, complete transistorization of the transmitter would result in less power output at frequencies above 100 mc than is required. Partial transistorizing would give a 25 per cent power saving in the transmitter. The battery saving based on a 17 per cent duty cycle was not considered commensurate with the effort involved in design at the time the project was started.

Until the recent development of the diffused based transistor,² transistor amplifiers at frequencies above 100 mc were impractical. This has resulted in transistorized vhf receivers in which rf gain has been avoided in attempts to fully transistorize the receiver or in which vacuum tubes have been employed in the rf por-

tions of the receiver. Commendable attempts to provide rf gain and selectivity in vhf receivers have been made using transistors whose upper limits are in this frequency region. The most successful effort has been with the tetrode transistor.³ Design with these units, however, has been dependent on selection from the best available tetrodes.

This paper describes an experimental vhf FM receiver which employs the diffused base transistor. It operates between 152 mc and 174 mc with a total power drain of 130 mw. This receiver is comparable in performance to existing mobile radio equipment in this frequency range.

GENERAL RECEIVER DESIGN

A block diagram of the transistorized FM receiver described herein is shown in Fig. 1. It is a double conversion superheterodyne receiver⁴ tunable for single-frequency crystal-controlled operation over a band from 152 to 174 mc. It has a sensitivity of 1.0 μ v (open circuit) for 20 db of noise quieting as shown in Fig. 2. Adjacent channel selectivity for 60-kc channel spacing is greater than 70 db and spurious response rejection at the first oscillator image frequency is greater than 90 db. Double conversion is desirable at this frequency with standard tuning elements, in order to achieve required adjacent channel selectivity and also to meet image rejection requirements with a reasonable number of components.⁵

The receiver employs a total of eleven diffused base transistors in the rf and IF stages. Although IF gain at 20.4 mc and 2 mc could reasonably be provided by several different available transistor types, the diffused base transistor was used because of the simplicity of design due to its high-frequency characteristics. The units used in the receiver have a collector capacitance of approximately 0.5 μ mf at 4.5 volts. The low-frequency alpha of the units range from 0.93 to 0.995. The alpha cutoff (grounded base) frequency is over 600 mc for all of the units with many units above 1000 mc. Noise figure measurements at 150 mc indicate some units with a noise figure as low as 8 db.

The receiver operates on a -6-volt collector supply voltage and a +1.5-volt bias supply. The total power drain is 130 mw. It will operate for over 100 hours on an 8-hour day duty cycle powered by a single battery

* Original manuscript received by the IRE, July 11, 1957; revised manuscript received, January 29, 1958.

† Bell Telephone Labs., Inc., Murray Hill, N. J.

¹ W. H. Timbie, "Industrial Electricity," John Wiley and Sons, Inc., New York, N. Y., 2nd ed., vol. I, p. 485; March, 1949.

² C. A. Lee, "A high frequency diffused base germanium transistor," *Bell Sys. Tech. J.*, vol. 35, pp. 23-34; January, 1956.

³ R. L. Wallace, L. G. Schimpf, and E. Dickton, "Junction transistor tetrode for high-frequency use," *PROC. IRE*, vol. 40, pp. 1395-1400; November, 1952.

⁴ D. E. Foster and J. A. Rankin, "IF values of FM wave receivers," *PROC. IRE*, vol. 29, p. 546; October, 1941.

⁵ F. E. Terman, "Radio Engineers Handbook," McGraw-Hill Book Co., Inc., New York, N. Y., pp. 658-659; 1943.

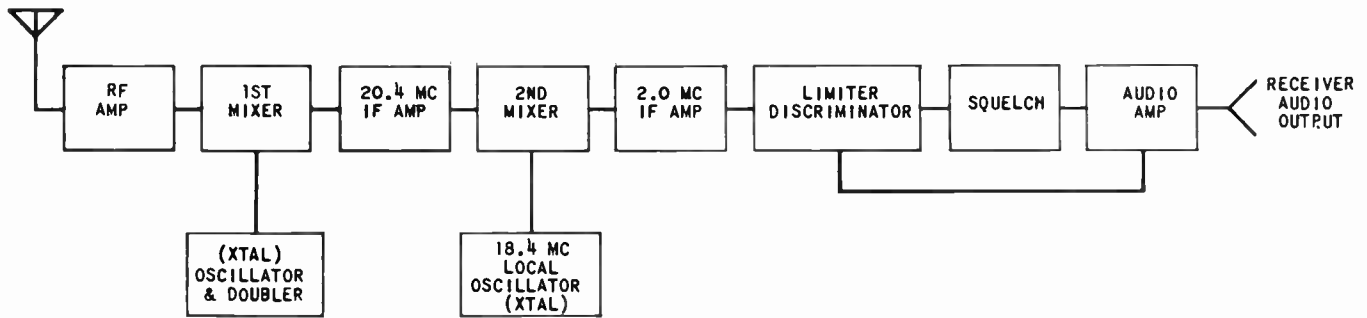


Fig. 1—Transistorized 150-mc FM receiver block diagram.

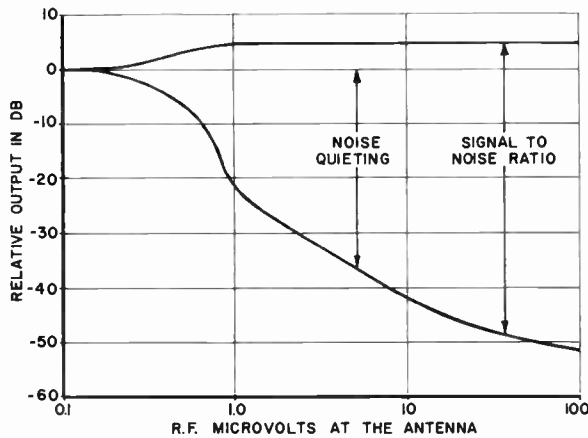


Fig. 2—Receiver sensitivity.

$1\frac{3}{4} \times 1\frac{3}{4} \times 2$ inches. Fig. 3 is a view of the complete receiver as a result of packaging to incorporate it in an experimental portable communications set.

RF TUNER DESIGN

The rf tuner is composed of two stages of rf gain, a crystal controlled oscillator, a frequency doubler, and a mixer. RF selectivity is obtained by a single-tuned antenna circuit and two capacitance-coupled double-tuned interstage coils. RF amplification is provided by two diffused base transistors in the circuit shown in Fig. 4 (opposite).

The basic rf amplifier is emitter biased at 1.5 ma from a 1.5-volt bias battery. At this bias current the input impedance at 150 mc is approximately 35 ohms. The collector voltage at this bias current is 4.5 volts. This results in a collector capacitance of less than $0.5 \mu\mu\text{f}$ in the diffused base transistor which is low enough to prevent excessive feedback to the 35-ohm input impedance of the transistor without neutralizing. The output resistance of the grounded base amplifier is 1500 ohms at 150 mc.

To meet spurious frequency rejection requirements, a total of five tuned circuits with a loaded Q of 25 each is necessary. The rf amplifier coils are impregnated and are wound on a shielded coil form.⁶ They provide a

⁶ Cambridge Thermionic Corp. Type LS9-3R.

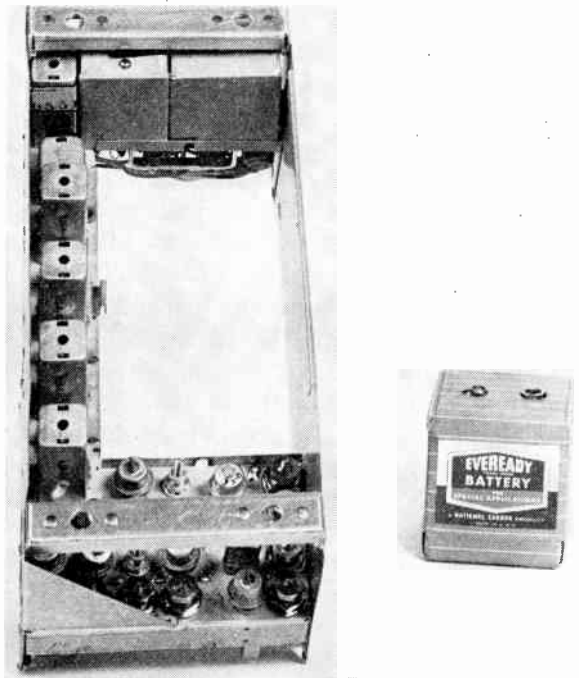


Fig. 3—150-mc FM experimental receiver with battery supply.

tunable inductance range from 0.06 to $0.08 \mu\text{h}$ with an unloaded Q of 90. The interstage tuned circuits are approximately critically coupled by capacitance. The primary circuit is driven from the collector of the preceding transistor and the secondary inductor is tapped to provide efficient coupling to the following stage. The coupling results in an effective loaded Q of 25 for each tuned circuit.

Bias voltage is prevented from appearing on the antenna by capacitive coupling to the amplifier. The antenna inductor is identical to the secondary coil in the interstage circuit, and since the antenna is approximately the same impedance as the input to the transistor, the antenna inductor functions only as a tuned selective element.

Diffused base transistors of average characteristics ($\alpha_0 = 0.95$, $f_{\alpha_0} = 600 \text{ mc}$, and $C_c = 0.5 \mu\mu\text{f}$) give an over-all two-stage rf gain at 150 mc of 22 db. Fig. 5 is the corresponding selectivity of the two-stage amplifier. The noise figure of the tuner is approximately 10 db

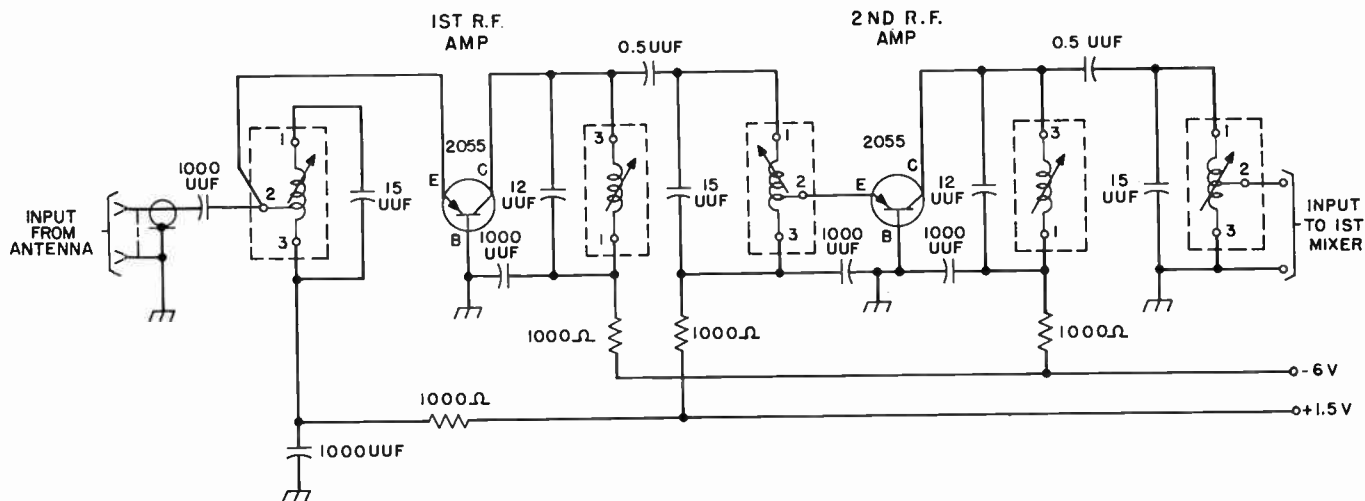


Fig. 4—Two-stage transistorized 150-mc rf amplifier.

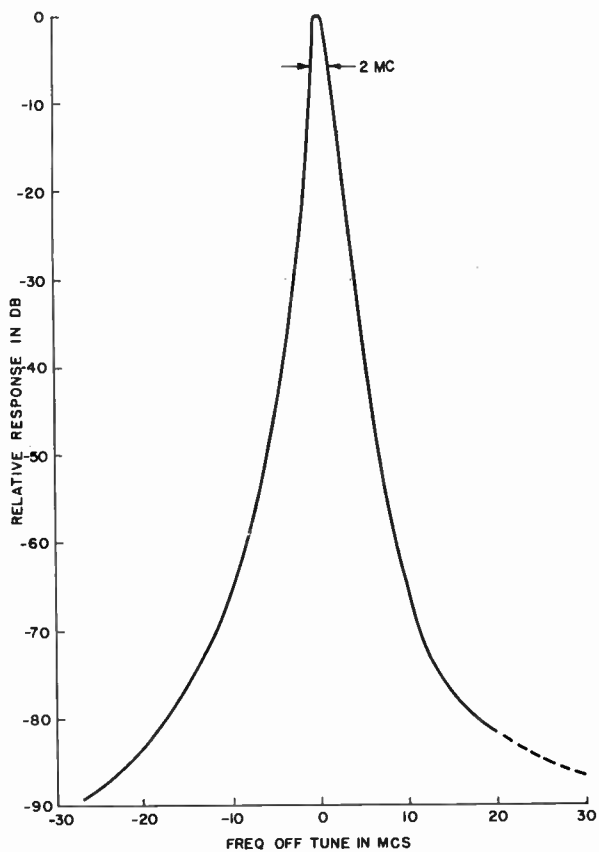


Fig. 5—Two-stage rf amplifier selectivity.

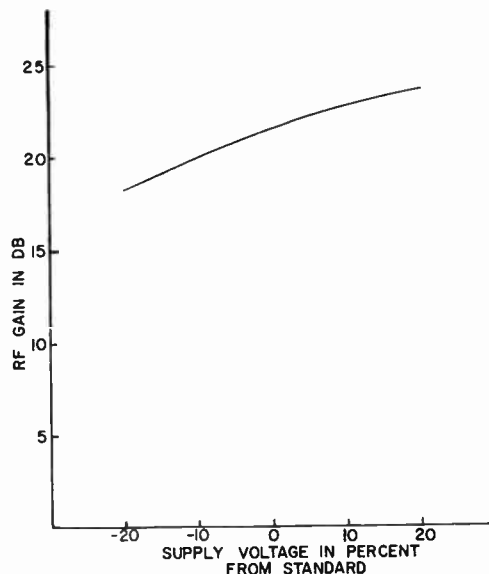


Fig. 6—150-mc rf amplifier gain change with supply voltage variation.

which is better than most vacuum tube equipment in this frequency range.

The change in amplifier gain with supply voltage variation of ± 20 per cent standard voltage is shown in Fig. 6. The use of emitter bias sufficient to maintain alpha over the variation is the main factor which makes the change in gain small.

The high-frequency local oscillator circuit is shown in Fig. 7. It is designed to operate at half the injection frequency in order to provide the desired frequency

stability with available crystals. The frequency is doubled by over-driving an amplifier stage following the oscillator and tuning its output to twice the oscillator frequency. The frequency doubler provides adequate drive to the first mixer with decreasing battery voltage to assure good modulation efficiency until the oscillator fails at approximately 3-volt collector supply.

The frequency stability of the oscillator with battery supply voltage variation is shown in Fig. 8. Fig. 9 shows the variation of frequency of the oscillator with respect to temperature change. This corresponds to a ± 0.001 per cent change in frequency for an 80°C temperature variation.

The mixer is biased similarly to the frequency doubler and the drive necessary for nonlinear operation is applied to the emitter by the frequency doubler. The rf signal is applied to the base of the same transistor and

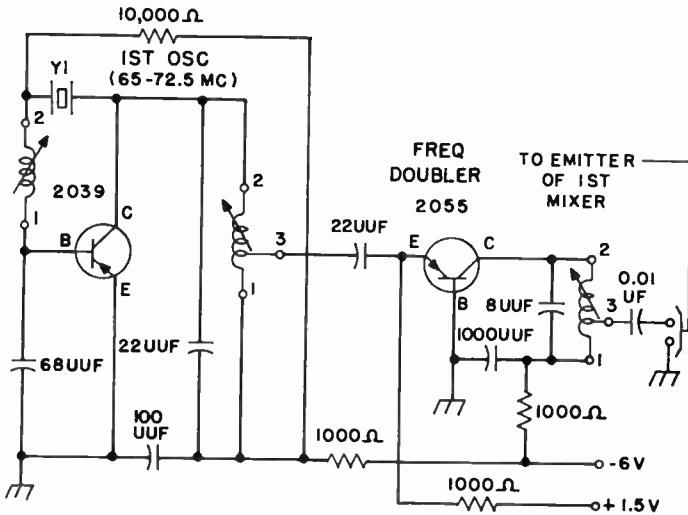


Fig. 7—High-frequency local oscillator and frequency doubler.

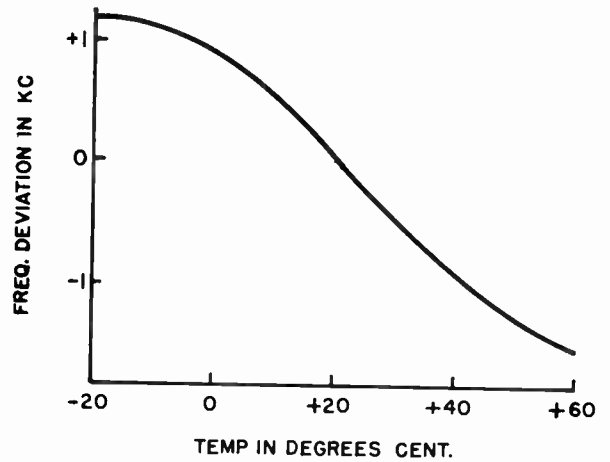


Fig. 9—Oscillator stability with temperature variation.

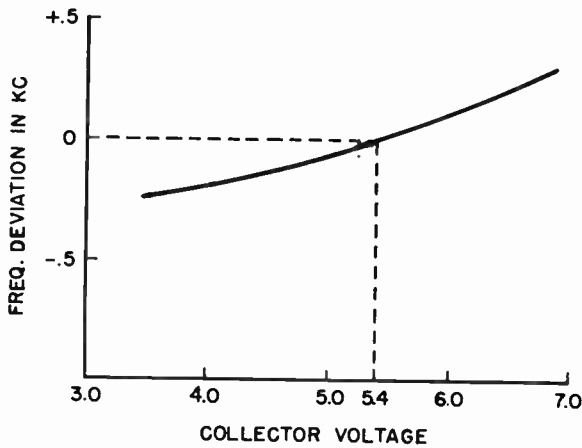


Fig. 8—High-frequency oscillator frequency deviation with supply voltage change.

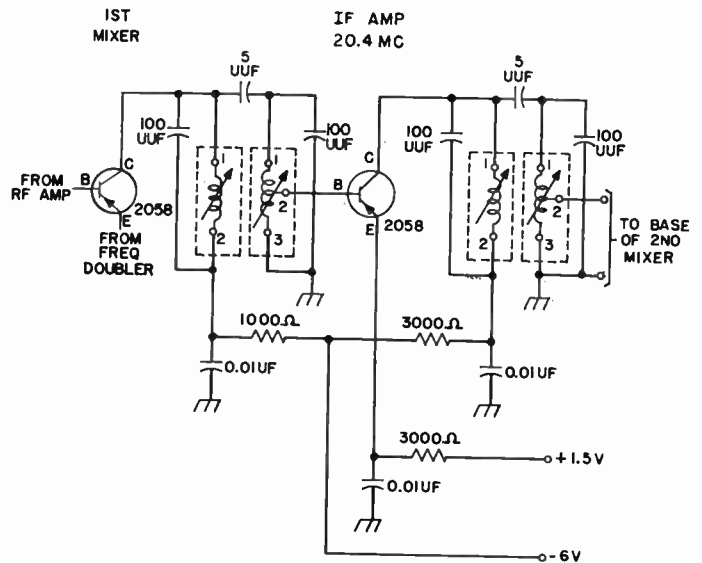


Fig. 10—High-frequency mixer and 20.4-mc IF amplifier.

the IF output at the collector is applied to the input tuned stage of the 20.4-mc IF amplifier as indicated in Fig. 10. The conversion gain is approximately 6 db.

20.4-MC IF AMPLIFIER

The primary function of the 20.4-mc IF is to allow the first oscillator to operate far enough from the carrier frequency so that its image can be rejected by the rf selectivity characteristic. Since 60-kc adjacent channel selectivity cannot be easily accomplished at this IF, a second lower IF is also required. The function of the 20.4-mc IF amplifier is to provide attenuation of the low-frequency oscillator image so that it will not create a spurious response.

The 70-db attenuation required at this image frequency is provided by a single diffused base transistor with double-tuned capacitively coupled input and output transformers. Inductors in this unit are wound on the same coil forms as the rf inductors with the exception that the adjustable powdered iron cores are

designed for 20-mc operation. Their nominal inductance is 0.6 μ h. Fig. 10 is the schematic diagram of this stage and Fig. 11 is the selectivity characteristic. The amplifier is emitter biased at 0.5 ma and has a gain of 20 db.

18.4-MC OSCILLATOR AND LOW-FREQUENCY MIXER

The modulating frequency to produce the 2-mc IF is provided by a crystal controlled 18.4-mc oscillator. The output from this circuit is sufficient to produce non-linear operation in the mixer over the complete range of operating supply voltage. No external bias is needed in this mixer because of the large signal output of the local oscillator at low power supply voltages.

The schematic diagram of the low-frequency mixer and the 18.4-mc oscillator is shown in Fig. 12.

2-MC IF AMPLIFIER

The low-frequency IF stages provide more than 70-db gain and the adjacent channel selectivity for the re-

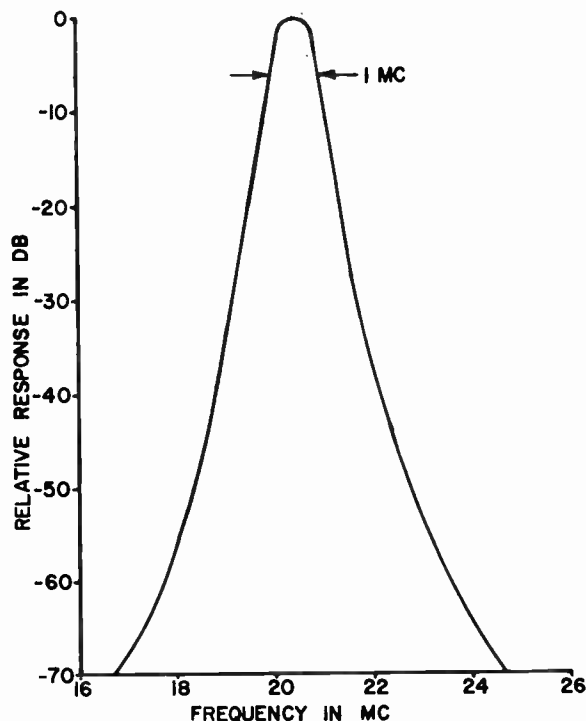


Fig. 11—20.4-mc amplifier selectivity.

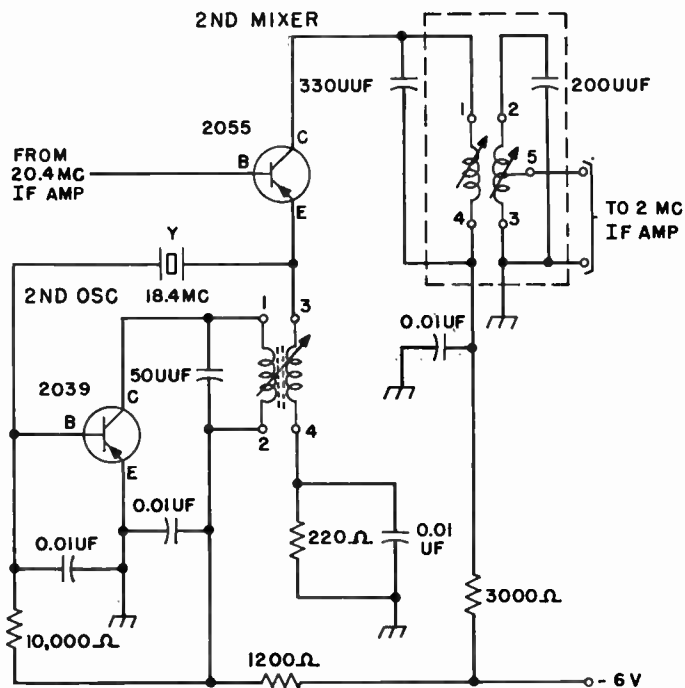


Fig. 12—18.4-mc oscillator and second mixer.

ceiver. The transistors are biased at 0.5 ma and the total drain of three stages at full battery voltage is only 11 mw. Neutralization is not required to prevent regeneration in the 2-mc stages because of the low collector capacitance of the diffused base units. The interstages are double-tuned inductively coupled inductors.⁷ The primary inductors are driven by the collector of the transistor. The secondary inductor is tapped to provide a match into the base of the following grounded emitter stage.

Although regenerative effects were not noticed on small signal voltages, the combination of low collector supply voltage and high quality interstage circuits was found to allow a sustaining oscillation to be produced if signal voltages sufficient to drive the collector voltage into a forward bias region were applied. This problem was eliminated by the insertion of a small unbiased load resistance in series with the tuned output. A value of 200 ohms was sufficient to stabilize the circuit and has a negligible effect on the gain of the stage since it is in series with a tuned circuit of 200-kilohms impedance at resonance.

Fig. 13 is a schematic diagram of a 2-mc IF stage. The complete IF consists of four inductively coupled double tuned interstage transformers and three diffused base transistors connected as indicated in the schematic. The input primary provides the tuned circuit output of the first mixer. The IF output drives the voltage limiter.

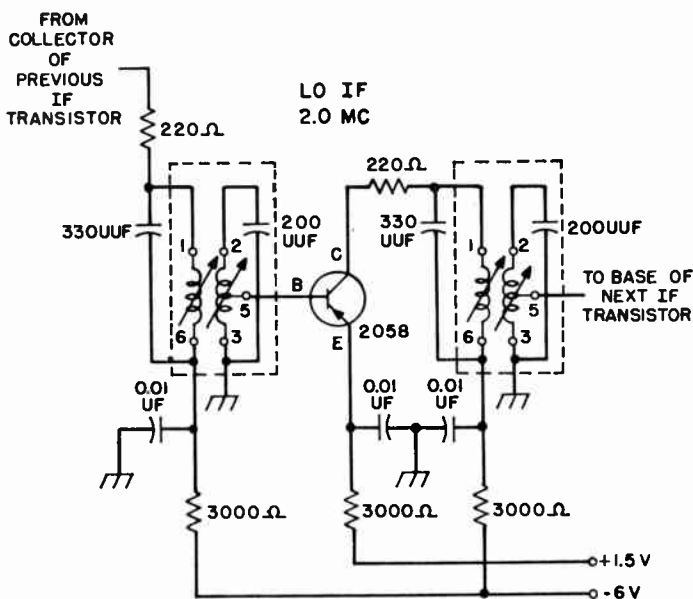


Fig. 13—2-mc IF amplifier.

LIMITER

The limiter stage is a single-tuned low-Q amplifier designed around a 20-mc f_{ab} alloy junction transistor.⁸ Neutralizing⁹ of this stage is necessary because of the high collector capacitance of these transistors. Limiting is accomplished by the action of two silicon diodes¹⁰

⁸ Raytheon 2N114.

⁹ T. O. Stanley and D. D. Holmes, "Stability Considerations in Transistor IF Amplifiers," RCA Labs., Camden, N. J., Rep. No. LB1014, pp. 1-15; December 20, 1955.

¹⁰ Hughes Diode HD-6005.

⁷ Automatic Manufacturing Co. EXO 5772.

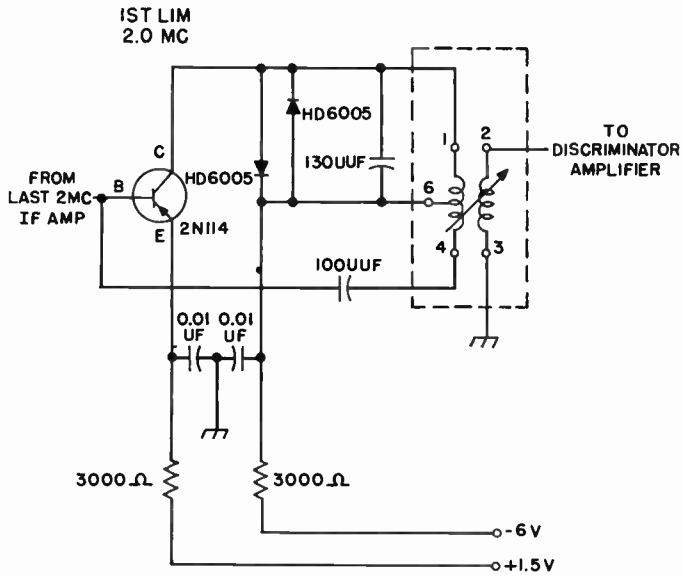


Fig. 14—Limiter stage employing silicon diodes.

duction direction. By tuning the capacitance of the diodes with the primary inductance of the output transformer, the limiter functions as a single-tuned IF amplifier until the voltage across the primary inductor reaches the forward breakdown voltage of the diodes. When this signal amplitude is reached, the diode conducts and limits the voltage swing to 1 volt peak to peak. This provides sharp limiting due to the diode characteristic and yet does not require a low impedance reference voltage to achieve it.

DISCRIMINATOR, AUDIO, AND SQUELCH

A Foster-Seeley discriminator is employed in the receiver. The design problems encountered in this stage were similar to vacuum tube problems with the exception of neutralizing and the impedance levels involved. These problems were overcome by the careful design of the discriminator transformer. The discriminator is more linear than required to meet standard mobile

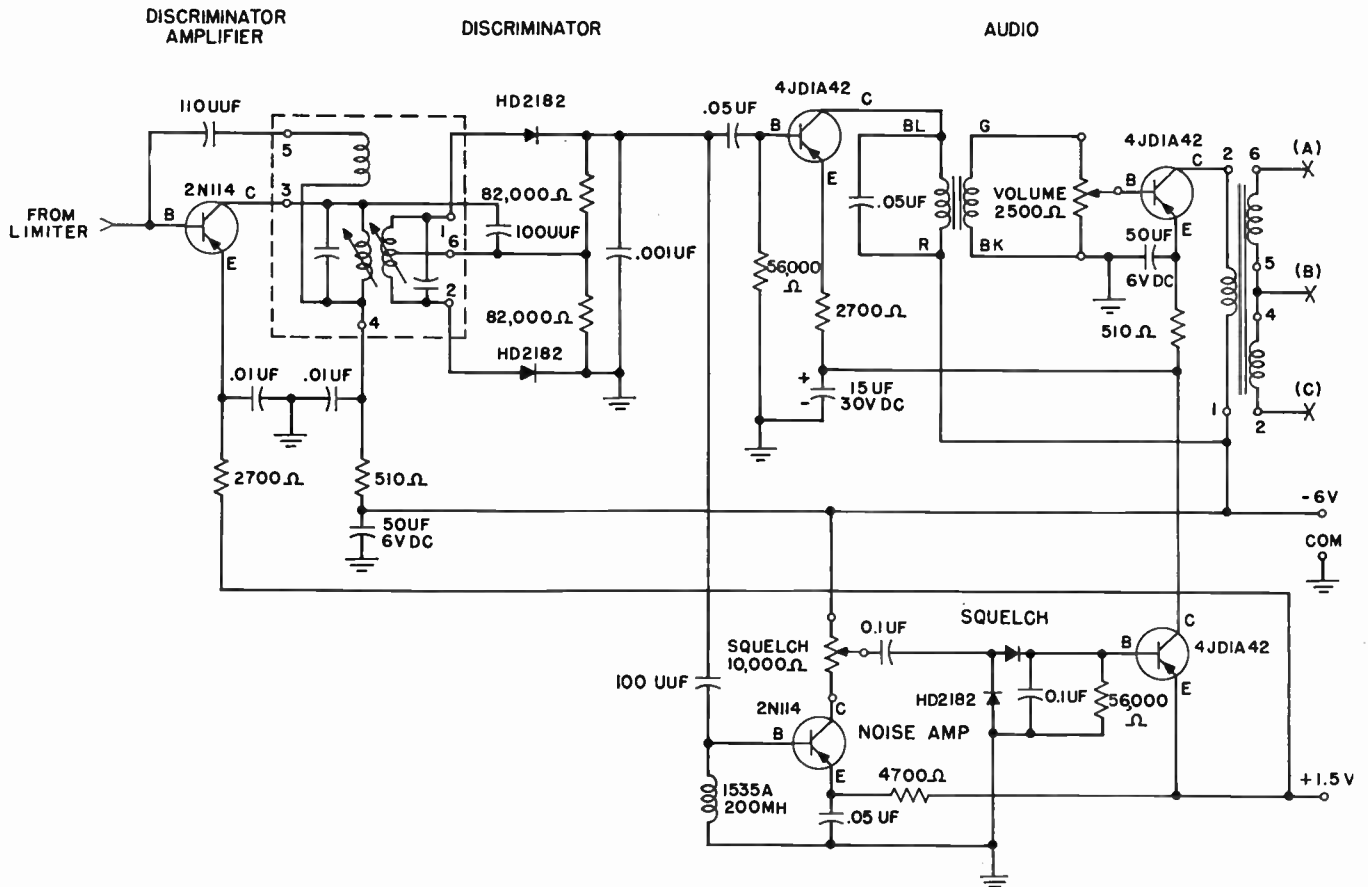


Fig. 15—Discriminator, squelch, and audio amplifier schematic diagram.

placed back to back across the output tuned primary inductor. Fig. 14 shows the schematic diagram of this stage. Use of silicon diodes for limiting is possible because of the voltage characteristic of these diodes. The sharp break between high conductivity and low conductivity occurs approximately 0.5 volt in the forward con-

duction direction. By tuning the capacitance of the diodes with the primary inductance of the output transformer, the limiter functions as a single-tuned IF amplifier until the voltage across the primary inductor reaches the forward breakdown voltage of the diodes. When this signal amplitude is reached, the diode conducts and limits the voltage swing to 1 volt peak to peak. This provides sharp limiting due to the diode characteristic and yet does not require a low impedance reference voltage to achieve it.

The audio amplifier provides standard de-emphasis for the receiver and amplifies the signal to provide 6 mw

at the handset. It utilizes General Electric 4JD1A42 transistors as the gain elements.

The squelch circuit disables the audio amplifier in the absence of received carrier by removing the bias from the audio stages. The squelch functions by measuring noise in a frequency band centered at 10 kc by means of a tuned series input circuit to the squelch amplifier. A partially by-passed emitter in this stage aids the low-frequency attenuation characteristic of this circuit. In the absence of carrier, the noise in this band is sufficient to cause the squelch circuit to control the bias to the audio amplifier by means of a transistor gate. When carrier is received, the quieting characteristic of the receiver reduces the power in this band to a value that cannot cause the squelch to cut off the audio bias. The loss in receiver sensitivity with the squelch control completely enabled is less than 5 db. Fig. 15 is the schematic diagram of the discriminator, audio, and squelch circuitry of the receiver.

PORTABLE 150-MC FM RADIO TELEPHONE

The transistorized receiver was packaged with a conventional 1-watt vacuum tube transmitter to provide a portable radio telephone as a demonstration aid. Packaging design was aimed at providing a unit that would be easy to handle and comfortable to use. Items that help to provide these features include a lightweight handset that can be worn on a head band for hands-free operation of the equipment. Also, convenient battery packs were packaged to power the equipment. One of these power packs is a rechargeable transistorized convertor supply that contains its own charging circuitry for 115-volt ac operation.

Fig. 16 is a photograph of the demonstration radio telephone. The unit as shown weighs 7 pounds and 14 ounces. It has a battery life of over 80 hours based on a 10 per cent transmitter duty cycle. The transmitter power supply requires two 67.5-volt B batteries and three 1.5-volt D cells to maintain a battery life comparable to the receiver and is therefore responsible for over 30 per cent of the total weight.

CONCLUSION

The electrical performance of the experimental transistorized receiver is comparable to existing vacuum tube equipment in the 150-mc frequency range. This is possible because of the low noise figure of the diffused based transistor and because of its ability to provide useful gain at 150 mc. The real advantage of the transistorized receiver is the long battery life possible due to the low power drain. In portable communication equipment, this is important since the receiver must monitor the channel continuously and, therefore, performs on nearly a 100 per cent duty cycle.

In providing a two-way communication unit for demonstrating the experimental receiver, miniaturization techniques and human engineering were used to

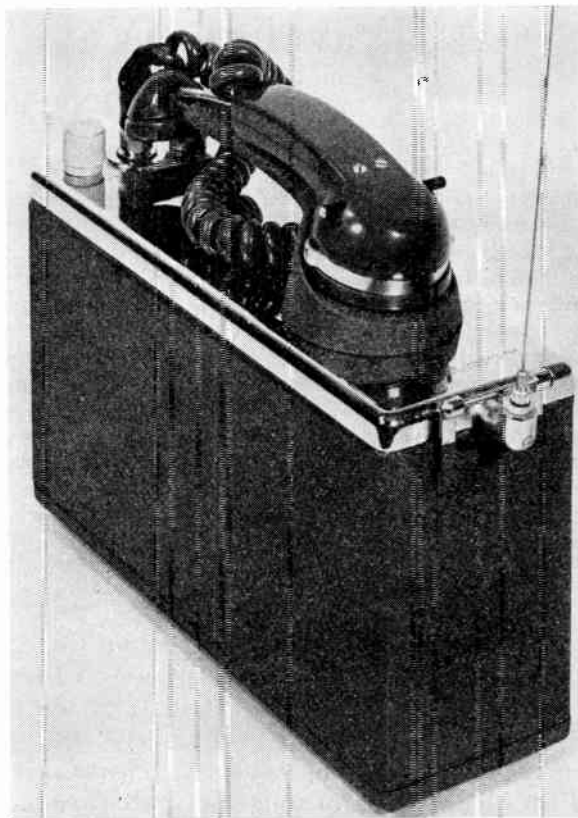


Fig. 16—Portable experimental 150-mc FM radio telephone containing a completely transistorized receiver.

provide a comfortable, efficient package. Because electrical design, using single- and double-tuned selectivity elements, was applied, and because the chassis mounting area of miniature vacuum tubes is approximately the same as that required for transistors, the receiver size is only slightly smaller than miniaturized vacuum tube models of this type. There is, however, a considerable size and weight saving in the receiver battery pack because of the lower power supply requirements of the transistorized receiver.

The value of a vhf receiver employing the diffused base transistor lies, therefore, in its ability to give equal and sometimes better performance than vacuum tubes while using an order of magnitude less power. This can make vhf mobile and portable equipment, where power drain is important, easier and cheaper to install and maintain.

The diffused base transistor used in this receiver is confined to model shop production for experimental purposes at present.

ACKNOWLEDGMENT

The design and construction of the receiver and portable radio telephone was made possible by the coordinated efforts of W. J. Chalmers, J. E. Farley, W. P. Kuebler, and A. J. Wier. Transistors were provided by the Transistor Development Department of Bell Telephone Laboratories.

A Traveling-Wave Ferromagnetic Amplifier*

P. K. TIEN†, MEMBER, IRE, AND H. SUHL†

Summary—A theory of a ferromagnetic traveling-wave amplifier of parametric type is presented here. Amplification of signal power in the form of growing waves is obtained in a propagating structure which is partially or totally embedded in a ferromagnetic medium. The structure, in one of its possible forms, possesses two propagating modes: one of the modes is excited by a signal at the input end, and the other is used as an idling circuit. The structure should also support a traveling wave supplied by a local oscillator which provides, through the motion of the magnetization, a time-varying coupling between the two propagating modes. The problem is essentially that of two coupled transmission lines with a time-dependent coupling coefficient. Optimum conditions for amplification are derived. A structure consisting of two pairs of parallel wires is calculated to illustrate the general principles.

I. INTRODUCTION

A FERROMAGNETIC amplifier in the microwave range has been recently proposed¹ by one of the authors and experimentally demonstrated by Weiss.² The amplifier may be described briefly as follows: microwave power of angular frequency ω is supplied by a local oscillator to a cavity which contains a ferrite sample. The cavity can support two resonant modes of angular frequencies ω_1 and ω_2 , respectively. The signal is fed into one of these modes. The cavity should also be resonant to the frequency of the local oscillator which drives the magnetization of the ferrite sample to precess uniformly. It is shown¹ that the uniform precession of the magnetization constitutes a time-varying coupling between the two cavity modes. If the frequency relation $\omega_1 + \omega_2 = \omega$ exists, the power supplied by the local oscillator is diverted through nonlinear effects to amplify the signal power. The physical principles of the amplifier can be understood from a simple low-frequency analogy: a pair of resonant circuits coupled through a time-varying reactance. The instability in circuits containing time-varying parameters is well known and was studied earlier by Manley and Rowe,³ and also by many others.⁴⁻⁶

It is conceivable that propagating structures may provide more bandwidth and more stability than resonant

circuits. It is the purpose of this paper to propose a traveling-wave amplifier which, in one of its possible forms, consists of two transmission lines (or two propagating modes of a transmission line) embedded in a ferromagnetic medium. The medium, in this case, is energized by a traveling wave supplied by a local oscillator and provides between the two transmission lines a coupling which varies in time and in distance. The signal is applied to the input end of one transmission line. Because of the time-varying coupling provided by the ferromagnetic medium, a wave known as the idling wave is induced in the other line, and both the signal and the idling waves grow with distance at the expense of the energizing power. Optimum conditions for amplification will be derived using transmission-line equations with proper coupling terms. A ferromagnetic amplifier, having a propagating structure in the form of two pairs of parallel wires, will then be calculated to illustrate the general principles. It should be pointed out here that the energizing power required from the local oscillator generally increases with the bandwidth of the circuit. The use of a ferromagnetic crystal of narrow line width to reduce necessary energizing power may be essential in this type of traveling-wave amplifier.

II. A TRANSMISSION-LINE SYSTEM

Before analyzing a microwave structure, complicated by the fact that the medium is no longer isotropic in the presence of the ferromagnetic material, a simpler low-frequency model will be studied which, as shown in Fig. 1, consists of two lossless transmission lines em-

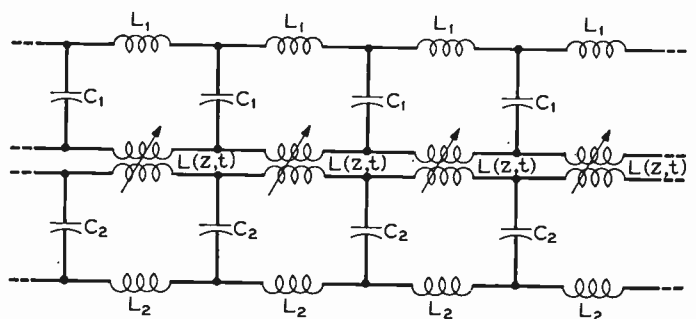


Fig. 1—A traveling-wave parametric amplifier.

bedded in an idealized nonlinear medium. The medium is energized by a traveling wave supplied by a local oscillator and is assumed to provide a variable coupling between the two transmission lines. For convenience, let us divide the transmission lines into small sections and represent each section by a filter circuit. The corre-

* Original manuscript received by the IRE, January 9, 1958.

† Bell Telephone Labs., Inc., Murray Hill, N. J.

¹ H. Suhl, "A proposal for a ferromagnetic amplifier in the microwave range," *Phys. Rev.*, vol. 106, pp. 384-385; April, 1957.

² M. T. Weiss, "Solid state microwave amplifier and oscillator using ferrites," *Phys. Rev.*, vol. 107, p. 317; July, 1957.

³ J. M. Manley and H. E. Rowe, "Some general properties of nonlinear elements—Part I. General energy relations," *Proc. IRE*, vol. 44, pp. 904-913; July, 1956.

⁴ R. V. L. Hartley, "Oscillation in systems with nonlinear reactance," *Bell. Sys. Tech. J.*, vol. 15, pp. 424-440; July, 1936.

⁵ L. W. Hussey and L. R. Wrathall, "Oscillations in an electromagnetic system," *Bell Sys. Tech. J.*, vol. 15, pp. 441-445; July, 1936.

⁶ V. D. Landon, "The use of ferrite-cored coils as converters, amplifiers and oscillators," *RCA Rev.*, vol. 10, pp. 387-396; September, 1949.

sponding sections of the two lines are coupled through a mutual inductance which varies in time and in distance and may be denoted as $L(z, t)$. Line no. 1 has a phase constant β_1 and a characteristic impedance Z_{01} at an angular frequency ω_1 , and line no. 2 has a phase constant β_2 and a characteristic impedance Z_{02} at an angular frequency ω_2 . We have

$$\beta_1 = \omega_1 \sqrt{L_1 C_1}; \quad Z_{01} = \sqrt{\frac{L_1}{C_1}} \quad (1)$$

$$\beta_2 = \omega_2 \sqrt{L_2 C_2}; \quad Z_{02} = \sqrt{\frac{L_2}{C_2}} \quad (2)$$

Line no. 1 is excited at the input end by a signal. The function of line no. 2 will be understood later. It acts essentially as an idling circuit and for simplification should be open at the input end and terminated at the output end by its characteristic impedance. In the presence of the nonlinear medium, the equations of the coupled system are

$$\frac{\partial V_1(z, t)}{\partial z} = -L_1 \frac{\partial I_1(z, t)}{\partial t} - \frac{\partial}{\partial t} [L(z, t) I_2(z, t)] \quad (3)$$

$$\frac{\partial I_1(z, t)}{\partial z} = -C_1 \frac{\partial V_1(z, t)}{\partial t} \quad (4)$$

$$\frac{\partial V_2(z, t)}{\partial z} = -L_2 \frac{\partial I_2(z, t)}{\partial t} - \frac{\partial}{\partial t} [L(z, t) I_1(z, t)] \quad (5)$$

$$\frac{\partial I_2(z, t)}{\partial z} = -C_2 \frac{\partial V_2(z, t)}{\partial t} \quad (6)$$

Here V_1 and I_1 are, respectively, the voltage and the current on line no. 1, and V_2 and I_2 are those on line no. 2. z is the distance along the direction of propagation and t is the time. The terms involving $L(z, t)$ are coupling terms which, as shown in Section VI, are in fact induced by the uniform precession of the magnetization. Here it is only assumed that $L(z, t)$ is in the form

$$L(z, t) = \frac{1}{2} [L(z) e^{j\omega t} + L^*(z) e^{-j\omega t}] \quad (7)$$

$$= \frac{1}{2} L [e^{j(\omega t - \beta z)} + e^{-j(\omega t - \beta z)}] \quad (8)$$

when the nonlinear medium is energized by a traveling wave of a phase constant β at an angular frequency ω . Here * denotes the complex conjugate.

We shall only consider waves of the frequency ω_1 on line no. 1 and waves of the frequency ω_2 on line no. 2 such that

$$\omega_1 + \omega_2 = \omega. \quad (9)$$

It may be seen from (3) and (5) that nonlinear terms given by waves of other frequencies appear to be out of synchronism with other terms in the equation and therefore cannot contribute substantial effects. Combining (3) and (4), and (5) and (6), we have, respectively,

$$\frac{\partial^2 I_1(z, t)}{\partial z^2} = C_1 L_1 \frac{\partial^2 I_1(z, t)}{\partial t^2} + C_1 \frac{\partial^2}{\partial t^2} [L(z, t) I_2(z, t)] \quad (10)$$

$$\frac{\partial^2 I_2(z, t)}{\partial z^2} = C_2 L_2 \frac{\partial^2 I_2(z, t)}{\partial t^2} + C_2 \frac{\partial^2}{\partial t^2} [L(z, t) I_1(z, t)]. \quad (11)$$

Put

$$I_1(z, t) = I_1(z) e^{j\omega_1 t} + I_1^*(z) e^{-j\omega_1 t} \quad (12)$$

$$I_2(z, t) = I_2(z) e^{j\omega_2 t} + I_2^*(z) e^{-j\omega_2 t}$$

then (10) and (11) may be reduced to

$$\frac{\partial^2 I_1(z)}{\partial z^2} = -\omega_1^2 L_1 C_1 I_1(z) - \frac{1}{2} \omega_1^2 L(z) C_1 I_2^*(z) \quad (13)$$

$$\frac{\partial^2 I_2^*(z)}{\partial z^2} = -\omega_2^2 L_2 C_2 I_2^*(z) - \frac{1}{2} \omega_2^2 L^*(z) C_2 I_1(z). \quad (14)$$

Similar equations may be obtained for $I_1^*(z, t)$ and $I_2(z, t)$ by simply interchanging the subscripts 1 and 2 in (13) and (14).

We shall first consider a simple case in which

$$\beta_1 + \beta_2 = \beta. \quad (15)$$

The general case which leads to a more complicated solution is discussed in the Appendix. Put

$$I_1(z) = A_1(z) e^{-j\beta_1 z}$$

$$I_1^*(z) = A_1^*(z) e^{j\beta_1 z}$$

$$I_2(z) = A_2(z) e^{-j\beta_2 z}$$

$$I_2^*(z) = A_2^*(z) e^{j\beta_2 z}. \quad (16)$$

We have also from (7) and (8),

$$L(z) = L e^{-j\beta z}$$

$$L^*(z) = L e^{j\beta z}.$$

Denote

$$L = \xi_1 L_1 = \xi_2 L_2 \quad (17)$$

where ξ_1 and ξ_2 are the ratios of the variable inductance to the fixed inductance of line no. 1 and line no. 2, respectively. ξ_1 and ξ_2 and so the coupling terms in (3) and (4) are assumed to be small, as is generally true in actual applications. $A(z)$'s in (16) are then slowly varying functions and the terms involving $\partial^2 A(z)/\partial z^2$'s may be neglected. Substituting (16) and (17) into (13) and (14), we have, respectively,

$$-2j\beta_1 \frac{\partial A_1(z)}{\partial z} - \beta_1^2 A_1(z) = -\omega_1^2 L_1 C_1 A_1(z) - \frac{1}{2} \omega_1^2 \xi_1 L_1 C_1 A_2^*(z) \quad (18)$$

$$2j\beta_2 \frac{\partial A_2^*(z)}{\partial z} - \beta_2^2 A_2^*(z) = -\omega_2^2 L_2 C_2 A_2^*(z) - \frac{1}{2} \omega_2^2 \xi_2 L_2 C_2 A_1(z). \quad (19)$$

Since $\beta_1^2 = \omega_1^2 L_1 C_1$ and $\beta_2^2 = \omega_2^2 L_2 C_2$, as given in (1) and (2), the above equations may be reduced to

$$\frac{\partial A_1(z)}{\partial z} = -\frac{1}{4} j \xi_1 \beta_1 A_2^*(z) \quad (20)$$

$$\frac{\partial A_2^*(z)}{\partial z} = \frac{1}{4} j \xi_2 \beta_2 A_1(z). \quad (21)$$

Combining (20) and (21), we have

$$\frac{\partial^2 A_1(z)}{\partial z^2} - \frac{1}{16} \xi_1 \xi_2 \beta_1 \beta_2 A_1(z) = 0. \quad (22)$$

The solution of (22) is

$$A_1(z) = a_1 e^{\alpha z} + b_1 e^{-\alpha z} \\ \alpha = \frac{1}{4} (\xi_2 \xi_1 \beta_1 \beta_2)^{1/2}. \quad (23)$$

Here a_1 and b_1 are arbitrary complex constants which should be determined by the boundary conditions. From (12), (16), and (23) we have finally

$$I_1(z, t) = e^{\alpha z} [a_1 e^{j(\omega_1 t - \beta_1 z)} + a_1^* e^{-j(\omega_1 t - \beta_1 z)}] \\ + e^{-\alpha z} [b_1 e^{j(\omega_1 t - \beta_1 z)} + b_1^* e^{-j(\omega_1 t - \beta_1 z)}] \quad (24)$$

$$I_2(z, t) = -j \sqrt{\frac{\xi_2 \beta_2}{\xi_1 \beta_1}} e^{\alpha z} [a_1^* e^{j(\omega_2 t - \beta_2 z)} - a_1 e^{-j(\omega_2 t - \beta_2 z)}] \\ + j \sqrt{\frac{\xi_2 \beta_2}{\xi_1 \beta_1}} e^{-\alpha z} [b_1^* e^{j(\omega_2 t - \beta_2 z)} - b_1 e^{-j(\omega_2 t - \beta_2 z)}]. \quad (25)$$

III. BOUNDARY CONDITIONS AND GENERAL DISCUSSIONS

It has been shown in (24) and (25) that for the case $\beta = \beta_1 + \beta_2$, both growing and decreasing waves may exist in the coupled transmission-line system. Since the growing wave is always dominant at the output end, the energy has to be transferred from the local oscillator to the growing waves. As mentioned earlier, line no. 1 is excited by a signal, and line no. 2 is open at the input end. The boundary conditions at the input end $z=0$ are therefore

$$I_1 = a \cos(\omega_1 t + \phi) \\ I_2 = 0. \quad (26)$$

Eqs. (24) and (25) then become

$$I_1(z, t) = \frac{1}{2} a [e^{\alpha z} \cos(\omega_1 t - \beta_1 z + \phi) \\ + e^{-\alpha z} \cos(\omega_1 t - \beta_1 z + \phi)] \quad (27)$$

$$I_2(z, t) = \frac{1}{2} a \sqrt{\frac{\xi_2 \beta_2}{\xi_1 \beta_1}} [e^{\alpha z} \sin(\omega_2 t - \beta_2 z - \phi) \\ - e^{-\alpha z} \sin(\omega_2 t - \beta_2 z - \phi)]. \quad (28)$$

We notice from the above equations that at the input end the growing and the decreasing waves are equal and in phase on line no. 1 and are equal and in opposite phases on line no. 2. At a few wavelengths from the input end, the decreasing wave becomes negligible as compared with the growing wave and may be generally ignored in the analysis.

For the general case, $\beta = \beta_1 + \beta_2 + \Delta\beta$, the solution given in the Appendix indicates that gain is generally reduced when $\Delta\beta$ deviates from zero. We may thus summarize the optimum conditions for amplification as follows:

- 1) $\omega = \omega_1 + \omega_2$
- 2) $\beta = \beta_1 + \beta_2$
- 3) $\left(\frac{d\omega}{d\beta}\right)_1 = \left(\frac{d\omega}{d\beta}\right)_2$.

It is obvious that in the propagating circuits, condition 1) is always satisfied. Condition 2) can be easily fulfilled by properly selecting the structures. Condition 3) is necessary in order that condition 2) can hold for a band of frequencies. It indicates that the group velocities of the two lines must be equal in the frequency band of amplification. It may be seen here that for extremely wide bandwidth, we may use the transmission-line type of structures ("TEM" modes) in which the group and the phase velocities are constant for all the frequencies. We may also use helices at the frequencies above their dispersive regions. With these structures, the bandwidth of the amplifier may extend from a very low frequency up to the energizing frequency.

IV. POWER RELATIONS

For simplicity we shall ignore the decreasing waves in (27) and (28). From (27), the power carried by line no. 1 is

$$P_1(z) = [I_1(z, t)^2 Z_{01}]_{\text{avg.}} = \frac{1}{8} a^2 e^{2\alpha z} \sqrt{\frac{L_1}{C_1}}. \quad (29)$$

Similarly from (28), the power carried by line no. 2 is

$$P_2(z) = [I_2(z, t)^2 Z_{02}]_{\text{avg.}} = \frac{1}{8} a^2 e^{2\alpha z} \frac{\omega_2}{\omega_1} \sqrt{\frac{L_1}{C_1}}. \quad (30)$$

The total power transferred from the local oscillator must be the sum of (29) and (30), which is

$$P_1 + P_2 = \frac{1}{8} a^2 e^{2\alpha z} \sqrt{\frac{L_1}{C_1}} \left(1 + \frac{\omega_2}{\omega_1}\right). \quad (31)$$

Comparing (29), (30), and (31), we find

$$\frac{P_1}{\omega_1} = \frac{P_2}{\omega_2} = \frac{P_1 + P_2}{\omega_1 + \omega_2}. \quad (32)$$

This, of course, is one of Manley's³ relations extended to the transmission-line system.

V. A SINGLE TRANSMISSION-LINE PARAMETRIC AMPLIFIER

We assumed earlier, for convenience, that the signal and the idling waves are carried by two separate transmission lines. We can easily show, however, that the signal, idling, and the energizing waves may be carried by a single transmission line or a propagating

mode. Amplification again is optimum when the three conditions shown in Section III are satisfied. The transmission line must contain a time-varying parameter which may be a distributed inductance, capacitance, or both. For example, in Fig. 2 we have a transmission line on which the three waves, signal, idling, and energizing all propagate. If the capacitance varies as

$$C(z, t) = C_0(1 + \frac{1}{2}\xi e^{j(\omega t - \beta z)} + \frac{1}{2}\xi e^{-j(\omega t - \beta z)})$$

the gain per unit distance is

$$\alpha = \frac{1}{4}(\xi^2 \beta_1 \beta_2)^{1/2}$$

which is in the same form of (23) with $\xi = \xi_1 = \xi_2$.

$$C(z, t) = C \left(1 + \frac{1}{2} \xi e^{j(\omega t - \beta z)} + \frac{1}{2} \xi e^{-j(\omega t - \beta z)} \right)$$

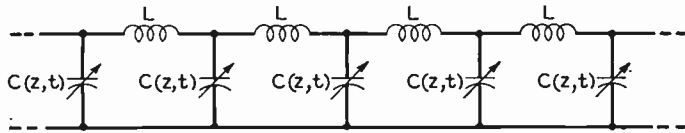


Fig. 2—A single transmission line parametric amplifier.

Later in Maxwell's equations, it will be found that in a ferrite medium the idling wave must have a component of the magnetic field parallel to the dc field and the signal wave, a component normal to the dc field, or vice versa. In the case of a single transmission line, we may place the line 45° from the dc field such that its magnetic field contains the components both parallel and normal to the dc field.

VI. A FERRITE TRAVELING-WAVE AMPLIFIER

Growing waves in a transmission line system containing time-varying parameters have been demonstrated. The calculation was made based on a low-frequency model. Next, a theory for an actual ferrite traveling-wave amplifier is worked out. In the presence of the ferromagnetic material, Maxwell's equations are necessarily complicated by the gyromagnetic character of the medium. Therefore it is important, for the present purpose, to select a simple propagating structure so that calculation can be carried out without using numerical methods.

Let us consider a structure shown in Fig. 3. It consists essentially of two pairs of parallel wires which are the two transmission lines described in Section II. Here we choose y axis as the direction of propagation. A dc field H_0 , uniform over the entire structure, is applied in the z direction. Line no. 1 has its two wires in the y - z plane, and line no. 2 has the wires in the x - y plane. All the wires are parallel to the direction of propagation and are totally embedded in a ferrite medium. The entire structure is surrounded by a circular waveguide which carries the energizing wave supplied by the local oscillator. To use the energizing power efficiently, the local oscillator must be operated at the frequency of the ferro-

magnetic resonance. We have therefore

$$\omega = \gamma \sqrt{H_0(H_0 - 2\pi M)}$$

where γ is the gyromagnetic ratio, H_0 is the dc applied magnetic field, and M is the total magnetization of the medium.

The magnetic fields associated with the two transmission lines are sketched in Fig. 3. It seems proper to assume for simplification that line no. 1 contains only E_{z1} , H_{x1} , and H_{y1} , and line no. 2 contains only E_{x2} and H_{z2} . These fields are also assumed to be uniform in the x and z directions. Again, we only consider waves of the frequency ω_1 on line no. 1, and waves of the frequency ω_2 on line no. 2 such that

$$\omega = \omega_1 + \omega_2.$$

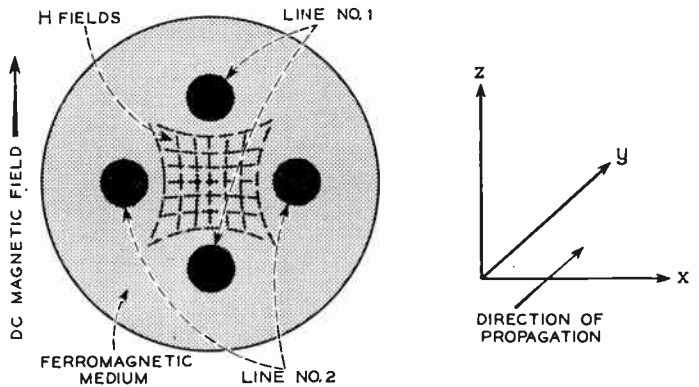


Fig. 3—A ferromagnetic traveling-wave amplifier with parallel-wire structure.

Put

$$\begin{aligned} H_{x,y1}(y, t) &= H_{x,y1}(y)e^{j\omega_1 t} + H_{x,y1}^*(y)e^{-j\omega_1 t} \\ E_{z1}(y, t) &= E_{z1}(y)e^{j\omega_1 t} + E_{z1}^*(y)e^{-j\omega_1 t} \\ M_{x,y,z1}(y, t) &= M_{x,y,z1}(y)e^{j\omega_1 t} + M_{x,y,z1}^*(y)e^{-j\omega_1 t} \\ H_{z2}(y, t) &= H_{z2}(y)e^{j\omega_2 t} + H_{z2}^*(y)e^{-j\omega_2 t} \\ E_{x2}(y, t) &= E_{x2}(y)e^{j\omega_2 t} + E_{x2}^*(y)e^{-j\omega_2 t} \\ M_{x,y,z2}(y, t) &= M_{x,y,z2}(y)e^{j\omega_2 t} + M_{x,y,z2}^*(y)e^{-j\omega_2 t}. \end{aligned} \quad (33)$$

We further assume that the local oscillator supplies an energizing wave of a phase constant β at an angular frequency ω which induces in the ferrite medium a circular polarized magnetization

$$\begin{aligned} M_x(y, t) &= \frac{1}{2} (M_0(y)e^{j\omega t} + M_0^*(y)e^{-j\omega t}) \\ &= \frac{1}{2} M_0(e^{j(\omega t - \beta y)} + e^{-j(\omega t - \beta y)}) \\ M_y(y, t) &= \frac{1}{2j} (M_0(y)e^{j\omega t} - M_0^*(y)e^{-j\omega t}) \\ &= \frac{1}{2j} M_0(e^{j(\omega t - \beta y)} - e^{-j(\omega t - \beta y)}). \end{aligned} \quad (34)$$

Define the precession angle as

$$\begin{aligned} \theta(y) &= M_0(y)/M; & \theta^*(y) &= M_0^*(y)/M; \\ \theta &= M_0/M. \end{aligned}$$

The propagating structure can be considered to be embedded in an infinite ferrite medium so that demagnetizing effects for the rf fields may be ignored. Since ω_1 and ω_2 are far from the ferromagnetic resonance, we may calculate the ω_1 and ω_2 components of magnetization from

$$\frac{d\vec{M}}{dt} = -\gamma[\vec{M} \times \vec{H}]. \quad (35)$$

Here H includes the dc and rf magnetic fields in the ferrite medium. We have thus after considerable algebraic work,

$$\begin{aligned} M_{x1}(y) &= XH_{x1}(y) + j\zeta H_{y1}(y) \\ &\quad - \theta(y) \frac{\omega_m(\omega + \omega_1)}{8\pi\Delta} H_{z2}^*(y) \\ M_{y1}(y) &= -j\zeta H_{x1}(y) + XH_{y1}(y) \\ &\quad + j\theta(y) \frac{\omega_m(\omega + \omega_1)}{8\pi\Delta} H_{z2}^*(y) \\ M_{z1}(y) &= 0 \\ M_{x2}(y) &= M_{y2}(y) = 0 \\ M_{z2}(y) &= -\frac{\theta(y)}{2} [M_{x1}^*(y) - jM_{y1}^*(y)]. \end{aligned} \quad (36)$$

Here

$$\begin{aligned} \omega_m &= 4\pi\gamma M \\ \Delta &= \omega^2 - \omega_1^2 \\ X &= \frac{\omega\omega_m}{4\pi(\omega^2 - \omega_1^2)} \\ \zeta &= \frac{\omega_1\omega_m}{4\pi(\omega^2 - \omega_1^2)}. \end{aligned} \quad (37)$$

If $\theta(y)=0$, we recognize immediately that (36) is the usual Polder relations between the magnetization and the magnetic fields. It may be seen that the uniform precession of the magnetization induced by the local oscillator, coupled through H_{z2}^* , excites additional fields on line no. 1. Through this type of couplings, the energy of the local oscillator is transferred to the signal and the idling waves. If ϵ is the dielectric constant of the ferromagnetic medium, Maxwell's equations of line no. 1 are

$$\begin{aligned} \frac{\partial H_{x1}(y)}{\partial y} &= -j \frac{\omega_1\epsilon}{c} E_{z1}(y) \\ \frac{\partial E_{z1}(y)}{\partial y} &= -j \frac{\omega_1}{c} [H_{x1}(y) + 4\pi M_{x1}(y)] \\ &= -j \frac{\omega_1}{c} \left[\mu H_{x1}(y) + i\kappa H_{y1}(y) \right. \\ &\quad \left. - \frac{\theta(y)}{2} \frac{\omega_m}{\Delta} (\omega + \omega_1) H_{z2}^*(y) \right] \\ 0 &= \mu H_{y1}(y) - j\kappa H_{x1}(y) \\ &\quad + j \frac{\theta(y)}{2} \frac{\omega_m}{\Delta} (\omega + \omega_1) H_{z2}^*(y) \end{aligned} \quad (38)$$

where

$$\begin{aligned} \mu &= 1 + 4\pi X \\ \kappa &= 4\pi\zeta \end{aligned}$$

and c is the velocity of light. Eliminating E_{z1} and H_{y1} , we get

$$\begin{aligned} \frac{\partial^2 H_{x1}(y)}{\partial y^2} &= -\frac{\omega_1^2\epsilon}{c^2} \frac{\mu^2 - \kappa^2}{\mu} H_{x1}(y) \\ &\quad + \frac{\omega_1^2\epsilon}{c^2} \frac{\mu - \kappa}{\mu} \frac{\theta(y)}{2} \frac{\omega_m(\omega + \omega_1)}{\Delta} H_{z2}^*(y). \end{aligned} \quad (39)$$

Similarly, Maxwell's equations for line no. 2 are

$$\begin{aligned} \frac{\partial H_{z2}^*(y)}{\partial y} &= -j \frac{\omega_2\epsilon}{c} E_{x2}^*(y) \\ \frac{\partial E_{x2}^*(y)}{\partial y} &= -j \frac{\omega_2}{c} [H_{z2}^*(y) + 4\pi M_{z2}^*(y)] \\ &= -j \frac{\omega_2}{c} \left[H_{z2}^*(y) \frac{\theta^*(y)}{2} [\mu + \kappa - 1] \right. \\ &\quad \left. + \frac{\mu + \kappa}{\mu} H_{x1}(y) \right]. \end{aligned} \quad (40)$$

Eliminating E_{x2}^* , we get

$$\begin{aligned} \frac{\partial^2 H_{z2}^*(y)}{\partial y^2} &= -\frac{\omega_2^2\epsilon}{c^2} H_{z2}^*(y) \\ &\quad + \frac{\omega_2^2\epsilon}{c^2} \frac{\theta^*(y)}{2} \frac{(\mu + \kappa - 1)(\mu + \kappa)}{\mu} H_{x1}(y). \end{aligned} \quad (41)$$

Comparing (39) and (41) to (13) and (14), we find that the terms

$$-\frac{\omega_1^2\epsilon}{c^2} \frac{\mu^2 - \kappa^2}{\mu} H_{x1} \quad \text{and} \quad -\frac{\omega_2^2\epsilon}{c^2} H_{z2}^*$$

correspond to the terms $-\omega_1^2 L_1 C_1 I_1 (= -\beta_1^2 I_1)$ and $\omega_2^2 L_2 C_2 I_2^* (= -\beta_2^2 I_2)$. Put

$$\begin{aligned} H_{x1}(y) &= e^{-i\beta_1 y} A_1(y) \\ H_{z2}^*(y) &= e^{i\beta_2 y} A_2^*(y) \end{aligned} \quad (42)$$

where

$$\beta_1 = \frac{\omega_1}{c} \sqrt{\frac{\epsilon(\mu^2 - \kappa^2)}{\mu}}$$

$$\beta_2 = \frac{\omega_2 \sqrt{\epsilon}}{c}$$

If $A_1(y)$ and $A_2^*(y)$ vary at a rate, slow compared to β_1 or β_2 , we may neglect $\partial A_1/\partial y$ by comparison with $\beta_1 A_1$ and $\partial^2 A_1/\partial y^2$ by comparison with $\beta_1(\partial A_1/\partial y)$. A similar situation also applies to A_2^* 's. Consider again the case

$$\beta = \beta_1 + \beta_2.$$

We have from (39) and (40),

$$-2j\beta_1 \frac{\partial A_1(y)}{\partial y} = \frac{\theta}{2} \frac{\beta_{10}^2(\mu - \kappa)}{\mu} \omega_m \frac{(\omega + \omega_1)}{\Delta} A_2^*(y) \quad (43)$$

$$-2j\beta_2 \frac{\partial A_2^*(y)}{\partial y} = \frac{\theta}{2} \beta_2^2 \frac{(\mu + \kappa - 1)(\mu + \kappa)}{\mu} A_1(y) \quad (44)$$

where

$$\beta_{10} = \frac{\omega_1 \sqrt{\epsilon}}{c}$$

Combining (43) and (44), we get

$$\frac{\partial^2 A_1(y)}{\partial y^2} - \frac{\theta^2}{16} \frac{\beta_{10}^2 \beta_2}{\beta_1} \frac{(\mu^2 - \kappa^2)(\mu + \kappa - 1)\omega_m(\omega + \omega_1)}{\mu^2 \Delta} A_1(y) = 0. \quad (45)$$

Eq. (45) should be compared to (22). The solutions of (45) are obviously in the exponential forms

$$\exp\left(\pm \frac{\theta}{4} \beta_{10} y \sqrt{\frac{\beta_2}{\beta_1} \frac{(\mu^2 - \kappa^2)(\mu + \kappa - 1)\omega_m(\omega + \omega_1)}{\mu^2 \Delta}}\right).$$

If the two transmission lines contain losses, we should add $2\alpha_1(\partial H_{x1}/\partial y)$ to the left hand of (39) and $2\alpha_2(\partial H_{x2}^*/\partial y)$ to the left hand of (41). Eq. (45) then becomes

$$\left(\frac{d}{dy} + \alpha_1\right)\left(\frac{d}{dy} + \alpha_1\right) A_1(y) = \frac{\theta^2}{16} \frac{\beta_{10}^2 \beta_2}{\beta_1} \frac{(\mu^2 - \kappa^2)(\mu + \kappa - 1)\omega_m(\omega + \omega_1)}{\mu^2 \Delta} A_1(y). \quad (46)$$

The net gain of the amplifier is therefore

$$\frac{\theta}{4} \beta_{10} \sqrt{\frac{\beta_2}{\beta_1} \frac{(\mu^2 - \kappa^2)(\mu + \kappa - 1)\omega_m(\omega + \omega_1)}{\mu^2 \Delta}} - \sqrt{\alpha_1 \alpha_2} \text{ nepers/cm}$$

or

$$\frac{\theta}{4} \beta_{10} \sqrt{\frac{\beta_2}{\beta_1}} \frac{\omega_m}{\omega - \omega_1} \sqrt{1 - \frac{\omega_1^2 \omega_m^2}{(\omega^2 + \omega \omega_m - \omega_1^2)^2}} - \sqrt{\alpha_1 \alpha_2} \text{ nepers/cm.} \quad (47)$$

In a particular case,

$$\beta_1 \cong \beta_{10}, \sqrt{1 - \frac{\omega_1^2 \omega_m^2}{(\omega^2 + \omega \omega_m - \omega_1^2)^2}} \cong 1, \alpha_1 = \alpha_2 = \alpha$$

(47) is reduced to

$$\frac{\theta}{4} \frac{\omega_m}{\omega - \omega_1} \sqrt{\beta_1 \beta_2} - \alpha \text{ nepers/cm} \quad (48)$$

which should be compared to (23).

VII. ENERGIZING POWER AND GENERAL CONSIDERATIONS

From (48), the power gain of the amplifier may be put in the form

$$8.686\alpha \left(\frac{\theta}{\theta_{\text{ert}}} - 1\right) = 8.686\alpha \left(\sqrt{\frac{P}{P_{\text{ert}}}} - 1\right) \text{ db/cm.}$$

Here θ_{ert} and P_{ert} are, respectively, the precession angle and the energizing power at which the net gain of the amplifier is equal to zero. Gain increases with the energizing power as is expected. In selecting the frequency of the local oscillator, it is important to avoid the instability due to the magnetostatic modes (Walker's modes).^{1,7} It is also important to keep the precession angle smaller than the value

$$\theta = \sqrt{\frac{\Delta H}{2\pi M}}$$

where ΔH is the line width of the ferromagnetic material. When θ is above the indicated value, an instability results from two quanta of the uniform precession going into two very short wavelengths spin-wave quanta. This has also been discussed previously.⁸

As a numerical example, we have

$$4\pi M = 2000 \text{ (yttrium iron garnet).}$$

$$\epsilon = 10.$$

$$\Delta H = 3 \text{ oersteds.}$$

$$H_0 = 3750 \text{ oersteds.}$$

$$\omega = \gamma \sqrt{H_0(H_0 - 2\pi M)} = 2\pi \times 9 \text{ kmc.}$$

$$\omega_m = 4\pi\gamma M = 2\pi \times 5.6 \text{ kmc.}$$

¹ L. R. Walker, "Magnetostatic modes in ferromagnetic resonance," *Phys. Rev.*, vol. 105, pp. 390-399; January, 1957.

⁸ H. Suhl, "Theory of the ferromagnetic amplifier," *J. Appl. Phys.*, vol. 28, pp. 1225-1236; November, 1957.

The lower limit of the magnetostatic mode is

$$\gamma(H_0 - 2\pi M) = 2\pi \times 7.7 \text{ kmc.}$$

Instability will not therefore occur by choosing

$$\omega_1 = 2\pi \times 6.5 \text{ kmc}$$

$$\omega_2 = 2\pi \times 2.5 \text{ kmc}$$

$$\theta = \frac{1}{20}.$$

$$\sqrt{1 - \frac{\omega_1^2 \omega_m^2}{(\omega^2 + \omega \omega_m - \omega_1^2)^2}} = 0.914.$$

The gain per unit distance calculated from (47) is 0.551 db/cm (ignoring copper loss of the circuit). Since ΔH is 3 oersteds, the energizing field is

$$h_{\text{energizing}} = \Delta H \times \theta = 0.15 \text{ oersted.} \quad (49)$$

To maintain this field, power must be supplied by the local oscillator mainly because of the ferromagnetic loss of the sample. If the volume of the sample is V_s in cm^3 , the ferromagnetic loss at the energizing frequency is

$$\begin{aligned} P_m &= \frac{\omega}{8\pi} \frac{4\pi M}{\Delta H} (h_{\text{energizing}})^2 V_s \times 10^{-7} \text{ watts} \\ &= 3.375 \times 10^3 V_s \text{ watts.} \end{aligned} \quad (50)$$

We notice from (49) and (50) that for a certain precession angle θ , the ferromagnetic loss is proportional to V_s and ΔH . The energizing power may be reduced by using a crystal of narrow line width and by keeping the vol-

where k_1 and k_2 are constants which satisfy the relation

$$k_1 + k_2 = 1. \quad (51)$$

Eqs. (18) and (19) then become

$$\begin{aligned} -2j(\beta_1 + k_1\Delta\beta) \frac{\partial A_1(z)}{\partial z} - (\beta_1 + k_1\Delta\beta)^2 A_1(z) \\ = -\beta_1^2 A_1(z) - \frac{1}{2}\xi_1\beta_1^2 A_2^*(z) \end{aligned} \quad (52)$$

$$\begin{aligned} 2j(\beta_2 + k_2\Delta\beta) \frac{\partial A_2^*(z)}{\partial z} - (\beta_2 + k_2\Delta\beta)^2 A_2^*(z) \\ = -\beta_2^2 A_2^*(z) - \frac{1}{2}\xi_2\beta_2^2 A_1(z). \end{aligned} \quad (53)$$

Put

$$\beta_1 + k_1\Delta\beta = \beta_1'$$

$$\beta_2 + k_2\Delta\beta = \beta_2'$$

and we have from (52) and (53),

$$\begin{aligned} \frac{\partial A_1(z)}{\partial z} - j \frac{k_1\Delta\beta(2\beta_1' - k_1\Delta\beta) A_1(z)}{2\beta_1'} \\ = -j \frac{1}{4} \xi_1 \frac{\beta_1^2}{\beta_1'} A_2^*(z) \end{aligned} \quad (54)$$

$$\frac{\partial A_2^*(z)}{\partial z} + j \frac{k_2\Delta\beta(2\beta_2' - k_2\Delta\beta) A_2^*(z)}{2\beta_2'} \quad (55)$$

$$= j \frac{1}{4} \xi_2 \frac{\beta_2^2}{\beta_2'} A_1(z)$$

Combining (54) and (55), we find

$$\begin{aligned} \left(\frac{\partial^2}{\partial z^2} - j \frac{\Delta\beta}{2} \left(\frac{k_1(2\beta_1' - k_1\Delta\beta)}{\beta_1'} - \frac{k_2(2\beta_2' - k_2\Delta\beta)}{\beta_2'} \right) \right) \frac{\partial}{\partial z} \\ + \frac{k_1 k_2 \Delta\beta^2 (2\beta_1' - k_1\Delta\beta)(2\beta_2' - k_2\Delta\beta)}{4\beta_1' \beta_2'} - \frac{1}{16} \xi_1 \xi_2 \frac{\beta_1^2 \beta_2^2}{\beta_1' \beta_2'} A_1(z) = 0. \end{aligned} \quad (56)$$

ume of the sample or the size of propagating structure small. We also notice from (23) and (47) that gain is proportional to β 's. A slow wave structure such as a helix, a loaded waveguide, or a filter type of circuit, may therefore be important for high gain amplifiers.

APPENDIX

If

$$\beta = \beta_1 + \beta_2 + \Delta\beta,$$

we put

$$I_1(z) = A_1(z) e^{-j(\beta_1 + k_1\Delta\beta)z}$$

$$I_1^*(z) = A_1^*(z) e^{j(\beta_1 + k_1\Delta\beta)z}$$

$$I_2(z) = A_2(z) e^{-j(\beta_2 + k_2\Delta\beta)z}$$

$$I_2^*(z) = A_2^*(z) e^{j(\beta_2 + k_2\Delta\beta)z}$$

For forward waves β_1' , β_2' , β_1 , and β_2 are positive and so the quantities

$$(2\beta_1' - k_1\Delta\beta) \quad \text{and} \quad (2\beta_2' - k_2\Delta\beta).$$

It is therefore always possible to find k_1 and k_2 so that the term involving $\partial/\partial z$ in (52) vanishes. We have finally

$$\begin{aligned} \frac{\partial^2 A_1(z)}{\partial z^2} = \frac{1}{16} \xi_1 \xi_2 \frac{\beta_1^2 \beta_2^2}{\beta_1' \beta_2'} \\ - \frac{k_1 k_2 \Delta\beta^2 (2\beta_1' - k_1\Delta\beta)(2\beta_2' - k_2\Delta\beta)}{4\beta_1' \beta_2'}. \end{aligned} \quad (57)$$

It is obvious that the last two terms in (57) are of opposite signs. The gain of the amplifier therefore reduces as $\Delta\beta$ deviates from zero.

Parametric Amplification of Space Charge Waves*

W. H. LOUISELL† AND C. F. QUATE†, MEMBER, IRE

Summary—The principle of using a variable reactance in a circuit to produce gain can be applied to an electron beam. The beam is strongly modulated by an rf wave at a frequency equal to twice the signal frequency. In such a beam the two normal space charge waves at the signal frequency break into two parts—one grows exponentially with distance and the second is attenuated. Either the “slow” or the “fast” space charge wave can be amplified. When this beam, which has been previously modulated at the double frequency, is coupled to a slow wave circuit, growing waves are found and again the “fast” space charge wave can be amplified. We stress the amplification of the fast wave since the noise theorems which apply to previous microwave amplifiers and establish a lower limit to the noise figure do not apply. Thus, in principle, we should be able to obtain lower values for the noise figure.

I. INTRODUCTION

THE devices which amplify at microwave frequencies have in general used dc power as their source of energy, but it is now recognized that the required power can equally well come from a continuous wave (cw) frequency which is related to the signal in a particular way. In one form of amplifier this cw source, denoted by the term “pump,” functions to vary the reactance of a circuit; this variable reactance converts power from the pumping frequency into the signal frequency. The term “parametric amplifier” has been used to describe these devices. Suhl¹ has illustrated this principle with his discussion of the ferrite model. He has shown that if a ferromagnetic sample is placed in a cavity resonant at frequencies ω , ω_1 , and ω_2 where $\omega = \omega_1 + \omega_2$ oscillation or amplification may occur at frequencies ω_1 or ω_2 . This is true provided that power is supplied at ω which is the frequency of uniform precession of the magnetization in a magnetic field H . Bridges² has shown that an electron beam can be used to vary the reactance of a microwave cavity and thereby achieve “parametric” gain. In this paper we will describe a distributed “parametric amplifier” which uses an electron beam and derives its power from a cw source oscillating at a frequency equal to twice the signal frequency.

Several early articles³⁻⁵ have described this method of using a variable reactance to amplify signals and the

current interest has been stimulated by the realization that, in principle, one can conceive of a parametric amplifier with a very low noise content. In turn this idea has come from the recent work on masers^{9,10} which is a form of amplifier that uses the cw “pump” frequency to invert the normal distribution of energy levels in the active material rather than to vary a reactance.

An amplifier of the most simple form is shown in Fig. 1(a). Here we have a single resonant circuit with a capacitance which is varied at a rate equal to twice the signal frequency. When the depth of modulation is such that¹¹

$$\frac{\Delta C}{C} = \frac{2}{Q},$$

the power delivered to the circuit from the pump is equal to the losses in the circuit, and the circuit will oscillate at ω . Below this value we can use the circuit as a regenerative amplifier, exhibiting negative resistance type of gain. A natural descendant of this circuit is shown in Fig. 1(b). In this distributed transmission line we modulate the shunt capacity with a traveling wave

tions,” Oxford University Press, New York, N. Y., pp. 69–70, 274–275; 1947.

⁶ J. D. Laudon, “The use of ferrite-cored coils as converters, amplifiers, and oscillators,” *RCA Rev.*, vol. 10, pp. 387–396; September, 1949.

⁷ E. Goto, “On the application of parametrically excited nonlinear resonators,” *J. Elec. Commun. Engrs. Japan*, vol. 38, pp. 770–775; June, 1955.

⁸ C. F. Edwards, “Frequency conversion by means of a nonlinear admittance,” *Bell Sys. Tech. J.*, vol. 35, pp. 1403–1416; November, 1956.

⁹ J. P. Gordon, H. J. Zeiger, and C. H. Townes, “The maser—new type of microwave amplifier, frequency-standard, and spectrometer,” *Phys. Rev.*, vol. 99, pp. 1264–1274; August 15, 1955.

¹⁰ J. P. Wittke, “Molecular amplification and generation of microwaves,” *Proc. IRE*, vol. 45, pp. 291–316; March, 1957.

¹¹ From Fig. 1(a), $C = C_0 + \Delta C \cos 2\omega_0 t$, the equation for the charge, y , is

$$\ddot{y} = \frac{R}{L} \dot{y} + \frac{1}{LC_0} \left(1 + \frac{\Delta C}{C_0} \cos 2\omega_0 t \right) y = 0.$$

If

$$y = v(t) \exp \left[\mu (LC_0)^{-1/2} \frac{R}{2L} \right] t,$$

$v(t)$ is periodic. From the theory of Mathieu equations (McLachlan, *op. cit.*), since

$$\frac{\Delta C}{C_0} \ll 1,$$

we find

$$\operatorname{Re}(\mu) \cong \frac{\Delta C}{4C_0}.$$

Thus, oscillation occurs when

$$\frac{\Delta C}{C_0} \geq \frac{2R}{\omega_0 L} = \frac{2}{Q}.$$

* Original manuscript received by the IRE, November 26, 1957; revised manuscript received, January 14, 1958.

† Bell Telephone Labs., Inc., Murray Hill, N. J.

¹ H. Suhl, “A proposal for a ferromagnetic amplifier in the microwave range,” *Phys. Rev.*, vol. 106, pp. 384–385; April, 1957.

² T. J. Bridges, “An electron beam parametric amplifier,” *Proc. IRE*, vol. 46, pp. 494–495; February, 1958.

³ W. L. Barrow, D. B. Smith, and F. W. Baumann, “A further study of oscillatory circuits having periodically varying parameters,” *J. Franklin Inst.*, vol. 221, pt. I, pp. 403–416, pt. II, pp. 509–529; March, 1936.

⁴ R. V. L. Hartley, “Oscillations in electromechanical systems,” *Bell Sys. Tech. J.*, vol. 15, pp. 441–445; July, 1936.

⁵ N. W. McLachlan, “Theory and Applications of Mathieu Func-

at the "pump" frequency. Tien has shown that growing waves appear on this circuit provided that the phase $\phi_1, \phi_2, \dots, \phi_n$ are properly chosen. Suhl and Tien¹² have discussed the case of two transmission lines coupled with reactive elements. Exponentially growing waves are obtained when the coupling is modulated with the proper traveling wave. Kompfner has considered the system of an electron beam coupled to a helix and modulated at twice the signal frequency. An analysis of this problem shows that waves, which grow with distance, occur; in a later section we will evaluate the various waves in such a system.

First, however, we will treat the problem of a single electron stream which is modulated at twice the signal frequency.

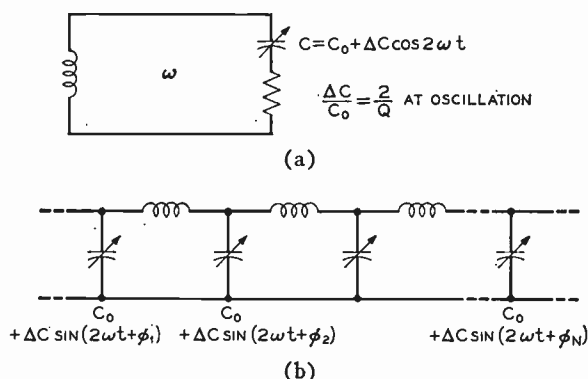


Fig. 1—Simple form of parametric amplifier. The single resonant circuit of (a) will exhibit negative resistance gain below the threshold of oscillation while the distributed circuit of (b) will exhibit exponential gain with distance along the circuit.

The two normal space charge waves on such a beam each divide into a wave which grows and a wave which attenuates with distance. Amplification of the "slow" space charge wave is of no interest since it can more easily be amplified by coupling the stream to such elements as a slow wave circuit to form a conventional twt¹³ or to a resistive wall amplifier.¹⁴ These amplifiers have a minimum noise figure which is determined by the noise parameters near the cathode potential minimum. At present, these amplifiers have been built with noise figures less than 4 db.¹⁵ The growing wave associated with the "fast" space charge wave is important since the theorems¹⁶ pertaining to the minimum noise figure of a "slow" wave amplifier do not apply and much lower noise figures should be possible.

¹² P. K. Tien and H. Suhl, "A ferromagnetic traveling wave amplifier," this issue, p 700.

¹³ J. R. Pierce, "Traveling Wave Tubes," D. Van Nostrand Co, Inc., New York, N. Y.; 1949.

¹⁴ C. K. Birdsall, G. R. Brewer, and A. V. Haeff, "The resistive wall amplifier," Proc. IRE, vol. 41, pp. 865-875; July, 1953.

¹⁵ M. R. Currie and D. C. Forster, "New results in noise reduction in electron beams," presented at Conference on Electron Tube Research, Berkeley, Calif., June, 1957.

¹⁶ H. A. Haus and F. N. H. Robinson, "The minimum noise figure of microwave beam amplifiers," Proc. IRE, vol. 43, pp. 981-991; August, 1955.

Adler¹⁷ has discussed this principle and suggested methods of amplifying the "fast" wave with deflection type circuits. Also, the work of Wade and Degrasse¹⁸ in which they obtain frequency division with feedback around two separate helices is quite likely related to the "parametric" gain of the slow wave as described in Section IV.

II. SINGLE ELECTRON STREAM MODULATED AT TWICE THE SIGNAL FREQUENCY

We will consider the waves on an electron beam which is modulated with a fast or slow wave at twice the signal frequency. The modulation will be assumed large as compared to the signal but still small enough so that it can be described with the linear theory. The beam will be assumed to be confined by a very large magnetic field.

We start from the three fundamental equations—namely Poisson's equation

$$\nabla \cdot E = \frac{1}{\epsilon_0} \rho, \quad (1)$$

the equation of continuity

$$\frac{\partial i}{\partial z} = -\frac{\partial \rho}{\partial t}, \quad (2)$$

and the equation of motion

$$\frac{dv}{dt} = \eta \frac{\partial V}{\partial z}, \quad (3)$$

where $\eta = e/m$ is the ratio of charge to mass of the electron and E is the electric field acting on the electron which is the gradient of the voltage as defined by

$$E = -\frac{\partial V}{\partial z}. \quad (4)$$

ϵ_0 = the dielectric constant of free space,

v = velocity of the electron beam,

ρ = charge per unit length in the stream,

i = current in the stream and is given by $i = \rho v$. (5)

We define as usual

$$\omega_p^2 = -\frac{\eta \rho_0}{\epsilon_0}. \quad (6)$$

Here ω_p is the plasma frequency for a one-dimensional beam of infinite cross section. ω_q is the plasma frequency for the cylindrical beam and is related to ω_p by the relation

$$\omega_q = R\omega_p. \quad (7)$$

¹⁷ R. Adler, "A new principle of signal amplification," presented at Conference on Electron Tube Research, Berkeley, Calif., June, 1957.

¹⁸ R. W. DeGrasse and G. Wade, "Microwave mixing and frequency dividing," Proc. IRE, vol. 45, pp. 1013-1015; July, 1957.

R is the plasma frequency reduction factor for a beam of finite cross section.¹⁹ Hereafter, we shall use ω_q in place of ω_p . Eq. (3) can be written in the form

$$\frac{\partial^2 v}{\partial t^2} + \frac{\partial^2}{\partial t \partial z} \left\{ \frac{v^2}{2} \right\} = \eta \frac{\partial^2 v}{\partial z \partial t} \tag{8}$$

and (1), (2), (4), and (6) can be combined to give

$$\eta \frac{\partial^2 V}{\partial z \partial t} = \omega_q^2 \frac{u_0}{I_0} i. \tag{9}$$

The equation of motion (8) is then

$$\frac{\partial^2 v}{\partial t^2} + \frac{\partial^2}{\partial z \partial t} \left\{ \frac{v^2}{2} \right\} = \omega_q^2 \frac{u_0}{I_0} i. \tag{10}$$

Similarly, if we combine (2) and (5) we can write

$$v^2 \frac{\partial i}{\partial z} = -v \frac{\partial i}{\partial t} + i \frac{\partial v}{\partial t}. \tag{11}$$

Eqs. (10) and (11) are the familiar equations which relate the velocity and current in an electron stream. The normal space charge waves on the stream come directly from (10) and (11) and are of the form

$$i = -I_0 + i_1 \exp \left[-j\beta_e \left(1 \mp \frac{\omega_q}{\omega} \right) z + j\omega t \right], \tag{12}$$

$$v = u_0 \mp \frac{\omega_q}{\omega} \frac{u_0}{I_0} i_1 \exp \left[-j\beta_e \left(1 \mp \frac{\omega_q}{\omega} \right) z + j\omega t \right], \tag{13}$$

where

- $\beta_e = \omega/u_0$,
- $I_0 =$ dc current,
- $u_0 =$ dc velocity.

These solutions were originally described by Hahn²⁰ and Ramo²¹ and we will briefly review their characteristics for they are the waves which we propose to amplify. The upper sign in (12) and (13) indicates a wave that travels faster than the dc beam velocity. This is the fast wave which will attract most of our attention. We see that the current and velocity are 180° out of phase as we move down the stream. With our particular definitions, a positive value of current indicates a reduction in the number of electrons below the average value. This antiphase condition means that the electron density is largest at the point of highest velocity. Therefore, in the presence of the fast wave the energy of the beam is increased over and above the dc energy. The second space charge wave associated with the lower sign in (12) and (13) has a phase velocity less than the dc velocity, and the rf current and velocity are in phase. The highest

electron density now occurs at the point of minimum velocity and the energy of the beam is reduced in the presence of this wave. These two waves are quite analogous to the forward and backward waves on an ordinary transmission line. There the current and voltage are in phase for the forward wave and the power flow is in the positive direction. The backward wave has a current and voltage which are out of phase and the power flow is in the negative direction. Chu²² has pointed out this similarity with the fast space charge wave corresponding to the forward wave and the slow space charge wave corresponding to the backward wave.

In a klystron, for example, both waves are equally excited at the input gap. Thus the beam energy is unchanged and it is commonly known that it requires no rf power to bunch a beam. After the beam passes through the output cavity the slow wave is much larger than the fast wave and the total beam energy is decreased by the energy flow through the output cavity. In a traveling-wave tube, amplification occurs at the point where the circuit phase velocity is equal to the velocity of the slow space charge wave. In this tube the slow wave grows exponentially with a continual decrease in beam energy. We will now consider the parametric amplifier and show that either the fast or the slow wave can be amplified independently of each other.

For the parametric amplifier we use a modulation at 2ω which is impressed on the beam in the form of a space charge wave

$$i_{2\omega} = I_m \exp \left[-j2\beta_e \left(1 - \frac{\omega_{q2}}{2\omega} \right) z + 2j\omega t \right],$$

$$v_{2\omega} = -\frac{\omega_{q2}}{2\omega} \frac{u_0}{I_0} I_m \exp \left[-j2\beta_e \left(1 - \frac{\omega_{q2}}{2\omega} \right) z + 2j\omega t \right], \tag{14}$$

where ω_{q2} is the reduced plasma frequency at the pump frequency. If we take ω_{q2} as positive we have modulation in the form of a fast wave, whereas if we use a negative value for ω_{q2} we have modulation in the form of a slow wave. In general, ω_{q2} is not equal to ω_q , the reduced plasma frequency at the signal frequency, and it is necessary to introduce a new parameter, a' , which relates these two as

$$a' = \frac{\omega_{q2}}{2\omega_q}. \tag{15}$$

The value of a' as calculated¹⁹ is plotted in Fig. 2. We see that it can range in value from +1 for a thin beam to a value of $\frac{1}{2}$ for an infinitely thick beam.

I_m is the peak ac current at the modulation frequency and we relate it to the dc current by

$$I_m = mI_0 \tag{16}$$

¹⁹ G. M. Branch and T. G. Mihran, "Plasma reduction factors in electron beams," IRE TRANS. ON ELECTRON DEVICES, vol. 2, pp. 3-11; April, 1955.

²⁰ W. C. Hahn, "Small signal theory of velocity modulated electron beams," Gen. Elec. Rev., vol. 42, pp. 258-270; June, 1939.

²¹ S. Ramo, "Space charge and field waves in an electron beam," Phys. Rev., vol. 56, pp. 276-283; August, 1939.

²² L. J. Chu, "A kinetic power theorem," presented at IRE Conference on Electron Devices, Durham, N. H.; June, 1951.

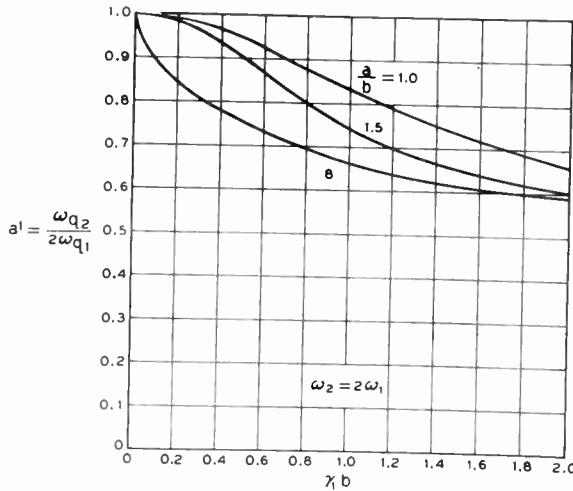


Fig. 2—A plot of a' vs γb . γb is the ratio of the circumference of the beam to the rf wavelength on the beam at the signal frequency. a' is equal to one-half of the ratio of the reduced plasma frequency at the pump frequency to the reduced plasma frequency at the signal frequency. It is thus a measure of the relative velocity of the space charge waves at the pump and signal frequencies.

where m expresses the depth of modulation. It is a complex number since the modulation can have any phase with respect to the signal frequency. We assume $I_m \gg i$ and therefore I_m can be considered constant with distance along the beam.

We can then write

$$i = -I_0 + \frac{m}{2} I_0 \exp \left[-2j\beta_e \left(1 - \frac{a'\omega_q}{\omega} \right) z + 2j\omega t \right] + cc \\ + \frac{1}{2} i_1(z) \exp \left[-j\beta_e \left(1 - \frac{a'\omega_q}{\omega} \right) z + j\omega t \right] + cc, \quad (17)$$

and

$$v = u_0 - \frac{a'\omega_q}{\omega} u_0 \frac{m}{2} \exp \left[-2j\beta_e \left(1 - \frac{a'\omega_q}{\omega} \right) z + 2j\omega t \right] + cc \\ + \frac{1}{2} v_1(z) \exp \left[-j\beta_e \left(1 - \frac{a'\omega_q}{\omega} \right) z + j\omega t \right] + cc \quad (18)$$

where cc indicates the complex conjugate. We must add the complex conjugates because of the quadratic terms which appear in the equations and represent coupling between the pump and signal frequencies. The form of these equations is convenient since it will turn out later that in the region of gain, $i_1(z)$ and $v_1(z)$ are real exponentials which means that the velocity of the signal frequency waves has shifted to become equal to the velocity of the pumping wave.

If we substitute (17) and (18) into (10) and (11), we obtain for the coefficients of the signal frequency terms

$$\frac{dv_1}{dz} + ja'\beta_q v_1 + ja'\beta_q \frac{m}{2} v_1^* = -j \frac{\beta_q^2}{\beta_e} \frac{u_0}{I_0} i_1, \quad (19)$$

and

$$\frac{di_1}{dz} + ja'\beta_q i_1 + j \frac{ma'}{2} \beta_q i_1^* + j \frac{\beta_e}{u_0} I_0 v_1 \\ - j \frac{m}{2} I_0 \frac{\beta_e}{u_0} v_1^* = 0 \quad (20)$$

where

$$\beta_q = \frac{\omega_q}{u_0}.$$

We will first consider the case for a thin beam where a' is unity. This indicates that the modulation is in the form of a fast wave which travels at the same velocity as the fast space charge wave at the signal frequency. We use (19) and (20) to write

$$\frac{d^2 v_1}{dz^2} + 2j\beta_q \frac{dv_1}{dz} - \beta_q^2 \frac{|m|^2}{4} v_1 - \frac{3m}{2} \beta_q^2 v_1^* = 0. \quad (21)$$

Eliminating v_1 or v_1^* between (21) and its cc ; and assuming solutions of the form

$$v_1 = v_0 e^{\mu\beta_q z}, \quad (22)$$

we obtain the secular equation for μ ,

$$\mu^4 + 4 \left(1 - \frac{|m|^2}{8} \right) \mu^2 - \frac{9|m|^2}{4} + \left(\frac{|m|^2}{4} \right)^2 = 0. \quad (23)$$

In (23) $|m|$ is always less than unity and we find approximate roots of the form

$$\mu_1 = \frac{3|m|}{4},$$

$$\mu_2 = \frac{3|m|}{4}, \quad (24)$$

$$\mu_3 = -j2, \quad (25)$$

$$\mu_4 = +j2.$$

We can see from (18) that the first two roots (μ_1, μ_2) represent waves traveling at the velocity of the fast wave at the pump frequency, one of which grows exponentially and the other of which attenuates exponentially. The third root (μ_3) is the slow wave and the fourth root (μ_4) is a new wave which travels faster than the fast wave. We will show later that this wave cannot be excited when the pump frequency modulation is removed.

For the case where $a' \neq 1$ we can combine (19) and (20) in the form

$$\frac{d^2 v_1}{dz^2} + 2ja'\beta_q \frac{dv_1}{dz} - \beta_q^2 \left[a'^2 \left(1 + \frac{|m|^2}{4} \right) - 1 \right] v_1 \\ - \beta_q^2 \frac{m}{2} (2a'^2 + 1) v_1^* = 0. \quad (26)$$

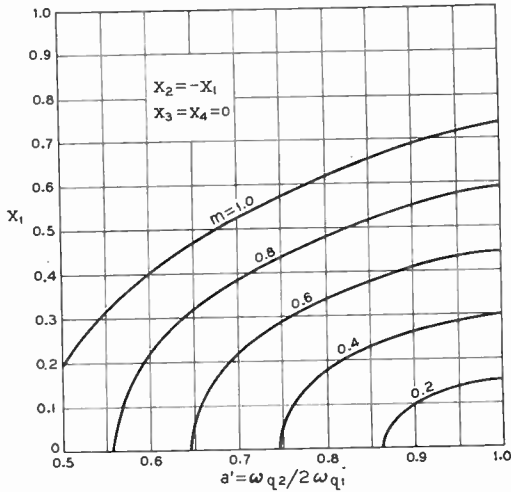


Fig. 3—The real part of the propagation constant for the two-frequency parametric beam. On such a beam waves propagate as

$$\exp -j\beta_0 \left(1 - a' \frac{\omega_q}{\omega}\right) z + \beta_q(x + jy)z + j\omega t.$$

Note that for $|a'| < 1$, which means that the space charge waves at the pump and signal frequencies do not travel at the same velocity, there is a minimum value of $|m|$ which will produce gain.

If we again eliminate v_1^* from (26) and its *cc* and assume that

$$v_1 = v_{01} e^{\mu \beta q z}, \tag{27}$$

we obtain

$$\mu^4 + 2 \left[a'^2 \left(1 - \frac{|m|^2}{4}\right) + 1 \right] \mu^2 + a'^4 \left(1 - \frac{|m|^2}{4}\right)^2 - \frac{3|m|^2}{2} a'^2 - 2a'^2 + 1 - \frac{|m|^2}{4} = 0. \tag{28}$$

The real roots of (28) are plotted in Fig. 3. As the velocity of the pump and signal waves become unequal, the gain per unit length decreases and there is a threshold value of modulation, m , below which no gain occurs. The imaginary parts of μ are shown in Fig. 4. This threshold value is plotted in Fig. 5. The straight line for μ_3 indicates a wave with a velocity

$$\frac{u_0}{1 + \frac{\omega_q}{\omega}}$$

which is the slow wave and for μ_4 a wave with a velocity

$$\frac{u_0}{1 - \frac{\omega_q}{u_0} (1 + 2a')}$$

which is the mirror of the slow wave about the pump velocity and travels faster than the fast wave.

We see that in (28) only even powers of a' occur. This means that we obtain the same roots for a' positive (fast wave modulation) or a' negative (slow wave modu-

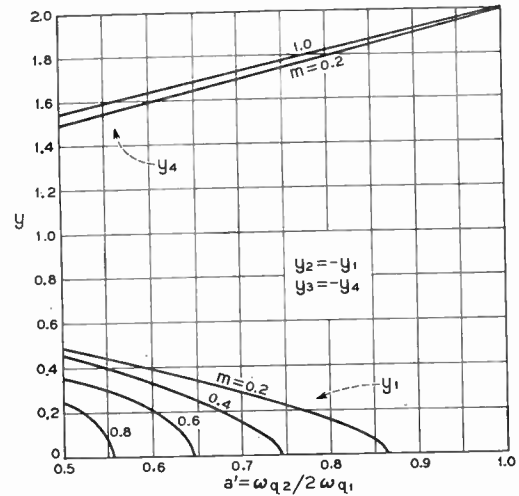


Fig. 4—The imaginary part of the propagation constant for the two-frequency parametric beam. On such a beam the waves propagate as

$$\exp -j\beta_0 \left(1 - a' \frac{\omega_q}{\omega}\right) z + \beta_q(x + jy)z + j\omega t.$$

For a' positive y_3 represents the normal slow space charge wave and y_4 is a wave which travels faster than the fast wave.

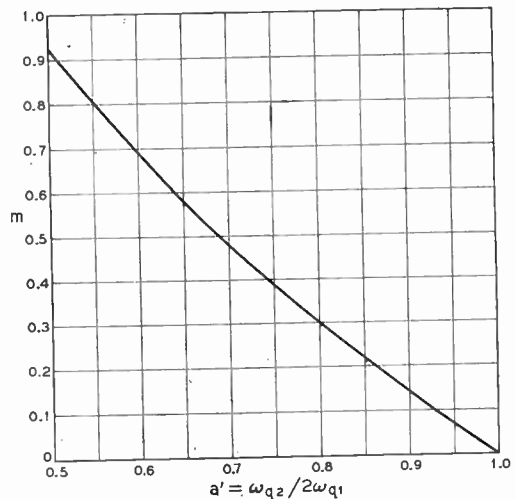


Fig. 5—The value of the minimum depth of modulation which will produce gain vs a' . We see that for a' equal to unity which represents a very thin beam there is no threshold value—whereas for a' equal to one-half which represents a beam of infinite cross section the threshold modulation is near unity.

lation). Of course, the way in which these waves are excited as determined by an examination of the boundary condition will depend upon the sign of a' . In Section III this will be illustrated by considering the boundary conditions for a beam which is modulated with a fast wave at the pump frequency which travels at the same velocity as the fast signal wave—($a' = +1$).

III. BOUNDARY CONDITIONS

At the input ($z = 0$) we can impress an ac current and velocity with an arbitrary amplitude and arbitrary phase. The phase of the signal with respect to the pump frequency modulation is a new and critical factor.

We can write at $z=0$,

$$\begin{aligned} v_1 + v_2 + v_3 + v_4 &= v_{in}, \\ v_1^* + v_2^* + v_3^* + v_4^* &= v_{in}^*, \\ i_1 + i_2 + i_3 + i_4 &= i_{in}, \\ i_1^* + i_2^* + i_3^* + i_4^* &= i_{in}, \end{aligned} \tag{29}$$

where again v_1 is the gaining wave, v_2 is the attenuated wave, v_3 is the ordinary slow wave, and v_4 is the new wave with the very fast velocity.

For the case of fast wave modulation or $a' = +1$ we use (19), (20), (24), and (25) and write (29) in terms of the four velocity components as follows

$$\begin{aligned} v_1 + v_2 + v_3 + v_4 &= v_{in} \\ j \frac{3|m|}{2} (v_1 - v_2) - 8v_4 &= v_{in}^* \\ -(v_1 + v_2) & \\ + j \frac{|m|}{2} (v_1 - v_2) + v_3 - \frac{1}{3} v_4 &= \frac{\omega_q}{\omega} \frac{u_0}{I_0} i_{in} \\ -j \frac{3|m|}{4} (v_1 - v_2) - 8v_4 &= \frac{\omega_q}{\omega} \frac{u_0}{I_0} i_{in}^*. \end{aligned} \tag{30}$$

Eq. (30) can now be solved to give

$$v_1 + v_2 = \frac{1}{2} \left(v_{in} - \frac{\omega_q}{\omega} \frac{u_0}{I_0} i_{in} \right) + \frac{m}{8} v_{in}^* \tag{31}$$

$$v_1 - v_2 = j \frac{m}{2|m|} \left(\frac{\omega_q}{\omega} \frac{u_0}{I_0} i_{in}^* - v_{in}^* \right) \tag{32}$$

$$\begin{aligned} v_3 &= \frac{1}{2} \left(v_{in} + \frac{\omega_q}{\omega} \frac{u_0}{I_0} i_{in} \right) \\ &+ \frac{m}{32} \left(3 \frac{\omega_q}{\omega} \frac{u_0}{I_0} i_{in}^* - v_{in}^* \right) \end{aligned} \tag{33}$$

$$v_4 = - \frac{3m}{32} \left(v_{in}^* + \frac{\omega_q}{\omega} \frac{u_0}{I_0} i_{in}^* \right). \tag{34}$$

Now we can consider two different input conditions at the signal frequency—either the fast wave or the slow wave. With the fast wave as an input we have the relation from (13).

$$v_{in} = - \frac{\omega_q}{\omega} \frac{u_0}{I_0} i_{in} \tag{35}$$

and

$$v_{in}^* = v_{in} \text{ and } i_{in}^* = i_{in}.$$

From (31)–(35) inclusive, we have

$$\begin{aligned} v_1 &= \frac{1}{2} (1 + j e^{i\phi}) v_{in} \\ v_2 &= \frac{1}{2} (1 - j e^{i\phi}) v_{in} \end{aligned} \tag{36}$$

where $m = |m| e^{i\phi}$. We can see that either the amplified wave or the attenuated wave can be set up depending on the phase of the pump. The critical phase required between the pump and signal frequencies would, of course, hinder the operation of a practical amplifier. This can be avoided by using a pump frequency which is not quite equal to twice the signal frequency. In this case, a third frequency is generated within the beam which is equal to the difference between the pump and signal frequencies. In this more general three-frequency type of operation the amplified and attenuated waves are set up equal in amplitude and the phase of the pump frequency is not important.

Returning to (36), we have for the condition $\phi = 3\pi/2$

$$v_1 = v_{in} \tag{37}$$

and from (17) and (18) we can write

$$v_{out} = v_{in} \exp \frac{3|m|}{4} \omega_q L - j \beta_e \left(1 - \frac{\omega_q}{\omega} \right) L + j \omega l,$$

$$\text{GAIN} = \left(\frac{v_{out}}{v_{in}} \right)^2 = 8.68 \frac{3|m|}{4} \beta_e L = 41 N_q \text{ db}, \tag{38}$$

where N_q is the number of plasma wavelengths along the beam of length L . Eq. (38) represents the maximum amount of gain; in an actual case the gain will be somewhat reduced since the velocity of the fast wave at the pump frequency is not in general equal to the velocity of the fast wave at the signal frequency.

With the slow wave as the input we have the relation from (13)

$$v_{in} = \frac{\omega_q}{\omega} \frac{u_0}{I_0} i_{in},$$

and therefore:

$$v_1 + v_2 = \frac{m}{8} v_{in},$$

$$v_1 - v_2 = 0,$$

$$v_3 = v_{in},$$

$$v_4 = - \frac{3|m|}{16} v_{in}, \tag{39}$$

which gives

$$v_1 = \frac{|m|}{16} v_{in}. \tag{40}$$

If we compare (40) with (37) we see that the ratio of the growing wave excited by the fast signal wave to that excited by the slow signal wave is greater than 23 db. Thus, we conclude that we can amplify the fast wave at the signal frequency alone for the slow wave will excite a growing wave of negligible amplitude. This is accomplished by properly modulating the beam again in the form of a fast wave at the pump frequency.

IV. PARAMETRIC BEAM COUPLED TO A SLOW WAVE CIRCUIT

We shall use a model in which a lossless transmission line is capacitively coupled to the electron beam. Let L_1 and C_1 be the inductance and capacitance per unit length of the transmission line, respectively, and let V_c and I_c be the voltage and current of the line, and i , the current in the electron beam. Then¹³

$$\left. \begin{aligned} \frac{\partial V_c}{\partial z} &= -L_1 \frac{\partial I_c}{\partial t} \\ \frac{\partial I_c}{\partial z} &= -C_1 \frac{\partial V_c}{\partial t} - \frac{\partial i}{\partial z} \end{aligned} \right\} \quad (41)$$

Let

$K = \sqrt{\frac{L_1}{C_1}}$ characteristic impedance of the line in the absence of the beam and,

$\Gamma_1 = \sqrt{L_1 C_1}$ = line propagation constant in beam absence.

If we write (41) in terms of the circuit voltage and stream current it becomes

$$\frac{\partial^2 V_c}{\partial z^2} - \frac{\Gamma_1^2}{\omega^2} \frac{\partial^2 V_c}{\partial t^2} - K\Gamma_1 \frac{\partial^2 i}{\partial z \partial t} = 0. \quad (42)$$

This is the equation which describes the coupling of the beam to the circuit. The equation of motion (10) must be modified for in addition to the space charge fields the circuit fields act on the beam and we can write as is done for the voltage, V_B ,¹³ which acts on the beam

$$V_B = V_c + V_{sc} \quad (43)$$

where V_{sc} is due to the space charge fields and is given by (9). With this (10) becomes

$$\frac{\partial^2 v}{\partial t^2} + \frac{\partial^2}{\partial z \partial t} \left(\frac{v^2}{2} \right) - \frac{u_0}{I_0} \omega_q^2 i = \eta \frac{\partial^2 V_c}{\partial z \partial t} \quad (44)$$

The equation of continuity (11) remains unchanged with the new coupling. We must now introduce normalizing parameters which allow us to simplify the problem.

We define

$$C^3 = K \frac{I_0}{4V_0} \quad (45)$$

which is familiar in the twt theory. Here however we must be careful to note that K is the circuit impedance at the signal frequency.

The space charge parameter at the signal frequency which has been denoted by $\sqrt{4QC}$ we will denote by a_0 ; i.e.,

$$\frac{\omega_{q1}}{\omega} = C\sqrt{4QC} = a_0 C. \quad (46)$$

We see immediately that the plasma frequency at the pump is given by

$$\frac{\omega_{q2}}{2\omega} = a' a_0 C. \quad (47)$$

Here again, as in the previous discussion, a' can range from $+1$ to $\frac{1}{2}$ if we modulate the beam at the pump frequency in the form of a fast wave and -1 to $-\frac{1}{2}$ if we modulate in the form of a slow wave.

We need the parameter which relates the circuit velocity to the beam velocity and we can use b as is conventional. Thus

$$\Gamma_1 = \frac{\omega}{v} = \frac{\omega}{u_0} (1 + Cb). \quad (48)$$

Here again if b is negative the circuit velocity is greater than u_0 and if b is positive the circuit velocity is less than the beam velocity.

We now assume

$$V_c = \frac{1}{2} V_{c1}(z) \exp \left[-j\beta_e \left(1 - a' \frac{\omega_q}{\omega} \right) z + j\omega t \right] + cc \quad (49)$$

and take the currents and velocity in the form of (17) and (18). Substituting for V_c and i in the circuit equation (42) and expanding in powers of C we have for the signal frequency term

$$\frac{dV_{c1}}{dz} + j\beta_e C (b + a' a_0) V_{c1} = j\beta_e C \frac{K}{2} i_1. \quad (50)$$

Similarly the equation of motion (44) becomes

$$\frac{dv_1}{dz} + ja'\beta_q v_1 + ja'\beta_q \frac{m}{2} v_1^* + j \frac{\beta_q^2}{\beta_e} \frac{u_0}{I_0} i_1 = \frac{\beta_e}{2} \frac{u_0}{V_0} V_{c1} \quad (51)$$

and the equation of continuity remains (20).

Eqs. (50), (51), and (20) together with their complex conjugates, constitute a set of six equations in v_1 , v_1^* , i_1 , i_1^* , and V_{c1} , V_{c1}^* . After decoupling we can look for solutions of the form

$$V_{c1} = V_{01} \exp [C\beta_e \{\delta' - ja'a_0\}z] \quad (52)$$

where $\delta' = x' + jy'$.

We are forced to use the prime notation since it is not possible to use the same numbering of the roots as is used in the twt equations. With this background we can now find the secular equation for δ' , from the set of six equations represented by (50), (51), and (20) as follows

$$\begin{aligned} &(\delta' - ja'a_0)^6 + [2a_0^2(1 + a'^2\theta) + (b + a_0a')^2](\delta' - ja'a_0)^4 \\ &+ \{2(b + 5a'a_0) + 2a_0^2[(b + a_0a')^2 - 4a_0^2a'^2] \\ &+ \theta[a_0^4(1 + 6a'^2) - 4a_0a' + 2a_0^2a'^2(b + a'a_0)^2 \\ &\quad + a_0^4a'^4\theta^2\}(\delta' - ja'a_0)^2 \\ &+ \{1 + (b + a'a_0)a_0^2\} \{-8a_0^2a'^2(b + a_0a') \\ &+ \theta[1 + a_0^2(b + a_0a')(1 + 6a'^2)]\} \\ &+ \theta^2 a'^4 a_0^4 (b + a'a_0)^2 = 0 \end{aligned} \quad (53)$$

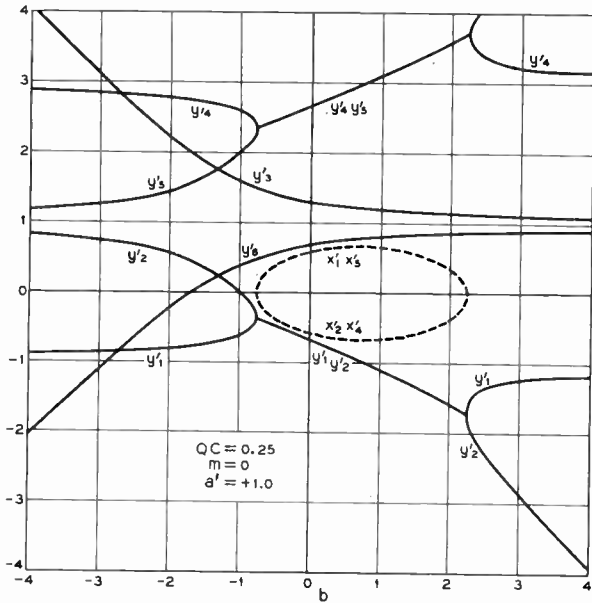


Fig. 6—The propagation constants for the two-frequency parametric beam which is coupled to a slow wave circuit. In this case waves propagate as

$$\exp[-j\beta_0 z + \beta_0 C(x' + jy')z + j\omega t].$$

This is the case for a thin beam with moderate space charge and no modulation. It is presented so as to clearly bring out the feature wherein the three new waves which appear are mirror images of the familiar twt waves about the value of y which represents the pump velocity—i.e., in this case the mirroring occurs about the line $y = +1$.

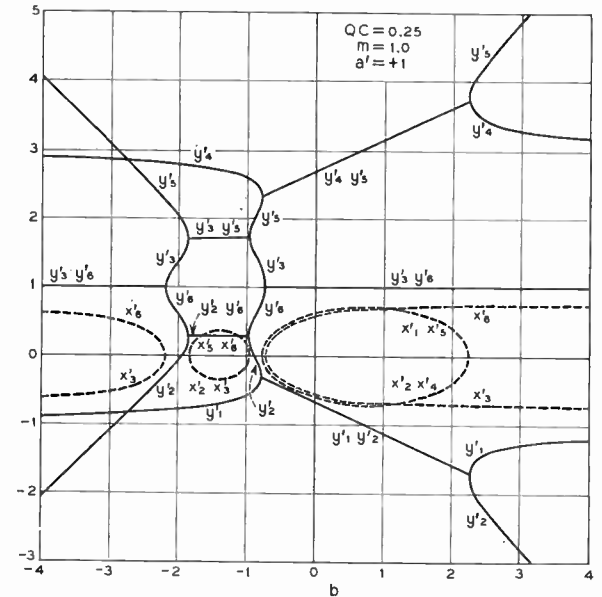


Fig. 8—The propagation constants for a two-frequency beam which is coupled to a slow wave circuit. In this case of moderate space charge the velocity of the modulating wave at the pump frequency is taken equal to the velocity of the space charge waves at the signal frequency. The beam is fully modulated by the pump and we note that the maximum value of x for the fast wave gain ($b = -1.4$) is slightly less than the largest value of x for the slow wave gain $b = +\frac{1}{2}$.

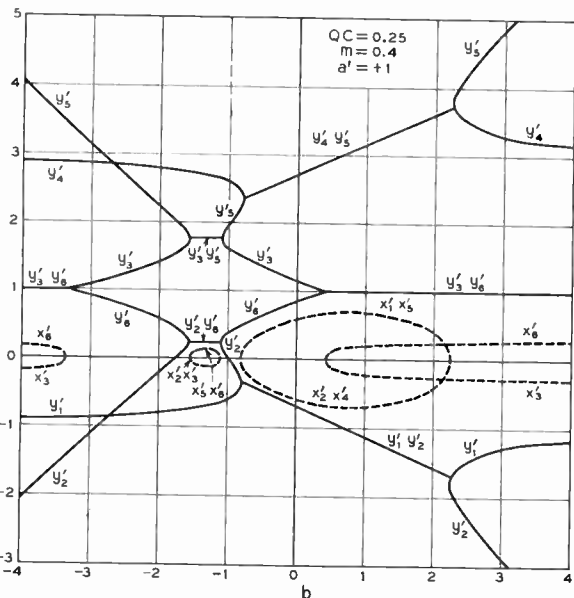


Fig. 7—The propagation constants for a two-frequency parametric beam which is coupled to a slow wave circuit. In Figs. 7 through 14 the pumping modulation is assumed to be in the form of the fast wave ($a' > 0$). For large values of b which indicates that the beam is decoupled from the circuit we get values of x_3' and x_4' identical with those of the single beam as in Fig. 3. As b becomes smaller these roots are suppressed except in the vicinity of $b = \pm 1$ where islands of gain appear. At $b = +1$ the velocity of the slow space charge wave is equal to the circuit wave and we obtain values of x_1' and x_2' which do not differ from those of Fig. 6 with no modulation. At $b = -1$ the velocity of the fast space charge wave is equal to the circuit wave and nearby we find another island of gain which is dependent upon the depth of modulation.

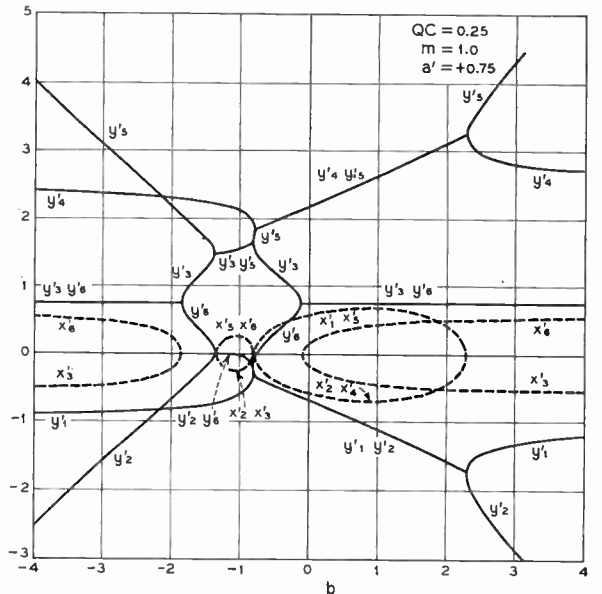


Fig. 9—The propagation constants in this case are similar to Fig. 8. Here the velocity of the wave on the beam at the pumping frequency is not equal to the velocity of the space charge waves at the signal frequency. This would represent a beam with γb near 1.

where

$$\theta = 1 - \frac{|m|^2}{4}$$

The roots of this equation are plotted in Figs. 6 through 16 (pp. 714–716). We see in these figures the solutions of the single beam alone appear as the circuit is decoupled from the beam by making b large. The effect

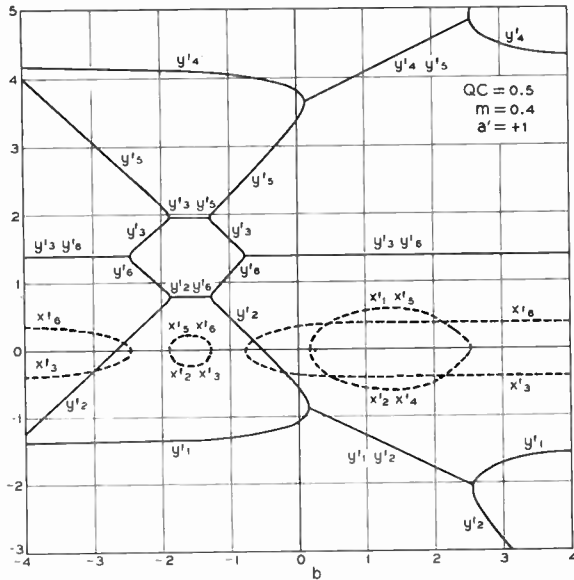


Fig. 10—The propagation constants for this case should be compared to those of Fig. 7. The increased values of space charge, or QC , results in a larger maximum value of x near the fast wave intersection.

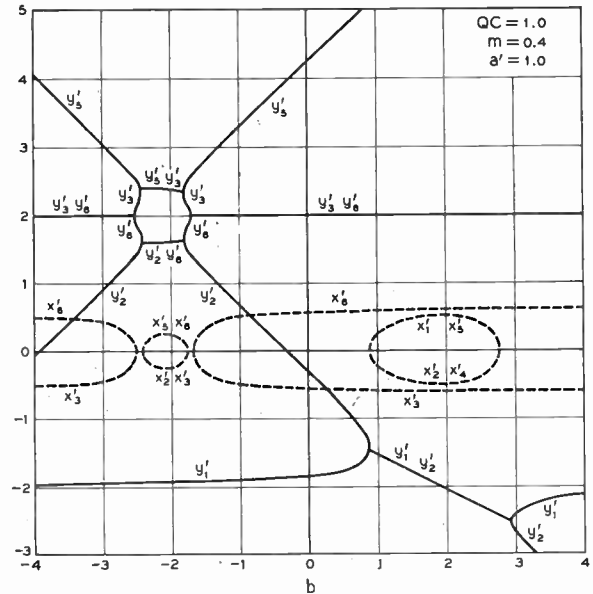


Fig. 12—The propagation constants for a thin beam with a large value of space charge and a moderate value of modulation. The character of the roots is similar to those in the previous figures.

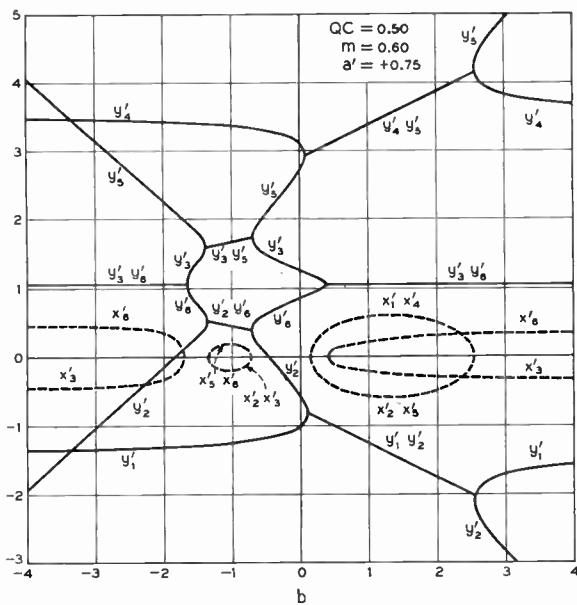


Fig. 11—The propagation constants for a case where the velocity of the waves at the pump frequency and signal frequency are not equal. Note the asymmetry of the roots about the point where the island of gain for the fast wave occurs.

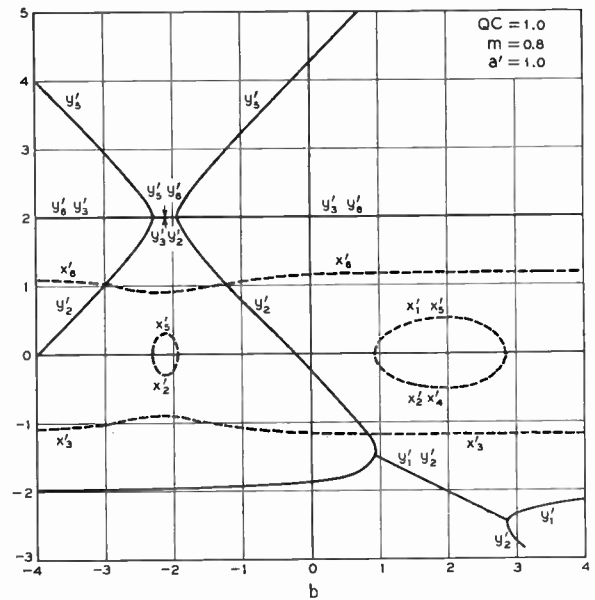


Fig. 13—Here we have the propagation constants for a thin beam with large space charge and heavy modulation at the pump frequency. The character of the roots is quite different for the gaining waves of the beam alone are so strong that coupling to the circuit does not suppress them. The islands of gain near the point where the circuit wave intersects the fast space charge wave and the slow space charge wave still appear.

of the double frequency modulation is to split the three normal waves—*i.e.*, circuit wave, slow space charge wave, and fast space charge wave—into two parts and we see that the three new waves are obtained as mirror images of the three original waves about the velocity of the pumping wave. In the single stream case the character of the roots was independent of the sign of a' whereas in the present case the sign of a' influences the roots. When the fast wave ($a' < 0$) at the pump frequency is used to modulate the beam, the real part of the roots for the beam alone are suppressed as the circuit velocity

approaches the beam velocity. The islands of complex roots occur at the signal frequency in the vicinity of the crossing of the fast space charge wave with the circuit wave and again where the slow wave crosses the circuit velocity. When the pumping modulation is in the form of the slow wave ($a' > 0$) we see that the real part of the roots for the beam alone can either be enhanced by the circuit coupling as in Fig. 15 or suppressed as in Fig. 16. It depends to a large extent on the value of a' or the

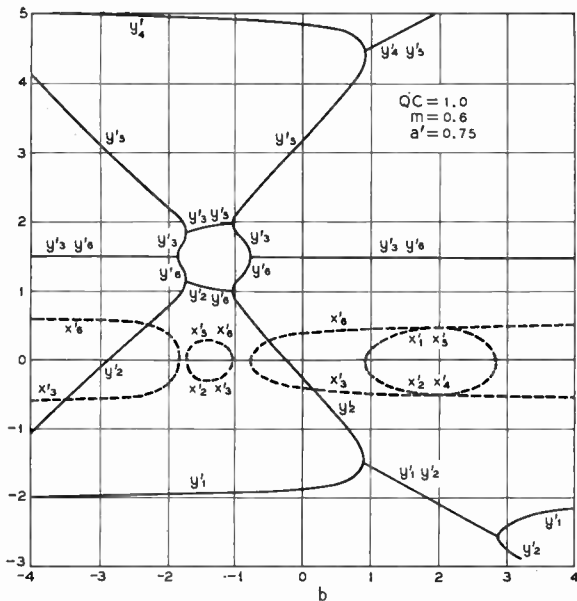


Fig. 14—The propagation constants for a case of large space charge and unequal velocities between the modulating wave and signal wave. The character of the roots is not greatly different from Fig. 12 where the two velocities are equal.

relative velocity of the pump wave as compared to the signal space charge wave and the depth of modulation.

V. CONCLUSION

It has been found that the normal space charge waves found in a drifting electron beam will convert to exponentially growing waves provided that one modulates the beam with a pumping frequency equal to twice the signal frequency. It is important to note that either the fast space charge wave or the slow space charge wave can be made to grow quite independently of each other. These new waves are of the parametric type and analogous to the growing exponential waves which are found on a transmission line whose distributed reactance is varied with a traveling wave at the pump frequency. The character of the growing waves on the electron beam are such that optimum growth occurs when the velocity of the pumping wave and the signal wave are equal. As the velocities become unequal a greater depth of modulation is required before the onset of exponential gain. These factors dictate the use of a thin beam not unlike the beams presently used in present klystrons and twt's.

A premodulated beam of this type can also be coupled to a circuit such as a helix whose phase velocity is reduced below that of free space. In this case we find six waves rather than three as in the normal twt. The nature of the roots depends on the form of the pumping modulation but in general there is more than one growing wave which occurs in the vicinity of the point where the fast space charge wave becomes equal to the circuit wave, and secondly, where the slow space charge wave is equal to the circuit wave.

The significance of this type of gain lies in the fact

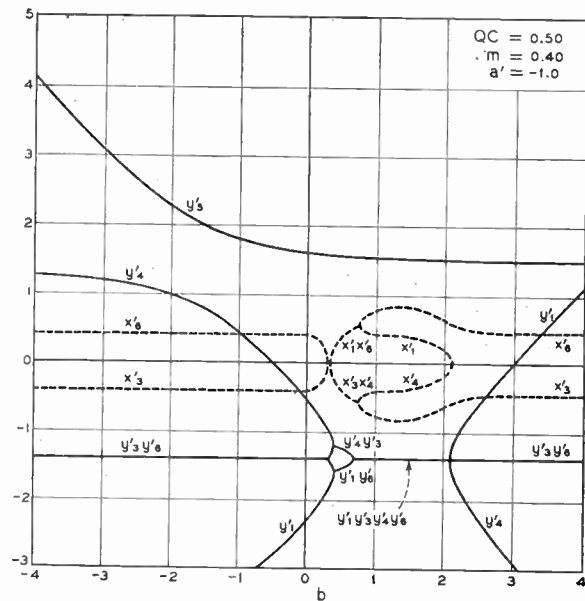


Fig. 15—The propagation constants for a case where the modulation is in the form of a slow wave ($a' < 0$) the gain in the region of the circuit wave equal to the slow space charge wave is enhanced. In the vicinity of the circuit wave velocity equal to the fast wave the roots seem to be very little affected by the presence of the circuit.

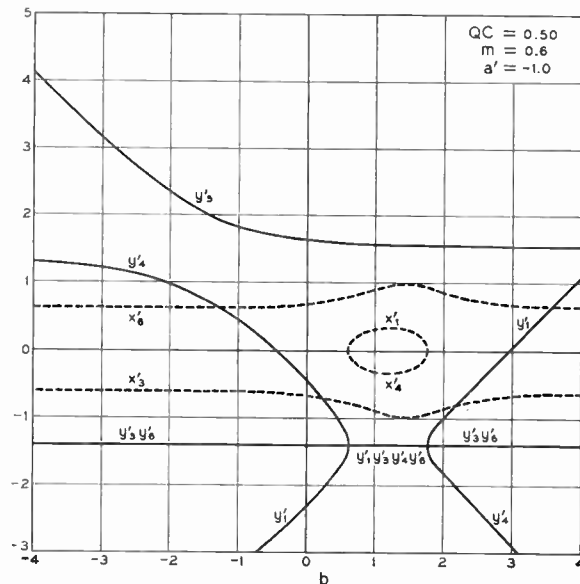


Fig. 16—A second case for the modulation wave in the form of a slow wave. The two complex roots for the uncoupled beam are not suppressed at all in this case. The roots are somewhat enhanced near the slow wave interaction point.

that the energy required for building up the signal waves comes from the pumping oscillator and not the dc beam. This allows for amplification of the fast space charge waves. Previous microwave amplifiers have amplified only the slow wave and the theorems which describe the minimum noise figure of such tubes are based directly on this fact. However, these theorems are not valid for a "fast" wave amplifier and in principle this form should prove to be less noisy than the slow wave amplifier.

A Gallium Arsenide Microwave Diode*

D. A. JENNY†, MEMBER, IRE

Summary—The semiconductor properties of gallium arsenide, particularly the high electron mobility and forbidden band gap, besides favorable point contact rectification characteristics, are of interest for microwave diode applications. The device feasibility evaluation described in this paper indicates that, both theoretically and experimentally, gallium arsenide is potentially superior to germanium and silicon in point contact diodes. Besides an improvement in mixer conversion loss, gallium arsenide diodes promise to be operable at appreciably higher temperatures than germanium and silicon units. The noise temperature values for the three materials are comparable. There are indications that gallium arsenide can be used advantageously in fast switching diodes.

INTRODUCTION

SILICON and germanium have been used extensively as semiconductor materials in point contact microwave diodes during and since World War II. Gallium arsenide is one of the new compound semiconductors of the III-V type, whose properties, compared with those of germanium and silicon, are most promising for microwave mixer applications. In addition to higher operating temperatures, a reduction in conversion loss can be expected from this material. These improvements are a consequence of the high forbidden energy gap of 1.35 eV, the high electron mobility of over 4500 cm²/volt/sec and the relatively low dielectric constant of about 11. The potential advantages of gallium arsenide led to this device feasibility investigation.

An exact theory of the high-frequency behavior of semiconductor point contact or small area mixers has not yet been developed. However, a linear approximation based on a simple passive equivalent network was used by Torrey and Whitmer¹ to analyze the conversion loss of point contact semiconductor diodes. This method was also used by Messenger and McCoy² in a comparison of silicon and germanium for microwave mixers. The noise of these diodes is so dependent upon such imponderables as processing, surface conditions, and contact homogeneity that one must resort to empirical methods for an evaluation of the various factors involved.

For the purpose of the following discussion, it is assumed that point contact rectifiers are essentially small-area metal-semiconductor contacts according to the well-known model introduced by Schottky.

* Original manuscript received by the IRE, October 23, 1957; revised manuscript received, December 20, 1957.

† RCA Laboratories, Princeton, N. J.

¹ H. C. Torrey and C. A. Whitmer, "Crystal Rectifiers," McGraw-Hill Book Co., Inc., New York, N. Y.; 1948.

² G. C. Messenger and C. T. McCoy, "Theory and operation of crystal diodes as mixers," Proc. IRE, vol. 45, pp. 1269-1283; September, 1957.

POINT CONTACT RECTIFIER CHARACTERISTICS AND FUNDAMENTAL PROPERTIES OF GALLIUM ARSENIDE

Gallium arsenide research has progressed to the point where a meaningful device feasibility evaluation on a comparative basis with germanium and silicon can be made for certain device applications. For this purpose, the pertinent semiconductor properties of gallium arsenide and the material dependent point contact rectifier characteristics are discussed briefly.

Experience has shown that *p*-type and *n*-type specimens of a particular semiconductor material behave very differently with respect to their point contact rectification characteristics. For instance, *p*-type silicon and *n*-type germanium readily yield point contact rectifiers which are relatively resistant to burn out and have high rectification ratios. On the other hand, *n*-type silicon and *p*-type germanium are very sensitive to burn-out and exhibit lower point contact rectification ratios. For this reason the preferred conductivity types for point contact devices are *p* type for silicon and *n* type for germanium. Gallium arsenide behaves similarly to germanium, namely *n*-type material exhibits far superior point contact rectification ratios and burn-out resistance than *p*-type material. Therefore, in a comparative evaluation of point-contact diodes, the properties of *p*-type silicon and *n*-type germanium on one hand must be compared with those of *n*-type gallium arsenide. As is well known, *p*-type silicon and *n*-type germanium are the preferred semiconductor materials in commercial point-contact diodes. The burn-out mechanism is still rather obscure and one is dependent on purely empirical observations for a comparison.

As will be shown in the Appendix, an optimum majority carrier concentration for a given operating temperature can be found for a specific semiconductor material to be used in microwave diodes. The optimum majority carrier concentrations are about 10¹⁸ cm⁻³ for germanium, about 5×10¹⁸ cm⁻³ for silicon, and about 2×10¹⁷ for gallium arsenide. A realistic comparison between different semiconductors must, therefore, be based on the properties of material with the respective optimum carrier concentration. This concerns particularly the majority carrier mobility which is carrier concentration dependent. The dielectric constant of the semiconductor enters into the barrier capacitance and should, therefore, be relatively low for good high-frequency performance.

The upper operating temperature limit of metal-semiconductor rectifiers, in contrast to *p-n* junction rectifiers, is not determined simply by the forbidden

energy band gap, but rather by the interface barrier height. Therefore, for a comparison of materials, it is necessary to use empirically obtained values of barrier height instead of the band gap. Table I gives several

TABLE I
SELECTED PROPERTIES OF GERMANIUM, SILICON,
AND GALLIUM ARSENIDE

Material	Barrier Height (ev)	Dielectric Constant	Majority Carriers	
			Optimum Concentration (cm^{-3})	Optimum Mobility ($\text{cm}^2/\text{volt}/\text{sec}$)
Ge (<i>n</i> type)	0.3 to 0.4	16	10^{18}	1500
Si (<i>p</i> type)	0.3 to 0.4	11	5×10^{18}	150
GaAs (<i>n</i> type)	0.6 to 0.8	11	2×10^{17}	4500

properties of the three semiconductor materials under investigation. The high metal-semiconductor interface barrier, the low dielectric constant, and the high electron mobility of gallium arsenide, as compared to germanium and silicon, make this the most promising semiconductor material for microwave diodes and other point contact devices.

EXPERIMENTAL RESULTS

Laboratory samples of gallium arsenide point contact diodes were prepared to check the predictions of the preceding section. For purposes of comparison, noise temperature measurements, comparative burn-out checks, and conversion loss determinations were made with germanium and silicon diodes similar to the gallium arsenide units. Technological problems, such as the choice of the point contact whisker material, surface treatment, and forming procedure were solved by an empirical approach to attain best performance.

Gallium arsenide is somewhat more brittle than silicon and germanium, so that tungsten whiskers under the necessary pressure caused crushing of the contact area. This manifested itself in high noise temperatures and electrical instabilities. Hardened beryllium copper and phosphor bronze gave more satisfactory results. The sharp point, necessary for small contact areas, was produced by electroforming. Various etching solutions, purely chemical as well as electrolytic, were investigated as surface treatments. However, sand blasting with very fine aluminum oxide powder before the application of the point contact yielded the best results. This may be partially due to a high surface recombination velocity which reduced minority carrier storage effects, although no evidence of minority carrier injection was found. Forming of the point contact was accomplished by repeated 60-cps current pulses or occasionally by dc pulses. The duration of the pulses was of the order of a second, or less, at various amplitudes until the most favorable dc rectification characteristic was attained.

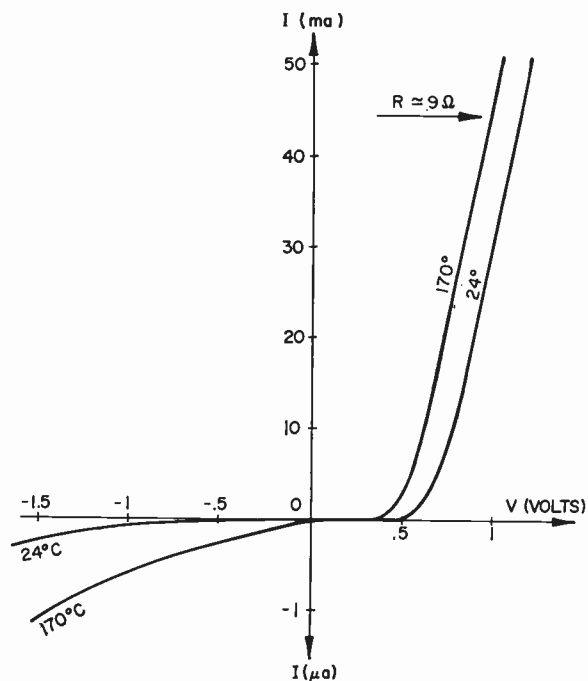


Fig. 1—Current-voltage characteristics of a gallium arsenide diode.

The criterion for this condition was derived from correlation of empirical results. Emphasis was necessarily placed on obtaining a steep forward current slope, indicating a low series or spreading resistance, without undue increase of the barrier capacitance. The reverse current and breakdown have to be kept within certain limits to maintain a minimum required rectification ratio. The units were mounted in the standard ceramic cartridges used for commercial microwave diodes, such as the 1N21. The gallium arsenide pellets were cut from single crystal material with an electron concentration of about 10^{17} cm^{-3} at room temperature and soft soldered to the brass support plug. Before soldering, a thin layer of copper was electrolytically deposited on the area of the gallium arsenide pellet to be soldered in order to insure a good mechanical joint as well as an ohmic contact.

Since this was a feasibility investigation to establish the attainable characteristics of gallium arsenide in comparison with germanium and silicon as a diode material, only the best results are reported. The following data represent the most favorable performance of gallium arsenide point contact diodes attained in the laboratory to date. Some improvement can be expected in the course of further development.

The dc current-voltage characteristics at room temperature and at 170°C are shown in Fig. 1. The upper temperature limit was imposed by the melting point of the solder rather than by an excessive reverse current. Recent work on high temperature devices with gallium arsenide indicates that much higher operating temperatures can ultimately be expected. The lower operating

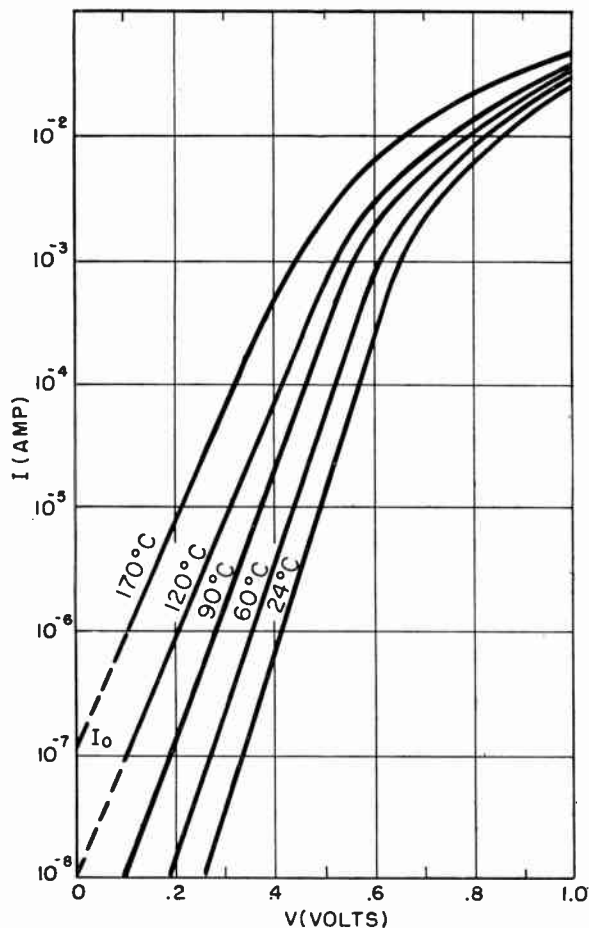


Fig. 2—Forward log I vs V of a gallium arsenide diode at different temperatures.

temperature limit is probably below -200°C as estimated from low temperature Hall and resistivity measurements. The spreading resistance as derived from the slope of the linear portion of the forward current is about 9 ohms. Somewhat lower spreading resistances have been observed. The semilogarithmic plot of the forward current vs forward voltage, shown in Fig. 2, allows the determination of the voltage factor λ in the exponent of the rectification equation $I = I_0(e^{\lambda V} - 1)$. The experimental value is 27 v^{-1} at room temperature, as compared with the theoretical 39 v^{-1} . Discrepancies of this type are regularly observed in silicon, and often in germanium, and a number of explanations have been proposed in the literature.³ The height E of the interface barrier can be determined from a $\log I_0$ vs $1/T$ plot, where I_0 is the extrapolated value of the linear portion of Fig. 2 to zero volts, according to the relation $I_0 = \text{const } e^{E/kT}$. This plot is shown in Fig. 3 where the slope of the straight line gives a barrier height, E , of about 0.8 ev. This is an appreciably higher barrier than generally observed in germanium and silicon

³ M. Cutler and H. Bath, "Surface leakage current in silicon fused junction diodes," Proc. IRE, vol. 45, pp. 39-43; January, 1957.

C. T. Sah, R. N. Noyce, and W. Shockley, "Carrier generation and recombination in p - n junctions and p - n junction characteristics," Proc. IRE, vol. 45, pp. 1228-1243; September, 1957.

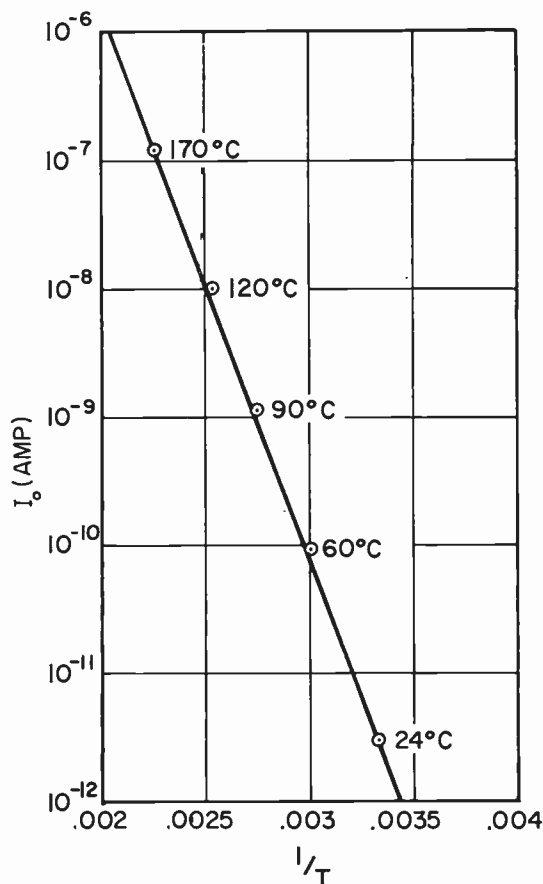


Fig. 3—Log I_0 vs $1/T$ of a gallium arsenide diode.

diodes. A direct manifestation of this is the low reverse current at elevated temperatures, as shown in Fig. 1, which in turn allows higher operating temperatures than with silicon and germanium.

Burn-out sensitivity was checked on a comparative basis by applying pulses of increasing amplitude simultaneously to commercial silicon and germanium diodes, as well as representative gallium arsenide diodes, until burn-out occurred. Several runs with different pulse durations were made. The gallium arsenide diodes were, in general, more resistant to burn out than 1N21, 1N23, or 1N263 types.

Minority carrier (holes) injection into the gallium arsenide could not be detected by several methods. This may be due either to extremely short hole lifetimes, which are too small to be detected with the equipment used, or to negligible hole injection. Whatever the reason, minority carrier storage effects should not interfere with operation except, perhaps, at very high frequencies. A few tests with gallium arsenide diodes in switching circuits tend to verify this conclusion, as the observed switching times were less than 10^{-9} seconds. These observations show also that gallium arsenide diodes of the type described are of interest for fast switching applications, particularly where high operating temperatures are anticipated, such as in compact computers and similar equipment.

Conversion loss and noise temperature measurements were made at 6000 mc. The measuring procedure was conventional. The results of comparative measurements with the best available silicon diodes of the 1N23B type and germanium diodes of the 1N263 type are shown in Table II. The characteristics for the gallium arsenide diode, presented in Table II, are the best over-all results among a number of laboratory samples.

TABLE II
MEASURED DIODE CHARACTERISTICS AT 6000 MC

Diode	Material	Conversion Loss (db)	Noise Temperature Ratio	IF Impedance (ohms)	Receiver Noise Factor (IF Noise Factor = 1.5 db)
Experimental Unit					
1N263	GaAs	4.8	1.25	420	6.97
1N23C	Ge	4.9	1.14	445	6.8
	Si	6	1.23	380	8.15

These diodes require a forward dc bias of a few tenths of a volt for optimum performance conditions. The noise temperature of 1.25 can be taken as an indication that gallium arsenide does not seem to present any unusual noise problems. Somewhat lower noise temperatures were observed in some diodes with higher conversion losses.

APPENDIX

A HIGH-FREQUENCY FIGURE OF MERIT FOR THE CONVERSION LOSS OF MICROWAVE DIODES

The following analysis is intended to give a semi-quantitative picture of the relation between the fundamental properties of the three semiconductors, germanium, silicon, and gallium arsenide, and the conversion loss of microwave diodes made from these materials.

Messenger and McCoy² carried out essentially the same analysis, though in less detail, to compare silicon and germanium for microwave mixer applications. More recent mobility values for silicon and germanium, used in the following, give better agreement between theory and experiment, thus lending further support to the usefulness of this simplified treatment. It must be borne in mind that several simplifying assumptions are made in this approach, such as a voltage-independent barrier capacitance and a voltage-independent forward resistance which, *a priori*, preclude a fully quantitative agreement with the experimental results. It is all the more surprising how well an agreement in optimum majority carrier concentration is obtained, so that the use of the theoretical results as a device design target is justified.

A point contact diode consists of the essential elements shown schematically in Fig. 4 and in the form of

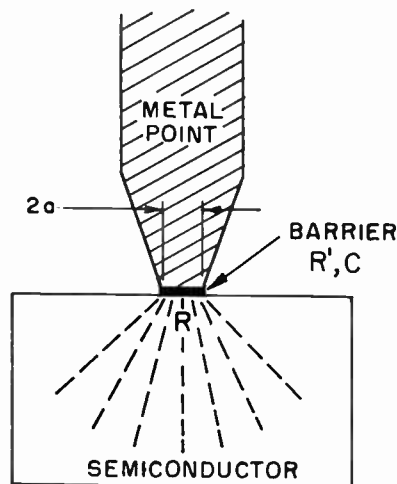


Fig. 4—Schematic of a small area metal-semiconductor contact.

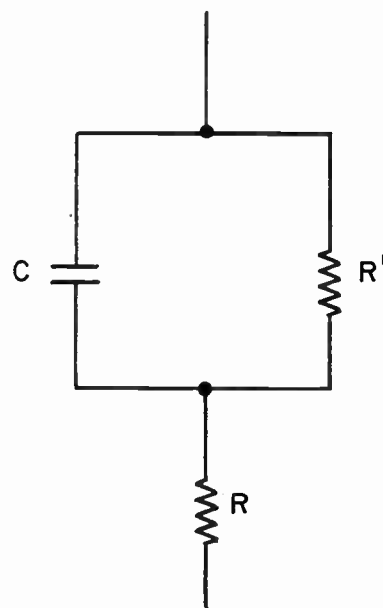


Fig. 5—Equivalent network of a small area metal-semiconductor contact.

an equivalent network in Fig. 5. The passive elements are the barrier resistance R' , the barrier capacitance C , and the spreading resistance R . For a circular contact area the latter can be expressed in terms of the contact radius a and the conductivity, $\sigma = en\mu$, of the semiconductor material.

$$R = \frac{1}{4a\sigma} = \frac{1}{4aen\mu} \tag{1}$$

where e is the electronic charge, μ the majority carrier mobility, and n the majority carrier concentration. The barrier resistance is a nonlinear function of the applied voltage and the barrier capacitance varies approximately as the square root of the voltage. However, the spreading resistance is essentially constant, if one neglects conductivity modulation in the forward direction. To apply the linear approximation used by Torrey and

Whitmer,¹ the voltage dependence of the barrier capacitance is neglected, and C is a constant. In the majority of practical mixer applications the oscillator amplitude is sufficiently high, so that the spreading resistance, R , dominates the barrier resistance, R' , in the forward direction, and the frequency, ω , is sufficiently high, so that $1/\omega C$ is much smaller than the barrier resistance R' in the reverse direction. With these two approximations, a dimensionless figure of merit for a microwave diode can be given as follows:

$$M = \frac{1}{\omega RC} \quad (2)$$

The only independent variable in a given semiconductor material, which can be adjusted at will, is the majority carrier concentration, n . This can be accomplished by appropriate doping with impurities. Therefore, it is necessary to express R and C in terms of n . The concentration dependence of R is not only as shown explicitly in (1), but an additional concentration term enters through the mobility. The actual charge carrier mobility is composed of two terms, namely the impurity scattering mobility μ_i and the lattice or thermal scattering mobility μ_t . The following first-order approximation is sufficiently accurate for this analysis:

$$\frac{1}{\mu} = \frac{1}{\mu_i} + \frac{1}{\mu_t}, \quad \text{or} \quad \mu = \frac{\mu_i \cdot \mu_t}{\mu_i + \mu_t} \quad (3)$$

The impurity mobility is given by the Conwell-Weisskopf⁴ equation

$$\mu_i = \frac{K_i \kappa^2 T^{3/2}}{m^{*1/2} n \log \left(1 + \frac{k_i \kappa^2 T^2}{n^{2/3}} \right)} \quad (4)$$

where m^* is the effective majority carrier mass, κ is the dielectric constant, T is the absolute temperature, and K_i and k_i are constants. The more accurate Brooks-Herring⁵ expression for μ_i coincides, for all practical purposes, with (4) in the carrier concentration range we are concerned with here. Therefore, the latter, analytically more convenient form, can be used. At low carrier concentrations the mobility is independent of n and follows the well known thermal or lattice scattering relation:

$$\mu_t = \frac{K_t S}{m^{*5/2} \kappa^{3/2}} \quad (5)$$

where K_t is a constant and S is a lattice scattering factor characteristic of the particular semiconductor material but independent of the impurity and/or carrier concentration. Without going into the details of the mecha-

nism determining the lattice scattering factor, it shall suffice to mention that S can be found with the help of available mobility data. Although the experimentally determined temperature dependence of μ_i and μ_t , in general, does not exactly follow the $T^{3/2}$ and $T^{-3/2}$ law, the deviations do not affect the qualitative result of this analysis.

The dependence of the barrier capacitance, C , on the carrier concentration, n , is obtained from the Schottky theory of metal-semiconductor contacts, where the bending of the energy bands near the interface assumes a parabolic form which follows from the solution of Poisson's equation. The width of the barrier and the dielectric constant, κ , enter into this solution, yielding

$$C \propto \sqrt{n\kappa} \quad (6)$$

Combining (1) through (6), an explicit relation between the figure of merit and the majority carrier concentration is obtained

$$M \propto \frac{\kappa^{1/2} \left(\frac{n}{T^3} \right)^{1/2}}{\frac{m^{*5/2}}{K_t \cdot S} + \frac{m^{*1/2}}{K_i \kappa^2} \cdot \ln \left[1 + \frac{k_i \kappa^2}{\left(\frac{n}{T^3} \right)^{2/3}} \right]} \quad (7)$$

It is not necessary to determine the proportionality factor in (7) to demonstrate certain temperature and carrier concentration effects, since M is a function of the variable n/T^3 . The numerical values of K_i , k_i , and K_t in (7) and the effective mass for silicon and germanium can be found from the literature.⁶ The constants are independent of the material used and are the same for gallium arsenide, silicon, and germanium. The effective mass of electrons, m^* , and the lattice scattering factor, S , for gallium arsenide can be obtained from the lattice scattering mobility of 7000 cm²/v per second, as estimated by Folberth and Weiss,⁷ and the measured mobility values at the carrier concentration of 2×10^{17} cm⁻³. The experimental mobility values are shown in Table I. Consequently, (7) becomes fully determined, except for the proportionality factor, and M can be plotted against n/T^3 , in arbitrary units, for n -type germanium, p -type silicon, and n -type gallium arsenide as shown in Fig. 6. The abscissa at the top gives the carrier concentration, n , at room temperature ($T = 300^\circ\text{K}$). The optimum room temperature carrier concentrations are, accordingly, 2×10^{17} cm⁻³ in gallium arsenide, 10^{18} cm⁻³ for germanium, and 5×10^{18} cm⁻³ for silicon as pre-

⁶ M. B. Prince, "Drift mobilities in semiconductors. I. Germanium," *Phys. Rev.*, vol. 92, pp. 681-687; November, 1953.

—, "Drift mobilities in semiconductors. II. Silicon," *Phys. Rev.*, vol. 93, pp. 1204-1206; March, 1954.

⁷ J. J. Morin and J. P. Maita, "Electrical properties of silicon containing arsenic and boron," *Phys. Rev.*, vol. 96, pp. 28-35; October, 1954.

⁸ O. G. Folberth and H. Weiss, "Herstellung und elektrische Eigenschaften von InP und GaAs," *Z. Naturf.*, vol. 10a, pp. 615-619; July, 1955.

⁴ E. Conwell and V. F. Weisskopf, "Theory of impurity scattering in semiconductors," *Phys. Rev.*, vol. 77, pp. 388-390; February, 1950.

⁵ H. Brooks, "Scattering by ionized impurities in semiconductors," *Phys. Rev.*, vol. 83, p. 879; August, 1951.

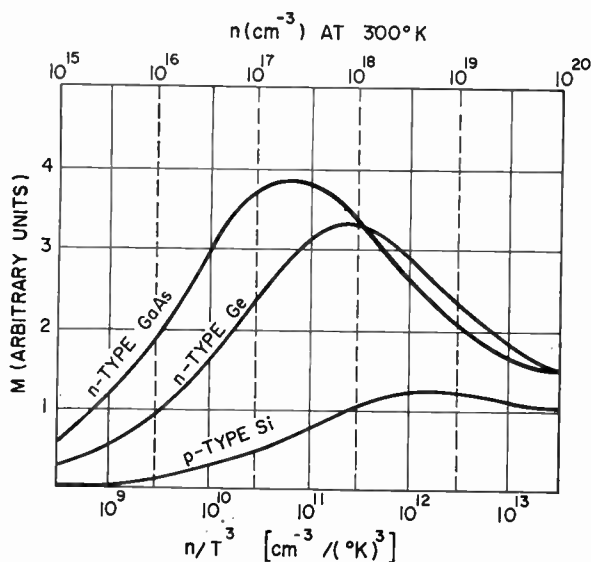


Fig. 6—Theoretical figure of merit for conversion loss M vs (n/T^3) for gallium arsenide, germanium, and silicon.

viously shown in Table I. The highest values of M are reached by gallium arsenide which indicates that this semiconductor material ought to yield lower conversion losses than germanium and silicon. It may be of interest to point out that gallium arsenide gives higher values of M in the n/T^3 range from about 2×10^{10} to about $3 \times 10^{11} \text{ cm}^{-3}(\text{°K})^{-3}$ than the maximum M for ger-

manium. This encompasses a temperature range, assuming constant n , of about 2.5:1 such as from 0°C to 400°C . The optimum electron concentration for this temperature range would, therefore, be $5 \times 10^{18} \text{ cm}^{-3}$. This example demonstrates how an optimum carrier concentration, introduced by proper doping, can be determined, for a certain temperature range and a certain semiconductor material, simply by making the values of M the same at the two temperature extremes.

Messenger and McCoy² found that M does not reach a maximum for silicon. This was due to the fact that they used a lattice scattering mobility for holes of $250 \text{ cm}^2/\text{volt}/\text{sec}$. More recent mobility data have, however, established a value of about $500 \text{ cm}^2/\text{volt}/\text{sec}$. The maximum shown in Fig. 6 is based on this value for the lattice scattering mobility. The experimental results of Messenger and McCoy, on the other hand, indicate a conversion loss minimum at a carrier concentration of about $5 \times 10^{18} \text{ cm}^{-3}$, which coincides exactly with the optimum n at room temperature for maximum M in silicon as shown in Fig. 6. Therefore, it is not necessary to resort to the onsetting degeneracy at high carrier concentrations as an explanation for their results.

ACKNOWLEDGMENT

The author wishes to gratefully acknowledge the contribution of F. Olesen who carried out the 6000-mc mixer measurements.

Some Applications of Ferrites to Microwave Switches, Phasers, and Isolators*

A. C. BROWN†, MEMBER, IRE, R. S. COLE†, AND W. N. HONEYMAN†

Summary—Two types of switch are described, one which is matched in both “on” and “off” positions, and the other is a very short, wide-frequency band, reactive switch suitable for switching at high repetition rates. A phaser is presented which is a reciprocal device and uses an unusual ferrite configuration. Although no particular isolator design has been included since this has been the subject of many previous articles, the effects of variations of temperature and dimensional parameters have been investigated and the results are presented here, together with some observations on scaling isolator designs into different frequency bands.

* Original manuscript received by the IRE, September 24, 1957; revised manuscript received, January 20, 1958.

† EMI Electronics Ltd., Middlesex, England.

INTRODUCTION

IN THE past decade a vast amount of research has been carried out on ferrites and their properties, thus opening an exciting new field of microwave components. The possibility of a one-way transmission system has now become a reality due to the non-reciprocal microwave properties of ferrites, while certain functions, for example phase or amplitude modulating, can now be performed electronically rather than mechanically. Many articles have been written describing these devices and, although those presented here perform the usual functions, such as switching and phasing,

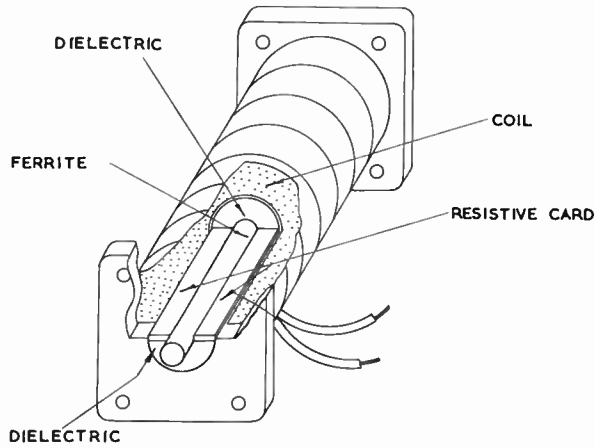


Fig. 1—Matched ferrite switch in upper X band.

they have certain novel features which make them of interest to the microwave engineer.

A MATCHED FERRITE SWITCH

The majority of ferrite switches which have been described¹ rely for their operation on a 90° rotation of the electric field vector which is then either reflected from a reactive mismatch or absorbed in a resistive card. Since they depend upon exactly 90° rotation for maximum attenuation, the variation of Faraday rotation with frequency in waveguide makes them narrow-banded. The switch, shown in Fig. 1, uses two pieces of resistive card which are placed alongside, instead of after, the ferrite. Using the configuration of Fig. 1, any rotation of the electric field vector over 90° results in absorption in the card as it rotates through 90°, giving rise to a broad-band matched switch. The performance of a switch, using a 2½ inch long, ¼ inch diameter rod of Ferramic R1 ferrite, is shown in Fig. 2(a) and 2(b), where two values of resistive card have been used. It can be seen that as the value of the resistive card is decreased, the switch becomes less sensitive due to the first insertion loss peak being suppressed.

The vswr of the switch is a function of the position of both the ferrite and the dielectric support of polytetrafluorethylene (ptfe) relative to the flange, and best positions were found by a method which effectively isolates one end of the switch. A tapered cylinder of iron loaded Araldite was used to absorb energy transmitted through the matching transition of the switch and the two parameters were then varied for the best match. The positions found were kept, but extra washers of ptfe were used to move the position of the iron Araldite load. The resulting points on a Smith chart formed a circle, the center of which gave the approximate vswr of the junction, its diameter being due to the mismatch of the load. This method of matching gave a vswr of less than 1.11 in both "on" and "off"

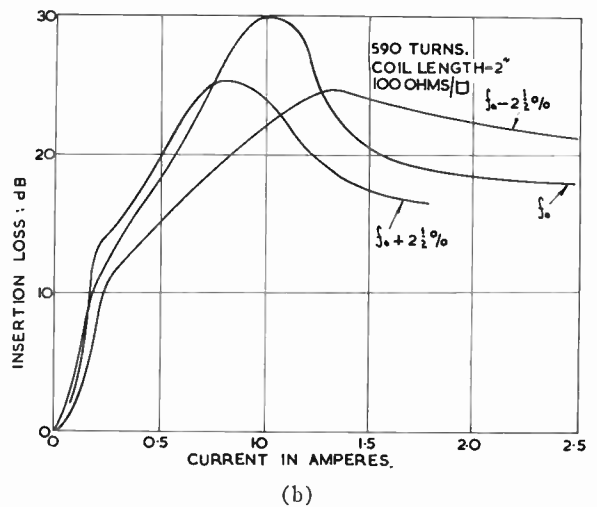
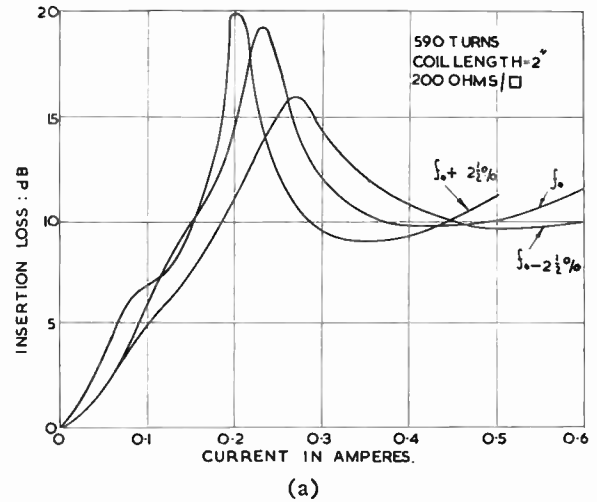


Fig. 2—Insertion loss—current characteristics of matched ferrite switch in upper X band.

positions over 5 per cent of upper X band, when butted directly onto waveguide 16 (0.900 inch \times 0.400 inch internal dimensions).

A BROAD-BAND REACTIVE FERRITE SWITCH

A reactive switch which rotates the plane of the electric field vector through 90° has been designed to have broad-band properties. It was pointed out above that a simple Faraday rotation device would be expected to be narrow banded. To overcome this, the Faraday rotation must be broad banded by means of dielectric slewing in the guide² or by making use of the anomalous effects which arise when a short length is combined with a large ferrite to waveguide diameter ratio. This has been carried out quite successfully in the device described here. It was found that the shorter the switch the larger the bandwidth obtained. For example, a switch 2½ inches long had a 2 per cent bandwidth greater than 20 db; 2 inches long, 5 per cent bandwidth; and

¹ J. N. Barry and W. W. M. Clarke, "Microwave modulator uses ferrite gyrator," *Electronics*, vol. 28, pp. 139-141; May, 1955.

² E. A. Ohm, "A broad-band microwave circulator," *IRE TRANS. ON MICROWAVE THEORY AND TECHNIQUES*, vol. 4, pp. 210-217; October, 1956.

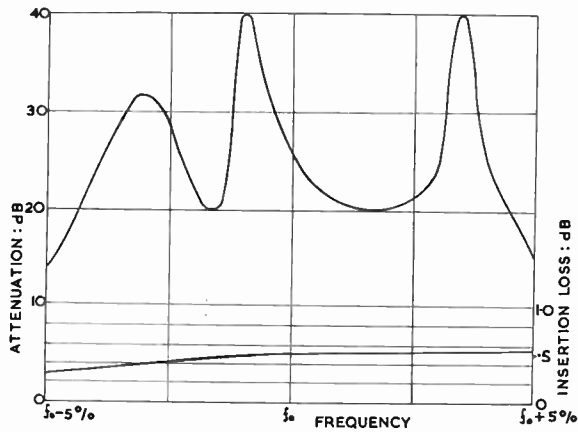


Fig. 3—Characteristic of reactive ferrite switch in upper X band.

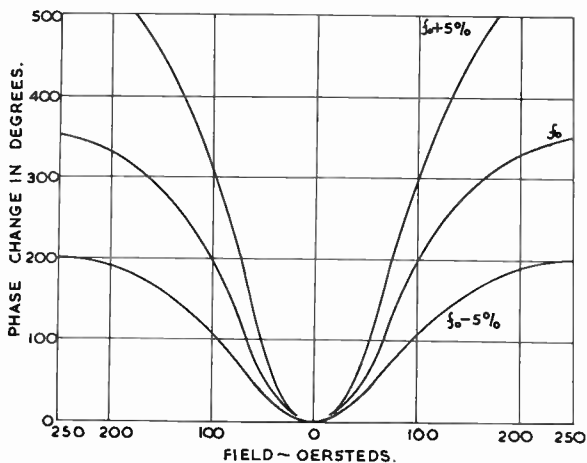


Fig. 4—Longitudinal magnetic field phaser characteristics.

$\frac{3}{4}$ inch long, 9 per cent bandwidth (Fig. 3). This large bandwidth is not yet fully understood but it would seem that the large peaks produced indicate anomalous reflections.

The switch $\frac{3}{4}$ inch long uses a $\frac{1}{4}$ -inch diameter rod of Ferramic R1 in $\frac{1}{2}$ -inch diameter pte filled waveguide. The matching technique and construction are similar to the matched switch already described but are without the resistive card. This switch was intended primarily for pulsing and had the waveguide constructed of Perspex (Lucite), the conducting wall being formed by evaporating a thin film of aluminum onto the inside surfaces of the Perspex.

The attenuation of this switch in its off position was better than 20 db and the insertion loss was less than 0.6 db over a 9 per cent frequency band at upper X band. Pulses of 0.4 μ sec long with rise times of 0.1 μ sec were applied and in all cases the microwave attenuation pulse appeared to follow the current pulse almost exactly.

Over a 1 per cent frequency band 30-db insertion loss could be achieved so two switches in series would provide the necessary receiver protection for a medium power radar. The advantage of ferrites over gas switches lies in the rapid recovery time and long life.

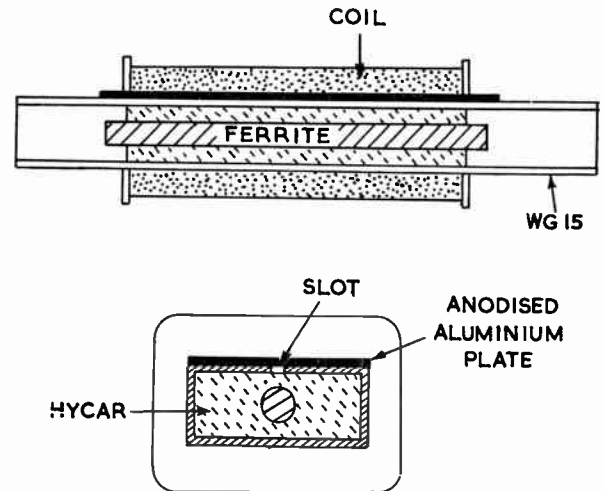


Fig. 5—2400-cps phaser.

A FERRITE PHASE SHIFTER

Several different types of microwave phase shifters based on the use of transversely magnetized slabs of ferrite either along the center or in a region of circular polarization in rectangular guide have been described in the literature.³ Phasers, employing a longitudinal magnetic field along a rod of ferrite in circular guide, preceded and followed by quarter-wave plates, have also been described.³

The phaser presented here employs a longitudinal magnetic field in rectangular waveguide using centrally disposed rods of ferrite supported in expanded acrylonitrile onazote (Hycar). It has been found that the variation of phase with frequency in this type of phaser is very much greater than the transverse field type where the ferrite is located near the side of the waveguide. For example, a transverse field phaser over 10 per cent of X band only gave a variation of $\pm 20^\circ$ at 200° phase change, whereas the variation using the longitudinal magnetic field was $\pm 100^\circ$ as shown in Fig. 4. However, this type of phaser has the advantage in some applications in that it is a reciprocal device and can be used in a two-way transmission path giving an equal phase shift in either direction of propagation. It can be seen from the characteristics (Fig. 4) that if a sinusoidal magnetic field is applied, any phase shift will occur at twice the applied frequency.

This device was required to sweep the phase by 180° over a 10 per cent frequency band at a modulation frequency of 2400 cps. This made it impossible to use normal waveguide because of eddy current losses in the waveguide walls. To overcome this difficulty, the waveguide was slotted along its length at the center of a broad face, but under these conditions the slot radiated power, probably due to field distortion. To prevent this, an anodized aluminum plate was placed over the slot

³ A. G. Fox, S. E. Miller, and M. T. Weiss, "Behavior and applications of ferrites in the microwave region," *Bell Sys. Tech. J.*, vol. 34, pp. 5-103; January, 1955.

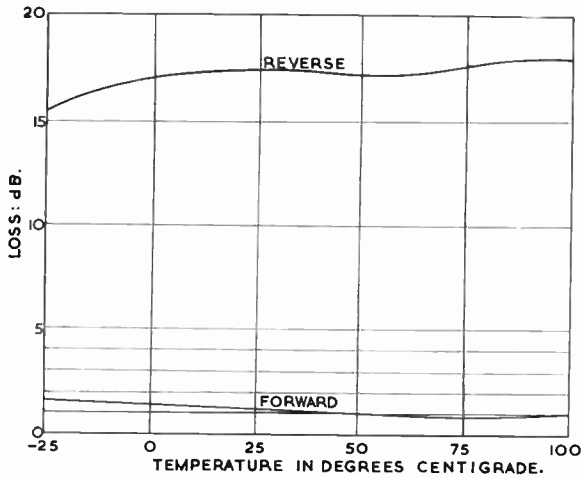


Fig. 6—Performance of R1 resonance isolator vs temperature.

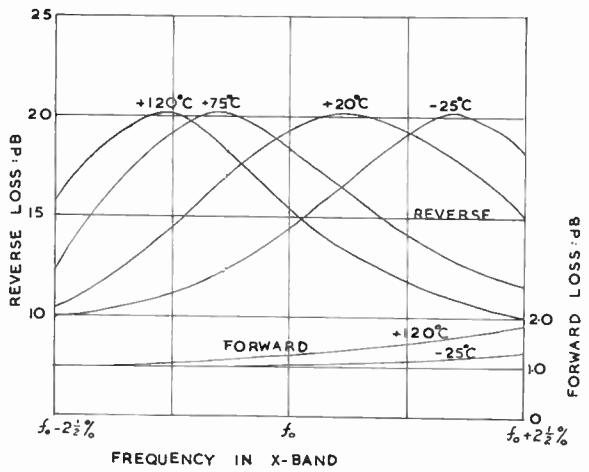


Fig. 8—Performance of F3 field displacement single-slab isolator.

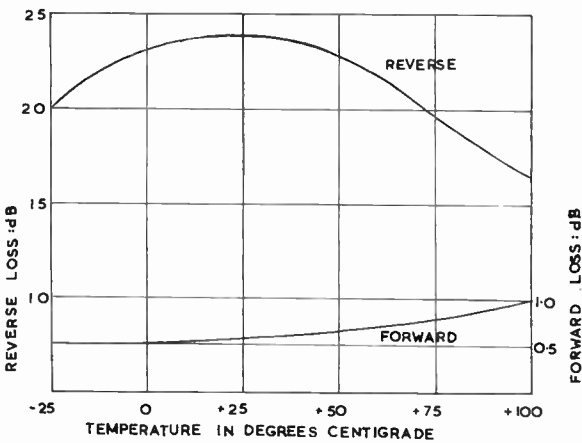


Fig. 7—Performance of R1 field displacement single-slab isolator.

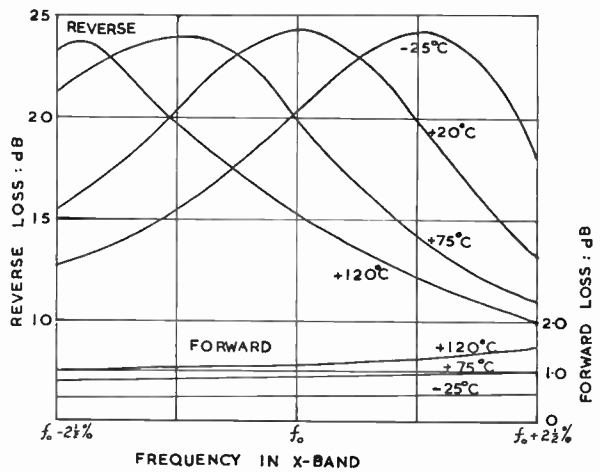


Fig. 9—Performance of R1 field displacement single-slab isolator.

(Fig. 5). This prevented leakage of microwave power, the microwave wall currents flowing through the capacity across the anodized surface. At the same time it prevented any large eddy current losses. Of course, in this instance, thin walled waveguide formed by evaporating aluminum onto a dielectric could have been used, but the method described is cheaper, easier to manufacture, and more robust.

An attempt was made to design a high-speed 350-kc sinusoidal phase modulator, but the temperature of the ferrite rose rapidly due to hysteresis losses in the ferrite itself. The best method of overcoming this effect would be the development of a ferrite with a narrow hysteresis loop, but a partial solution of the problem would be achieved by cooling or perhaps by using larger quantities of ferrite and much smaller fields.

ISOLATORS

Temperature Effects on Isolators

Many articles have been published on isolators,^{3,4} but little information is available on their temperature char-

acteristics.^{5,6} Two isolators of comparable performance, one utilizing ferromagnetic resonance absorption and the other relying for its operation on field displacement, and both one inch long, were compared over a temperature range of -25°C to $+100^{\circ}\text{C}$ (Figs. 6 and 7), both of these isolators using Ferramic R1. It can be seen from the curves that the resonance type isolator has a better performance than the field displacement type over this temperature range. A curve published by Duncan and Swern⁶ shows practically no variation of resonance absorption in the temperature region 25°C to 100°C for Ferramic R1. This is in agreement with Fig. 6. The temperature dependence of the field displacement isolator employing different ferrites and using the same ferrite configuration is shown in Figs. 8 and 9. The performance of the Ferramic R1 is very similar to that of F3, an experimental nickel aluminum ferrite of ap-

⁵ S. Boronski, "Some properties and applications of ferrites at 3-cm wavelength," *Proc. IEE*, pt. B, vol. 104, supplement no. 6, pp. 331-337; 1957.

⁶ B. J. Duncan and L. Swern, "Temperature behavior of ferromagnetic resonance in ferrites located in waveguide," *J. Appl. Phys.*, vol. 27, pp. 209-215; March, 1956.

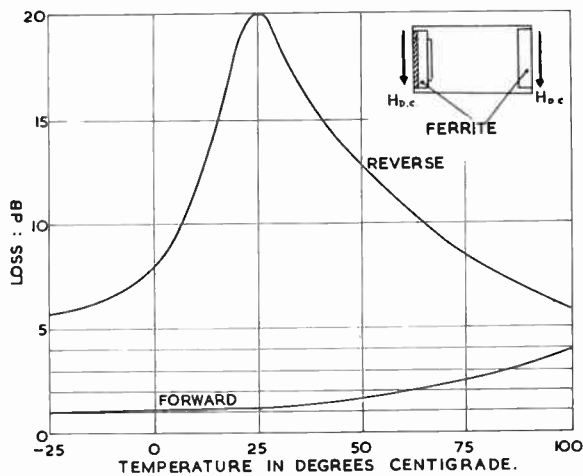


Fig. 10—Performance of R1 field displacement double-slab isolator vs temperature.

proximately the same saturation magnetization, but having a Curie temperature around 500°C . This ferrite was produced by Derry and Wills of Admiralty Research Laboratories, Teddington, England.⁷

Since the F3 ferrite has a higher Curie temperature than Ferramic R1, which is generally accepted to be in the region of 300°C , it was thought that an isolator constructed with F3 ferrite would have a superior performance. However, in the temperature range concerned this was not so, and it would seem that the Curie temperature has little effect.

Generally, as the temperature increases, it can be seen that the center frequency of the isolator bandwidth is lowered. The performance at the center frequency can be recovered at any temperature by changing the dimensions of the ferrite.

Fig. 10 shows the temperature characteristic of a double slab isolator using Ferramic R1. The performance is inferior to the single slab case, and it would seem that the geometry of the ferrite configuration plays an important part in its temperature properties.

VARIATION OF ISOLATOR PARAMETERS

Besides the temperature characteristics of isolators, a thorough investigation has been carried out using Ferramic R1 on the variation of different parameters in the design of field displacement isolators. The work which has been done has concentrated mainly on designing very short isolators where the tolerances for an optimum performance are very critical compared to an isolator four or five times the length.

The following parameters, as shown in Fig. 11, were varied:

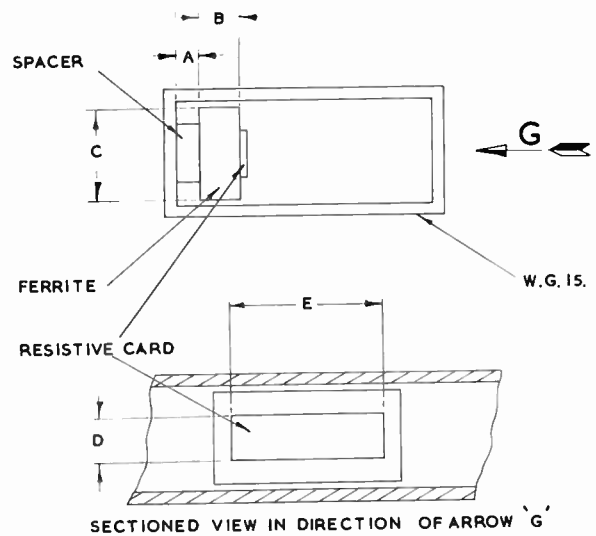


Fig. 11—Field displacement isolator.

- A) Spacing of the ferrite from the sidewall of the guide (Fig. 12).
- B) Thickness of the ferrite (Fig. 13).
- C) Height of the ferrite (Fig. 14).
- D) Breadth of the resistance card (Fig. 15).
- E) Length of the resistance card (Fig. 16).

For very short isolators the first two parameters mentioned are very critical and tolerances of ± 0.001 inch have to be kept, in order to obtain a good performance at the frequencies required. It can be seen from the curves that the parameters A), B), and C) decrease with increasing frequency. The vswr of the device can be improved by reducing the height of the ferrite, the best vswr coinciding with maximum bandwidth. Further decrease in the height results in a narrow-banded, but very high back-to-front ratio isolator. The isolation depends very critically on parameter D), but remains fairly constant over a comparatively large change in length E). This is in disagreement with a curve published by Weisbaum and Seidel⁴ for an isolator 5 inches long which showed that the isolation rises to a single peak. This disagreement is probably due to the fact that fringing fields and evanescent modes at the ends of the ferrite in a very short isolator are relatively more important than in a long one.

It should be realized that all the parameters indicated are interdependent, and in the graphs where the isolation has deteriorated it can be recovered by altering another variable.

SCALING OF FERRITE ISOLATORS

The design of a field displacement isolator in any frequency band is basically empirical since the number of variables is so large. When a suitable isolator has been designed in one frequency band, the ability to scale into another band reduces the development time. This scal-

⁷ R. Derry and M. S. Wills, "Microwave Faraday effect and conductivity in nickel ferrite and ferrite aluminates," *Proc. IEE*, pt. B, vol. 104, supplement no. 6, pp. 324-330; 1957.

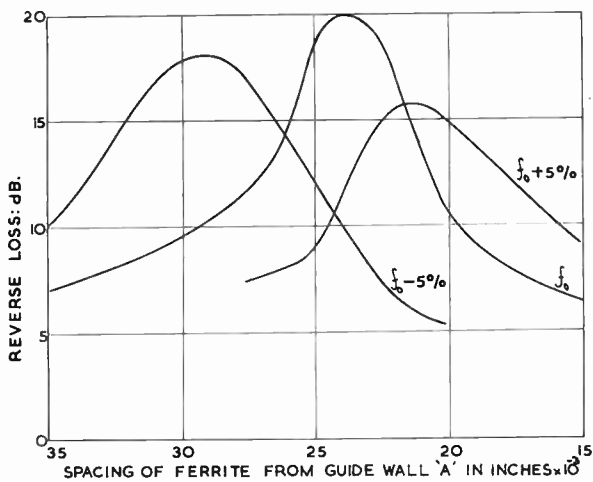


Fig. 12—Reverse loss—ferrite spacing for various frequencies at lower X band.

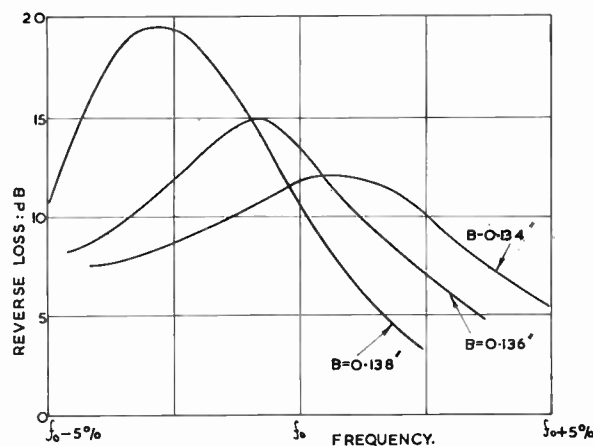


Fig. 13—Reverse loss—frequency characteristic for various ferrite thicknesses B at lower X band.

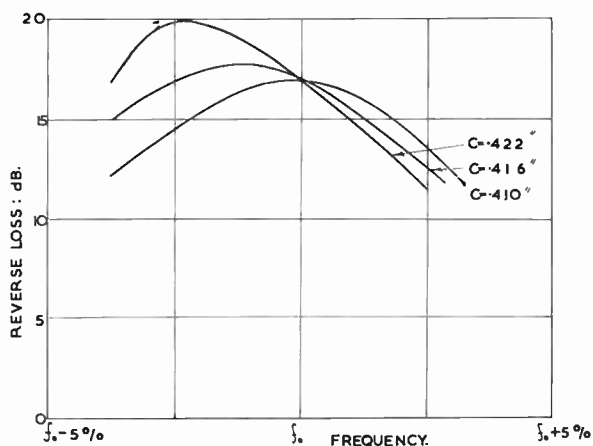


Fig. 14—Reverse loss—frequency characteristic for various ferrite heights C at lower X band.

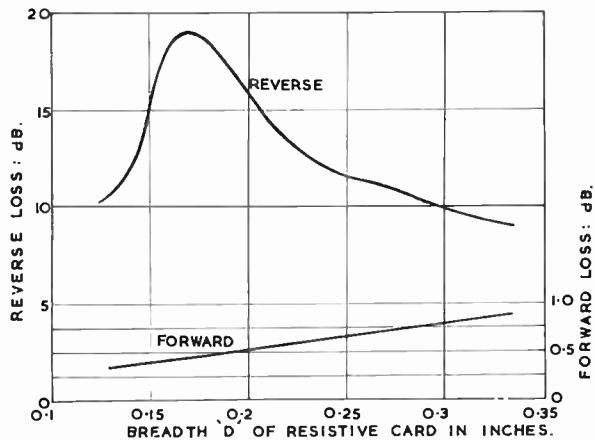


Fig. 15—Forward and reverse loss vs breadth of resistive card.

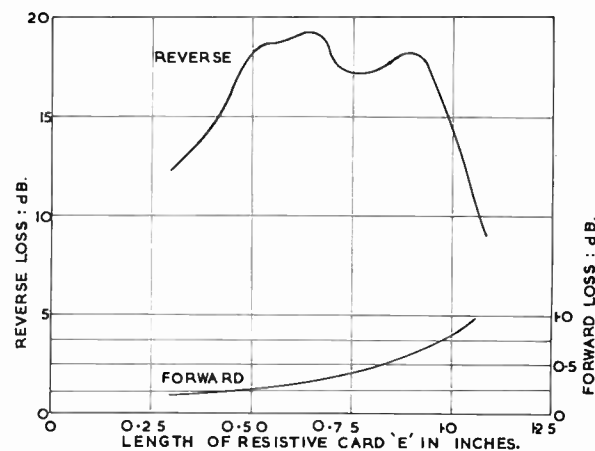


Fig. 16—Forward and reverse loss vs length E of resistive card at lower X band.

The following parameters were scaled as indicated:

- 1) A), B), and C) were scaled inversely with frequency.
- 2) The magnetic field was scaled proportionally with frequency.
- 3) If a different ferrite is to be used, the dimensions must be scaled in proportion to the two saturation magnetizations.

If the ferrite is larger than the guide size after scaling, another ferrite with a different saturation magnetization must be used. It has been found that the dimensions are critical to within 0.001 inch, whereas the magnetic field may be varied by ± 10 per cent without undue effect on the performance. These results are in agreement with those obtained by Weisbaum and Seidel.⁴

ACKNOWLEDGMENT

The authors wish to express their thanks to EMI Electronics Ltd., Feltham, Middlesex, England, for permission to publish this article and to their colleagues of the Microwave Division for their invaluable assistance.

ing technique has been carried out successfully from a short isolator with an optimum performance at X band to one of similar performance using a different ferrite at KU band (British designation: J band).

Theory of Stronger-Signal Capture in FM Reception*

ELIE J. BAGHDADY†, MEMBER, IRE

Summary—The characteristics of the FM disturbance that is caused by two-signal interference are pointed out and compared with the characteristics of message modulation. The comparison suggests a new role for the amplitude limiter in FM receivers. The limiter spreads out the spectrum which carries the FM disturbance over a frequency range that often exceeds many times the bandwidth requirements of the message modulation. This makes it possible to reject important parts of the interference spectrum by proper filtering in the output of the limiter without substantially affecting the spectrum of the message modulation. A repeated cycle of amplitude limiting and spectrum filtering is found to be an effective scheme for suppressing the disturbance ahead of the discriminator stage, and for improving the capture capabilities of an FM receiver.

I. INTRODUCTION

THE basis for the pronounced capture capabilities of a wide-band FM system lies in the properties of FM disturbances as compared with message modulation. Similar considerations account for the inherent vulnerability of AM systems to cochannel disturbances. In this paper we discuss the characteristic features of FM disturbances caused by high-level interference between two signals. Then, after a re-examination of an earlier suggestion for improving the capture ability of an FM receiver, we present a new approach that is based on the effect of a repeated process of amplitude limiting followed by narrow-band filtering upon the instantaneous frequency of the resultant of two carriers that differ in both frequency and amplitude.

In contrast to the work of previous investigators, we should like to emphasize that our philosophy is not merely guided by the desire to specify the requirements that would lead to the realization of an ideal frequency demodulator. For such a demodulator (in addition to being insensitive to amplitude changes) has been interpreted as producing a rectified output that varies linearly with the instantaneous-frequency variations caused by message and by disturbance under all possible disturbance conditions. Therefore, such a demodulator has been divorced of any contribution to the inherent capture capabilities of the FM receiver. We shall demonstrate that the realization of this demodulator as a limiter-discriminator combination (or some other amplitude-insensitive device) that will reproduce the instantaneous-frequency variations caused by high-level interference and convert them into an undistorted, rectified, voltage output is not only undesirable, but often im-

practicable. Our results will also show that it is possible to minimize the FM disturbance (in the limiter section) before detecting it. Consequently, the only necessary properties for the ideal FM demodulator, which will adequately meet the requirements for interference rejection, are the amplitude insensitivity and the linear variation of the detected output with only the message modulation—and not the disturbance.

II. CHARACTERISTICS OF FM INTERFERENCE

Consider that two carriers of relative strengths 1 and a ($a < 1$) and of frequencies p and $(p+r)$ radians per second ($r \ll p$) fall within the linear pass band of a frequency-modulation receiver. For simplicity, assume that the signals are either momentarily unmodulated in amplitude and frequency or, at worst, have a frequency modulation that is so slow relative to the frequency difference, r , that the signal frequencies are not appreciably changed during several periods of $2\pi/r$ second. The terms "interference ratio" and "weaker-to-stronger-signal amplitude ratio" will be used synonymously.

The resultant signal at the input of the first limiter is $e(t) = A(t) \cos [pt + \theta(t)]$. The instantaneous frequency of this signal is

$$\begin{aligned} \omega_i(t) &= p + \frac{d\theta}{dt} \\ &= p + \frac{1}{2} r \left[1 - \frac{1 - a^2}{1 + 2a \cos rt + a^2} \right]. \end{aligned} \quad (1)$$

Clearly, $d\theta/dt$ represents the instantaneous deviation of the frequency of the resultant signal from that of the stronger signal. It therefore represents the extraneous instantaneous-frequency perturbations caused by the superposition of the weaker signal upon the desired stronger signal. Plots of $d\theta/dt$ are shown in Fig. 1, for $a = 0.8$ (solid curve) and $a = 1/0.8$ (dashed curve). The spike pattern will reverse polarities if $r \rightarrow -r$, or if a becomes greater than 1.

It is important to observe that the average frequency of the resultant signal over a period of $2\pi/r$ second is precisely the frequency of the stronger signal. Thus, if the FM demodulator can eliminate the amplitude changes and deliver a rectified output voltage that is linearly related to the instantaneous-frequency variations of the input signal, the output of this demodulator, before any audio (or video) filtering, is equal to some constant multiplied by $[E_0(p) + d\theta/dt]$, where $E_0(p)$ is a direct-voltage level dictated by the frequency p . Since $d\theta/dt$ averages to zero over a period of $2\pi/r$ second, the average value of the detected voltage will correspond

* Original manuscript received by the IRE, March 14, 1957; revised manuscript received, November 18, 1957; second revised manuscript received, January 9, 1958. This work was supported in part by the U. S. Army (Signal Corps), the U. S. Air Force (Office of Sci. Res., Air Res. and Dev. Com.), and the U. S. Navy (Office of Naval Res.).

† Dept. of Elec. Eng. and Res. Lab. Electronics, Mass. Inst. Tech., Cambridge, Mass.

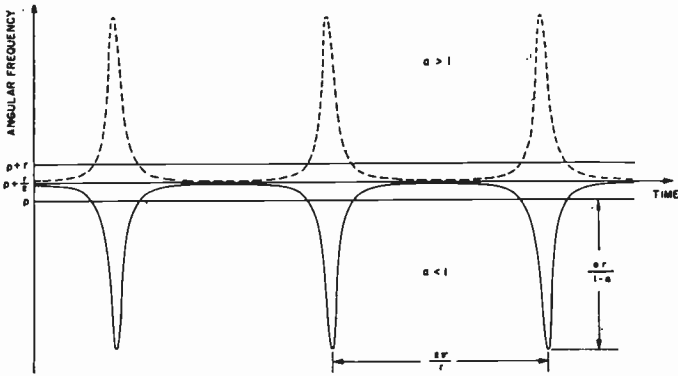


Fig. 1—FM disturbance pattern caused by two-carrier interference, plotted for $a=0.8$ and $a=1/0.8$.

to the direct-voltage level dictated by the frequency p of the stronger signal. A slow message modulation carried by p will be delivered by the direct-voltage level corresponding to p at the output. The rectified output voltage will also contain sinusoidal components at frequency r radians per second and at harmonics of r .

From the viewpoint of audio filtering after proper demodulation, if a disturbance of the type shown in Fig. 1 is delivered at the output of the discriminator, the amplitudes of its Fourier components, as well as the number of these components that go through the low-pass filter, will vary with r . The rate, r , at which the disturbance pattern recurs is, therefore, an important distinguishing feature of the disturbance. For, if $r/2\pi$ lies outside the expected audio (or video) band, the disturbance will be completely wiped out by the low-frequency filtering after the discriminator. If $r/2\pi$ lies within the audio band, then several factors combine to reduce the effectiveness of the disturbance that leaks through to a small fraction of full message modulation. These factors relate to the dependence of the amplitudes of the Fourier components of the disturbance waveform upon r , the properties of wide-band FM systems, and the possible use of a de-emphasis filter.

Let us now determine the requirements for reproducing a reasonable approximation to the disturbance pattern of (1) in the response of a filter (that follows an ideal limiter) and for converting the FM to AM by a discriminator circuit.

In general, if a frequency-modulated wave is impressed upon a band-pass filter, the frequency modulation of the filter response will be a reasonable approximation to the frequency modulation of the excitation only to the extent that the filter can be said to follow the excitation through quasi-stationary states. For, if the filter is able to respond in a quasi-static manner, its response can be computed by the instantaneous-frequency method. This method assumes that the response of the filter at, let us say, time $t=t_1$ is essentially given by its steady-state response to a sinusoid whose frequency is given by $\omega_i(t_1)$, the value of the instantaneous frequency at that time. If a given filter is able to re-

spond in this manner to a specified FM excitation, then, henceforth, the filter will be referred to as "wide-band" relative to that excitation. If the filter is unable to follow the excitation in a quasi-stationary manner, we shall refer to it as a "narrow-band," or "sluggish," filter relative to the specified excitation.

We have shown¹ that for purposes of quasi-stationary analysis a filter that is characterized by a system function with poles entirely in the left-half of the complex-frequency plane may be characterized by an index of sluggishness k and by its bandwidth (BW) between half-power points. (For a single-tuned circuit, $k=8$; for a pair of critically coupled tuned circuits, $k=20$.) If the given excitation has a phase-modulation function, $\theta(t)$, then an upper bound on the error incurred in assuming that the complex amplitude of the filter response is given by the quasi-stationary solution, is given by

$$\epsilon = \frac{1}{2} \frac{k}{(BW)^2} \cdot |\theta''(t)|_{\max}. \tag{2}$$

Tolerable engineering errors in the complex amplitude of the response will result if $\epsilon \leq 1/10$.

Thus the most important feature of an FM disturbance, as far as the reproduction of this disturbance is concerned, is the maximum slope of its waveform. In our problem this is

$$|\theta''(t)|_{\max} = B_{\lim}^2 \left(\frac{1+a}{1-a} r \right)^2, \tag{3}$$

where B_{\lim} is as plotted in Fig. 2. This value should be compared with

$$|\theta''(t)|_{\max} = \frac{1}{2} \omega_m (BW)_{if}$$

which holds for a sine-wave modulation given by

$$\theta'(t) = \frac{1}{2} (BW)_{if} \sin \omega_m t.$$

The ratio of the maximum (rate of frequency sweep) for interference and the maximum for a sine-wave modulation is

$$|\theta_{N''}|_{\max} / |\theta_{S''}|_{\max} = 2 \left[B_{\lim} \frac{1+a}{1-a} \right]^2 \frac{(BW)_{if}}{\omega_m}.$$

If $\omega_m/2\pi = 15$ kc, $(BW)_{if}/2\pi = 150$ kc, and a is in the range $0.4 < a < 1$, this ratio is

$$3.2 \left(\frac{1+a}{1-a} \right)^2.$$

If we combine (2) and (3), we find that the filter that follows the first ideal limiter [if r is given its maximum value of one $(BW)_{if}$] must have a bandwidth given by

$$(BW)_{\lim} = KB_{\lim} \frac{1+a}{1-a} (BW)_{if}, \tag{4}$$

¹ E. J. Baghdady, "Theory of Low-Distortion Transmission of FM Signals Through Linear Systems," M.I.T., Res. Lab. Electronics, Cambridge, Mass. Tech. Rep. 332; July 30, 1957. (To be published.)

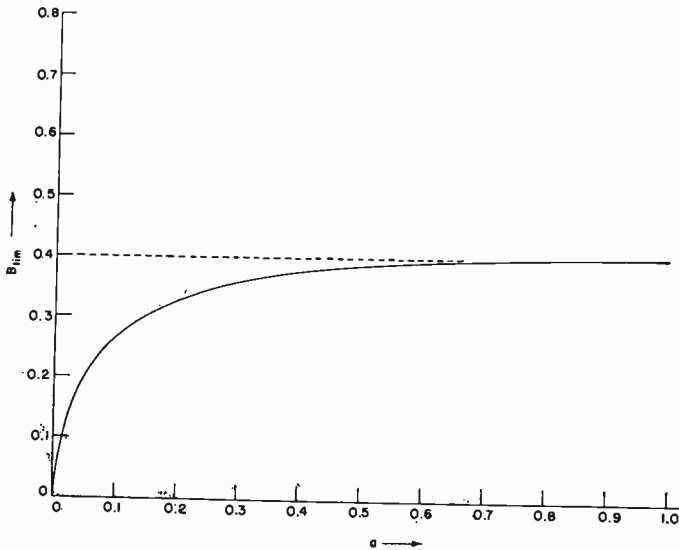


Fig. 2—Variation of B_{lim} , of (3) and (4), with a .

where

$$K = \sqrt{\frac{k}{2\epsilon}} \quad \text{and} \quad \epsilon \leq 1/10,$$

in order to follow the amplitude-limited resultant of the two input carriers through quasi-stationary states. Otherwise the limiter filter will be too sluggish. For a between 0.4 and 1, $B_{lim} \cong 0.4$, and if $\epsilon \leq 1/10$, we have

$$KB_{lim} \geq \begin{cases} 2.5 & \text{for a single-tuned circuit} \\ 4 & \text{for a maximally flat double-tuned circuit.} \end{cases}$$

For a value of $a = 0.95$, (4) indicates that a single-tuned circuit will reproduce an acceptable approximation to the disturbance pattern if $(BW)_{lim} \geq 100(BW)_{if}$. For a maximally flat double-tuned circuit,

$$(BW)_{lim} \geq 160(BW)_{if}!!$$

Next, let us assume that the discriminator FM-to-AM conversion filter is excited by the amplitude-limited resultant of the two signal carriers. Such a filter is best represented by a pair of high- Q , stagger-tuned, parallel-resonant circuits. The rectified output of the discriminator often is (or is equivalent to) a superposition of the envelope of one tank-circuit response upon the envelope of the other tank-circuit response reversed in polarity. If the bandwidth of each circuit is taken as 2α radians per second, then best linearity in the discriminator characteristic is achieved if the resonant frequencies of the circuits are 2.45α radians per second apart. With this separation, the extent of the linearity of the discriminator characteristic will be (nearly) α radians per second centered about the center frequency of operation. A prerequisite for proper operation is quasi-static response by each of the parallel-resonant circuits. Since the resonant frequencies are not normally swept by the FM excitation, we can show that α must satisfy the requirement

$$\alpha \geq 2.5\sqrt{|\theta''(t)|_{\max}}$$

For a between 0.4 and 1, this means that

$$\alpha \geq \frac{1+a}{1-a} (BW)_{if}$$

This condition states that α , which also equals the extent of the discriminator linearity, must be equal to the frequency range that the largest spikes can cover. Consequently, the peak-to-peak separation of the discriminator characteristic must be approximately

$$2.5 \frac{1+a}{1-a} (BW)_{if}$$

For $a = 0.95$, this separation is of the order of $100(BW)_{if}$. Since 100 per cent message modulation is only $\pm \frac{1}{2}(BW)_{if}$, a discriminator characteristic of this width represents no tangible sensitivity and is, indeed, useless, not to mention the prospect of its construction.

Finally, we need to consider the properties of the spectrum that is required for the reproduction of the FM disturbance depicted in Fig. 1. This spectrum makes up the amplitude-limited resultant of the two input signals which is given by

$$\begin{aligned} e(t) &= \cos [pt + \theta(t)] \\ &= \sum_{n=-\infty}^{\infty} A_n(a) \cos (p - nr)t. \end{aligned} \quad (5)$$

Ten-place tables of the spectral amplitudes $A_{\pm n}(a)$ were computed by Granlund.² The detailed properties of this spectrum have been explored by the author.^{3,4} Only the characteristics that are pertinent to the present discussion are summarized here.

We note that the amplitude of the spectral component that has the frequency of the stronger of the two input signals is A_0 . The component with amplitude A_{-1} has the frequency of the weaker signal. The amplitudes of the side-frequency components are not symmetrically distributed about the center-frequency component A_0 . This lack of symmetry conforms to our physical expectations. On an instantaneous-frequency basis, the instantaneous frequency of the resultant signal (see Fig. 1) keeps this signal much longer on one side of the center frequency than on the other. This means that the power in the composite signal will not be equally shared by the two sidebands. Since the instantaneous frequency of the composite signal lingers in the vicinity of the mean of the two carrier frequencies (that is, $p + (1/2)r$ radians per second) during the greater part of

² J. Granlund, "Interference in Frequency-Modulation Reception," M.I.T., Res. Lab. Electronics, Cambridge, Mass., Tech. Rep. 42; January 20, 1949.

³ E. J. Baghdady, "Frequency-modulation interference rejection with narrow-band limiters," Proc. IRE, vol. 43, p. 51; January, 1955.

⁴ E. J. Baghdady, "Interference Rejection in FM Receivers," M.I.T., Res. Lab. Electronics, Cambridge, Mass., Tech. Rep. 252; September 24, 1956.

the frequency-difference cycle, more signal power should reside in each of the two components that have frequencies closest to the average frequency (namely, A_0 and A_{-1}) than in any of the other components. This is confirmed by the computed values for the amplitudes. The magnitude of A_0 is larger than that of A_{-1} , and this may be appreciated by noting that the instantaneous frequency of the composite signal always puts it on the A_0 side of the mean frequency ($p + (1/2)r$) radians per second. Inasmuch as the spectral components are basically the "building blocks" of the resultant signal, the components that tend to pull the instantaneous frequency of the resultant signal toward the frequency of the weaker signal must logically be those that lie on the same side relative to the frequency p (of the stronger signal) as the frequency of the weaker signal. The components in the opposite sideband provide the necessary balancing for preserving the desired average value, p , of the frequency of the resultant signal.

The extent of the significant spectrum of the amplitude-limited resultant of the two input carriers can be determined from Fig. 3. In a process whereby the amplitude-limited resultant of the two signals is resynthesized from its Fourier components, ΔS in Fig. 3 gives the fractional amount by which the original spike magnitude has been decreased by rejecting those portions of the spectrum that fall outside a bandwidth of

$$\beta_{lim} \cdot \left(\frac{1+a}{1-a} \right) (BW)_{if},$$

when the various components are spaced $r = (BW)_{if}$ radians per second apart. The value of β_{lim} that will result in a 10 per cent decrease in the spike magnitude is approximately 2.6. For a decrease of 1 per cent, $\beta_{lim} \cong 5.5$.

III. AN EARLY PROPOSAL: THE "WIDE-BANDING" THEORY

The first important proposal aimed at specifying the design conditions for ensuring suppression of two-path interference at arbitrarily high levels was made by Arguimbau and Granlund.⁵⁻⁸ Their proposal prescribes that the FM demodulator (limiter-discriminator section) approach the ideal in the sense of being amplitude insensitive and of delivering a rectified voltage output that is linearly related to the instantaneous-frequency variations of the resultant of the two input signals over the entire range covered by the spike pattern described by (1). The FM disturbance could then be suppressed or minimized after it is detected.

⁵ L. B. Arguimbau and J. Granlund, U. S. Patent 2,674,690; April, 1954.

⁶ L. B. Arguimbau, "Vacuum-Tube Circuits and Transistors," John Wiley and Sons, Inc., New York, N. Y.; 1956.

⁷ L. B. Arguimbau and J. Granlund, "Transatlantic FM transmission," *Proc. Natl. Electronics Conf.*, vol. 3, p. 644; November, 1947.

⁸ L. B. Arguimbau and J. Granlund, "Sky-wave FM receiver," *Electronics*, vol. 22, pp. 101-103; December, 1949.

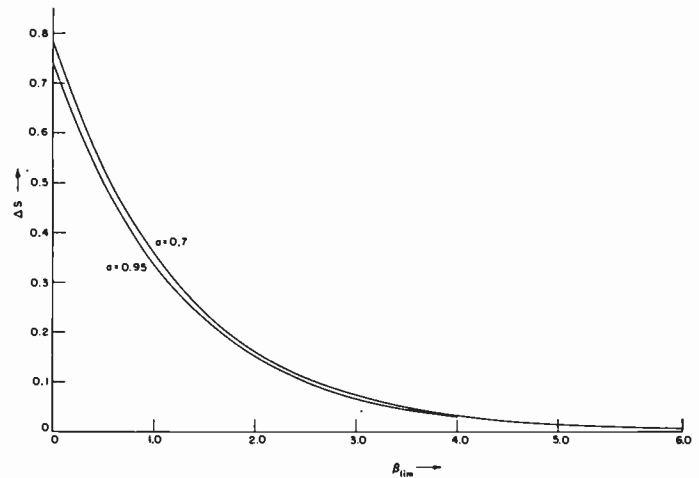


Fig. 3—Degree of reduction in intensity of FM disturbance as a function of the normalized bandwidth of the ideal narrow-band limiter. 100 ΔS represents the percentage of reduction in the magnitude of the FM disturbance spike.

At the basis of the "wide-banding" theory lies the argument that if the instantaneous-frequency variations caused by the interference can be kept substantially undistorted in going through the nonlinear sections (limiter and discriminator), then it can be guaranteed that their average over one cycle of the frequency difference between the two carriers will always be zero. We have demonstrated^{3,4} that it is possible to distort this instantaneous-frequency pattern by proper filtering without in any way affecting the desired zero average deviation from the desired frequency. This proves that although this first fundamental assumption of the "wide-banding" theory is a sufficient condition for suppressing the interference, it certainly is not necessary.

Next, in attempting to provide limiter-bandwidth design criteria that ensure the absence of harmful distortion of the instantaneous-frequency pattern, the "wide-banding" theory makes the (unjustified)⁹ assumption that if this filter bandwidth is designed on the basis of the extent of the frequency spikes, then a quasi-stationary analysis is permissible. Consequently, it can safely be said that the instantaneous-frequency disturbance pattern of the filter response will be substantially identical with that of the excitation. This assumption proves to be completely invalid, except for values of a that are close to zero. For, if account is taken of the situation in which the stronger signal has the higher frequency, then, from Fig. 1, the instantaneous frequency of the resultant signal can range over a bandwidth given by

⁹ Granlund, *op. cit.*, pp. 39-53. Granlund performed the Fourier analysis indicated in (5), "with the idea of determining whether the . . . range covered by the instantaneous-frequency spikes . . . is a reasonable estimate of the extent of the spectrum after limiting. Thus, the result was to be used as a guide in determining limiter and discriminator bandwidths." He concludes: "Further study is indicated before a receiver can be properly designed with narrow-banding."

$$(BW)_s \equiv \frac{1+a}{1-a} (BW)_{if}, \quad (6)$$

where r has been assigned its maximum permissible value of one IF bandwidth. Eq. (4) shows that this bandwidth is only $1/KB_{lim}$ (or less than $\frac{1}{3}$) of the value that a physical filter must have in order for its response to be satisfactorily approximated by a quasi-stationary solution. This can also be established from a consideration of the extent of the significant spectrum of the amplitude-limited resultant signal.

We must therefore conclude that the bandwidths prescribed by the "wide-banding" theory are not sufficiently wide: that is to say, the "wide band" of the "wide-banding" theory is less than one third as wide as the "wide-banding" theory fundamentally intended it to be. Indeed, wide as these bandwidths were believed to be, they still fall safely within the classification of narrow-band filters. The extent of the maximum instantaneous-frequency deviation is not always a reliable basis for estimating the necessary bandwidth for the validity of an instantaneous-frequency approach.¹ The only reliable basis is the maximum rate of change that the instantaneous frequency of the excitation will experience.

Finally, basing the argument on a quasi-stationary approach to the limiter-filter response problem, the "wide-banding" theory draws the conclusion that if the limiter bandwidth is given by (6), then the FM detection characteristic must be linear over the same range, if the worst situation in which $r = (BW)_{if}$ is to be successfully handled. This conclusion is, of course, invalidated by the invalidity of the quasi-stationary argument. Our results indicate that the bandwidth requirement in the discriminator can only be stated after the number of limiter stages and the bandwidth of each have been specified. If only one such stage with the bandwidth specified by (6) is used, the discriminator-characteristic linearity need only extend over two thirds of the range specified by (6). Lower figures follow the use of narrower limiter bandwidths and of more than one narrow-band limiter stage, as the results of this paper will show.

Before concluding this section, we would like to point out that upon a re-examination of the receiver whose performance is discussed by Arguimbau and Granlund in their publications, this author became convinced that their observations should be reinterpreted in the light of the results presented in this paper.

IV. A NEW APPROACH TO THE PROBLEM

In view of the difficulty of meeting the FM demodulator design requirements for faithful reproduction of the FM disturbance, we propose to suppress, or at least minimize, this disturbance *before* (rather than *after*) it is detected. Various methods could be used to achieve this end. We propose to discuss a method that is based upon subjecting the two-carrier resultant signal to a repeated

process of amplitude-limiting followed by narrow-band filtering. In this method the limiter does more than just eliminate undesirable variations in the amplitude—it also contributes to the abatement of the FM disturbance.

Before we present the quantitative justification for this method, a heuristic argument can be made. We recall (from Section II) that under conditions of high-level interference [$a > 0.4$ and $r \sim (BW)_{if}$] the maximum slope of the disturbance waveform is many orders of magnitude greater than the greatest slope that can be expected in the message waveform. This should make it possible to insert filters at appropriate places in the signal path that would be too sluggish to follow the disturbance without distorting the message modulation. The appropriate places for these filters in the high-frequency sections of the receiver are not in the linear stages, because in these stages the desired carrier and the interference combine linearly and their resultant spectrum is fully accommodated within the IF pass band. This concentration of the spectrum within the IF pass band makes it impossible to separate the two signals, or to improve the predominance of the stronger one, purely by linear filtering. But a process of amplitude limiting will spread out the significant spectrum (which is necessary for the reproduction of the FM disturbance) over a frequency range that exceeds many times the IF bandwidth. Since the instantaneous frequency of the desired signal will always place it within the extent of one IF bandwidth, it should be possible, by filtering after the limiting process, to exclude sizable portions of the interference spectrum without affecting the message-bearing spectrum. The minimum requirement of one IF bandwidth for the limiter filter is calculated to meet the prerequisites of undistorted reproduction of the expected message modulation.

One stage of limiting and filtering, however, can be expected to retain at its output a spectrum with a significant amount of the interference in the form of components that could not be rejected without impairing the message or upsetting the desired average instantaneous frequency. Therefore, several repetitions of the narrow-band limiting process may be necessary in order to reduce the maximum disturbance to some desired level.

The results that we now present will uphold the following important statement.

Theorem 1

The only necessary properties for an ideal FM demodulator that will properly handle and suppress interference are: 1) insensitivity to amplitude variations of the resultant impressed signal; 2) the detected output must vary linearly with the instantaneous frequency of the input signal over a minimum permissible range which need only be slightly greater than twice the frequency deviation of the expected message modulation.

Evidently, in order for these properties to be also

sufficient to realize proper suppression of interference, the disturbance must be substantially suppressed before it reaches the FM-to-AM converter (or discriminator) part of the demodulator. The cascading of narrow-band limiters ahead of the discriminator is only one important means for achieving this result. Various interesting schemes have resulted from other arrangements that involve narrow-band limiters.¹⁰

V. EFFECT OF ONE IDEAL NARROW-BAND LIMITER

The first step in the development of the new scheme for interference suppression is to determine the minimum permissible limiter bandwidths. This has been done in terms of an ideal limiter followed by an ideal filter.³ In brief, the limiter bandwidth must be so chosen that it will always pass configurations of sideband components that will add up to a resultant signal whose average frequency is equal to the frequency of the stronger of the two input carriers. A bandwidth equal to one IF bandwidth is sufficient for all $a \leq 0.863$, while a bandwidth equal to three IF bandwidths will be sufficient for all $a \leq 0.98$.

The necessary minimum extent of the linearity of the frequency-detection characteristic is dictated by the maximum instantaneous-frequency deviation of the resultant signal that drives the discriminator circuit. It is, therefore, of practical importance to describe the intensity of the interference in terms of the necessary minimum extent of the linearity of the discriminator characteristic as dictated by the most adverse interference condition. For simplicity, we shall, henceforth, use the term "discriminator bandwidth" [or $(BW)_{disc}$] to refer to the extent of the linear range of the frequency-detection characteristic.

The degree of reduction in the intensity of the interference that is achieved by a limiter with a specified bandwidth will vary with the limiter bandwidth. One way to gauge the amount of improvement in the capture conditions as a function of the limiter bandwidth is provided by the variation in the necessary minimum extent of the linearity in the discriminator characteristic with $(BW)_{lim}$. This variation is described³ by

$$\beta_{disc} = 1 - \zeta(a)e^{-0.791\beta_{lim}} \tag{7}$$

where $\beta_{lim} \equiv (BW)_{lim}/(BW)_s$, $\beta_{disc} \equiv (BW)_{disc}/(BW)_s$, $(BW)_s$ is defined in (6), and $\zeta(a) = 0.30a + 0.44$. In quoting this formula we have used the expression

$$k(a) = 0.791 \left(\frac{1-a}{1+a} \right)$$

which appears to fit the computed values of $k(a)$. A plot of β_{disc} vs β_{lim} appears in Fig. 4. It is important to observe that when $\beta_{lim} = 1$, indicating that

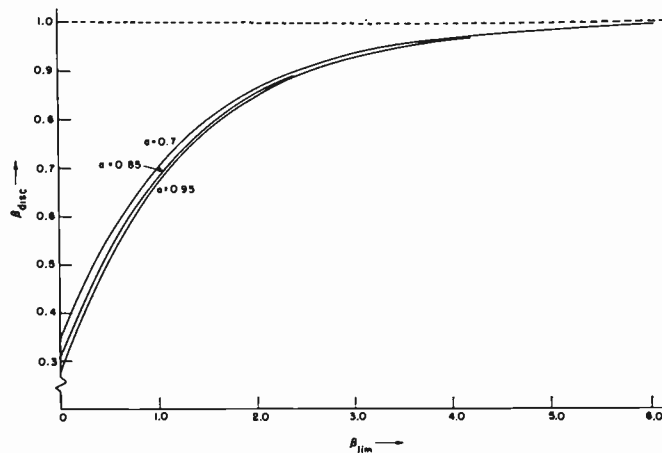


Fig. 4—Variation of the required normalized minimum extent of discriminator linearity with the normalized bandwidth of the limiter. Plot shows the amount of reduction in the required minimum value of β_{disc} caused by one stage of ideal narrow-band limiting.

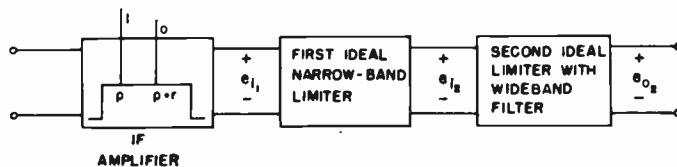


Fig. 5—Block diagram of a two-stage cascading scheme.

$$(BW)_{lim} = \left(\frac{1+a}{1-a} \right) (BW)_{it}$$

β_{disc} is only equal to $\frac{2}{3}$.

VI. EFFECT OF CASCADING NARROW-BAND LIMITERS

Consider the block diagram shown in Fig. 5. The first-limiter stage is assumed to have a bandwidth of W_{L1} times the IF bandwidth. Our immediate task is to study the disturbance carried by e_{o2} when the worst spectral composition of e_{i2} that corresponds to an assumed value of W_{L1} is impressed at the input of the second limiter. We first need to probe the restrictions (if any) on the permissible bandwidths after the second limiter.

Theorem 2

The minimum permissible bandwidth for the idealized filter associated with an amplitude limiter is, theoretically, one IF bandwidth for all values of $a \leq 0.863$. This requirement on the bandwidth of any limiter stage is independent of the number and of the bandwidths of the limiter-filter units in a cascaded chain which may precede that stage.

If the chosen limiter is the first in the chain, then the theorem states a fact that has already been established.³ If it is the second in the chain, then two situations are possible: the bandwidth of the first limiter is either equal to or greater than the IF bandwidth. If the bandwidth of the first limiter is equal to $(BW)_{it}$, then this

¹⁰ E. J. Baghdady, "Theory of feedback around the limiter," 1957 IRE NATIONAL CONVENTION RECORD, pt. 8; pp. 176-202.

value of bandwidth imposes an *a priori* restriction upon the usefulness of the combined cascade of limiters to interference ratios (at the input of the first limiter in the chain) that are less than 0.863. The bandwidths of the limiters following the first may, therefore, be $\geq (BW)_{if}$. Next, let the first-limiter bandwidth be greater than $(BW)_{if}$. A consideration of the most adverse spectral configuration that can arise at the output of the second-limiter filter when its bandwidth equals $(BW)_{if}$ will show that the criterion for the permissibility of only one IF bandwidth for the second-limiter filter is identical to the criterion for the first-limiter filter. This means that the minimum permissible bandwidth for the idealized second-limiter filter is one $(BW)_{if}$ for all $a \leq 0.863$. The argument that will establish this conclusion for the n th limiter in a chain is now obvious, and Theorem 1 is proved.

The actual computation of the minimum bandwidths permissible after the second limiter for $a > 0.863$ is possible, but too laborious. Moreover, the significance of the numerical results does not justify the effort. For the purposes of the ensuing discussion, it suffices to know that any desired values of idealized-filter bandwidth that are equal to or greater than the minimum permissible value after the first limiter³ can be safely assumed for any limiter filter in a chain.

The first "cascading" theorem that we shall demonstrate follows.

Theorem 3

If a system of cascaded ideal narrow-band limiters, each of bandwidth $(BW)_{if}$, is incorporated in an FM receiver, then the most adverse condition of two-signal interference will occur at both input and output of the scheme when the two signals differ in frequency by one $(BW)_{if}$, provided that the input interference ratio, a , is less than 0.84. The spectrum at the output of the scheme will then consist of only two sinusoids which correspond to the input sinusoids, with the ratio of weaker-to-stronger signal amplitude reduced from its input value of $a < 0.84$ to a value that can be made as small as desired by cascading the necessary number of narrow-band limiters.

The first part of this theorem is demonstrated by the plots of Fig. 6. In this figure, N represents the number of upper sideband components passed along with the desired component $A_0(a)$ [see (5)] by an idealized limiter filter whose bandwidth equals one $(BW)_{if}$. In this analysis the upper sideband components will tend to upset the desired average frequency in favor of the interference, because the frequency of the interference is above the desired frequency. Fig. 6 clearly shows that the situation in which only the components $A_0(a)$ at p radians per second and $A_{-1}(a)$ at $p+r$ radians per second are passed represents the most adverse disturbance condition for all $a < 0.84$, when the idealized limiter-filter pass band is one $(BW)_{if}$ radians per second wide. Under this condition of interference, the output

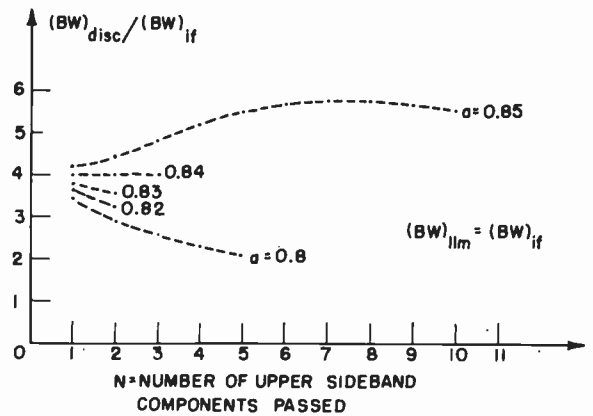


Fig. 6—Variation of the required minimum discriminator bandwidth with the upper sideband components passed by the ideal-limiter filter when the filter bandwidth equals the IF bandwidth.

of the first narrow-band limiter (like its input) consists of the sum of one sinusoid at p radians per second and another at $p + (BW)_{if}$ radians per second with a ratio of weaker-to-stronger signal amplitude that is given by $A_{-1}(a)/A_0(a) < a$. This indicates a reduction in the amplitude of the interference relative to the desired stronger signal. The amount of reduction is illustrated by the plot (first made by Granlund)² of $A_{-1}(a)/A_0(a)$ against a shown in Fig. 7. The greatest reduction arises when a is less than $\frac{1}{2}$, and the reduction then amounts to halving the interference ratio. It turns out that this represents the greatest interference reduction that can be achieved with one stage of narrow-band limiting unaided by additional unconventional schemes, such as, for example, feedback.¹⁰

The effectiveness of the scheme in which idealized narrow-band limiters, each of which has one IF bandwidth, are cascaded ahead of the amplitude-insensitive discriminator is illustrated in Fig. 8 by a plot of the required minimum discriminator bandwidth against the number of cascaded stages for values of a given by $a = 0.8$ and $a = 0.7$. If we denote by a_0 the ratio of weaker-to-stronger signal amplitude at the input of the first limiter and by a_n the corresponding ratio at the output of the n th stage, then

$$a_0 = a, \quad a_1 = A_{-1}(a)/A_0(a), \quad \text{and} \quad a_{n+1} = \frac{A_{-1}(a_n)}{A_0(a_n)}.$$

The plot of Fig. 7, therefore, describes the mathematical law which relates a_{n+1} to a_n , where $n = 0, 1, 2, \dots$.

When the interference ratio a exceeds 0.84, the spectrum that will carry the greatest disturbance at the output of the first limiter will consist of more than two components whether or not $W_{L1} > 1$. We shall now establish quantitative evidence for the effectiveness of the cascading scheme in suppressing the interference for values of $a > 0.84$ and $W_{L1} > 1$. For simplicity, we shall consider only two specific values of W_{L1} , namely $W_{L1} = 3$ and $W_{L1} = 7$. The spectrum that carries the

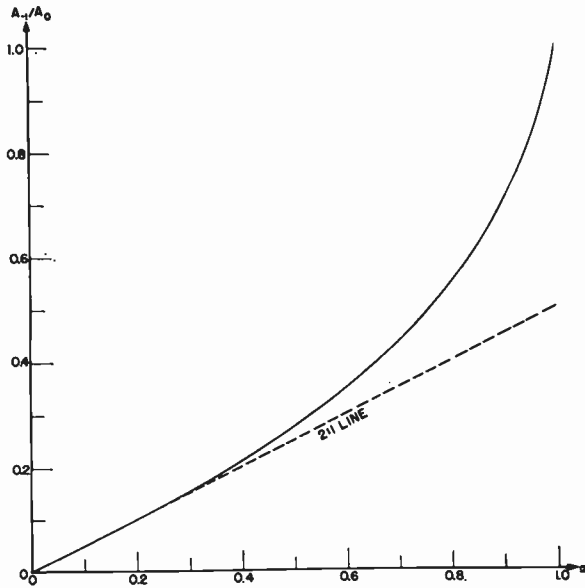


Fig. 7—Effect of the ideal amplitude-limiting process upon the amplitude, $A_{-1}(a)$, of the component that has the frequency of the weaker signal relative to the amplitude, $A_0(a)$, of the component that has the frequency of the stronger signal.

are brought out by Fig. 9. The amplitude-limiting process will thus spread out the significant spectrum of the resultant signal, again, largely at the expense of the troublesome components of the input signal.

Let us first assume that the first-limiter filter has a bandwidth of $3(BW)_{if}$. Let $B_n(a)$ denote the amplitude of the component at $p - nr$ radians per second in the spectrum of e_{o2} (in Fig. 5) when e_{i2} is described by $M = 1$, $N = 2$. If the bandwidth of the second limiter is restricted to one $(BW)_{if}$, the spectrum that appears at its output is made up of $B_0(a)$ at p radians per second and $B_{-1}(a)$ at $p + r$ radians per second. These components correspond to the two signals delivered by the IF amplifier. Under the worst condition of interference, therefore, a scheme composed of two limiters in cascade, the first of which has a bandwidth of $3(BW)_{if}$ and the second of $(BW)_{if}$, will deliver at its output only two sinusoids with the ratio of weaker-to-stronger signal amplitude (or interference ratio) reduced from its input value of a to the value $B_{-1}(a)/B_0(a)$ at the output. If $a = 0.85$, $B_{-1}(a)/B_0(a) = 0.49$, a significant reduction. Therefore, the indicated scheme demonstrates an interference suppression effect for all $a < 0.863$, which is analogous to the effect that a single stage with one IF bandwidth will exhibit for all $a < 0.84$. The output interference may be operated upon by additional cascaded limiter-filter units, each of which has a bandwidth of one $(BW)_{if}$, to produce further reductions in the interference. The speed with which this will decrease the minimum permissible discriminator bandwidth, $(BW)_{disc}$, is illustrated by one of the plots in Fig. 8.

Let us next assume that the second limiter, as well as the first, has a bandwidth of $3(BW)_{if}$. The present case is illustrated by the plots of Fig. 10. In this figure, the undistorted FM disturbance $\Omega_0(t)$ is transformed into $\Omega_1(t)$ by the first narrow-band limiter. $\Omega_1(t)$ is, in turn, transformed to $\Omega_2(t)$ by the second narrow-band limiter. The corresponding values of required minimum discriminator bandwidth are shown in Fig. 8.

As a final illustration, let $W_{L1} = 7$ and let $C_n(a)$ denote the amplitude of the component at $p - nr$ radians per second in the spectrum of e_{o2} (in Fig. 5) when e_{i2} is described by $M = 3$, $N = 4$. The worst condition of interference will arise at the input of the scheme, as well as at the output of each stage and of the whole scheme, when $r = (BW)_{if}$. Therefore, when $W_{L2} = 3$, the minimum required $(BW)_{disc}$ will be dictated by the spectrum $M = 1$, $N = 2$ at the output of the second limiter. The values dictated when $a = 0.85$, 0.9 , and 0.95 are plotted in Fig. 8. The corresponding values for $W_{L2} = 7$ are also plotted in this figure.

The decrease in the required value of $(BW)_{disc}$, brought about by each scheme, suggests that the required minimum $(BW)_{disc}$ will converge faster toward a prescribed value when the second and later limiter bandwidths are $3(BW)_{if}$ rather than $7(BW)_{if}$. In general, fewer stages with limiter bandwidths of $3(BW)_{if}$ would be needed after the first limiter to reduce the

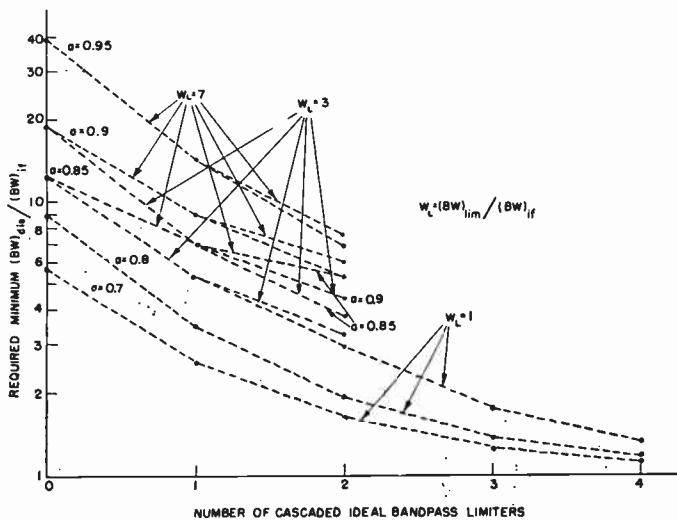


Fig. 8—Variation of the required minimum discriminator bandwidth with the number of cascaded narrow-band limiters.

most severe disturbance, when $W_{L1} = 3$, is specified by $M = 1$, $N = 2$ with $r = (BW)_{if}$ for all $a \leq 0.91$. The corresponding spectrum, when $W_{L1} = 7$, is specified by $M = 3$, $N = 4$ with $r = (BW)_{if}$ for values of a that include 0.95 . The method of treatment is independent of the specific spectral configurations that are considered and of the values of first-limiter bandwidth that are assumed.

A Fourier analysis⁴ of the amplitude-limited resultant of each of the two aforementioned spectral configurations reveals that the components of the troublesome sideband are all decreased in magnitude relative to the desired component (at p radians per second) while the relative amplitude of at least the leading component in the helpful sideband is increased. These observations

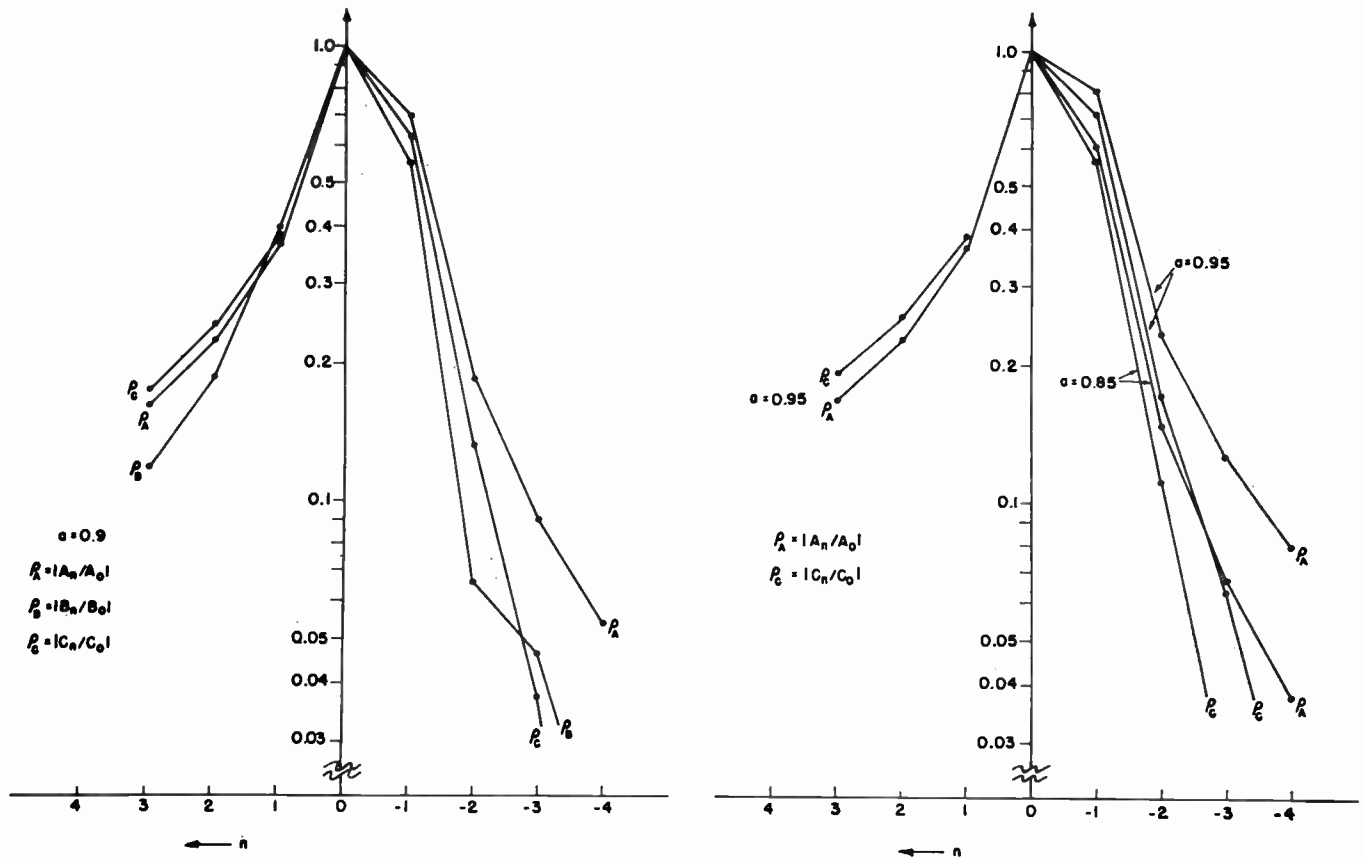


Fig. 9—Relative amplitudes of spectral components of interference spectrum at the output of the first and second limiters. Amplitude of component at $p - nr$ radians per second is:

$$B_n(a) \text{ if } W_{L1} = 3 \text{ and } M = 1, N = 2$$

$$C_n(a) \text{ if } W_{L1} = 7 \text{ and } M = 3, N = 4.$$

minimum permissible discriminator bandwidth to a prescribed value than with higher values of limiter bandwidth. In particular, as the bandwidth of the second limiter is increased from its minimum permissible value to higher and higher values, the minimum discriminator bandwidth required after this second limiter increases from a small value to a larger value that is dictated by the worst configuration delivered by the first limiter in the absence of the second. This larger value is achieved when the second-limiter bandwidth becomes sufficiently large to accommodate all of the spectral components of significance in the structure of the amplitude-limited resultant of e_{32} .

We may now induce the following conclusion.

Theorem 4

Under conditions of two-signal interference and for all values of the interference ratio that are less than unity (as delivered by the intermediate-frequency amplifier), the required minimum discriminator bandwidth can be reduced to a value that is as close to one IF bandwidth, as is desired, by cascading the necessary number of ideal narrow-band limiters with appropriately chosen bandwidths.

This theorem must be true generally because it can be

demonstrated for any specific situation by the methods that lead to the results summarized in Fig. 8.

VII. CONCEPT OF EQUIVALENT INTERFERENCE RATIO

Under conditions of two-signal interference, it is convenient to specify the capture conditions at any point within the high-frequency section of the receiver by a corresponding ratio of weaker-to-stronger signal amplitude. This specification is unambiguous only if the resultant signal at the chosen point is still composed of only two sinusoids. In the more general case it is desirable to introduce a measure of the interference level which is based upon a two-signal equivalent representation and embodies an acceptable extension of the meaning of "interference ratio." This may be done as follows.

With reference to Fig. 11, if the given configuration of sideband components arises with a value of frequency difference, r , and, in turn, gives rise to an instantaneous-frequency spike of normalized magnitude

$$\lambda = [\Delta\omega]/r, \quad (8)$$

then an equivalent frequency-spike magnitude, recurring every $2\pi/r$ second will also be produced when all

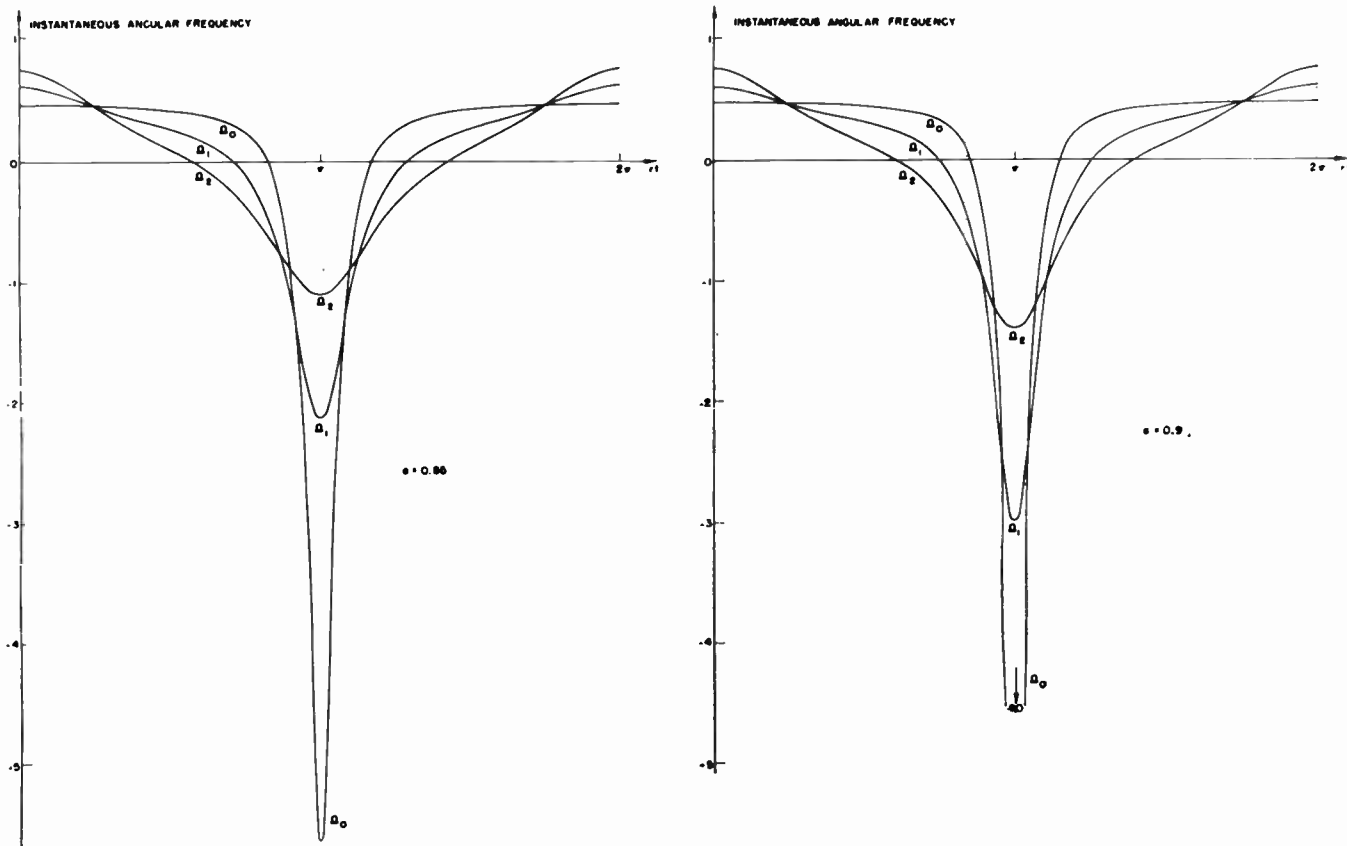


Fig. 10—Instantaneous deviations from the frequency of the stronger signal experienced by the frequency of the resultant signal.

$\Omega_0(t)$ = undistorted FM disturbance.

$\Omega_1(t)$ = distorted FM disturbance at output of one narrow-band limiter whose bandwidth equals $3(BW)_{if}$.

$\Omega_2(t)$ = distorted FM disturbance at output of two identical narrow-band limiters, each of bandwidth equal to $3(BW)_{if}$.

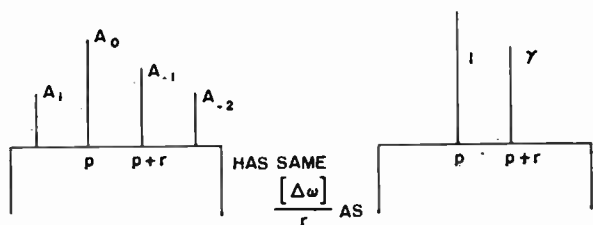


Fig. 11—Definition of γ , the equivalent interference ratio.

the sideband components that are passed are replaced by one component at $p+r$ radians per second whose amplitude relative to the component at p radians per second is given by γ , where

$$\gamma = \frac{\lambda}{1 + \lambda} \tag{9}$$

The "equivalent interference ratio" is, by definition, given by γ .

The following theorems formalize the results of this paper. The term "primary spectrum" is used in reference to the spectrum described by (5).

Theorem 5

If the band-pass filter following an idealized limiter is capable of following the instantaneous-frequency

variations of the amplitude-limited resultant of two carriers through quasi-stationary states—or, equivalently, if the filter pass band is sufficiently wide to accommodate the entire significant primary spectrum caused by the ideal limiting action—then the equivalent interference ratio of the composite signal delivered to the limiter will not be affected by the band-pass limiting action. Such a band-pass limiter will, however, deliver a constant-amplitude signal at its output.

Theorem 6

The equivalent interference ratio of a composite signal will be diminished by a band-pass filter only if the significant spectrum of the resultant impressed signal is spread out beyond the extent of the filter pass band. Under these conditions, a process of instantaneous-frequency limiting is exhibited by the response of the narrow-band filter, because this filter is unable to follow closely the fast rates of instantaneous-frequency variations of the excitation.

Theorem 7

When the ratio of weaker-to-stronger signal amplitude delivered by the IF amplifier is less than 0.84, the greatest reduction in the equivalent interference ratio that results from passing a composite signal through a nar-

row-band limiter is achieved when the limiter bandwidth has the smallest permissible value of one IF bandwidth.

Corollary

When the ratio of weaker-to-stronger signal amplitude delivered by the IF amplifier is less than 0.84, the number of cascaded stages of narrow-band limiting that is necessary to achieve a prescribed decrease in the equivalent interference ratio delivered to an amplitude-insensitive discriminator is smallest when the least permissible bandwidth of one IF bandwidth is used in each stage of limiting.

Theorem 8

Under conditions of two-signal interference, in which the ratio of weaker-to-stronger signal amplitude is less than unity, the equivalent interference ratio can be reduced by any desired amount by passing the composite signal through an appropriate number of cascaded narrow-band limiters with appropriately chosen bandwidths.

VIII. LOW-FREQUENCY FILTERING OF DISTURBANCE

In the wake of the reductions in the effectiveness of the interference are some valuable relaxations in the design requirements on limiters and discriminators that are intended for handling high-level interference. We have already noted the substantial reductions in the minimum permissible discriminator bandwidth. The important increases in the upper bounds on the discriminator and limiter low-frequency time constants that result from the narrow-band limiting process can now be anticipated.^{4,11}

We shall now comment on the low-frequency filtering of the disturbance. In general, after a proper detection of the instantaneous-frequency variations of the signal that drives the discriminator, the output voltage variations that are caused by the disturbance are modified by the action of the de-emphasis and audio filters that follow the discriminator circuit. If the frequency difference between the two input carriers lies beyond the range of audibility, the Fourier components of the recurrent spike train will all be filtered out. However, if the frequency difference between the two paths is audible, the component with the fundamental frequency of recur-

rence, plus a number of harmonics, depending upon the position of this frequency in the audible spectrum, will pass through the low-pass filters and will, therefore, disturb the output signal.

Two factors play more or less obvious roles in minimizing the importance of the unfilterable disturbance: 1) the de-emphasis filter attenuates most of the harmonic components, and 2) the magnitude of the FM disturbance (hence the amplitude of each of its constituent Fourier components) varies directly with r . Thus, with r well within the audio band, the increased number of unfilterable harmonics does not imply a proportionately increased disturbance because the amplitudes of the harmonics decrease with r .

A third factor that tends to minimize the audible disturbance is introduced by the partial suppression of the interference before it is detected. Computations,⁴ made with the assumption that the interference suppressor is a narrow-band limiter, show that the Fourier components of the modified FM disturbance have smaller amplitudes than their counterparts in the undistorted disturbance. Also, the fundamental component (of frequency r) becomes increasingly predominant in amplitude over the components at harmonics of r . This effect is more pronounced with increasing values of the frequency difference r and the interference ratio a . This is readily seen from the fact that, for a fixed value of a , the degree of disturbance suppression achieved through narrow-band limiting is greatest when the two carriers are farthest apart in frequency. As the frequency difference between the two carriers decreases, the intensity of the disturbance will decrease, and so will the degree of improvement in the capture conditions achievable with each stage of narrow-band limiting. When the frequency difference decreases to a value r_{\min} that is specifiable as a small fraction of the limiter-filter bandwidth, the extraneous modulation caused by the interference becomes sufficiently slow for the filter to follow it through quasi-stationary states, and the disturbance will pass through unabated. The closer the interference amplitude ratio approaches unity, the smaller the value of r_{\min} which marks the limit of noticeable improvement in the capture. An expression for r_{\min} , which follows from (2) and (3), is

$$r_{\min} = \rho \frac{1 - a}{1 + a} (BW)_{\text{lim}}, \quad (10)$$

where $\rho = 1/KB_{\text{lim}}$. In the range $0.4 < a < 1$, ρ may be taken as $\frac{2}{3}$ for a single-tuned circuit, and $\frac{1}{4}$ for a maximally flat double-tuned circuit.

¹¹ E. J. Baghdady, "FM-demodulator time-constant requirements for interference rejection," *PROC. IRE*, vol. 46, pp. 432-440; February, 1958.



Exact Ladder Network Design Using Low- Q Coils*

LOUIS WEINBERG†, SENIOR MEMBER, IRE

Summary—In preceding papers, tables were presented for the design of lossless networks terminated in resistance at one or both ends. Networks with uniform dissipation and a resistance termination only at the load end are considered in this paper. The tables give the element values of normalized low-pass ladders with one of the following characteristics: maximally flat magnitude (Butterworth), equal-ripple magnitude (Tchebycheff), and maximally flat time delay (Bessel polynomial). The low-pass to band-pass frequency transformation can be used on the Butterworth and Tchebycheff networks to yield the element values for the band-pass case.

INTRODUCTION

MOST of the practical synthesis procedures yield lossless networks terminated in resistance. Tables of element values for such networks have been presented in previously published papers.¹⁻⁴ Because of unavoidable dissipation in reactive elements, building the network to have the prescribed characteristics may be difficult. Though capacitors can be manufactured to have negligible dissipation, this is not true of coils. The parasitic resistances associated with the coils may introduce a discrepancy between the designed and the actual characteristics of a network. We can attempt, of course, to make the discrepancy negligible by the use of high- Q coils, but the concomitant increase in coil size and weight may be intolerable for many applications.

As discussed in the Appendix, there is a simple transformation of the frequency variable that permits parasitic losses to be taken into account in such a way that the *desired characteristic is realized exactly*. The method is called *predistortion*. It provides a series resistance with every inductance of the network, and a shunt conductance with every capacitance, without changing the shape of the magnitude or phase of the prescribed transfer function. The elements of the network are equally dissipative so that the network is said to possess *uniform dissipation*. The only change in the transfer function is in the constant multiplier. Thus a *flat loss* is introduced by the method.

* Original manuscript received by the IRE, October 30, 1957; revised manuscript received, December 18, 1957. This paper is based on the author's report of the same title, Hughes Res. Labs., Culver City, Calif., Tech. Memo. No. 482; February, 1957.

† Hughes Res. Labs., Culver City, Calif.

¹ L. Weinberg, "Network design by the use of modern synthesis techniques and tables," *Proc. Natl. Electronics Conf.*, vol. 12, pp. 794-817; 1956.

² —, "Additional tables for design of optimum ladder networks," *J. Franklin Inst.*, vol. 264, pp. 7-24, 127-138; July (Part I), August (Part II), 1957.

³ —, "Tables of networks whose reflection coefficients possess alternating zeros," *IRE TRANS. ON CIRCUIT THEORY*, vol. 4, pp. 313-320; December, 1957.

⁴ S. D. Bedrosian, E. L. Luke, and H. N. Putschi, "On the tabulation of insertion loss low-pass chain matrix coefficients and network elements values," *Proc. Natl. Electronic Conf.*, vol. 11, pp. 697-717; 1955.

The method is simple and it is exact. On the other hand, it has the undesirable effect in the low-pass case of introducing dissipation where it is not needed, namely, across the capacitances. This loss, however, is useful when the low-pass to band-pass transformation is used. It is of interest to mention, furthermore, that there is another exact transformation that yields one value of dissipation for the inductances and another for the capacitances. With this transformation, networks can be designed for zero dissipation across the capacitances. Such networks are exceedingly useful for the low-pass case, and tables for their design may be presented in a future paper.

As in the author's previous papers,¹⁻³ the tables give the element values for the reactances of a normalized low-pass filter with one of the following characteristics: Butterworth (maximally flat magnitude), Tchebycheff (equal-ripple magnitude), or Bessel polynomial (maximally flat time delay).^{1,2}

The impedance level of the networks given by the tables is normalized with respect to the load resistance, and the frequency is normalized with respect to the cutoff frequency for the Butterworth and Tchebycheff networks, and with respect to $\omega_0 \equiv 1/T_0$ (where T_0 is the zero-frequency time delay) for the maximally flat time-delay networks. It is assumed that the reader is familiar with the simple process for removing the normalizations; this also has been discussed.^{1,2}

The new feature of the networks given by the tables of this paper is the uniform dissipation. Each of the reactances has an associated dissipation; the reciprocal of the time constant of each reactance and its dissipation is given by d , where d is a constant representing the amount of frequency shift.

For each type of network four values of d have been tabulated—1/4, 1/10, 1/20, and 1/30. Thus, as shown in the Appendix, the corresponding Q 's of the coils and capacitors for the low-pass case are 4, 10, 20, and 30. Each table is therefore divided into four parts, one for each value of d . Table I gives the element values for the Butterworth networks; Tables II-VII give the Tchebycheff networks for the respective ripple factors of 1/10 db, 1/4 db, 1/2 db, 1 db, 2 db, and 3 db; and Table VIII gives the Bessel polynomial networks.

Inspection of the tables shows that networks are not given for certain values of n . As shown in the Appendix, in order for the uniformly dissipative network to exist, d must be less than the absolute value of the real part of the pole closest to the j axis. Networks omitted from the tabulation do not exist, that is, the value of d is too large for these cases.

TABLE I
ELEMENT VALUES (IN HENRYS, FARADS) FOR A NORMALIZED BUTTERWORTH FILTER WITH UNIFORM DISSIPATION

Value of n	C_1 or L'_1	L_2 or C'_2	C_3 or L'_3	L_4 or C'_4	C_5 or L'_5	L_6 or C'_6	C_7 or L'_7	L_8 or C'_8	C_9 or L'_9	L_{10} or C'_{10}
a) $d = 1/4$										
1	1.3333									
2	1.0938	1.2895								
3	0.8000	1.7857	1.1487							
4	0.6199	1.6087	2.0388	0.9400						
5	0.5035	1.3854	2.0032	2.4354	0.6558					
6	0.4231	1.1981	1.8176	2.4099	6.8653	0.1711				
b) $d = 1/10$										
1	1.1111									
2	0.8236	1.3979								
3	0.5882	1.4805	1.4020							
4	0.4518	1.2402	1.7006	1.3622						
5	0.3655	1.0385	1.5490	1.7947	1.3093					
6	0.3064	0.8860	1.3716	1.7141	1.8444	1.2496				
7	0.2636	0.7699	1.2168	1.5731	1.8131	1.8777	1.1845			
8	0.2312	0.6796	1.0880	1.4347	1.7035	1.8799	1.9076	1.1138		
9	0.2058	0.6077	0.9814	1.3109	1.5843	1.7936	1.9310	1.9425	1.0364	
10	0.1854	0.5493	0.8924	1.2029	1.4714	1.6915	1.8603	1.9760	1.9908	0.9508
c) $d = 1/20$										
1	1.0526									
2	0.7609	1.4104								
3	0.5405	1.4032	1.4570							
4	0.4144	1.1557	1.6356	1.4547						
5	0.3349	0.9609	1.4596	1.7399	1.4385					
6	0.2806	0.8168	1.2802	1.6266	1.7939	1.4168				
7	0.2413	0.7083	1.1296	1.4780	1.7267	1.8247	1.3923			
8	0.2116	0.6244	1.0066	1.3397	1.6074	1.7912	1.8439	1.3661		
9	0.1884	0.5578	0.9057	1.2190	1.4861	1.6961	1.8351	1.8566	1.3385	
10	0.1697	0.5038	0.8222	1.1153	1.3742	1.5915	1.7595	1.8666	1.8660	1.3098
d) $d = 1/30$										
1	1.0345									
2	0.7421	1.4126								
3	0.5263	1.3792	1.4726							
4	0.4033	1.1302	1.6155	1.4817						
5	0.3258	0.9377	1.4326	1.7241	1.4763					
6	0.2729	0.7962	1.2528	1.6008	1.7813	1.4652				
7	0.2347	0.6899	1.1035	1.4497	1.7027	1.8145	1.4513			
8	0.2058	0.6079	0.9822	1.3114	1.5796	1.7686	1.8351	1.4359		
9	0.1832	0.5430	0.8832	1.1917	1.4572	1.6692	1.8134	1.8485	1.4195	
10	0.1650	0.4903	0.8013	1.0891	1.3455	1.5628	1.7333	1.8453	1.8576	1.4025

TABLE II
ELEMENT VALUES (IN HENRYS, FARADS) FOR A NORMALIZED TCHEBYCHEFF FILTER WITH UNIFORM DISSIPATION
AND WITH 1/10-DB RIPPLE ($\epsilon = 0.1526$, $\epsilon^2 = 0.0233$)

Value of n	C_1 or L'_1	L_2 or C'_2	C_3 or L'_3	L_4 or C'_4	C_5 or L'_5	L_6 or C'_6	C_7 or L'_7	L_8 or C'_8	C_9 or L'_9	L_{10} or C'_{10}
a) $d = 1/4$										
1	0.1587									
2	0.5341	0.6727								
3	0.8412	1.2730	0.8597							
4	1.2441	1.9137	4.0539	0.2242						
b) $d = 1/10$										
1	0.8115									
2	0.4603	0.7038								
3	0.6102	1.1529	1.0200							
4	0.7124	1.3481	1.5466	1.0350						
5	0.8039	1.4838	1.7814	1.6228	1.0093					
6	0.8991	1.6081	1.9948	1.9737	2.1632	0.6018				

TABLE II (Cont'd)

c) $d = 1/20$									
1	0.0382								
2	0.4401	0.7106							
3	0.5590	1.1192	1.0575						
4	0.6235	1.2689	1.4957	1.1519					
5	0.6694	1.3532	1.6427	1.5931	1.2285				
6	0.7081	1.4139	1.7297	1.7237	1.7362	1.1565			
7	0.7445	1.4646	1.7972	1.7990	1.8923	1.7058	1.1312		
8	0.7806	1.5113	1.8587	1.8605	2.0001	1.9024	1.8625	0.9132	
9	0.8179	1.5569	1.9210	1.9243	2.1215	2.1300	2.6566	8.2810	0.1218
d) $d = 1/30$									
1	0.1534								
2	0.4337	0.7125							
3	0.5438	1.1082	1.0688						
4	0.5986	1.2449	1.4821	1.1853					
5	0.6340	1.3164	1.6108	1.5923	1.2826				
6	0.6613	1.3639	1.6801	1.7033	1.7273	1.2513			
7	0.6850	1.4006	1.7283	1.7601	1.8439	1.7086	1.2764		
8	0.7070	1.4319	1.7674	1.7987	1.9057	1.8228	1.7982	1.1840	
9	0.7285	1.4605	1.8023	1.8300	1.9516	1.8829	1.9414	1.7419	1.1516
10	0.7499	1.4877	1.8355	1.8585	1.9935	1.9319	2.0349	1.9337	1.8632
									0.9453

TABLE III

ELEMENT VALUES (IN HENRYS, FARADS) FOR A NORMALIZED TCHEBYCHEFF FILTER WITH UNIFORM DISSIPATION AND WITH 1/4-DB RIPPLE ($\epsilon = 0.2434$, $\epsilon^2 = 0.0593$)

Value of n	C_1 or L'_1	L_2 or C'_2	C_3 or L'_3	L_4 or C'_4	C_5 or L'_5	L_6 or C'_6	C_7 or L'_7	L_8 or C'_8	C_9 or L'_9	L_{10} or C'_{10}
a) $d = 1/4$										
1	0.2592									
2	0.7712	0.7507								
3	1.2748	1.4258	0.8796							
b) $d = 1/10$										
1	0.2495									
2	0.6263	0.8212								
3	0.8101	1.2820	1.1346							
4	0.9513	1.4755	1.7337	1.0044						
5	1.0562	1.6100	2.0236	1.6700	0.9551					
c) $d = 1/20$										
1	0.2464									
2	0.5894	0.8372								
3	0.7223	1.2513	1.1841							
4	0.7993	1.3924	1.6506	1.1728						
5	0.8356	1.4620	1.7869	1.6171	1.2754					
6	0.9139	1.5316	1.9053	1.7467	1.8426	1.1019				
7	0.9687	1.5834	1.9924	1.8314	2.0528	1.6958	1.0781			
8	1.0260	1.6338	2.0842	1.9233	2.2897	2.1966	2.9454	0.4173		
d) $d = 1/30$										
1	0.5780									
2	0.2454	1.9826								
3	0.6971	1.2409	1.1985							
4	0.7588	1.3680	1.6311	1.2189						
5	0.7812	1.4237	1.7433	1.6234	1.3409					
6	0.8374	1.4786	1.8323	1.7284	1.8225	1.2297				
7	0.8703	1.5140	1.8857	1.7814	1.9504	1.6921	1.3000			
8	0.9025	1.5450	1.9325	1.8192	2.0259	1.8151	1.8740	1.1083		
9	0.9350	1.5742	1.9777	1.8534	2.0934	1.8977	2.0877	1.7240	1.0557	
10	0.9686	1.6028	2.0245	1.8899	2.1721	2.0051	2.3880	2.5688	20.2841	0.0495

TABLE IV
ELEMENT VALUES (IN HENRYS, FARADS) FOR A NORMALIZED TCHEBYCHEFF FILTER WITH UNIFORM DISSIPATION
AND WITH 1/2-DB RIPPLE ($\epsilon=0.3493$, $e^2=0.1220$)

Value of n	C_1 or L'_1	L_2 or C'_2	C_3 or L'_3	L_4 or C'_4	C_5 or L'_5	L_6 or C'_6	C_7 or L'_7	L_8 or C'_8	C_9 or L'_9
a) $d = 1/4$									
1	0.3827								
2	1.0804	0.7573							
3	1.9884	1.6160	0.7886						
b) $d = 1/10$									
1	0.3620								
2	0.8159	0.8858							
3	1.0494	1.3379	1.2414						
4	1.2541	1.5269	1.9539	0.9135					
5	1.4870	1.7002	2.5769	1.9821	0.6738				
c) $d = 1/20$									
1	0.3555								
2	0.7544	0.9159							
3	0.9067	1.3208	1.3008						
4	1.0026	1.4502	1.8057	1.1475					
5	1.0840	1.5233	1.9821	1.5832	1.3370				
6	1.1639	1.5795	2.1110	1.7194	1.9796	0.9976			
7	1.2481	1.6319	2.2453	1.8434	2.3758	1.7639	0.8758		
d) $d = 1/30$									
1	0.3534								
2	0.7359	0.9246							
3	0.8674	1.3144	1.3172						
4	0.9398	1.4301	1.7759	1.2083					
5	0.9942	1.4893	1.9129	1.6030	1.4189				
6	1.0426	1.5295	1.9944	1.7007	1.9329	1.1723			
7	1.0895	1.5619	2.0606	1.7517	2.0856	1.6307	1.3257		
8	1.1371	1.5912	2.1243	1.7936	2.1978	1.7816	1.9902	0.9693	
9	1.1868	1.6198	2.1924	1.8411	2.3366	1.9774	2.6692	2.5435	0.4897

TABLE V
ELEMENT VALUES (IN HENRYS, FARADS) FOR A NORMALIZED TCHEBYCHEFF FILTER WITH UNIFORM DISSIPATION
AND WITH 1-DB RIPPLE ($\epsilon=0.5088$, $e^2=0.2589$)

Value of n	C_1 or L'_1	L_2 or C'_2	C_3 or L'_3	L_4 or C'_4	C_5 or L'_5	L_6 or C'_6	C_7 or L'_7	L_8 or C'_8
a) $d = 1/4$								
1	0.5830							
2	1.6730	0.6712						
b) $d = 1/10$								
1	0.5361							
2	1.1139	0.8953						
3	1.4528	1.3136	1.3923					
4	1.8089	1.5093	2.4122	0.7061				
c) $d = 1/20$								
1	0.5221							
2	1.0023	0.9501						
3	1.1928	1.3263	1.4641					
4	1.3284	1.4371	2.0457	1.0581				
5	1.4560	1.4998	2.2818	1.4716	1.4202			
6	1.5917	1.5532	2.5065	1.6573	2.3074	0.7568		

TABLE V (Cont'd)

d) $d = 1/30$									
1	0.5176								
2	0.9699	0.9663							
3	1.1257	1.3297	1.4810						
4	1.2203	1.4284	1.9913	1.1412					
5	1.2984	1.4769	2.1529	1.5099	1.5351				
6	1.3732	1.5096	2.2623	1.6008	2.1287	1.0487			
7	1.4497	1.5370	2.3656	1.6584	2.3606	1.5002	1.3379		
8	1.5311	1.5638	2.4820	1.7308	2.6649	1.9214	2.9594	0.4545	

TABLE VI

ELEMENT VALUES (IN HENRYS, FARADS) FOR A NORMALIZED TCHEBYCHEFF FILTER WITH UNIFORM DISSIPATION AND WITH 2-DB RIPPLE ($\epsilon = 0.7648$, $\epsilon^2 = 0.5849$)

Value of n	C_1 or L'_1	L_2 or C'_2	C_3 or L'_3	L_4 or C'_4	C_5 or L'_5	L_6 or C'_6	C_7 or L'_7
a) $d = 1/4$							
1	0.9456						
2	3.2915	0.4438					
b) $d = 1/10$							
1	0.8281						
2	1.6561	0.8022					
3	2.2840	1.1616	1.6313				
4	3.1624	1.5299	7.1328	0.1745			
c) $d = 1/20$							
1	0.7952						
2	1.4208	0.8962					
3	1.7012	1.2149	1.7435				
4	1.9372	1.3007	2.5116	0.8636			
5	2.1908	1.3573	2.9752	1.2645	1.4823		
d) $d = 1/30$							
1	0.7848						
2	1.3566	0.9245					
3	1.5678	1.2360	1.7576				
4	1.7156	1.3105	2.3862	0.9815			
5	1.8526	1.3444	2.6232	1.3018	1.7516		
6	1.9951	1.3686	2.8298	1.4014	2.5579	0.7977	
7	2.1517	1.3943	3.0891	1.5507	3.5806	2.0400	0.6235

TABLE VII

ELEMENT VALUES (IN HENRYS, FARADS) FOR A NORMALIZED TCHEBYCHEFF FILTER WITH UNIFORM DISSIPATION AND WITH 3-DB RIPPLE ($\epsilon = 0.9976$, $\epsilon^2 = 0.9953$)

Value of n	C_1 or L'_1	L_2 or C'_2	C_3 or L'_3	L_4 or C'_4	C_5 or L'_5	L_6 or C'_6
a) $d = 1/4$						
1	1.3291					
2	6.9013	0.2378				
b) $d = 1/10$						
1	1.1082					
2	2.2477	0.6808				
3	3.3643	1.0200	1.7908			
c) $d = 1/20$						
1	1.0500					
2	1.8352	0.8034				
3	2.2359	1.0737	2.0265			
4	2.6207	1.1480	3.0638	0.6797		
5	3.0817	1.2251	4.2145	1.3540	1.0683	

TABLE VII (Cont'd)

d) $d = 1/30$

1	1.0319											
2	1.7294	0.8410										
3	2.0111	1.1078	2.0378									
4	2.2309	1.1658	2.8163	0.8286								
5	2.4520	1.1924	3.1791	1.1130	1.9485							
6	2.6976	1.2178	3.6020	1.2898	3.3258	0.4981						

TABLE VIII

ELEMENT VALUES (IN HENRYS, FARADS) FOR A NORMALIZED MAXIMALLY FLAT TIME-DELAY NETWORK WITH UNIFORM DISSIPATION

Value of n C_1 or L'_1 L_2 or C'_2 C_3 or L'_3 L_4 or C'_4 C_5 or L'_5 L_6 or C'_6 C_7 or L'_7 L_8 or C'_8 C_9 or L'_9 L_{10} or C'_{10} C_{11} or L'_{11}

a) $d = 1/4$

1	1.3333											
2	0.4000	1.0811										
3	0.1905	0.5263	0.8593									
4	0.1111	0.3157	0.4864	0.7199								
5	0.0727	0.2102	0.3279	0.4337	0.6271							
6	0.0513	0.1498	0.2373	0.3117	0.3885	0.5612						
7	0.0381	0.1120	0.1795	0.2380	0.2897	0.3522	0.5119					
8	0.0294	0.0869	0.1404	0.1880	0.2292	0.2683	0.3232	0.4735				
9	0.0234	0.0693	0.1127	0.1522	0.1867	0.2175	0.2495	0.2996	0.4425			
10	0.0190	0.0566	0.0923	0.1254	0.1554	0.1816	0.2052	0.2325	0.2802	0.4170		
11	0.0158	0.0470	0.0771	0.1053	0.1309	0.1537	0.1740	0.1937	0.2186	0.2642	0.3954	

b) $d = 1/10$

1	1.1111											
2	0.3571	1.0332										
3	0.1754	0.4978	0.8445									
4	0.1042	0.2997	0.4721	0.7146								
5	0.0690	0.2007	0.3172	0.4265	0.6250							
6	0.0490	0.1438	0.2295	0.3050	0.3848	0.5603						
7	0.0366	0.1080	0.1740	0.2324	0.2855	0.3502	0.5116					
8	0.0284	0.0841	0.1363	0.1835	0.2253	0.2657	0.3221	0.4734				
9	0.0227	0.0673	0.1097	0.1486	0.1832	0.2147	0.2478	0.2990	0.4425			
10	0.0185	0.0551	0.0900	0.1226	0.1525	0.1790	0.2034	0.2315	0.2799	0.4170		
11	0.0154	0.0459	0.0753	0.1030	0.1285	0.1514	0.1721	0.1924	0.2180	0.2640	0.3955	

c) $d = 1/20$

1	1.0526											
2	0.3448	1.0167										
3	0.1709	0.4888	0.8391									
4	0.1020	0.2947	0.4674	0.7124								
5	0.0678	0.1977	0.3137	0.4240	0.6241							
6	0.0483	0.1419	0.2271	0.3028	0.3834	0.5599						
7	0.0362	0.1067	0.1722	0.2306	0.2841	0.3495	0.5114					
8	0.0281	0.0832	0.1350	0.1821	0.2240	0.2648	0.3217	0.4733				
9	0.0224	0.0666	0.1087	0.1475	0.1821	0.2138	0.2473	0.2988	0.4424			
10	0.0183	0.0546	0.0893	0.1217	0.1515	0.1782	0.2028	0.2312	0.2798	0.4170		
11	0.0153	0.0455	0.0747	0.1023	0.1277	0.1506	0.1714	0.1920	0.2178	0.2640	0.3955	

d) $d = 1/30$

1	1.0345											
2	0.3409	1.0111										
3	0.1695	0.4858	0.8372									
4	0.1014	0.2931	0.4658	0.7117								
5	0.0674	0.1967	0.3125	0.4232	0.6238							
6	0.0481	0.1412	0.2262	0.3020	0.3830	0.5598						
7	0.0360	0.1063	0.1716	0.2300	0.2837	0.3492	0.5113					
8	0.0280	0.0829	0.1346	0.1816	0.2236	0.2645	0.3215	0.4732				
9	0.0224	0.0664	0.1084	0.1471	0.1818	0.2135	0.2471	0.2987	0.4424			
10	0.0183	0.0544	0.0890	0.1214	0.1512	0.1779	0.2025	0.2311	0.2797	0.4170		
11	0.0152	0.0454	0.0745	0.1020	0.1274	0.1504	0.1712	0.1918	0.2177	0.2639	0.3955	

For the Butterworth characteristic, the absolute value of the real part of the pole closest to the j axis becomes *smaller* as n increases. Thus if d is too large for $n = x$, all networks for $n > x$ will also not exist. The same property holds for the Tchebycheff networks. In addition, for a fixed value of n , the pole closest to the j axis of a Tchebycheff transfer function moves closer as the ripple factor increases. Thus it is possible to tabulate more networks for the smaller ripple factors. For the Bessel polynomial networks no difficulty occurs; all the networks exist for the four values of d used in this paper. Unlike the Butterworth and Tchebycheff cases, the absolute value of the real part of the pole closest to the j axis becomes *larger* as n increases. Since for $n = 1$ the pole lies at $s = -1$, networks exist for all values of n if d is chosen smaller than unity. These properties of the poles of the different functions may be derived analytically or may be verified by consulting the previous tabulations¹ of the poles.

In the previous tables,¹⁻³ a number of values of the input-to-output resistance ratio were used for the tabulation. For these dissipative networks, however, resistance terminations at both ends were not considered essential. Therefore, all the networks possess a resistance termination only at the load end (the resistance, of course, being normalized to one ohm). The reader should note that this does not mean an ideal voltage or current source must always be used. When a generator resistance is also required, it may be *supplied by part of the dissipation associated with the first reactance on the input side of the network*.

The element values of band-pass networks may be obtained by the low-pass to band-pass transformation. If necessary, the reader should consult the references for a discussion of this transformation, and also for discussions of the duality and reciprocity theorems. These theorems help to convert the networks of the tables to alternative practical configurations. There are, of course, other techniques for converting the networks to forms that can be built more easily. To cite just one example, it may be found that in a band-pass network, the coil in the series arm is so large that its self-resonance frequency may cause difficulty; tapping down on the shunt coils on either side of the series arm, with appropriate changes in the element values of the series arm, may eliminate the difficulty. Most of these techniques, however, may be found in filter textbooks and therefore are not discussed further here.

In the first part of the paper we discuss how to use the tables to design low-pass uniformly dissipative networks, and then show how to obtain band-pass networks in which the *capacitors have no dissipation and the coils have uniform dissipation*. In the second part two examples are given to illustrate the use of the tables. The Appendix is devoted to the derivation of the formulas and the procedure used to generate the tables. The steps for using the tables can be followed without knowledge of their derivation, but for a complete under-

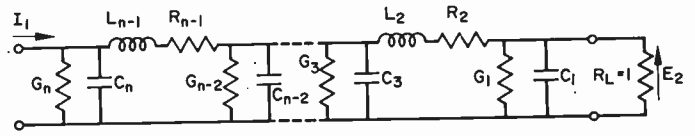


Fig. 1—General form of low-pass ladder network with a current-source input and n odd.

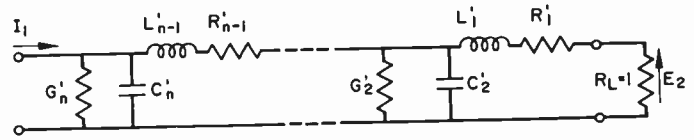


Fig. 2—General form of low-pass ladder network with a current-source input and n even.

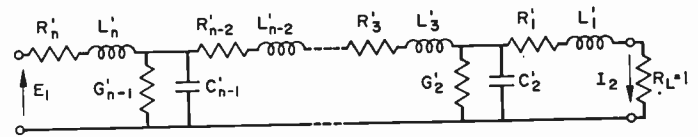


Fig. 3—General form of low-pass ladder network with a voltage-source input and n odd.

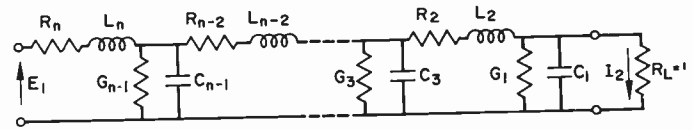


Fig. 4—General form of low-pass ladder network with a voltage-source input and n even.

standing of these steps it is recommended that the Appendix be read first.

USE OF THE TABLES

The elements in the columns of the tables are either primed or unprimed. The primed elements give networks that are duals of the networks given by the unprimed elements. This allows both transfer impedances and transfer admittances (or transfer voltage ratios) to be realized. When a current source is to be used, the transfer impedance $Z_{21} \equiv E_2/I_1$ is required; transfer admittance $Y_{21} \equiv I_2/E_1$ applies for a voltage-source input.

The network forms obtained for Z_{21} from the tables of element values are shown in Figs. 1 and 2.

1) For n odd the *unprimed* tabulated values yield the network of Fig. 1 with a current-source input and a voltage output. The values of the L 's and C 's are given by the tables. The values of the resistances associated with the coils and the conductances associated with the capacitors are given by the d of each table. The constant d is equal to the reciprocal of the time constant, that is, $d = R_v/L_v = G_\mu/C_\mu$. Thus, $R_v = dL_v$ ohms and $G_\mu = dC_\mu$ mhos.

2) For n even the *primed* tabulated values yield the network of Fig. 2. As in 1), d is the reciprocal of the time constant so that $R_v' = dL_v'$ ohms and $G_\mu' = dC_\mu'$ mhos.

For the transfer admittance Y_{21} the network forms are shown in Figs. 3 and 4, which are the respective duals of the networks in Figs. 1 and 2.

1) For n odd the primed values yield the network shown in Fig. 3. Again, $R_v' = dL_v'$ ohms and $G_\mu' = dC_\mu'$ mhos.

2) For n even the unprimed values yield the network of Fig. 4. As before, the d of the table that is used yields the resistance and conductance values: $R_v = dL_v$ ohms and $G_\mu = dC_\mu$ mhos.

Each of the networks is shown driven by an ideal source. However, when a finite and nonzero generator resistance is required, part or all of the dissipation associated with the last reactance on the left may be assigned as the resistance of the source. For example, G_n in Fig. 1 may be used as the generator resistance so that the capacitance C_n must now be furnished by a lossless capacitor.

It is also possible to use Thévenin's or Norton's theorem to effect a source conversion and thus obtain new network configurations. For example, Thévenin's theorem applied to G_n and the current source in Fig. 1 yields a voltage source and a series resistance. In this way a transfer admittance or transfer voltage ratio may be realized with shunt capacitance branches at both ends of the coupling network.

It is shown in the Appendix that the Q of each of the reactors used in the low-pass network (henceforth designated by Q_{LP}) is equal to $1/d$, where Q_{LP} is defined at the cutoff frequency ω_{co} . In symbols,

$$Q_{LP} = \omega_{co} L_v'' / R_v'' = G_\mu'' / (\omega_{co} C_\mu''), \quad (1)$$

where the double primes have been used to designate the element values after the removal of the frequency and impedance normalizations.

For the band-pass case a capacitance is added in series with each inductance in the low-pass network, and an inductance is added in parallel with each capacitance. The quality factor of the coils defined at the center frequency ω_0 , i.e., $Q_{BP} = \omega_0 L_v'' / R_v''$, is then given by (5), which is repeated below for convenience:

$$Q_{BP} = Q_{\text{circuit}} Q_{LP}, \quad (2)$$

where Q_{circuit} is defined as $\omega_0 / (\omega_b - \omega_a)$ or, equivalently, ω_0 / ω_{co} . Here ω_b and ω_a are the respective upper and lower frequency limits of the pass band.

One more equation is needed before the design of a filter can be carried out, namely, the equation for the calculation of the flat loss introduced by the uniform dissipation. This is given by (11) as

$$\text{loss (db)} = -20 \log (b_0/a_0). \quad (3)$$

The reader should consult the Appendix for the derivation and use of this equation.

Except for the choice of the shift d , the methods for determining whether a Butterworth, Tchebycheff, or Bessel polynomial filter is appropriate, and the calculation of the required value of n , are the same as in the previous papers on tabulated ladder networks. In a typical problem, one part of the specifications will give

the maximum Q_{LP} or Q_{BP} , or the maximum flat loss that can be tolerated. From this specification and the use of (1), (2), or (3), the table with the required value of d can be chosen. The procedure is illustrated in the examples below.

ILLUSTRATIVE EXAMPLES

In this section, two examples are given that illustrate the use of the tables. So that a comparison can be made between the previously tabulated networks containing lossless reactances and the ones derived below, the first example incorporates the specifications of Example 2-1.¹ Of course, we add a specification that determines the amount of dissipation. The second example uses some of the data of Example 3-1¹ so that a comparison is also possible here.

Example 1

We wish to design a low-pass filter that has a resistance termination only at the output. The filter is to be of the Butterworth type with a cutoff frequency $\omega_{co} = 10,000$ radians/second and an output resistance of 750 ohms. At a frequency $\omega = 3\omega_{co}$ the magnitude response is to be down at least 50 db from its zero-frequency value. The input source is a cathode follower which approximates an ideal voltage source. The Q_{LP} of the coils is not to be greater than 25.

The value of n is determined in the usual way by the specification in the attenuation band:

$$\begin{aligned} \frac{1}{1 + \omega^{2n}} \Big|_{\omega=3} &= 10^{-5}, \\ (1 + \omega^{2n}) \Big|_{\omega=3} &= 10^5, \\ 3^{2n} &\cong 10^5, \\ n &= 5.23. \end{aligned}$$

Thus the next larger integer $n = 6$ is used.

Because $Q_{LP} \leq 25$ all values of d except $d = 1/30$ are acceptable. We show two alternative designs by using Table I(b) and (c) corresponding to $d = 1/10$ and $d = 1/20$, respectively.

Since the input is a voltage source and n is even, the network form of Fig. 4 is applicable. We therefore use the unprimed values of Table I(b) and (c) to obtain the following normalized element values:

$d = 1/10$	$d = 1/20$
$C_1 = 0.3064$	$C_1 = 0.2806$
$L_2 = 0.8860$	$L_2 = 0.8168$
$C_3 = 1.3716$	$C_3 = 1.2802$
$L_4 = 1.7141$	$L_4 = 1.6266$
$C_5 = 1.8444$	$C_5 = 1.7939$
$L_6 = 1.2496$	$L_6 = 1.4168$

Using the relationships $R_v = dL_v$ ohms and $G_\mu = dC_\mu$ mhos yields the normalized resistances and conductances:

$d = 1/10$ $d = 1/20$

$G_1 = 0.0306$	$G_1 = 0.0281$
$R_2 = 0.0886$	$R_2 = 0.0817$
$G_3 = 0.1372$	$G_3 = 0.1280$
$R_4 = 0.1714$	$R_4 = 0.1627$
$G_5 = 0.1844$	$G_5 = 0.1794$
$R_6 = 0.1250$	$R_6 = 0.1417$

To achieve a load resistance R_L of 750 ohms, we multiply all R 's and L 's by $R_L = 750$ and divide all G 's and C 's by 750. To change the cutoff frequency to $\omega_{co} = 10,000$ radians/second every L and C must be divided by this value.

The final values, designated by double primes, are therefore:

$d = 1/10$

$C_1'' = 4.09 \times 10^{-8}$	$G_1'' = 4.09 \times 10^{-5}$
$L_2'' = 6.65 \times 10^{-2}$	$R_2'' = 66.5$
$C_3'' = 1.83 \times 10^{-7}$	$G_3'' = 1.83 \times 10^{-4}$
$L_4'' = 1.29 \times 10^{-1}$	$R_4'' = 129$
$C_5'' = 2.46 \times 10^{-7}$	$G_5'' = 2.46 \times 10^{-4}$
$L_6'' = 9.37 \times 10^{-2}$	$R_6'' = 93.7$

$d = 1/20$

$C_1'' = 3.74 \times 10^{-8}$	$G_1'' = 3.74 \times 10^{-5}$
$L_2'' = 6.13 \times 10^{-2}$	$R_2'' = 61.3$
$C_3'' = 1.71 \times 10^{-7}$	$G_3'' = 1.71 \times 10^{-4}$
$L_4'' = 1.22 \times 10^{-1}$	$R_4'' = 122$
$C_5'' = 2.39 \times 10^{-7}$	$G_5'' = 2.39 \times 10^{-4}$
$L_6'' = 1.06 \times 10^{-1}$	$R_6'' = 106$

The network is shown in Fig. 5.

It is pointed out in passing that since G_1 serves no real purpose here, it is possible to increase the gain of the network by combining G_1 with the normalized load resistance $G_L = 1/R_L = 1$. This gives a load resistance of $R = 1/1.031$ for $d = 1/10$ and $R = 1/1.028$ for $d = 1/20$. Now to remove the impedance normalization the factor to be used in place of 750 is 750×1.031 for $d = 1/10$ and 750×1.028 for $d = 1/20$.

The flat loss of the network in Fig. 5 is now calculated for each value of d . For the Butterworth polynomials $a_0 = 1$. To evaluate b_0 we first consult Table 2.2' for the coefficients of the Butterworth polynomial of the sixth degree. We find $q(-1/10) = 0.680$ and $q(-1/20) = 0.825$. Thus the flat loss for $d = 1/10$ is 3.4 db, and for $d = 1/20$ the loss is 1.7 db.

Example 2

A ladder network is desired with the following properties.

- 1) The network is to be a band-pass filter with a peak-to-peak ripple in the squared magnitude characteristic not exceeding 15 per cent of the maximum value.

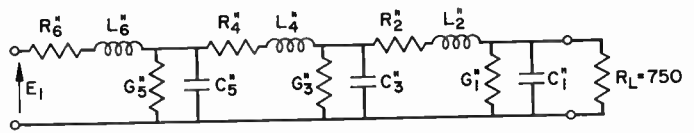


Fig. 5—Network obtained for Example 1. (Values of R , G , L , and C are in ohms, mhos, henrys, and farads, respectively.)

2) The pass band has a bandwidth $\omega_{co} \equiv \omega_b - \omega_a = 5000$ radians/second (the bandwidth being measured at the minimum value of the ripple).

3) The center frequency ω_0 is equal to 100,000 radians/second.

4) A resistance termination of 1000 ohms is required only at the load end.

5) The response is to be down at least 50 db at $\omega = 4\omega_{co}$.

6) The network is to be driven by a pentode which approximates a current source.

7) The Q_{BP} of the coils must not exceed 250.

The required value of ϵ^2 is first calculated. At a trough of the ripple we have

$$\frac{1}{1 + \epsilon^2 T_n^2(1)} = 1 - 0.15$$

$$= 0.85$$

$$1 + \epsilon^2 = \frac{20}{17}$$

$$\epsilon^2 = 0.176.$$

Since this value lies between $\frac{1}{2}$ -db and 1-db ripple, Table IV must be used.

Next we calculate n . At $\omega = 4$

$$\frac{1}{1 + \epsilon^2 T_n^2(4)} = 10^{-5}$$

$$\epsilon^2 T_n^2(4) \cong 10^5$$

$$T_n(4) = 753.$$

We now use an equation expressing the attenuation of the Tchebycheff curve to calculate n :

$$\frac{(\omega + \sqrt{\omega^2 + 1})^n + (\omega + \sqrt{\omega^2 - 1})^{-n}}{2} \Big|_{\omega=4} = 753$$

$$(\omega + \sqrt{\omega^2 - 1})^n \Big|_{\omega=4} \cong 1506$$

$$(7.88)^n = 1506$$

$$n = 3.58.$$

Therefore, $n = 4$ is used.

Consulting Table IV shows that the network for $n = 4$ exists when $d = 1/10$. We now check whether this value of d satisfies the requirements on Q_{BP} . Since $Q_{circuit} = \omega_0/\omega_{co} = 10^5/(5 \times 10^3) = 20$ and $Q_{LP} = 1/d = 10$, we have by use of (2), $Q_{BP} = 20 \times 10 = 200$. Therefore, use of Table IV(b) is satisfactory for this requirement.

Consulting Table IV(b) for $n = 4$ gives the normalized

values for the low-pass network; we use the primed values and the configuration of Fig. 2 since the input is a current source and n is even. Removing the normalizations by multiplying all C 's by

$$\frac{1}{R_L \omega_c} = \frac{1}{5 \times 10^6},$$

all L 's by $R_L/\omega_c = \frac{1}{5}$, all R 's by $R_L = 1000$, and all G 's by $1/R_L = 10^{-3}$, we obtain

$$L_1'' = \frac{1}{5} L_1' = 0.251 \quad R_1'' = 1000 R_1' = 126$$

$$C_2'' = \frac{1}{5 \times 10^6} C_2' = 0.305 \times 10^{-6} \quad G_1'' = 10^{-3} \times G_2' = 153 \times 10^{-6}$$

$$L_3'' = \frac{1}{5} L_3' = 0.391 \quad R_3'' = 1000 R_3' = 196$$

$$C_4'' = \frac{1}{5 \times 10^6} C_4' = 0.183 \times 10^{-6} \quad G_4'' = 10^{-3} \times G_4' = 92 \times 10^{-6}.$$

The transformation to a band-pass network is now made by causing each of the L 's and C 's of the low-pass network to resonate at ω_0 : a capacitance is added in series with each L , and an inductance in parallel with each C . The values of these additional elements are

$$C_1'' = \frac{1}{\omega_0^2 L_1''} = 3.98 \times 10^{-10}$$

$$L_2'' = \frac{1}{\omega_0^2 C_2''} = 3.28 \times 10^{-4}$$

$$C_3'' = \frac{1}{\omega_0^2 L_3''} = 2.56 \times 10^{-10}$$

$$L_4'' = \frac{1}{\omega_0^2 C_4''} = 5.46 \times 10^{-4}.$$

The network is shown in Fig. 6. The Q_{BP} of each of the shunt and series coils is 200.

CONCLUSION

The tables of this paper make possible the design of a uniformly dissipative ladder network with a maximally flat, an equal ripple, or a maximally flat time-delay characteristic. The tabulated element values apply to the normalized low-pass network. The corresponding band-pass networks may be obtained by a simple transformation of the low-pass networks.

APPENDIX

Here we briefly explain the procedure used to design uniformly dissipative networks.^{5,6} First, the frequency shift called predistortion, namely, the substitution of

⁵ H. W. Bode, "Network Analysis and Feedback Amplifier Design," D. Van Nostrand Co., New York, N. Y., pp. 216-222; 1945.

⁶ S. Darlington, "Synthesis of reactance 4-poles which produce prescribed insertion loss characteristics," *J. Math. Phys.*, vol. 18, pp. 336-340; 1939.

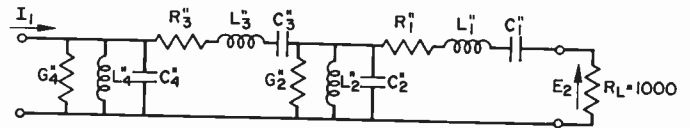


Fig. 6—Network realizing the data of Example 2. (Values of R , G , L , and C are in ohms, mhos, henrys, and farads, respectively.)

$s-d$ for s , is considered and its effect on the network made clear. This discussion yields the relationship between the shift d and the Q of the reactors for the low-pass network. The derivation of the corresponding relationship for the band-pass network is also shown. Next, the simple expression for calculating the flat loss is derived. The Appendix concludes with an outline of the complete synthesis procedure used to generate the tables of this paper.

Any transfer function of a network may be obtained by the proper combination of the driving-point functions of the network elements. The truth of this becomes clear when a transfer impedance or admittance is evaluated as the ratio of a cofactor and the determinant of the Kirchhoff equilibrium equations for the network. Thus, the effect of a frequency transformation on a transfer function can be determined from its effect on the element driving-point functions.

What is the effect on a network when s is replaced by $s+d$, where s is the complex frequency variable and d is a positive constant? Since the impedance of a resistance does not depend on frequency, the resistances of a network are not changed by the transformation. The impedances of an inductance L_v and a capacitance C_μ , however, are frequency dependent, being given respectively by $L_v s$ and $1/(C_\mu s)$. If s is changed to $s+d$, these impedances become $L_v(s+d)$ and $1/[C_\mu(s+d)]$. As shown in Fig. 7 the first represents the impedance of an inductance L_v in series with a resistance $R_v = dL_v$, whereas the second is the impedance of a capacitance C_μ in parallel with a conductance $G_\mu = dC_\mu$. The constant d is thus equal to the reciprocal of the time constant of each impedance, $d = R_v/L_v = G_\mu/C_\mu$. For ω equal to unity, d represents the resistance-reactance ratio associated with each inductive impedance, and the conductance-susceptance ratio associated with each capacitive impedance.

As will be seen later, the above transformation of $s+d$ for s is used to remove the effect of an original predistortion transformation. Therefore, if a resistance-terminated lossless network has been designed to give a predistorted low-pass filter characteristic with $\omega = 1$ as the cutoff frequency, then the removal of the predistortion makes d equal to $1/Q$ for each coil and capacitor, where Q , defined at the cutoff frequency, is L_v/R_v or G_μ/C_μ . When the frequency normalization is removed, $\omega = 1$ becomes the cutoff frequency $\omega = \omega_{co}$, and L_v becomes L_v/ω_{co} . If the Q of the coils is again defined at the cutoff frequency, then $Q = \omega_{co}(L_v/\omega_{co})/R_v = L_v/R_v$. Thus the relationship between d and Q continues to hold after

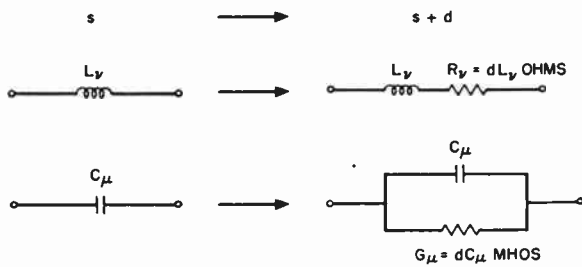


Fig. 7—Conversion of reactances when $s+d$ is substituted for s .

the frequency normalization is removed. The equality of the Q 's of the elements leads to the designation of such a network as uniformly dissipative.

For the band-pass filter, obtained by a frequency transformation from the low-pass case, a relation between the shift d and the required Q of the coils (both the coil in the series arm and the coil added across the capacitance in the shunt arm) also exists. Since different Q 's must be used in the analysis, it is convenient to designate the Q for the low-pass filter discussed in the preceding paragraph by Q_{LP} . We further designate the coil Q we wish to use in each branch of the band-pass filter by Q_{BP} and the Q of the band-pass magnitude curve by $Q_{circuit}$. If we let L_v'' and R_v'' designate the inductance and resistance values after the frequency and impedance normalizations have been removed, then in terms of these quantities,

$$Q_{LP} = \frac{1}{d} = \frac{\omega_{co}L_v''}{R_v''}$$

Finally, we use the conventional definitions

$$Q_{BP} = \frac{\omega_0 L_v''}{R_v''}$$

$$\omega_0 = \sqrt{\omega_a \omega_b}$$

$$Q_{circuit} = \frac{\omega_0}{\omega_b - \omega_a}$$

$$= \frac{\omega_0}{\omega_{co}} \tag{4}$$

where $\omega_b - \omega_a = \omega_{co}$ defines the bandwidth of the band-pass filter and ω_0 is its center frequency. By straightforward manipulations of Q_{BP} , we have

$$Q_{BP} = \frac{\omega_0 \omega_{co} L_v''}{\omega_{co} R_v''}$$

$$= Q_{circuit} Q_{LP} \tag{5}$$

Therefore, if we have a small percentage bandwidth filter, the required Q_{BP} of the coils will be large. For example, if $d = \frac{1}{4}$ and thus $Q_{LP} = 4$, and $Q_{circuit} = 50$, the coil Q_{BP} will be 200. Expressed in another way, the tables in this paper cannot be used for a band-pass filter with a percentage bandwidth of less than 2 per cent if the Q of the coils is limited to 200.

The above analysis is in terms of the coil in the series

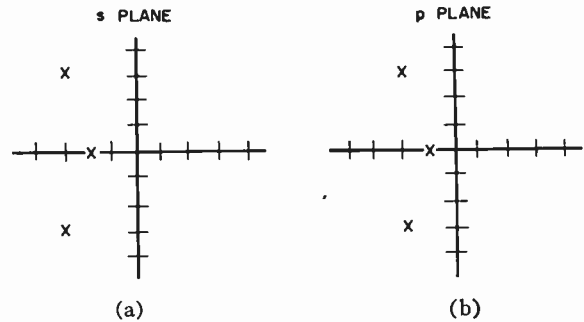


Fig. 8—Movement of critical frequencies as a result of predistortion. (a) Poles of Z_{21} in s plane. (b) Poles of Z_{21}^T in p plane.

arm of the network. The same results can be obtained for the parallel capacitance-conductance combination in the shunt arm. But when $Q_{BP} \geq 10$, the conductance across the shunt capacitance may be completely assigned as the loss of the parallel coil that is introduced by the transformation to a band-pass network.⁷ Thus the Q_{BP} of the coils in the shunt branches is also given by (5).

Now suppose we desire to realize a prescribed low-pass transfer function by a network with uniform dissipation. The synthesis procedure that must be used, however, is the Darlington one, which yields a lossless quadripole terminated in resistance. Therefore, it is first necessary to transform the prescribed function to one that describes the network with the lossless quadripole. The lossless network is simply the final one in which the uniform dissipation has been removed from each of the reactance elements. Corresponding to this network change, the transformation⁸ $s = p - d$ is made in the prescribed function. In other words, the given function [here assumed for illustration as a transfer impedance $Z_{21}(s)$] is predistorted to yield the transformed function

$$Z_{21}^T(p) = Z_{21}(p - d) \tag{6}$$

It is pointed out that the new transfer impedance Z_{21}^T has no physical significance. It is merely an intermediate function for which we realize a lossless network. As a final step, uniform dissipation is added to the realized network; this cancels the effect of the original predistortion because it corresponds, as we have seen, to the substitution of $s+d$ for p in Z_{21}^T .

Predistorting a function moves its critical frequencies d units to the right. In Fig. 8 the critical frequencies in the s and p planes are shown for which $Z_{21} = 1/[(s+2)(s^2+6s+18)]$ and $d=1$, so that $Z_{21}^T = 1/[(p+1)(p^2+4p+13)]$. Since Z_{21}^T must remain a function realizable by a resistance-terminated network, its poles must lie in the left half-plane. Thus one restriction on the amount of predistortion becomes apparent: d must be less than the absolute value of the real part of the pole of Z_{21} closest to the imaginary axis.

⁷ T. S. Gray, "Applied Electronics," John Wiley and Sons, Inc., New York, N. Y., 2nd ed., pp. 547-550; 1954.

⁸ For clarity and to simplify the following discussion a new frequency variable p is introduced.

There are other restrictions which should be mentioned.⁶ If Z_{21}^T is to be realized by a lossless network terminated in resistance, its numerator must be an even or odd polynomial. However, if Z_{21} has a numerator that is even or odd (but is not merely a constant), the transformation $s = p - d$ cannot possibly yield an even or odd numerator for Z_{21}^T . Thus predistortion followed by use of the Darlington procedure for the lossless quadripole will not work in this case. For the characteristics treated here, the numerator of each transfer function is a constant so that no difficulty arises.

In addition, the constant multiplier on Z_{21}^T must be adjusted before the synthesis is begun. For example, suppose Z_{21} is given as the form of transfer function considered in this paper,

$$Z_{21} = \frac{H}{q(s)} = \frac{H}{s^n + a_{n-1}s^{n-1} + \dots + a_1s + a_0}, \quad (7)$$

where H is a constant multiplier, and we wish to realize a uniformly dissipative ladder network with a resistance termination only at the load end. Thus we can realize Z_{21}^T by the ladder shown in Fig. 9, for which

$$Z_{21}^T = \frac{b_0}{q(p-d)} = \frac{b_0}{p^n + b_{n-1}p^{n-1} + \dots + b_1p + b_0}, \quad (8)$$

where

$$b_0 = q(s)|_{s=-d}. \quad (9)$$

It is necessary that the constant multiplier be b_0 since inspection of the network in Fig. 9 for $s = 0$ shows that $Z_{21}^T(0)$ must equal unity.

If Z_{21} instead of Z_{21}^T were realized by the network of Fig. 9, H would equal a_0 . However, Z_{21} is realized by the uniformly dissipative ladder of Fig. 10, and thus

$$Z_{21} = Z_{21}^T(s+d) = \frac{b_0}{q(s)} = \frac{b_0}{a_0} \frac{a_0}{q(s)}. \quad (10)$$

The fixed loss introduced by the dissipation, therefore, is given in db by

$$\text{loss (db)} = -20 \log (b_0/a_0). \quad (11)$$

It is pointed out that this is added loss when the network is driven by an ideal generator. When the generator has internal resistance, the loss introduced by this resistance must be subtracted from the above loss.

The fixed loss is therefore easy to compute, since b_0 is obtained by (9). Frequently, the use of the remainder

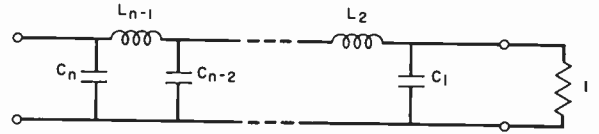


Fig. 9—Ladder network for realizing Z_{21}^T .

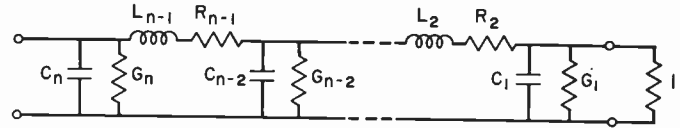


Fig. 10—Uniformly dissipative ladder.

theorem simplifies the computation. The polynomials $q(s)$ —that is, the Butterworth, Tchebycheff, and Bessel polynomials—have been tabulated.¹ Inspection of those tables¹ also shows that for the Butterworth polynomials

$$a_0 = 1 \quad (\text{for all } n), \quad (12)$$

for the Tchebycheff polynomials

$$a_0 = \frac{1}{2^{n-1}\epsilon} \quad (\text{for } n \text{ odd})$$

$$a_0 = \frac{\sqrt{1 + 1/\epsilon^2}}{2^{n-1}} \quad (\text{for } n \text{ even}), \quad (13)$$

and for the Bessel polynomials

$$a_0 = \frac{(2n)!}{n!2^n} = 1 \cdot 3 \cdot 5 \cdot \dots \cdot (2n - 1) \quad (14)$$

for all values of n . The quantity ϵ^2 is the ripple factor; its value is given in the title for each table of equal-ripple networks.

Based on the above description, the procedure for realizing a uniformly dissipative low-pass network is summarized by the following steps.

1) Determine the realizable $Z_{21}^T(p)$ from the specified $Z_{21}(s)$ by making the substitution $s = p - d$.

2) After performing the necessary adjustment of the constant multiplier of Z_{21}^T , realize Z_{21}^T by a network whose reactances have no associated dissipation.

3) Make the realized network uniformly dissipative by adding a resistance $R_\nu = dL_\nu$ in series with each inductance L_ν of the network, and adding a conductance $G_\mu = dC_\mu$ in parallel with each capacitance C_μ appearing in the network.

4) The uniformly dissipative network realizes the $Z_{21}(s) = Z_{21}^T(s+d)$; this is equal to the given transfer impedance within a constant multiplier. The flat loss introduced by the added dissipation can be calculated by use of (11).

ACKNOWLEDGMENT

The author expresses his thanks to Tadayoshi Suzuki, Mathematics Section, Systems Analysis Laboratory, Hughes Aircraft Company, for carrying out most of the calculations.

Minimum Energy Triggering Signals*

L. A. BEATTIE†, ASSOCIATE MEMBER, IRE

Summary—In switching problems, the efficiency of the switching circuits is often of considerable importance. In the past the basic switching mechanism has been actuated by pulses of simple functions of voltage, current, or force, and efforts to obtain increased efficiency have led to the use of transistors, development of better relays, and the improvement of other components. This paper considers, as an alternative or complementary approach to the problem, the optimization of the function of time which is used for triggering so as to minimize the energy required of the triggering signal.

The general problem of determining the optimum triggering signal for a lumped-constant, linear circuit is considered. The optimum signal is defined as that which produces a given current through, or a voltage across, a resistive output element at time $t = T$ while at the same time requiring a minimum of energy from the generator driving the circuit. The output resistance is considered as characterizing the input terminals of a monostable or bistable element such as a thyratron, multivibrator, or a magnetic relay.

An equation characterizing the optimum signal is derived, and the conditions under which the equation is valid are noted. There are two types of circuits for which a characteristic equation is not obtained. However, both of these types of circuits are unrealistic in the practical sense because they do not allow for generator internal resistance or stray capacitance across the input terminals. For equivalent circuits of practical importance the characteristic equation is always valid.

The solution of the characteristic integral equation is discussed, and it is shown that the Laplace transform can be used to reduce the integral equation into an algebraic one which is susceptible of simple solution. Finally, a sample problem is proposed and the solution outlined. This example, in addition to demonstrating the general solution, also presents a method for finding the undetermined constants involved in the equations.

INTRODUCTION

SWITCHING is of great importance in almost all fields of engineering endeavor. The problems range all the way from the trivial ones of mechanically turning an equipment on and off to the complicated problems associated with automatic telephone exchanges and computers. Regardless of the complexity, however, the basic switching mechanism in the past has been actuated by pulses or predetermined functions in time of voltage, current, or force. In some of the complex problems in switching much attention has been paid to the efficiency of the switching process. However, the improvements in efficiency have resulted from reducing the energy requirements of the switching elements by building better relays and other terminal devices, and from increasing the efficiency of the associated circuits such as might result through the use of transistors. Thus, improved switching has re-

sulted from the improvement of the switching circuits. One might consider an alternative or complementary approach to the switching problem. In many cases it might be desired to operate a remotely located switch by radio. Here the energy required of the transmitter may be of primary importance and one may or may not have optimized the receiver efficiency. Thus, in this type of problem the receiver may be fixed and one may only be free to adjust the transmitter parameters. Here, it might be quite inefficient to select arbitrarily some given type of triggering signal, such as a pulse, for example, and it might be of considerable benefit to optimize the function of time which is chosen for the triggering signal.

The minimum energy signal problem might also be couched in the terminology of a signal detection problem in which one desires to determine that voltage or current as a function of time, which if applied to the input terminals of a given linear receiver results in some peak deflection to root-mean-square (rms) background noise deflection ratio on an oscilloscope screen, while at the same time requiring a minimum of energy from the signal driving the circuit.

The triggering problem and the signal detection problem, as defined above, are identical except for the ultimate use which is made of the peak output voltage. However, for convenience the remainder of this paper is written in terms of triggering signals.

Before considering the solution to the optimum triggering signal problem, it may be well to review some of the accomplishments in the field of signal detection since, at first glance, it appears that the solution to the signal detection problem might yield a solution to the optimum triggering signal problem. However, it will be shown that the two problems are very different in nature, and the solution to one suggests nothing in the way of a solution to the other.

The part of the signal detection problem which bears the closest relationship to the optimum triggering signal problem is probably best defined by referring to Van Vleck and Middleton's treatment of the problem.¹ To summarize briefly, these authors considered a signal known exactly to be applied to the input terminals of a filter, the output of which is used to produce a deflection on an oscilloscope screen. Their problem was that of determining that filter characteristic which would result in a maximization of the peak output signal to the rms noise output.

* Original manuscript received by the IRE, June 27, 1957; revised manuscript received, November 18, 1957. This work was sponsored by the U. S. Army Signal Corps, and is abstracted from Tech. Rep. No. 56, "Minimum energy triggering signals," by L. A. Beattie.

† Dept. of Elec. Eng., University of Idaho, Moscow, Idaho; formerly with Electronic Defense Group, University of Michigan, Ann Arbor, Mich.

¹ J. H. Van Vleck and D. Middleton, "A theoretical comparison of the visual, aural, and meter reception of pulse signals in the presence of noise," *J. Appl. Phys.*, vol. 17, pp. 940-971; November, 1946.

The first theoretical treatment of this type of problem was made by North.² He showed that to maximize the ratio of the peak signal, known exactly, to the rms noise, the filter characteristic should be the complex conjugate of the Fourier transform of the pulse.

In addition to optimizing the filter characteristic for the detection of signals known exactly, there have also been investigations leading to the optimization of pulse widths, repetition rates, scanning rates, etc.^{1,3} These optimizations lead to the choice of the parameters of some signal of a given type. However, the general problem of determining, if possible, the best function of time for peaking the filter output for a given filter does not appear in the literature.

Without a critical examination, it appears at first glance that North's determination of the best filter for peaking the ratio of the output signal to the rms noise output might be applied conversely to the determination of the best signal for a given filter. However, there is a basic difference between the two problems. Suppose first that we have some signal known exactly and that we want to determine the best filter for maximizing the ratio of the peak output signal to rms noise. In this problem it is assumed that there is some given noise level at the filter input. It is clear that we do not want to simply select the filter characteristic to maximize the output signal, because this in general might also peak the output noise. For example, the best circuit for peaking the output signal would be an ideal transformer with infinite turns ratio. However, this transformer would also peak the output noise and thus would not maximize the signal-noise ratio. In signal detection, therefore, the choice of the filter involves inherently a choice of the noise output.

In the optimum triggering signal problem noise plays no role whatsoever. In this case it is assumed that the filter or circuit is given. But if the filter is given, it then follows that the noise output from the filter is also given. The choice of the optimum triggering signal therefore involves no choice of the noise output from the circuit. In this case, optimizing the input signal to maximize the peak output also maximizes, on the average, the ratio of the peak output signal to the noise output. Thus, one would not expect in general that the optimum triggering signal is, using North's theorem in converse, the complex conjugate of the inverse Fourier transform of the filter characteristic.

MINIMUM ENERGY TRIGGERING SIGNALS

The problem which is considered is that of activating a critical monostable or bistable element, located at the output terminals of a circuit, with a minimum of energy

delivered to the input terminals of the circuit. The critical element is envisioned, for example, as a biased thyatron or a bistable multivibrator. These types of critical elements require that some minimum instantaneous voltage be exceeded at least once between a sensitive pair of tube elements in order that triggering occur and conduction take place. Another example would be a relay which requires some minimum current through the pull-in coil in order for the relay to be activated. In general, the circuit with the critical element at the output terminals is considered to be stable and made up of lumped-constant, linear elements, such as resistances, inductances, capacitances, and linear vacuum tubes. In practice the critical element to be triggered can always be considered as purely resistive; *i.e.*, thyatrons, multivibrators, and relay coils can all be considered to have a resistive component of input impedance and the reactive components can all be lumped into the remainder of the network. The description of the critical element as a pure resistance allows the activating output signal to be described in terms of a current through a resistance. Thus this type of subterfuge allows all triggering problems to be resolved into a single type in which one wishes to establish some minimum current through an output resistance at some instant in time.

Consider then the circuit as characterized by the block diagram of Fig. 1. Here $g_{11}(t)$ is the current $i_1(t)$

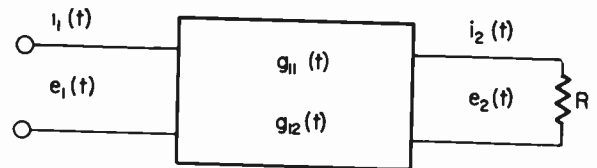


Fig. 1—Block diagram characterizing the circuit to be triggered.

which flows in response to a voltage $e_1(t)$ when $e_1(t)$ is a unit impulse. $g_{12}(t)$ is the current $i_2(t)$ which flows in response to $e_1(t)$ when $e_1(t)$ is a unit impulse. With these definitions we can write⁴

$$i_1(t) = \int_0^t e_1(\tau) g_{11}(t - \tau) d\tau, \quad (1)$$

and

$$i_2(t) = \int_0^t e_1(\tau) g_{12}(t - \tau) d\tau \quad (2)$$

where $e_1(t)$ is now an arbitrary driving function but equal to zero for $t < 0$, and where the initial energy stored in the network is assumed to be zero.

Let us now consider a time interval $0 \leq t \leq T$, where T defines both the instant of triggering and also the allowable elapsed time interval of the driving function.

² D. O. North, "Analysis of Factors Which Determine Signal-Noise Discrimination in Pulsed Carrier Systems," unpublished RCA Rep. PTR-6C, Princeton, N. J.; June 25, 1943.

³ J. L. Lawson and G. E. Uhlenbeck, "Threshold Signals," M.I.T. Rad. Lab. Ser., McGraw-Hill Book Co., Inc., New York, N. Y., vol. 24; 1948.

⁴ M. F. Gardner and J. L. Barnes, "Transients in Linear Systems," John Wiley and Sons, Inc., New York, N. Y., vol. 1; 1952.

If T represents the instant of triggering, then $i_2(T)$ must equal some critical minimum current which will establish the conduction of a tube or the pulling in of a relay. Thus we want

$$i_2(T) = I_c = \int_0^T e_1(t)g_{12}(T - t)dt. \quad (3)$$

Now, the total energy input to the circuit in the interval $0 \leq t \leq T$ is then

$$E(T) = \int_0^T e_1(t)i_1(t)dt = \int_0^T e_1(t) \int_0^t e_1(\tau)g_{11}(t - \tau)d\tau dt. \quad (4)$$

Expressed mathematically, then, the optimization problem becomes that of minimizing the integral given by (4) subject to the constraint that (3) is also satisfied. In the following treatment of the optimum triggering signal problem the variational calculus will be used.^{5,6}

We first assume that there is some function $e_1(t)$ satisfying the above conditions, and then examine what happens when we use a function perturbed away from the optimum, instead of using the optimum driving function. Thus, if we let $e_1(t)$ be the optimum driving function, we will consider a perturbed driving function

$$e_1(t) + \epsilon\eta(t), \quad (5)$$

where ϵ is some small arbitrary constant and $\eta(t)$ is some arbitrary continuous function of t with $\eta(0) = \eta(T) = 0$. Also, in order to incorporate both (3) and (4) into a single equation, we make use of the Lagrangian multiplier λ , where λ is an arbitrary constant to be chosen finally to satisfy the boundary conditions of the problem.⁷ We therefore consider the minimization of

$$E(T) - \lambda i_2(T) = \int_0^T \left[e_1(t) \int_0^t e_1(\tau)g_{11}(t - \tau)d\tau - \lambda e_1(t)g_{12}(T - t) \right] dt. \quad (6)$$

Now in (6) we substitute for $e_1(t)$ the perturbed driving function given by (5). Eq. (6) then becomes

$$E(T) - \lambda i_2(T) = \int_0^T \left[e_1(t) \int_0^t e_1(\tau)g_{11}(t - \tau)d\tau - \lambda e_1(t)g_{12}(T - t) \right] dt + \epsilon \int_0^T \left[\eta(t) \int_0^t e_1(\tau)g_{11}(t - \tau)d\tau - \lambda \eta(t)g_{12}(T - t) \right] dt$$

$$+ e_1(t) \int_0^t \eta(\tau)g_{11}(t - \tau)d\tau - \lambda \eta(t)g_{12}(T - t) \Big] dt + \epsilon^2 \int_0^T \eta(t) \int_0^t \eta(\tau)g_{11}(t - \tau)d\tau dt. \quad (7)$$

It can now be argued that if $e_1(t)$ is such as to minimize (6), then any perturbation can only serve to increase the value of (7). Note that the first term of (7) is the original unperturbed function given by (6). The second term of (7) has a multiplier ϵ . If we allow ϵ to have either positive or negative values, then to guarantee that the perturbation has increased the original function [this implies that $e_1(t)$ minimizes the function $E(T) - \lambda i_2(T)$] the coefficient of ϵ must be zero. The third term has ϵ^2 as a multiplier, which is always positive, and, in addition, the coefficient of ϵ^2 is the energy input to the network due to the perturbing signal acting alone, which must also be positive. Thus if we set the coefficient of ϵ equal to zero, we will have established a condition on $e_1(t)$ such that any perturbations of $e_1(t)$ always result in an increase in the value of (6). This is exactly the condition which minimizes the quantity given by (4) and satisfies (3). Equating the coefficient of ϵ to zero gives

$$0 = \int_0^T \eta(t) \int_0^t e_1(\tau)g_{11}(t - \tau)d\tau dt + \int_0^T e_1(t) \int_0^t \eta(\tau)g_{11}(t - \tau)d\tau dt - \lambda \int_0^T \eta(t)g_{12}(T - t)dt. \quad (8)$$

As it stands, it would appear that the solution of this equation for $e_1(t)$ would lead to a function of the network parameters, g_{11} and g_{12} , and also of $\eta(t)$. But if $e_1(t)$ is given in terms of the perturbation then we have not truly found an optimizing function, but have optimized only with respect to the perturbation. However, if the right-hand side of (8) can be resolved into the form

$$\int_0^T \eta(t)f[e_1(t), g_{11}(t), g_{12}(t)]dt, \quad (9)$$

then we could satisfy (8) by insisting that $f[e_1(t), g_{11}(t), g_{12}(t)]$ be identically equal to zero. If this is possible, then the description of $e_1(t)$ will be independent of the perturbation and will be given in terms of only the network functions $g_{11}(t)$ and $g_{12}(t)$.

RESTRICTIONS ON $g_{11}(t)$ FOR STABLE, LUMPED-CONSTANT, LINEAR NETWORKS, AND NATURE OF THE CORRESPONDING SOLUTIONS

Before looking for solutions to (8), we will first observe some of the general characteristics of $g_{11}(t)$ and consider some of the restrictions on $e_1(t)$ since they are important in the mathematical treatment of the problem.

⁵ A. R. Forsyth, "Calculus of Variations," Cambridge University Press, Cambridge, Eng.; 1927.

⁶ C. Fox, "An Introduction to the Calculus of Variations," Oxford University Press, New York, N. Y., 1950.

⁷ I. S. Sokolnikoff "Advanced Calculus," McGraw-Hill Book Co., Inc., New York, N. Y.; 1939.

Consider now only the input terminals of the network to be triggered. The Laplace transformed equation relating input current to input voltage is

$$i_1(s)z_{11}(s) = e_1(s), \quad (10)$$

where $z_{11}(s)$ is a complex impedance function describing the driving point impedance of the network. If $e_1(t)$ is a unit impulse $u_1(t)$, then $i_1(t)$ is, by definition, equal to $g_{11}(t)$. We have, therefore,

$$g_{11}(s) = 1/z_{11}(s). \quad (11)$$

Now, because $z_{11}(s)$ is a driving point impedance function, it can be written as the ratio of two polynomials in s , subject to the restriction that the degree of the numerator does not differ by more than one from the degree of the denominator. This is in consequence of the restriction that driving point impedances can have no more than simple poles on the imaginary axis.⁸ Thus $g_{11}(s)$ can in general be written

$$g_{11}(s) = k_1s + k_2 + N(s)/D(s), \quad (12)$$

where k_1 or k_2 , or both, may be equal to zero, and where $N(s)$ is at least one degree less than $D(s)$. $g_{11}(t)$ is therefore of the form

$$g_{11}(t) = k_1u_2(t) + k_2u_1(t) + \text{other terms}, \quad (13)$$

where $u_2(t)$ is a unit doublet and $u_1(t)$ is a unit impulse. In general, the "other terms" in (13) can be expressed as powers of t times damped sinusoids, *i.e.*, in the form

$$t^n e^{-at} \sin(\omega t + \theta). \quad (14)$$

This form results because the zeros of $D(s)$ lie either on the negative real axis or else appear in complex conjugate pairs.

Because of (13), we can characterize $g_{11}(t)$ as belonging to one of three possible classes. These are: 1) $g_{11}(t)$ contains neither a unit doublet nor a unit impulse, 2) $g_{11}(t)$ contains no unit doublet, but does contain a unit impulse, and 3) $g_{11}(t)$ contains a unit doublet.

In addition to the restriction on $g_{11}(t)$ which results from the restrictions on the types of networks being considered, there are also restrictions on $e_1(t)$ because of the nature of the problem, *i.e.*, $e_1(t)$ is to be a minimum-energy type signal.

It will be shown later that if certain conditions are met by $g_{11}(t)$, $g_{12}(t)$, and $e_1(t)$ then the integral equation characterizing solutions to the optimum triggering signal problem can be reduced to an algebraic equation in the variable s by using the Laplace transform. The optimum driving voltage is therefore first found as the ratio of two polynomials in s . Because of this we can say that unboundedness in the optimum signal can only result through the appearance of impulses, doublets, etc.

Let us now consider the energy input to a network for the three classes of $g_{11}(t)$ when subjected to unbounded driving voltages of the above types. However, before doing so, it is to be noted that in a finite non-zero time interval any given output voltage can be realized with a properly chosen step function with a resulting finite energy input to the network. We first conclude, therefore, that an optimum signal can deliver only a finite energy to a network.

Case I. $g_{11}(t)$ Contains Neither a Doublet Nor an Impulse

Consider a driving function, $e_1(t)$ which contains a unit impulse. Then from (10)–(12) it can be seen that $i_1(t)$ will be bounded. Let the maximum value of $i_1(t)$ on the interval $0 \leq t \leq T$ be M . Then the energy input to the network due to the impulse of voltage is no greater than that given below.

$$\begin{aligned} E &\leq \int_0^T M u_1(t) dt \\ &= M. \end{aligned} \quad (15)$$

For this case then it can be seen that the optimum driving signal can be unbounded.

Case II. $g_{11}(t)$ Contains an Impulse But Not a Doublet

From (10)–(12) it is seen that any term contained in $e_1(s)$ is also contained in $i_1(s)$. Let us now take $e_1(t) = u_1(t)$ and let $u_1(t)$ be defined as

$$u_1(t) = \lim_{a \rightarrow 0} \frac{u(t) - u(t-a)^9}{a} \quad (16)$$

where $u(t)$ is the unit step function. For case 2, $i_1(t)$ will contain a term $ku_1(t)$ and the input energy contribution due to the impulses of voltage and current can be written

$$\begin{aligned} E &= \lim_{a \rightarrow 0} \int_0^a \frac{1}{a} \frac{k}{a} dt \\ &= \lim_{a \rightarrow 0} \frac{k}{a} \rightarrow \infty. \end{aligned} \quad (17)$$

Similarly, higher order terms in $e_1(t)$ would also result in infinite energy input to the network, and thus we conclude that if $g_{11}(t)$ contains a unit impulse then the optimum driving function must be bounded.

Case III. $g_{11}(t)$ Contains a Unit Doublet

Now a doublet of current in $g_{11}(t)$ only results for circuits with shunt capacitance across the input terminals and no internal generator resistance. This situation is unrealizable in practice and can only be considered as

⁹ Note that the step function definition is arbitrary and one could as well have chosen some other appropriate definition such as one involving distribution functions. However, the other definitions of $u_1(t)$ also lead to the notion that the integral of a unit impulse squared is unbounded in the limit.

⁸ E. A. Guillemin, "Modern methods of network synthesis," in "Advances in Electronics," vol. 3, pp. 263–264; 1951.

the limit of the case in which an internal generator resistance is assumed and is allowed to become vanishingly small. With regard to unbounded driving voltages, in the limit this case is not well defined. Thus for energy input considerations we consider this case to be only an approximation for a circuit of case II.

Theorem: A sufficient condition for the optimum driving function to be bounded is for $g_{11}(t)$, the input impulse response of the network, to contain a unit impulse but not a doublet.

EQUATION CHARACTERIZING SOLUTIONS TO THE OPTIMUM TRIGGERING SIGNAL PROBLEM

The basic equation for optimum triggering signals for linear, lumped-constant networks is given by (8). It was suggested that it is desirable to write this equation in the form of (9) in order to obtain an equation for $e_1(t)$ independent of the perturbation. It turns out that this is possible if it is known that $e_1(t)$ is bounded and sectionally continuous in the interval $0 \leq t \leq T$. But, from the preceding section, we know that if $g_{11}(t)$ does not contain a unit doublet but does contain a unit impulse then the boundedness and continuity conditions on $e_1(t)$ will be satisfied. Thus, we restrict our attention to $g_{11}(t)$ in the form

$$g_{11}(t) = k_1 u_1(t) + k_2 g_{11c}(t) \tag{18}$$

where $g_{11c}(t)$ is sectionally continuous. Substituting (18) into (8) gives

$$\int_0^T \left\{ \eta(t) \int_0^t e_1(\tau) [k_1 u_1(t - \tau) + k_2 g_{11c}(t - \tau)] d\tau + e_1(t) \int_0^t \eta(\tau) [k_1 u_1(t - \tau) + k_2 g_{11c}(t - \tau)] d\tau - \lambda \eta(t) g_{12}(T - t) \right\} dt = 0. \tag{19}$$

Now, all terms except those in the second inner integral in the above expression are already in the form of (9). We therefore consider the second integral separately.

$$\int_0^T e_1(t) \int_0^t \eta(\tau) [k_1 u_1(t - \tau) + k_2 g_{11c}(t - \tau)] d\tau dt = \int_0^T k_1 e_1(t) \eta(t) dt + \int_0^T e_1(t) \int_0^t k_2 \eta(\tau) g_{11c}(t - \tau) d\tau dt. \tag{20}$$

In the last term in (20) the order of integration can be reversed by integrating over the triangle of Fig. 2 first in t and then in τ . This gives

$$\int_0^T e_1(t) \int_0^t \eta(\tau) g_{11c}(t - \tau) d\tau dt = \int_0^T \eta(t) \int_t^T e_1(\tau) g_{11c}(\tau - t) d\tau dt. \tag{21}$$

Thus, (19) finally becomes

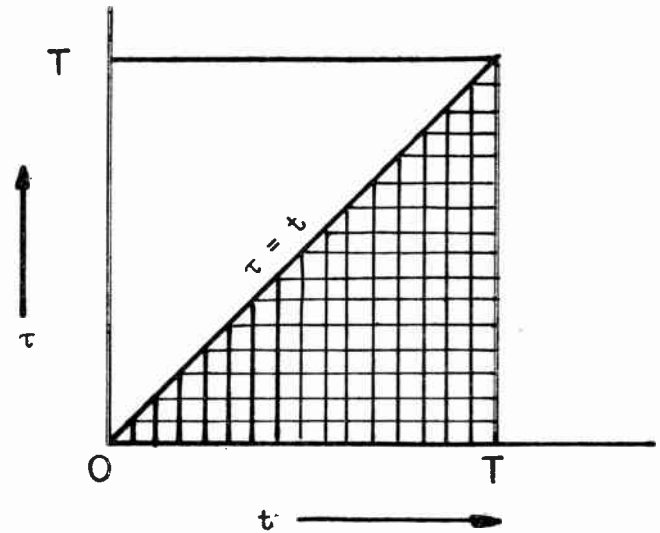


Fig. 2—Region of integration in the τ, t plane.

$$\int_0^T \eta(t) \left\{ \int_0^t e_1(\tau) [k_1 u_1(t - \tau) + k_2 g_{11c}(t - \tau)] d\tau + k_1 e_1(t) + k_2 \int_t^T e_1(\tau) g_{11c}(\tau - t) d\tau - \lambda g_{12}(T - t) \right\} dt = 0. \tag{22}$$

This can be satisfied independently of η by setting

$$2k_1 e_1(t) + k_2 \int_0^t e_1(\tau) g_{11c}(t - \tau) d\tau + k_2 \int_t^T e_1(\tau) g_{11c}(\tau - t) d\tau - \lambda g_{12}(T - t) = 0. \tag{23}$$

Eq. (23) will henceforth be called the characteristic equation.

METHOD OF SOLUTION

A method which is sufficiently powerful to allow solution of (23) even in cases where $g_{11}(t)$ and $g_{12}(t)$ are complicated functions is that of taking the Laplace transform of the characteristic equation. This reduces the original integral equation into an algebraic equation which is always susceptible of relatively simple solution.

First it is noted that the characteristic (23) contains only three different types of terms. These are: 1) direct functions of t , 2) convolution integrals of the form $\int_0^t e_1(\tau) g_{11c}(t - \tau) d\tau$, and 3) integrals of the form $\int_t^T e_1(\tau) g_{11c}(\tau - t) d\tau$. The Laplace transform of the first two types are taken directly. For terms of the third type we first expand the integral as the difference of two integrals as follows:

$$\int_t^T e_1(\tau) g_{11c}(\tau - t) d\tau = \int_0^T e_1(\tau) g_{11c}(\tau - t) d\tau - \int_0^t e_1(\tau) g_{11c}(\tau - t) d\tau, \tag{24}$$

and treat each of the resulting integrals separately. The second integral on the right-hand side of (24) is in the

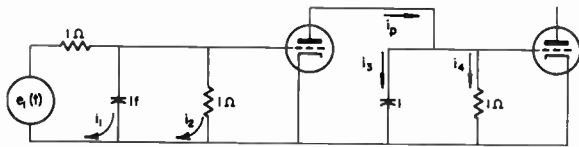


Fig. 3—Circuit to be triggered, containing an RC coupled amplifier and a biased thyatron.

form of a convolution integral. However, the first integral on the right-hand side of (24) is not a convolution integral and must therefore be treated in a different manner. In general it can be shown that $g_{11_c}(\tau - t)$ can be written as a sum of terms each of which is in the form $f(t)g(\tau)$. Thus, the first integral on the right-hand side of (24) can be expanded into the sum of a number of terms, each of which can be written as a function of t times an integral whose limits are constants. Now the integrals with constant limits are in themselves constants, and can be determined after solving for the general form of $e_1(t)$. Thus, the integral (23) readily reduces into an algebraic equation.

This completes the discussion of optimum driving voltages. It deserves mention that through the principle of duality the preceding theory can be written equally well in terms of optimum driving currents. However, for the optimum current case the input and transfer characteristics of the network must be written as the response of the network to a unit impulse of current rather than of voltage.

Example: A Single-Stage RC Coupled Amplifier Whose Output Is Used to Trigger a Biased Thyatron

The purpose of this section is to demonstrate the applicability to a particular problem of the theory contained in the preceding sections. Many notions of practical significance are difficult to discuss in general terms. One such notion, for example, is that of the minimum energy requirement necessary to cause triggering. One can only examine a minimum energy requirement after having found the optimum driving function, and, of course, one cannot find such a function unless $g_{11}(t)$ and $g_{12}(t)$ are specified. One particularly interesting facet of the optimum triggering signal problem is the study of the relationship between energy required and the time allowed for triggering. In the following example the solution to a particular problem is demonstrated and the energy input to the network for the optimum signal is discussed.

A type of problem which might be of practical interest is one involving vacuum tubes. Let us now consider the optimum driving voltage to be applied to a single-stage RC coupled amplifier whose output is used to trigger a biased thyatron. For purposes of simplicity we will use simple values for the circuit constants.¹⁰ Consider the circuit of Fig. 3.

¹⁰ Even for simple circuits with simple element values the algebra required to find a solution is considerable. For complicated circuits a computer might be required.

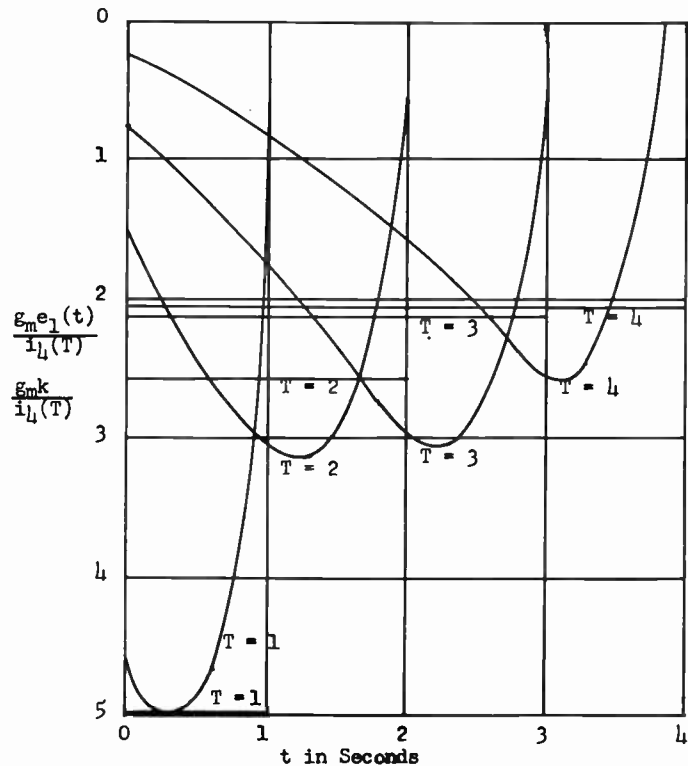


Fig. 4—Optimum triggering signals and step functions for various values of the triggering time T .

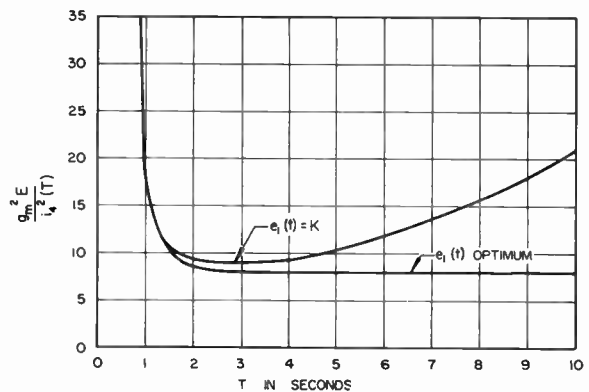


Fig. 5—Triggering energy vs firing time.

In this case we wish to establish some critical $i_4(T)$ at some given time $t = T$ with a minimum of energy delivered to the input circuit by the generator $e_1(t)$. We proceed first to the determination of the input impulse response, $g_{11}(t)$, and the transfer impulse response, $g_{12}(t)$. The transfer current in this case is $i_4(t)$. For this circuit one finds

$$g_{11}(t) = u_1(t) - e^{-2t} \tag{25}$$

and

$$g_{12}(t) = g_m e^{-t} + g_m e^{-2t}. \tag{26}$$

For this problem, then, $g_{11}(t)$ contains a unit impulse plus continuous terms. Using (25) and (26) in (23) gives for $e_1(s)$

$$e_1(s) = \frac{s^2(k + \lambda g_m e^{-2T} - \lambda g_m e^{-T}) + s(k + \lambda g_m e^{-2T}) + (4\lambda g_m e^{-T} - 2\lambda g_m e^{-2T} - 2k)}{2(s-1)(s-\sqrt{2})(s+\sqrt{2})}, \tag{27}$$

where

$$k = \int_0^T e_1(\tau) e^{-2\tau} d\tau. \tag{28}$$

The inverse Laplace transform of (27) gives $e_1(t)$. Integrating (28) allows one to find k . Then using the relation

$$i_4(s) = g_{12}(s)e_1(s) \tag{29}$$

one can solve for λ in terms of $i_4(T)$. Finally, using

$$i_1(s) = g_{11}(s)e_1(s), \tag{30}$$

one can find $i_1(t)$, and upon integrating the product of $e_1(t)$ times $i_1(t)$ over the interval from 0 to T , one finds the energy input to the network over the same interval. The results of these operations are,

$$e_1(t) = \frac{-i_4(T)}{g_m} \left\{ \frac{[(-3/2 - 9\sqrt{2}/8)e^{-(3-\sqrt{2})T} + (-3/2 + 9\sqrt{2}/8)e^{-(3+\sqrt{2})T}]e^t + [(5/4 + 5\sqrt{2}/4)e^{-2T} + (1/4 - \sqrt{2}/4)e^{-(3+\sqrt{2})T}]e^{\sqrt{2}t}}{(1 - 13\sqrt{2}/16)e^{-(2-\sqrt{2})T} + (1 + 13\sqrt{2}/16)e^{-(2+\sqrt{2})T} + (3/2 + 17\sqrt{2}/16)e^{-(4-\sqrt{2})T} + (3/2 - 17\sqrt{2}/16)e^{-(4+\sqrt{2})T} - 5e^{-3T}} \right. \\ \left. + \frac{[(5/4 - 5\sqrt{2}/4)e^{-2T} + (1/4 + \sqrt{2}/4)e^{-(3-\sqrt{2})T}]e^{-\sqrt{2}t}}{(1 - 13\sqrt{2}/16)e^{-(2-\sqrt{2})T} + (1 + 13\sqrt{2}/16)e^{-(2+\sqrt{2})T} + (3/2 + 17\sqrt{2}/16)e^{-(4-\sqrt{2})T} + (3/2 - 17\sqrt{2}/16)e^{-(4+\sqrt{2})T} - 5e^{-3T}} \right\}. \tag{31}$$

and

$$E = \frac{i_2^2(T)[(7/64 + \sqrt{2}/32) - (71/32)e^{-2\sqrt{2}T} + (33/16 + 39\sqrt{2}/32)e^{-4\sqrt{2}T} + (-99/64 - 35\sqrt{2}/32)e^{-2T} + (3/32)e^{-(2+2\sqrt{2})T}]}{g_m^2[(1 - 13\sqrt{2}/16) + (1 + 13\sqrt{2}/16)e^{-2\sqrt{2}T} + (3/2 + 17\sqrt{2}/16)e^{-2T} + (3/2 - 17\sqrt{2}/16)e^{-(2+2\sqrt{2})T} - 5e^{-(1+\sqrt{2})T}]^2} \\ + \frac{i_2^2(T)[(-99/64 + 37\sqrt{2}/32)e^{-(2+4\sqrt{2})T} + (5/2 + 15\sqrt{2}/8)e^{-(1+\sqrt{2})T} + (5/4 - 51\sqrt{2}/16)e^{-(1+3\sqrt{2})T}]}{g_m^2[(1 - 13\sqrt{2}/16) + (1 + 13\sqrt{2}/16)e^{-2\sqrt{2}T} + (3/2 + 17\sqrt{2}/16)e^{-2T} + (3/2 - 17\sqrt{2}/16)e^{-(2+2\sqrt{2})T} - 5e^{-(1+\sqrt{2})T}]^2}. \tag{32}$$

For comparison purposes, let us now find the energy delivered to the same circuit by a step of voltage of sufficient amplitude to cause triggering at time $t=T$. For the step of voltage we have

$$e_1(t) = k, \tag{33}$$

and one finds that

$$i_4(t) = k g_m (-1/2 + e^{-t} - e^{-2t}/2). \tag{34}$$

Therefore,

$$e_1(t) = k = \frac{2i_4(T)}{g_m(-1 + 2e^{-T} - e^{-2T})}. \tag{35}$$

One also finds that the energy delivered to the circuit by this voltage in the interval 0 to T is

$$E = \frac{i_4^2(T)(2T - e^{-2T} + 1)}{g_m^2(1 - 2e^{-T} + e^{-2T})^2}. \tag{36}$$

Eqs. (31) and (35) are plotted in Fig. 4 for various values of the parameter T . Eqs. (32) and (36) are plotted in Fig. 5.

It can be seen from Fig. 5 that the energy for the optimum signal is always less than that for a unit step. However, we see that for T small the energy required

of the optimum signal approaches that required for a step function. From Fig. 5 it is seen that the optimum signal begins with a step and then increases in value in the negative direction. Note that near the end of the period 0 to T the optimum signal makes an attempt to recover some of the energy stored in the input capacity. For T decreasing the optimum signal approaches the step function both in energy and in shape. Thus, if separate considerations dictate a small allowable triggering time, there is little advantage to the optimum function, and a step function becomes a very good approximation.

CONCLUSIONS AND SPECULATIONS

It has been shown that if a network contains a unit impulse in its input impulse response then there is an

optimum way for a signal to expend energy so as to produce across some output resistance a given voltage at some preselected time $t=T$. Applications to straight-forward triggering problems come readily to mind. In the introduction it was suggested that the theory might find application in the field of signal detection. For example, an optimum shaped radar pulse would produce greater deflection than a rectangular pulse for a given average radiated power. However, the usefulness of the optimum signal theory will depend on how much increased range can be realized at the cost of a certain amount of pulse shaping circuitry. Apart from electrical problems the theory might find application to any system capable of being described or approximately described by a family of linear differential-integral equations. A sufficient condition for the theory to be applicable is for the system to have an electrical analog in which the forcing function acts through a series resistance into a capacitive energy storage element. A mechanical application which comes to mind and which is of current interest is that of realizing maximum rocket energy storage (potential plus kinetic) with a given available expendable energy. The theory contained in this paper suggests that there might be some optimum way to program a rocket's thrust so as to realize a maximum final energy for a given fuel supply.

Some Studies on Delayed Feedback Circuits*

HIDEO SEKI†, SENIOR MEMBER, IRE

Summary—This paper attempts to describe a new method by which periodic signals in noise can be detected easily without the aid of an expensive correlator. In principle, the circuit consists of a delay network which is inserted as a part of a unidirectional loop connected with the main circuit through a hybrid coil. The delay time must be equal to, or an integral multiple of, the signal period to be detected. The delay time also must be longer than the inverse figure of the preceding network bandwidth. Successive noises will be superimposed one after another at random in circulation, while the signals are superimposed in phase. This means an improvement in the signal-to-noise ratio. Theoretically, the ideal basic delayed feedback circuit gives an improvement in the snr of 7.66 db, and in the apparent Q of 9.06. Further improvement can be expected by the use of active circuits. Possible applications are for producing artificial reverberation, a narrow-band filter, and a short-time memory circuit. The response of the delayed feedback circuit is like a comb filter. The circuit also can extract complicated periodic waves without an appreciable distortion.

INTRODUCTION

NEGATIVE feedback circuit is effective in reducing internal noise although it is useless against external noise. Delayed feedback circuit, on the other hand, may improve the input snr. Of course, periodic signals in noise can be detected effectively by any type of correlator,¹ but in general, they are complicated and very expensive. It is desirable, therefore, to simplify them to fit the ordinary radio receiver in order to reduce external noise. The delayed feedback circuit may be regarded as a simplified correlator, since its frequency, as well as its time response, are of a similar character. Since its frequency response is comb-like, it is exactly the same as synchronously commutated capacitors.² Therefore, it is understandable that comb filters can be obtained through both mechanical and electrical means. The time delay circuits were used by Calvert in a control device,³⁻⁵ but his chief interest was directed to the improvement of waveform of command signals. To apply his circuit to our present purpose of snr im-

provement, it is better to choose the delay time of each element as equal to, or integral multiples of, some definite time duration. Interesting characteristics of such a finite arrangement of delay network without feedback may be deduced easily from the following discussion, and therefore it will not be necessary to go into further detail here. Electrically, the delayed feedback circuit can also be regarded as a positive feedback or a regenerative circuit, except for the time delay in the feedback loop. Time delay in the loop is a vital factor for improvement of the snr. Nevertheless, there is another interesting application of the delayed feedback circuit—that of artificial reverberation.⁶ In this case, it is not necessary to keep the delay time in the feedback loop within an exact value, but it must be adjustable within certain limits for practical applications.

This paper proposes to discuss the theoretical details which are considered useful for all these applications.

DESCRIPTION OF THE FUNDAMENTAL CIRCUIT

Fig. 1 shows the fundamental circuit to which the delayed feedback principle has been applied ideally. Half of the input signal power passes through the lossless hybrid coil H to the loop circuit and the rest appears directly on the output terminals 3-3'. The delay network N is inserted in any part of the loop. Delay time is chosen to superimpose the circulated periodic signals in phase with the waves newly arriving at input terminals 1-1'. Incoming random noise is also halved in power and passes through the two routes in the same manner as the signal. However they are combined at the junction point in a random phase because noise is not a periodic function. If the input impedance is 600 ohms, the loop circuit and output impedance both must be 1200 ohms. To satisfy these circuit conditions, we need an ideal amplifier to provide power gain unity in some part of the loop. In such an ideal case, the rms voltage of random noise, because of its subtraction and addition, can be treated merely by power due to its randomness. The phase, however, must be taken into consideration for the summation of signals. For the convenience of further development, Fig. 1 is simplified symbolically, as shown in Fig. 2, according to Mason's signal flow graphs,⁷ because of the linearity of our circuit. The terminals 1-1', 3-3', and the hybrid coil correspond to source, sink, and index nodes, respectively.

* Original manuscript received by the IRE, February 11, 1957; revised manuscript received, November 22, 1957. The original paper was read before a meeting of the Studying Committee of JIECEJ on Circuit and Information Theories. Part of the manuscript was published in the Japanese journal of JIECEJ. On June 27, 1956, a revised paper was read before the IRE Tokyo Section meeting.

† Iwasaki Tsushinki Co., Tokyo, Japan.

¹ Y. W. Lee, "Application of Statistical Methods to Communication Problems," Electronics Res. Lab., M.I.T., Cambridge, Mass., Tech. Rep. No. 181; September, 1950.

² W. R. LePage, C. R. Cahn, and J. S. Brown, "Analysis of a comb filter using synchronously commutated capacitors," *Trans. AIEE*, vol. 72, pp. 63-68; March, 1953.

³ D. J. Gimpel and J. F. Calvert, "Signal component control," *Trans. AIEE*, vol. 71, pt. II, pp. 339-343; November, 1952.

⁴ D. J. Ford and J. F. Calvert, "The application of short-time memory devices to compensator design," *Trans. AIEE*, vol. 73, pt. II, pp. 88-93; May, 1954.

⁵ T. W. Sze and J. F. Calvert, "Short-time memory devices in closed-loop system—steady-state response," *Trans. AIEE*, vol. 74, pt. II, pp. 340-344; November, 1955.

⁶ P. E. Axon, C. L. S. Gilford, and D. E. L. Shorter, "Artificial reverberation," *Proc. IEE*, vol. 102, pt. B, pp. 624-642; September, 1955.

⁷ S. J. Mason, "Feedback theory—some properties of signal flow graphs," *Proc. IRE*, vol. 41, pp. 1144-1156; September, 1953.

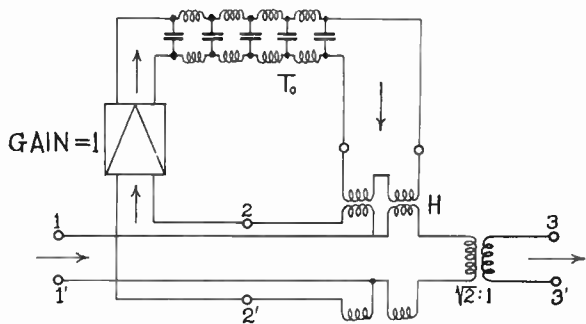


Fig. 1—Delayed feedback circuit.

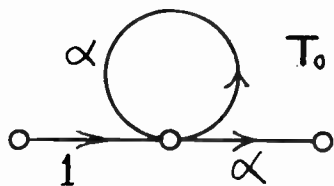


Fig. 2—Signal flow graph.

Branch gains $1/\sqrt{2}$ appear twice in the fundamental circuit and frequently in the derived circuit. Let us take general branch gain α as being $1/\sqrt{2}$ in the special case of an ideal circuit. Then, branch gains of self-loop and output branches will both be α , while those of the input branch will be unity as shown in Fig. 2. Note that we have added a new symbol expressing the delay time beside the branch gain.

It is important to note that the following three conditions are required to improve the snr in our delayed feedback circuit.

- 1) Denoting the delay time as T_0 and the period of incoming signal as T , it is required that

$$T_0 = NT$$

where N is any positive integer.

- 2) Denoting the bandwidth of incoming white noise as B , it is required by the uncertainty principle that

$$T_0 > \frac{1}{2B} \text{ or at least } T_0 > \frac{1}{B\sqrt{\pi}}.$$

- 3) Branch gain of the self-loop must remain within certain limits, so as not to cause parasitic oscillations. In the special case of a single loop circuit, this limit can be taken as unity.

If the noise band B is very wide, N can be taken as unity, but the narrower the noise band, the larger N must be. Condition 2) can be derived from the autocorrelation function of random noise.¹

$$\phi_{11}(\tau) = \int_{-\infty}^{\infty} \Phi_{11}(\omega) \cos \omega\tau d\omega. \tag{1}$$

Let us assume that the power density spectrum function $\Phi_{11}(\omega)$ is

$$\Phi_{11}(\omega) \approx a^2 e^{-s\omega^2}, \tag{2}$$

or Gaussian spectrum, where

$$x \equiv 2Q \frac{f - f_0}{f_0}$$

and s is the number of single-tuned circuits inserted between amplifiers in cascade, where center frequency is f_0 and quality factor is Q . Then the equivalent noise band (or effective band) can be evaluated as follows:

$$B = \int_0^{1.5/f_0} e^{-sx} df = \frac{f_0}{2Q} \int_{-1}^{1/2} e^{-sx} dx.$$

This integral may be evaluated only by infinite series instead of simple form. However, if $s/4$ is large enough to be able to neglect

$$\int_{-\infty}^{-1} e^{-sx^2} dx \text{ and } \int_{1/2}^{\infty} e^{-sx^2} dx,$$

as compared to the above integral, its value would depend mainly on the function near $x = 1$. We can approximate the integral without appreciable error as

$$\int_{-1}^{1/2} e^{-sx^2} dx \approx \int_{-\infty}^{\infty} e^{-sx^2} dx$$

which brings us the simple expression

$$B = \frac{f_0}{2Q} \sqrt{\frac{\pi}{s}}. \tag{3}$$

Thus we obtain the approximate formula for autocorrelation function by putting (2) and (3) into (1):

$$\phi_{11}(\tau) = 2\pi a^2 B e^{-\pi(B\tau)^2} \cos \omega_0\tau \tag{4}$$

which gives condition 2), or

$$\pi(B\tau)^2 > 1 \text{ or } T_0 > \frac{1}{\sqrt{\pi}B}. \tag{5}$$

As another limiting case, let us choose that of noise passing a single-tuned circuit, of which Lee and Stutt² have made a thorough study. Let us assume that the random noise has a uniform spectrum $\Phi_{11}(\omega) = a^2$ at the input. The autocorrelation function of this random noise after it passes through a single-tuned circuit becomes

$$\phi_{11}(\tau) = \frac{\pi}{2} a^2 L^2 Q \omega_0^3 e^{-\omega_0|\tau|/2Q} \left(\cos \omega_0|\tau| - \frac{1}{2Q} \sin \omega_0|\tau| \right). \tag{6}$$

¹ Y. W. Lee and C. A. Stutt, "Statistical Prediction of Noise," Electronics Res. Lab., M.I.T., Tech. Rep. No. 129; July 12, 1949.

This conforms to condition 2) that $\phi_{11}(\tau)$ drops to $1/e$; i.e.,

$$|\tau| > \frac{2Q}{\omega_0}.$$

As the noise equivalent band in this case is

$$\beta = \frac{\omega_0}{4Q}, \quad (7)$$

condition 2) becomes

$$|\tau| > \frac{1}{2\beta} \quad \text{or} \quad T_0 > \frac{1}{2\beta}. \quad (8)$$

Condition 3) is absolutely necessary in our case, because we are not concerned with oscillation as produced by a pulse generator.⁹ However, there remains some margin to insert an active network in the self-loop branch. In the basic network of Fig. 1, $\alpha=0.707$, and this may be increased to near unity depending on the circuit stability.

SNR IMPROVEMENT

Let us assume that the periodic signal has lasted for a finite time, say n periods. Then the output signal amplitudes should be α , $\alpha+\alpha^2$, $\alpha+\alpha^2+\alpha^3$, \dots , and $\alpha+\alpha^2+\alpha^3+\dots+\alpha^n$, respectively, during the first, second, third, \dots , and n th period. After the $(n+1)$ th period, the signal amplitudes should decay without limit. The largest amplitude occurs at the n th period, and it would be

$$v_s^{(n)} = \sum_{m=1}^n \alpha^m = \frac{1-\alpha^{n+1}}{1-\alpha} \alpha \quad (9)$$

$$\therefore \lim_{n \rightarrow \infty} v_s^{(n)} = \frac{\alpha}{1-\alpha} \equiv v_s. \quad (10)$$

If the autocorrelation function $\phi_{11}(\tau)$ of unity power noise drops to a negligible value after time T , then the resultant noise power $N_2^{(n)}$ should be the simple summation of $\alpha^2, \alpha^4, \dots, \alpha^{2n}$, i.e.,

$$N_2^{(n)} = \sum_{m=1}^n \alpha^{2m} = \frac{1-\alpha^{2n+2}}{1-\alpha^2} \alpha^2 \quad (11)$$

$$\therefore \lim_{n \rightarrow \infty} N_2^{(n)} = \frac{\alpha^2}{1-\alpha^2} = N_2. \quad (12)$$

Assuming now, without losing its generality, that

S_1 : input signal power = unity

N_1 : input noise power = unity,

we get

S_2 : output signal power = $[v_s^{(n)}]^2$

N_2 : output noise power = $N_2^{(n)}$.

⁹ C. C. Cutler, "The regenerative pulse generator," *PROC. IRE*, vol. 43, pp. 140-148; February, 1955.

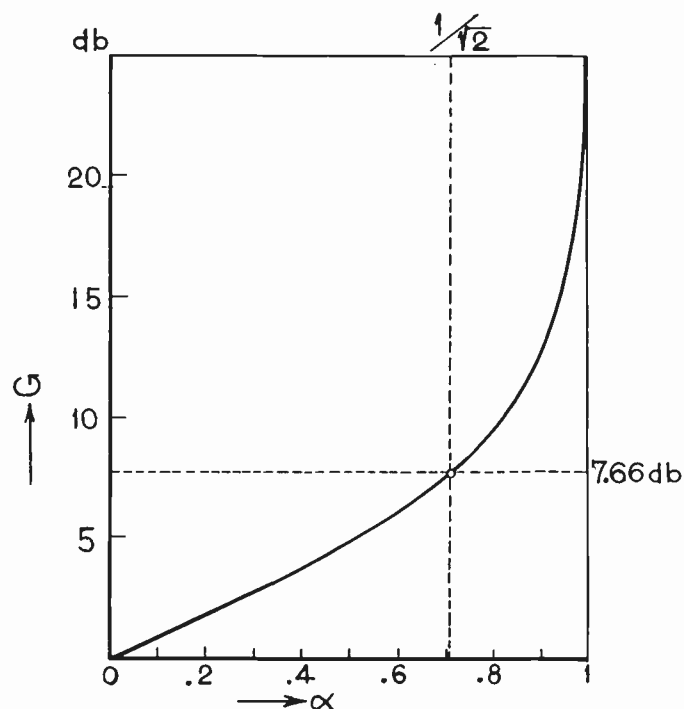


Fig. 3—SNR improvement vs loop gain α .

Then this will be followed by the snr improvement ratio G as follows:

$$G^{(n)} = \frac{S_2/N_2}{S_1/N_1} = \frac{1+\alpha}{1-\alpha} \frac{1-\alpha^n}{1+\alpha^{2n}} \quad (13)$$

$$\therefore \lim_{n \rightarrow \infty} G^{(n)} = \frac{1+\alpha}{1-\alpha} \equiv G. \quad (14)$$

This quantity is always larger than unity in our case. The inverse of G seems to correspond to the noise figure F , although not exactly, because it has not been corrected with respect to frequency bandwidth of the network in question. Otherwise, the inverse of G is always less than unity. $G=5.83$ (7.66 db) for $\alpha=1/\sqrt{2}$; and $G=9$ for $\alpha=0.8$. The nearer α approaches unity, the more unstable our circuit becomes, because of the increase in G without limit (Fig. 3). Our experience has shown that it is better to keep α around 0.8.

TRANSIENT OR BUILD-UP TIME

The waveform of the periodic signal remains similar, as shown in Fig. 4, but it grows after each period. The amplitude variation $G^{(n)}$ with respect to the number of period n is shown in Fig. 5, for the numerical example of $\alpha=1/\sqrt{2}$. Even after the last period of the signal, the output signal will not disappear, but will damp gradually period after period, as long as the signal circulates along the feedback loop. These phenomena are independent of the periodic waveform of the incoming signal. For example, a sawtooth wave in Fig. 6 will keep its form in the delayed feedback circuit so far as its bandwidth is wide enough to include the higher harmonics. Meanwhile, noise power N_2 is kept constant

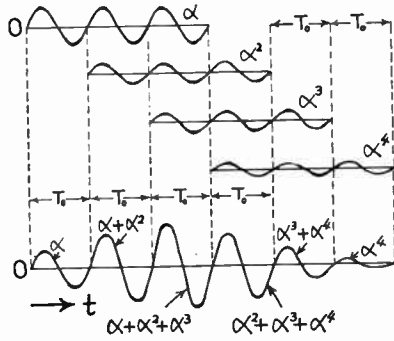


Fig. 4—Process of amplitude build-up with time (example).

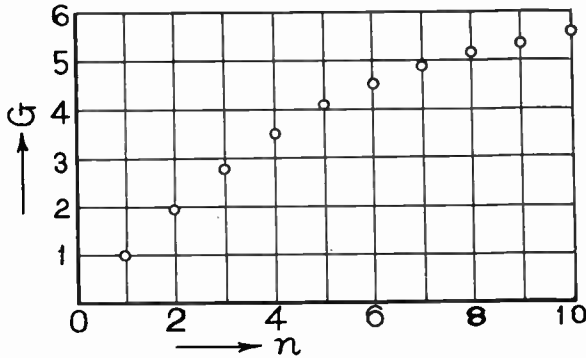


Fig. 5—SNR improvement (G) vs number of circulations (n) in delayed feedback circuit.

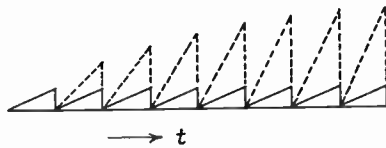


Fig. 6—Example of transient current (— input, - - - output).

even after it passes through the fundamental delayed feedback circuit, because $\alpha = 1/\sqrt{2}$; $\alpha^2 = 0.5$ in (12).

Now take the ratio of signal voltage at n th period to the saturated voltage and equate with $(1 - e^{-1})$, or

$$\frac{v_s^{(n)}}{v_s} = 1 - \alpha^n = 1 - e^{-}$$

and define time constant as $\tau_c \equiv nT_0$. We have then a definition for the time constant of a delayed feedback network of

$$\tau_c \equiv \frac{T_0}{\log\left(\frac{1}{\alpha}\right)}, \quad (15)$$

where T_0 and α are delay time and loop branch gain (voltage), respectively. This equation can be simplified further, if α is nearly unity, or $\alpha = 1 - \epsilon$, *i.e.*,

$$\tau_c = \frac{T_0}{\epsilon} \quad (16)$$

where ϵ is a very small number.

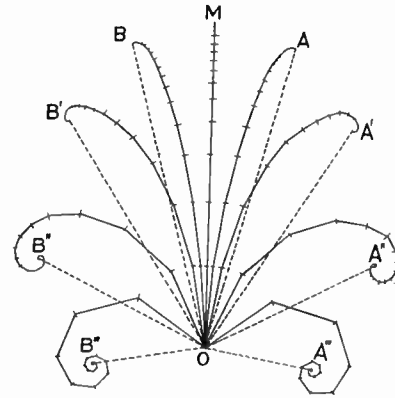


Fig. 7—Vector diagram for delayed feedback waves.

FREQUENCY RESPONSE

Frequency response of the delayed feedback network, when treated as a transmission system, is exactly the same as that of a mechanical commutator type comb filter.² Instead of series (8) or $\alpha + \alpha^2 + \alpha^3 \dots$, we take

$$v_s^{(n)} = \sum_{m=1}^n \alpha^m e^{jm\theta} = \frac{1 - \alpha^n e^{jn\theta}}{1 - \alpha e^{j\theta}} \alpha \quad (17)$$

where

$$\theta \equiv 2\pi\left(1 - \frac{T}{T_0}\right) = 2\pi\left(1 - \frac{f_0}{f}\right); \quad f_0 = \frac{1}{T_0}$$

This is an angle between two subsequent vectors of the series (17) and their resultants are $OA, OA', \dots, OB, OB', \dots$ as shown in Fig. 7. In the work of Le Page *et al.*,² this angle is replaced by $a = 2\pi - \theta$, and the frequency response function is written as

$$\bar{F}(a) = \frac{1}{\sqrt{1 + \frac{2}{(1 - \alpha)^2} (1 - \cos a)}} \angle \phi \quad (18)$$

where

$$\phi = -\tan^{-1} \frac{\alpha \sin a}{1 - \alpha \cos a}$$

For the special case where α is nearly unity and f is around resonance or f_0 , this function may be rewritten approximately as

$$F^2(f) \approx \frac{1}{1 + \left\{ \frac{2\pi}{\log\left(\frac{1}{\alpha}\right)} \right\}^2 \left(1 - \frac{f_0}{f}\right)^2}, \quad (19)$$

while the frequency response of ordinary single resonance circuit with inductance and capacity is

$$F^2(f) = \frac{1}{1 + 4Q^2 \left(1 - \frac{f_0}{f}\right)^2}. \quad (20)$$

Comparing these two equations, we get the equivalent Q of the delayed feedback circuit near resonance as

$$Q = \frac{\pi}{\log\left(\frac{1}{\alpha}\right)} \tag{21}$$

This is also written as

$$Q = \pi \frac{\tau_c}{T_0} \tag{22}$$

by (15). Note that τ_c/T_0 is nearly equal to the signal voltage amplification A , which can also be defined as the ratio of the final to the initial value of the infinitely repeated periodic signal, *i.e.*, from (10)

$$A = \frac{v_s}{\alpha} = \frac{1}{1 - \alpha} \approx \frac{1}{\log\left(\frac{1}{\alpha}\right)} = \frac{\tau_c}{T_0} \tag{23}$$

as α approaches unity. Phase angle θ near m th harmonic frequency must be m times larger than that near the fundamental or f_0 , because of the general principle that the retardation in an ideal delay circuit should be constant independent of frequencies. This allows us to put

$$\theta = 2\pi m \left(1 - \frac{f_0}{f}\right)$$

instead of the definition of θ in (17). Then we have

$$Q = m \frac{\pi}{\log\left(\frac{1}{\alpha}\right)} \tag{24}$$

and this transforms the effective bandwidth β in (7) to

$$\beta = \frac{m\omega_0}{4Q} = \frac{1}{2} f_0 \log\left(\frac{1}{\alpha}\right) \tag{25}$$

This result shows that the effective bandwidth β near the harmonic frequencies $2f_0, 3f_0, \dots, mf_0$ in Fig. 8 are all equal to that near f_0 . Now, let us consider the frequency range B which includes m such harmonics in it. Then the over-all noise, which had uniform spectrum at the input of the network, should be within the effective band $B_e = m\beta$ at the output, *i.e.*,

$$B_e = \frac{1}{2} mf_0 \log\left(\frac{1}{\alpha}\right) = \frac{1}{2} B \log\left(\frac{1}{\alpha}\right) \tag{26}$$

or

$$\frac{B}{B_e} = \frac{2}{\log\left(\frac{1}{\alpha}\right)}$$

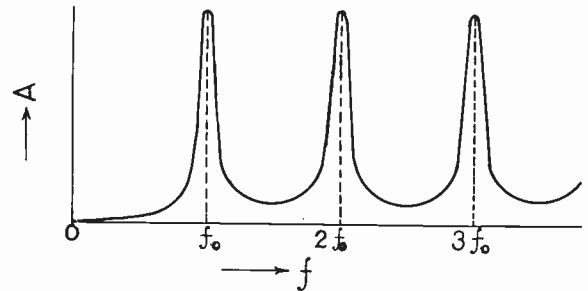


Fig. 8—Frequency response of delayed feedback circuit.

It is clear that we should take B_e as the effective band in the definition of noise figure F , which we may compute by

$$F = \frac{N}{GkTB_e} = \frac{N}{GkTB} \frac{B}{B_e} = F_a \frac{B}{B_e},$$

where F_a is an apparent noise figure and is given by the reciprocal of G in (14), and (14) may be written approximately for the value of α near unity, as

$$F_a = \frac{1 - \alpha}{1 + \alpha} \approx \frac{1}{2} \log\left(\frac{1}{\alpha}\right) \tag{27}$$

Thus the equation of noise figure F can be reduced to

$$F \approx 1$$

by combining (26) and (27). The smaller the value of F_a , the more exactly this relation will hold.

APPLICATIONS

Feeder Circuit Noise Elimination

A delayed feedback circuit may be inserted between the antenna and receiver input so as to eliminate static or industrial noise. It is also applicable to the cases of nuclear magnetic resonance and microwave spectroscopy where detection of periodic signal in noise is needed. The circuit shown in Fig. 9 is usable at frequencies below the hf range. It will be more convenient if phase and gain adjustments are available together with the vacuum tube amplifiers. Fig. 10 is for the vhf or uhf range, while Fig. 11 is for shf. In the latter case, delay time usually will be higher multiples of the signal period, and a fine adjustment of delay time will be difficult.

Low-Frequency Circuit

If the signal is still periodic after final detection in a receiver, the delayed feedback circuit should also be effective in a low-frequency circuit. Such cases sometimes occur in A2 telegraphy and radar, but not in telephony or phototelegraphy. The period for A2 telegraphy must be equal to the modulation wave period, while that for radar must be equal to prf. Fig. 12 gives experimental data obtained through low-frequency delayed feedback.

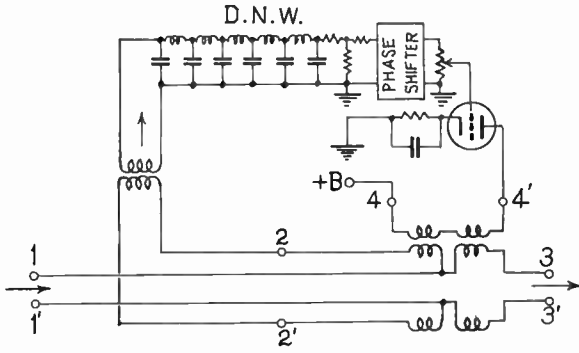


Fig. 9—Application for hf or lower frequency bands.

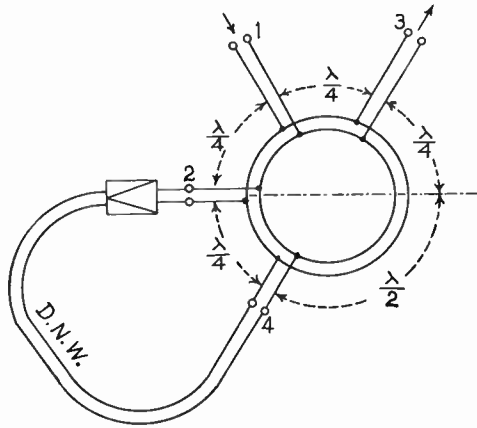


Fig. 10—Application for vhf or higher frequency bands.

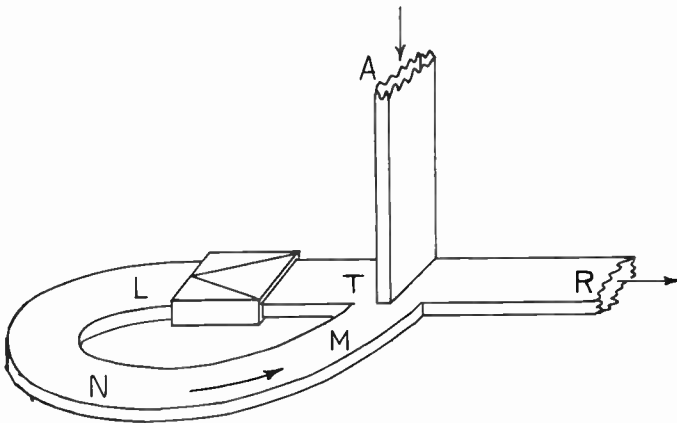


Fig. 11—Application for shf or higher frequency bands.

Artificial Reverberation⁸

Details on the practical applications have already been reported by Axon and others, who treated the case of a multiple delayed feedback circuit. There would be no meaning in improving the snr in this case. Therefore, the delay time need not be adjusted to an exact value.

Filter for Special Code Selection

Delayed feedback circuits can be used for all cases where comb filters are needed. For example, detection of

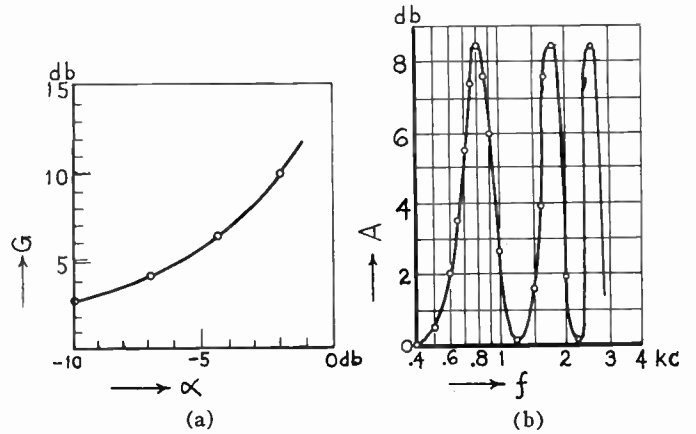


Fig. 12—Experimental data on (a) the snr improvement and (b) the frequency response.

repeated call signals or distress signals can be improved by this method. In some cases where delay time is so long that an electrical filter is too expensive, a rotary drum magnetic recording device may be useful, although extremely high mechanical accuracy would be necessary for stable operation.

CONCLUSION

- 1) Delayed feedback circuits are effective when the signal is periodic and the noise frequency band is sufficiently wide.
- 2) Delay time must be equal to or integral multiples of the signal period and longer than the inverse of the noise frequency band.
- 3) In the basic delayed feedback circuit, snr improvement is 7.66 db, time constant is 2.89 times the delay time, and the apparent Q is 9.06.
- 4) The apparent noise figure of the fundamental delayed feedback circuit seems to be less than unity. But the true noise figure is just unity in an ideal case, taking account of the effective band.
- 5) The signal to be selected need not be a sine wave, but any periodic waveform.
- 6) Effective values of input and output noise are equal to the fundamental delayed feedback circuit after a steady state is reached.
- 7) SNR improvement can be increased by inserting an active network in the feedback loop. But it must be carefully done so as not to cause oscillation.
- 8) There are also several applications such as artificial reverberation and special filters in addition to the snr improvement.

ACKNOWLEDGMENT

The author wishes to acknowledge the helpful advice of Dr. K. Ohashi of the Iwasaki Tsushinki Company and Messrs. Nakajima, Okuse, Hayakawa, and Koyama for their aid in conducting experiments. Mr. Sato prepared the graphs for this paper. Finally, Mr. Ninoseki kindly checked the sentences.

IRE Standards on Piezoelectric Crystals: Determination of the Elastic, Piezoelectric, and Dielectric Constants—The Electromechanical Coupling Factor, 1958*

(58 IRE 14. S1)

COMMITTEE PERSONNEL

Subcommittee on Methods for Measurement of the Elastic, Piezoelectric, and Dielectric Constants 1957-1958

R. Bechmann
I. E. Fair

Committee on Piezoelectric and Ferroelectric Crystals

1957-1958

E. A. GERBER, *Chairman*
I. E. FAIR, *Vice-Chairman*

J. R. Anderson
J. H. Armstrong
H. G. Baerwald
R. Bechmann
W. G. Cady
W. A. Edson

W. D. George
R. L. Harvey
E. J. Huibregtse
Hans Jaffe
E. D. Kennedy
T. M. Lambert

W. P. Mason
W. J. Merz
C. F. Pulvari
P. L. Smith
R. A. Sykes
K. S. VanDyke

Standards Committee

1957-1958

M. W. BALDWIN, JR., *Chairman*
C. H. PAGE, *Vice-Chairman*

R. F. SHEA, *Vice-Chairman*
L. G. CUMMING, *Vice-Chairman*

J. Avins
W. R. Bennett
J. G. Brainerd
D. R. Brown
T. J. Carroll
P. S. Carter
A. G. Clavier
G. A. Deschamps
S. Doba, Jr.
J. E. Eiselein
G. Espersen
D. Frezzolini

E. A. Gerber
A. B. Glenn
H. Goldberg
V. M. Graham
R. A. Hackbusch
H. C. Hardy
D. E. Harnett
A. G. Jensen
I. M. Kerney
J. G. Kreer, Jr.
W. A. Lynch
A. A. Macdonald
Wayne Mason

D. E. Maxwell
H. R. Mimno
L. H. Montgomery
G. A. Morton
J. H. Mulligan, Jr.
W. Palmer
R. L. Pritchard
R. Serrell
H. R. Terhune
J. E. Ward
E. Weber
W. T. Wintringham

Measurements Coordinator

R. F. Shea

* Approved by the IRE Standards Committee, December 12, 1957. Reprints of this Standard, 58 IRE 14. S1, may be purchased while available from the Institute of Radio Engineers, 1 East 79th Street, New York, N. Y., at \$0.75 per copy. A 20 per cent discount will be allowed for 100 or more copies mailed to one address.

INTRODUCTION

IN 1949, Standards on Piezoelectric Crystals [1] were issued covering the definition of axes for piezoelectric crystals and their relation to rectangular axes, standards for specifying crystal plate orientation and nomenclature referring to the piezoelectric relations, symbols, and units. In 1957, the IRE Standards on Piezoelectric Crystals [2] was issued covering the piezoelectric vibrator: definition and measurements. It is the object of these present Standards to specify a method for determining the basic elastic, piezoelectric, and dielectric constants of crystals. In addition, the electromechanical coupling factor and the relations to these constants are considered. Among the several known methods for the determination of the elastic and piezoelectric constants, the resonance method has been proven simple and reliable. These constants are derived from the motional parameters of the equivalent electric circuit of piezoelectric vibrators made from the material considered. The motional parameters and their measurements are specified in the 1957 IRE Standards [2].

The expressions relating measured quantities to basic coefficients are different for crystals of various symmetry classes. A complete presentation covering all symmetry classes is rather complex. Fortunately, most piezoelectric materials of practical interest belong to crystal classes having several symmetry elements, so that the problem of determining the elastic and piezoelectric constants is considerably simplified when compared to the most general case of the asymmetric class. Determination of the constants may be further simplified by choosing cuts specially oriented in relation to the symmetry planes or axes of the material considered. Therefore it is not necessary to use the theoretical relationships in their complete tensor form. Reference is made to the general elastic and piezoelectric equations in the 1949 IRE Standards and several textbooks (see [3]-[5]).

1. THE PIEZOELECTRIC EQUATIONS

The piezoelectric equations usually are expressed as relations between the six tensor components of the stress T_p and the strain S_q as elastic variables, the three vector components of the electric field E_i and the electric displacement D_j as electric variables, and the scalars temperature θ and entropy σ as thermal variables. In the notation used in these Standards, the symbols for subscripts numbered from 1 to 6 will be represented by p, q indicating second-order tensors, and those for subscripts numbered from 1 to 3 by i, j indicating vectors.

For the present purpose, one of the thermal scalars, the entropy, is taken as constant, and only the elastic and electric properties under adiabatic conditions are considered.

Four sets of equations for any piezoelectric crystal can be given depending upon which of the elastic quantities (stress, strain) or electric quantities (electric field, electric displacement) are taken as independent vari-

ables. Each form consists of a set of nine equations comprising a group of six elastic equations (corresponding to $p=1$ to 6), together with three electric equations (corresponding to $i=1$ to 3).

Two sets of equations refer to controlled field conditions, the other two to open circuit conditions. For the present purpose of determination of the elastic and piezoelectric constants, only the equations referring to controlled field conditions are of interest.

The piezoelectric equations of state for the most general cast (triclinic crystal, hemihedral class C_1), where the components of stress and electric field are taken as independent variables (controlled field conditions), while the components of strain and electric displacement are taken as dependent variables, are

$$\begin{aligned}
 S_1 &= s_{11}^E T_1 + s_{12}^E T_2 + s_{13}^E T_3 + s_{14}^E T_4 + s_{15}^E T_5 \\
 &\quad + s_{16}^E T_6 + d_{11} E_1 + d_{21} E_2 + d_{31} E_3 \\
 S_2 &= s_{12}^E T_1 + s_{22}^E T_2 + s_{23}^E T_3 + s_{24}^E T_4 + s_{25}^E T_5 \\
 &\quad + s_{26}^E T_6 + d_{12} E_1 + d_{22} E_2 + d_{32} E_3 \\
 S_3 &= s_{13}^E T_1 + s_{23}^E T_2 + s_{33}^E T_3 + s_{34}^E T_4 + s_{35}^E T_5 \\
 &\quad + s_{36}^E T_6 + d_{13} E_1 + d_{23} E_2 + d_{33} E_3 \\
 S_4 &= s_{14}^E T_1 + s_{24}^E T_2 + s_{34}^E T_3 + s_{44}^E T_4 + s_{45}^E T_5 \\
 &\quad + s_{46}^E T_6 + d_{14} E_1 + d_{24} E_2 + d_{34} E_3 \\
 S_5 &= s_{15}^E T_1 + s_{25}^E T_2 + s_{35}^E T_3 + s_{45}^E T_4 + s_{55}^E T_5 \\
 &\quad + s_{56}^E T_6 + d_{15} E_1 + d_{25} E_2 + d_{35} E_3 \\
 S_6 &= s_{16}^E T_1 + s_{26}^E T_2 + s_{36}^E T_3 + s_{46}^E T_4 + s_{56}^E T_5 \\
 &\quad + s_{66}^E T_6 + d_{16} E_1 + d_{26} E_2 + d_{36} E_3 \\
 D_1 &= d_{11} T_1 + d_{12} T_2 + d_{13} T_3 + d_{14} T_4 + d_{15} T_5 \\
 &\quad + d_{16} T_6 + \epsilon_{11}^T E_1 + \epsilon_{12}^T E_2 + \epsilon_{13}^T E_3 \\
 D_2 &= d_{21} T_1 + d_{22} T_2 + d_{23} T_3 + d_{24} T_4 + d_{25} T_5 \\
 &\quad + d_{26} T_6 + \epsilon_{12}^T E_1 + \epsilon_{22}^T E_2 + \epsilon_{23}^T E_3 \\
 D_3 &= d_{31} T_1 + d_{32} T_2 + d_{33} T_3 + d_{34} T_4 + d_{35} T_5 \\
 &\quad + d_{36} T_6 + \epsilon_{13}^T E_1 + \epsilon_{23}^T E_2 + \epsilon_{33}^T E_3
 \end{aligned} \tag{1}$$

where s_{pq}^E are the elastic compliances at constant field strength, d_{jp} the piezoelectric strain constants, and ϵ_{ij}^T the dielectric permittivities at constant stress.

In matrix notation the equations of state (1) can be more simply written [1]

$$\begin{aligned}
 S &= s^E T + d_i E \\
 D &= d T + \epsilon^T E.
 \end{aligned} \tag{2}$$

Alternatively, when the strain S and the electric field E are taken as independent variables,

$$\begin{aligned}
 T &= c^E S - e_i E \\
 D &= e S + \epsilon^S E.
 \end{aligned} \tag{3}$$

where the subscript t signifies a transposed matrix. In (2), s^E are the elastic compliances at constant field strength, d the piezoelectric strain constants, and ϵ^T the dielectric permittivities at constant stress. In (3), c^E are the elastic stiffnesses at constant field strength, e the piezoelectric stress constants, and ϵ^S the dielectric permittivities at constant strain. The matrices s , c , and ϵ are symmetric; e.g., $s_{pq} = s_{qp}$; $c_{pq} = c_{qp}$; and $\epsilon_{ij} = \epsilon_{ji}$. Eq. (1) through (3) are written in rationalized 4π -free units. The relationship between the elastic stiffnesses and compliances, and between the piezoelectric stress constants and strain constants, can be found in the 1949 IRE Standards [1].

1.1 The Elasto-Piezo-Dielectric Matrix

A simplified presentation of the elasto-piezo-dielectric matrix for all seven crystal systems and thirty-two classes, using both Hermann-Mauguin's and Schoenflies' notation (the former in parentheses), is shown in Chart I (pp. 767-768) [6]. The tetragonal system and the trigonal system are divided into two groups designated as (a) and (b). For the tetragonal system IV(b), s_{11} equals zero; for the trigonal system V(b), s_{25} equals zero. Of all the thirty-two crystal classes, twenty are piezoelectric and are denoted by the following Schoenflies' symbols

$$\begin{aligned} C_1, C_{1v} (=C_s) \\ C_n, C_{nv}, D_n \quad n = 2, 3, 4, 6 \\ S_4, D_{2d}, C_{3h}, D_{3h}, T, T_d. \end{aligned}$$

The twenty schemes of piezoelectric constants reduce to sixteen independent schemes, since the symmetry operations for $n=4$ or $n=6$ have the same effect on the piezoelectric scheme and the schemes for classes T and T_d are identical. The arrangement of the classes in Chart I is in accordance with generally accepted practice. The numbers on the right side of each scheme indicate, from top to bottom, the number of the independent elastic, piezoelectric, and dielectric constants.

Table I gives some known examples of crystals belonging to various crystal systems for which the elastic and piezoelectric coefficients have been determined. Elastic and piezoelectric constants of crystals belonging to the classes of the tetragonal system IV(a) and the trigonal system V(a) have not been determined.

The symmetry type of polarized polycrystalline ceramic material; e.g., barium titanate ceramics, is associated with the crystallographic class C_{6v} of the hexagonal crystal system in regard to all those physical properties that are described by tensors of ranks up to four and which include dielectric, piezoelectric, and elastic phenomena.

2. THE RESONANCE METHOD FOR DETERMINATION OF THE ELASTIC AND PIEZOELECTRIC CONSTANTS

2.1 Resonance Method—General

The method for determining the values for the elastic and piezoelectric constants of piezoelectric crystals

TABLE I
SOME KNOWN PIEZOELECTRIC CRYSTALS

Crystal System and Class			Material
II	Monoclinic	C_2	Ethylene diamine tartrate (EDT). Potassium tartrate (DKT). Lithium sulphate monohydrate.
III	Orthorhombic	D_2	Rochelle salt.
IV (b)	Tetragonal	C_{4v} D_{2d}	Barium titanate single crystal. Ammonium dihydrogen phosphate (ADP).
V (b)	Trigonal	D_3	Alpha-quartz.
VI	Hexagonal	D_6	Beta-quartz.
VII	Isometric	T	Sodium bromate. Sodium chlorate.

should be simple and reliable. To determine the elastic and piezoelectric constants, the simplest method is the resonance method (see also [5], [7], [15]).

The main properties of a piezoelectric vibrator; e.g., the frequency and the parameters of the equivalent electric circuit, are expressed in terms of elastic, piezoelectric, and dielectric constants. Therefore, the values for these constants can be derived from measurements of resonance frequency, parameters of the equivalent electric circuit, and the dimensions and density of a suitably oriented specimen, when the theory for the mode of motion for the specimen is known. The relation between the elastic and piezoelectric constants and the measurable quantities of the piezoelectric vibrator are best expressed in terms of the frequency constant N , the motional capacitance constant Γ , and the capacitance ratio r . Further, each of these constants in turn can be described by a general expression including a factor adaptable to any mode, even though the modes have different strain-stress systems. These factors are derived from the differential equations of vibration under the appropriate boundary conditions.

2.2 Frequency Constant (N)

The frequency constant N of a vibrator is defined as the product of the series resonance frequency f_s and the linear dimension h which determines the frequency of the specimen; e.g., length l for the length-extensional mode of bars and contour modes of square plates, diameter ϕ for contour modes of disks, thickness t for thickness modes (see Section 2.5).

$$N = f_s h = \frac{F}{2} \sqrt{\frac{q}{\rho}} \quad (4)$$

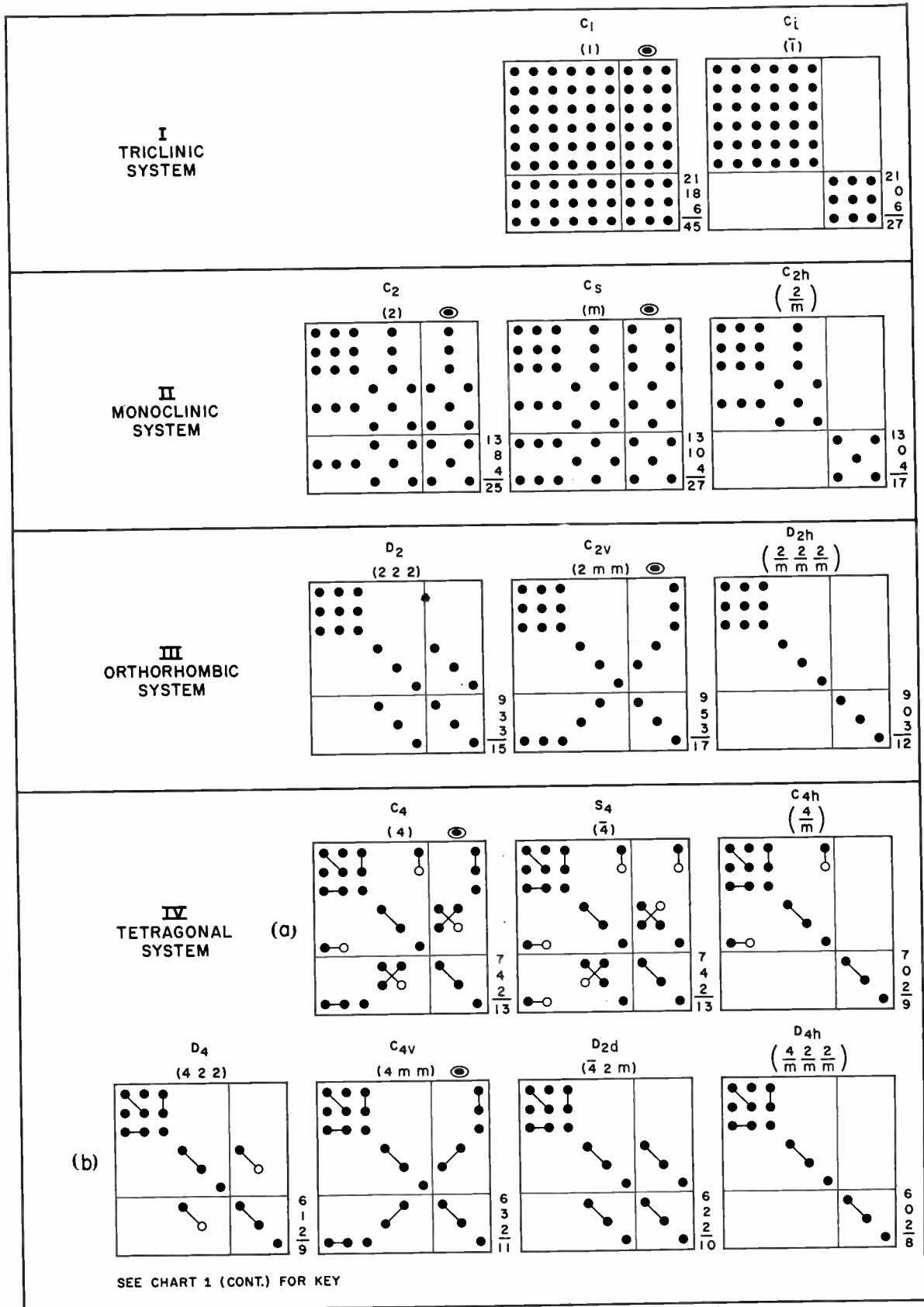
where q is the effective elastic modulus, ρ the density of the material, and

$$F = \frac{2\kappa}{\pi}, \quad (5)$$

F being a factor which is related to the eigen value κ of the mode.

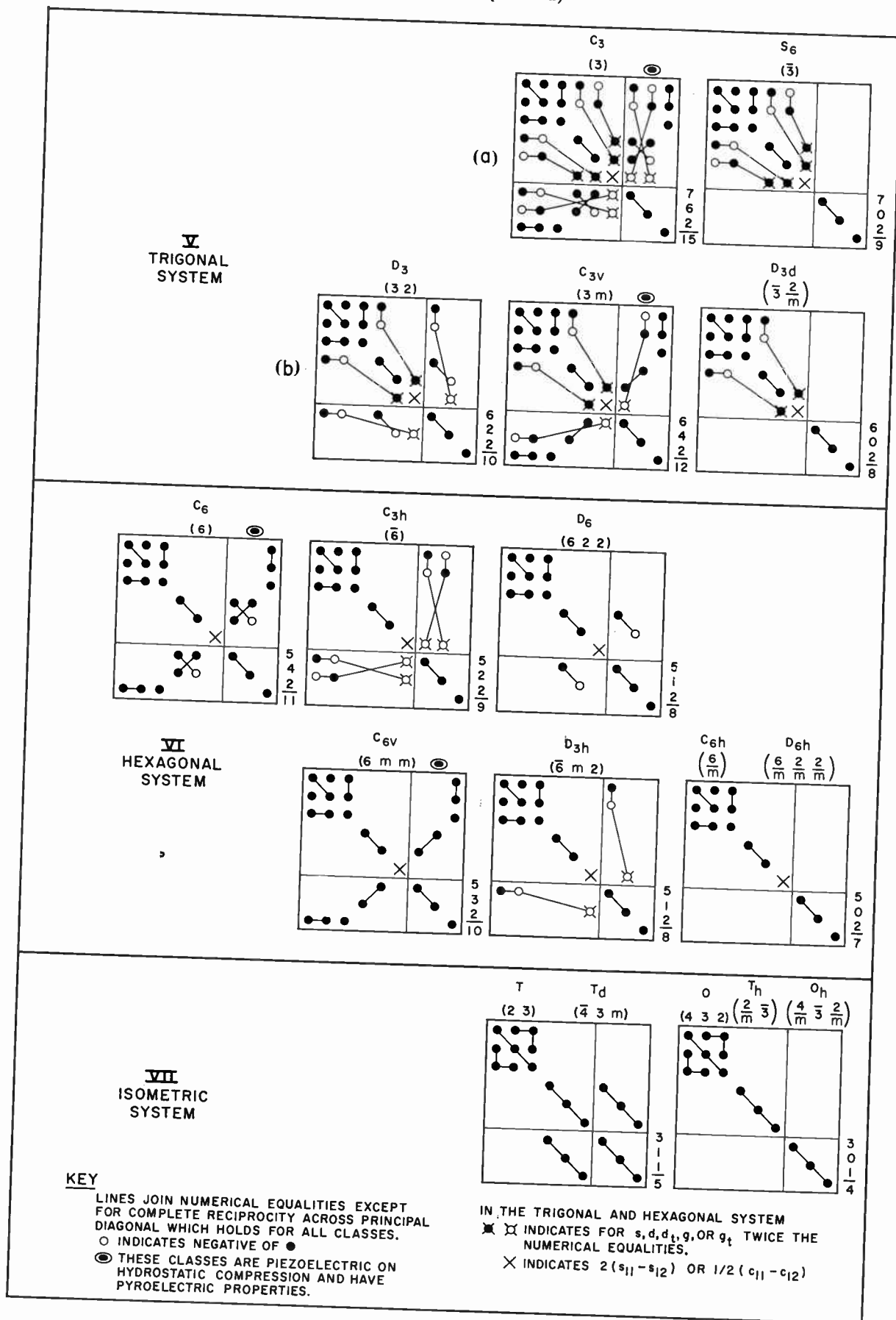
CHART I*

ELASTO-PIEZO-DIELECTRIC MATRIX OF VARIOUS CRYSTAL CLASSES



* The numbers on the right side of each scheme indicate, from top to bottom, the number of the independent elastic, piezoelectric, and dielectric constants.

CHART I (Cont'd)*



When the frequency f is measured in cycles per second and the linear dimension h is measured in meters, N is expressed in msec^{-1} which is numerically equal to kc-mm . For the units of g , κ , and F see Section 6.

2.3 Motional Capacitance Constant (Γ)

The motional capacitance constant is defined as $\Gamma = C_1(t/a)$, where C_1 is the motional capacitance of the vibrator, t is the linear dimension (thickness) parallel to the direction of the electric field, and a is the area of the fully plated specimen. This constant can be related to the vibrator properties by the equation

$$\Gamma = \rho\beta\delta^2N^2 \quad (6)$$

where N is the frequency constant, ρ the density, δ the effective piezoelectric strain constant, and β is a numerical factor following from the theory of vibration of the mode considered, taking into account the distribution of the mechanical displacement.

When the motional capacitance C_1 is measured in farads and the linear dimensions in meters, Γ is expressed in Fm^{-1} ($=10^9 \mu\mu\text{f mm}^{-1}$). Γ has the same dimension as a permittivity.

2.4 Capacitance Ratio (r)

The capacitance ratio $r = C_0/C_1$ of a vibrator, where C_0 is the shunt capacitance and C_1 the motional capacitance, is related to the series resonance frequency f_s and the parallel resonance frequency f_p , and is expressed by the constants describing the vibrator properties (in rationalized units)

$$\frac{1}{r} = \frac{f_p^2 - f_s^2}{f_s^2} = \frac{\Gamma}{\Gamma_0} = \frac{\rho\beta\delta^2N^2}{\epsilon^m}, \quad (7)$$

where $\Gamma_0 = C_0(t/a) = \epsilon^m$, the shunt capacitance constant, is the dielectric constant ϵ^m for the mode of the specimen considered.

The reciprocal of r is the square of the motional coupling factor (see Section 4). The capacitance ratio r is related to the appropriate static coupling factor k (see Section 4.6) in first approximation by the equation

$$\frac{1 - k^2}{rk^2} = p. \quad (8)$$

For more complete expressions, see Section 4.6. The numerical quantity p is used to eliminate ϵ^m and to determine the static coupling factor from the capacitance ratio (see Section 2.8.1).

2.5 Modes of Motion

Some commonly encountered modes of motion of bars and plates which can be excited piezoelectrically by a homogeneous electric field are now considered. The modes used to determine the elastic compliances and piezoelectric strain constants by the resonance method are the length-extensional mode and the overtone contour-shear mode of narrow bars, contour-extensional modes and contour-shear mode of square plates. The

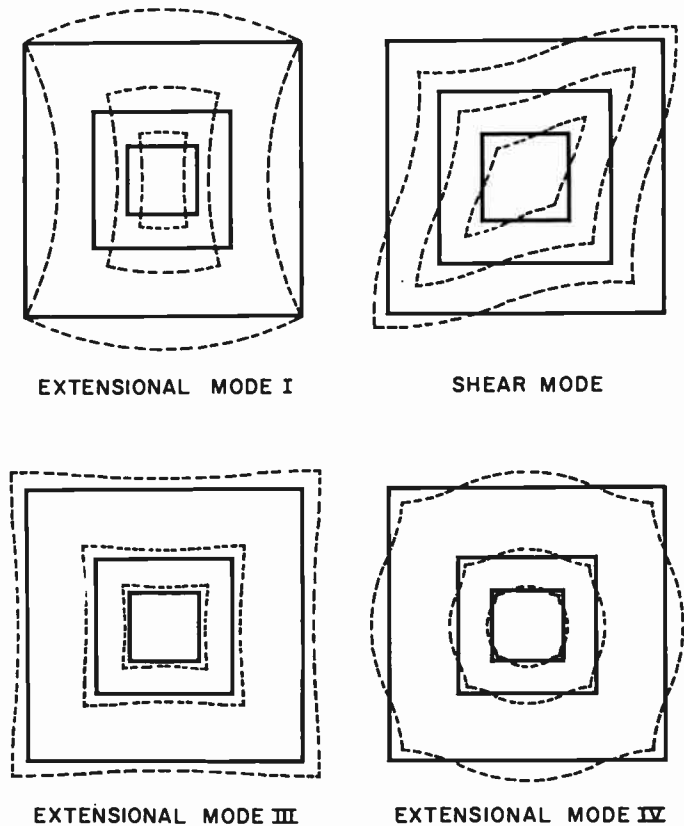


Fig. 1—Displacement of the various contour modes of square plates.

contour-extensional mode (radial mode) of disks and a contour-extensional mode of square plates are also used to determine some of the elastic and piezoelectric coefficients of crystals belonging to classes C_{3v} , C_6 , and C_{6v} . The thickness modes of plates are used to determine the elastic stiffnesses and piezoelectric stress constants. The type of displacement for the four contour modes of square plates considered is shown in Fig. 1.

The constants and parameters introduced in (4) to (8) inclusive, describing the mechanical properties g , κ , F , and the piezoelectric properties δ , β , p , of the various modes are listed in Table II. These quantities refer to infinitely narrow bars or infinitely thin plates. For convenience, specimens listed in Table II are assumed to be a (zx) cut, that is a z -cut bar or plate with length parallel to X . According to the actual orientation of the bars and plates used, the appropriate transformation for the elastic and piezoelectric constants must be applied. The transformation equations for the elastic, piezoelectric, and dielectric constants can be found in various references, [3]–[5]. Constants related to rotated axes are distinguished by primes; e.g., s' , d' from the unprimed constants s , d , which are related to the rectangular X , Y , Z crystal axes, as defined in the 1949 IRE Standards.

2.6 Measurements—General

The elastic, piezoelectric, and dielectric constants designated by subscripts refer to a specified system of rectangular axes. The crystallographic and rectangular axes should be chosen in accordance with the 1949 IRE

TABLE II
MODE CONSTANTS AND PARAMETERS

Specimen	Mode	Constant						Condition for Excitation	Remarks
		q	κ	F	δ	β	p		
Narrow Bar	Length-Extensional	$\frac{1}{s_{11}}$	$\frac{\pi}{2}$	1	d_{31}	$\frac{32}{\pi^2}$	$\frac{8}{\pi^2}$		
Square Plate	Contour-Extensional I	$\frac{1}{s_{11}' - s_{12}'} = \frac{2}{s_{66}}$	$\frac{\pi}{2}$	1	$d_{31}' = \frac{d_{36}}{2}$	$\frac{512}{\pi^4}$	$\frac{64}{\pi^4}$	Diagonal of the plate parallel to 2-, 4-, or 6-fold symmetry axis. $d_{31}' = -d_{32}'$. $s_{11}' = s_{22}'$, $s_{16}' = s_{26}'$.	Symmetry axis is X or Y. The primed values refer to a plate (zxt) 45°. See Fig. 1, mode I, Reference [8].
	Contour-Shear	$\frac{1}{s_{66}}$	$\frac{\kappa_0 \alpha}{\text{Footnote 1 below}}$	$\frac{2\kappa}{\pi}$	d_{36}	$\frac{4\pi^2 a}{\kappa_0^2(\kappa_0^2 + 2)}$	$\frac{4\alpha^2 a}{\kappa_0^2 + 2}$	One side parallel to 2-, 4-, or 6-fold symmetry axis.	Symmetry axis is X or Y. See Fig. 1, mode II, and Footnote 1 below, Reference [8].
	Contour-Extensional III	$\frac{1}{s_{11}}$	$\kappa(\sigma)$	$\frac{F_{III}}{\text{Table III}}$	d_{31}	for $\sigma=0$: $\frac{64}{\pi^2}$ for $\sigma \neq 0$: Table IV	for $\sigma=0$: $\frac{8}{\pi^2}$ for $\sigma \neq 0$: Table IV	Plate perpendicular to 3-, 4-, or 6-fold symmetry axis. Sides parallel to the other axes, $d_{31} = d_{32}$. $s_{11} = s_{22}$.	$\sigma = -\frac{s_{12}}{s_{11}}$ is Poisson's ratio. See Fig. 1, mode III, References [9], [10].
	Contour-Extensional IV	$\frac{1}{s_{11}}$	$\kappa(\sigma)$	$\frac{F_{IV}}{\text{Table III}}$	d_{31}	for $\sigma=0:0$		Plate perpendicular to 3- or 6-fold symmetry axis. $d_{31} = d_{32}$.	$\sigma = -\frac{s_{12}}{s_{11}}$ See Fig 1, mode IV, References [9], [10].
Disk	Contour-Extensional	$q_0 = \frac{1}{s_{11}}$	$\frac{\kappa_d(\sigma)}{\text{Table III}}$	$\frac{F_d}{\text{Table III}}$	d_{31}	$\frac{\beta_d}{\text{Table IV}}$	$\frac{p_d}{\text{Table IV}}$	Plate perpendicular to 3- or 6-fold symmetry axis. $d_{31} = d_{32}$.	$\sigma = -\frac{s_{12}}{s_{11}}$ See Footnote 2, below, References [7], [11].
Plate	Thickness-Shear	c_{44}	$\frac{n\pi}{2}$	n	$\frac{e_{34}}{c_{44}}$	$\frac{32}{n^2\pi^2}$	$\frac{8}{n^2\pi^2}$	Plate parallel to 2-, 4-, or 6-fold symmetry axis.	Y axis assumed to be a two-fold symmetry axis. $n=1, 3, 5, \dots$, =order of mode. (See Footnote 3, below.)
Prismatic Bar	Overtone Contour-Shear	$\left. \begin{matrix} 1 \\ s_{66} \\ 1 \\ s_{66} \end{matrix} \right\}$	$\frac{n\pi}{2}$	n	$\left. \begin{matrix} d_{36} \\ d_{36} \end{matrix} \right\}$	$\frac{32}{n^2\pi^2}$	$\frac{8}{n^2\pi^2}$	Vibration in the XY plane, h parallel to Y. Vibration in the ZX plane, h parallel to Z.	Length parallel to axis of symmetry. n =order of mode.

¹ κ_0 is root of the equation: $\tan \kappa_0 + \kappa_0 = 0$. The first root is $\kappa_0 = 2.0288$. α and a are corrections of the form

$$\alpha = 1 - 0.05015\mu^{1/2} \text{ and } \mu = \frac{s_{11} + s_{22}}{2s_{66}}$$

$$a = 1 - 0.0691\mu$$

² Usually

$$q = \frac{s_{11}}{s_{11}^2 - s_{12}^2} = \frac{1}{s_{11}(1 - \sigma^2)} \text{ and } F = \frac{2\kappa}{\pi}$$

In this table q_0 and F_d are used instead of q and F giving identical results:

$$q = q_0 = \frac{1}{s_{11}}, F_d = \frac{2\kappa}{\pi} (1 - \sigma^2)^{-1/2}$$

$\kappa_d = \kappa$ is root of equation: $\kappa J_0(\kappa) - (1 - \sigma) J_1(\kappa) = 0$, where J_0 and J_1 are Bessel functions of the order zero and one. In the vicinity of $\sigma = 0.30$, the first root for κ is given by [12]

$$\kappa = 2.04885 + 0.62323(\sigma - 0.30) - 0.202(\sigma - 0.30)^2$$

$$\beta_d = \frac{4\pi^2}{\kappa^2} \frac{(1 + \sigma)^2}{\kappa^2 - 1 + \sigma^2}, \quad p_d = \frac{2(1 + \sigma)}{\kappa^2 - 1 + \sigma^2}$$

³ To avoid correction factor for frequency constant, use f_p instead of f_s . The values for β and p refer to a uniform strain distribution. A more complete solution for a finite plate is given by Mindlin [13].

Standards. All specimens measured should be oriented with respect to these axes.

The bars and plates should be mounted in such a way that the intended mode of motion is relatively unrestricted. For bars and plates to be excited in length-extensional and contour modes, respectively, the surfaces perpendicular to the electric field, which is in the thickness direction, are fully plated with very thin conducting layers as electrodes, the other surfaces being free from conducting layers. Silver, gold, or aluminum layers, deposited by evaporation, are known to be suitable.

For an exact determination of the constants, various influences must be taken into account. The conditions under which the bars and plates are measured must agree with the conditions on which the formulas were based; for example, bars must be narrow enough or plates large enough to render unimportant any errors due to the influence of the width-length or thickness-length ratio. Tests must be made to insure that no disturbing frequencies are present which might influence the results. It is necessary to so choose the linear dimensions for the resonators that no other mode of motion is nearby in frequency. In particular, when bars having certain dimensional ratios are vibrating longitudinally, flexural modes can be excited by coupling. For example, in a bar of any material, of which the width is about 0.2 to 0.3 times the length, the frequency of the second flexural mode coincides with that of the longitudinal mode. If any coupling between the longitudinal and shear modes is not zero, the properties of the coupled vibration differ from those of the longitudinal vibration, and ratios near this critical value should therefore be avoided. Occasionally, it may be necessary to alter the dimensions of the specimen. Slight changes in plate dimensions should suffice to determine if a clear region is available. In general, bars having a width-length ratio smaller than 0.1 and plates having a thickness-length ratio smaller than 0.1 approximate an assumed infinitely narrow bar or an infinitely thin plate. The values for zero ratios can be derived by extrapolating the results obtained from bars and plates of varying width-length or thickness-length ratios. On the other hand, adequate corrections of the Rayleigh type for the width-length or thickness-length ratio may be applied.

The resonance method for the determination of piezoelectric constants, for which the formulas contain only the squares of these quantities, and, in general, the square of a combination of such values, results in an ambiguity in the sign which must be considered. The sign of one of the piezoelectric constants, as defined in the 1949 IRE Standards, must be determined by a static test.

The accuracy of the constants determined dynamically is influenced by various factors. First, the accuracy depends on the mechanical preparation and measure-

ment of the specimen itself, the measurement of its orientation with respect to the crystallographic axes, and the influences already mentioned. For the accuracy of piezoelectric stress constants, see Section 2.9. Second, the accuracy depends on the methods of measurement of the frequency and of the parameters of the equivalent electric circuit. The accuracy of these measurements in turn depends on the values of Q and the capacitance ratio r of the specimen measured and the approximation used in terms of these quantities. Methods for measurement of the parameters of the equivalent electric circuit and the various approximations, taking into consideration the influence of Q and r , are covered in the 1957 IRE Standards [2]. The expression for the motional capacitance is independent of the dielectric constant. When high accuracy is of importance, methods should be used which avoid the shunt capacitance. A bridge method for measuring the motional capacitance at various frequencies near that of resonance, preferably differing from the resonance frequency by from 0.5 per cent to 5 per cent, is most accurate. If there are no unwanted modes, the motional capacitance of the equivalent electric circuit can be measured to within 0.2 per cent. Because of temperature dependence of the various constants, all measurements should be made at a specified temperature.

2.7 Elastic Constants

From measurements of the series resonance frequency f_s of a particular mode of a given specimen, the dimension h controlling the frequency, and the density ρ , the effective elastic constant q can be determined according to (4),

$$q = \frac{4\rho N^2}{F} \quad (9)$$

where $N = f_s h$ is the frequency constant and F is the appropriate mode factor given in Table II.

The elastic constant q is equal to the reciprocal of the compliance $1/s$ for the extensional mode of thin bars and for contour modes of thin plates. In the case of a fully plated specimen, the compliance for constant electric field s^E is thus obtained. The elastic constant q obtained from a thickness mode is the stiffness c^D measured at constant normal displacement. The elastic constant q , obtained from the overtone contour-shear mode of a (zx) cut bar, is $1/s_{66}^E$, where the direction of the displacement is perpendicular to the direction of the electric field and is $1/s_{55}^D$, where the direction of the displacement is parallel to the direction of the electric field. In the latter case, the parallel resonance frequency f_p should be used instead of the series resonance frequency f_s in the expression for the frequency constant.

2.7.1 Elastic Compliances From Length-Extensional and Contour-Shear Modes: Measurements of the length-

TABLE III

THE CONSTANTS F_{III} , F_{IV} , κ_d , F_d AS FUNCTIONS OF σ

σ	F_{III}	F_{IV}	F_{IV}/F_{III}	κ_d	F_d
0.25	1.1218	1.7012	1.5164	2.0172	1.3272
0.26	1.1277	1.6974	1.5052	2.0236	1.3348
0.27	1.1336	1.6938	1.4942	2.0300	1.3422
0.28	1.1396	1.6903	1.4832	2.0362	1.3503
0.29	1.1458	1.6869	1.4723	2.0425	1.3587
0.30	1.1519	1.6836	1.4615	2.0488	1.3673
0.31	1.1582	1.6804	1.4509	2.0551	1.3761
0.32	1.1646	1.6773	1.4403	2.0612	1.3851
0.33	1.1710	1.6744	1.4299	2.0673	1.3943
0.34	1.1775	1.6716	1.4197	2.0735	1.4037
0.35	1.1841	1.6690	1.4096	2.0795	1.4132

TABLE IV

THE CONSTANTS β_{III} , ρ_{III} , β_d , ρ_d AS FUNCTIONS OF σ

σ	β_{III}	ρ_{III}	β_d	ρ_d
0.25	6.38	0.746	4.841	0.797
0.26	6.37	0.749	4.839	0.796
0.27	6.36	0.748	4.838	0.795
0.28	6.35	0.742	4.837	0.794
0.29	6.34	0.738	4.836	0.792
0.30	6.32	0.734	4.834	0.791
0.31	6.31	0.730	4.832	0.789
0.32	6.29	0.725	4.831	0.788
0.33	6.27	0.720	4.829	0.786
0.34	6.25	0.715	4.828	0.785
0.35	6.23	0.710	4.827	0.783

extensional modes of a sufficient number of independently oriented bars, cut from an asymmetric material (class C_1), will result in the determination of nine of the possible elastic compliances

$$s_{11}, s_{22}, s_{33}, s_{15}, s_{16}, s_{24}, s_{26}, s_{34}, s_{35}$$

and six combinations of the other twelve constants,

$$s_{44} + 2s_{23}, s_{55} + 2s_{13}, s_{66} + 2s_{12}, s_{14} + s_{56}, s_{25} + s_{46}, s_{36} + s_{45}.$$

For the other crystal systems, the number of elastic compliances, determinable from measurements on bars, decreases with increasing symmetry. The compliances and their combinations for the different crystal systems reduce to

II	Monoclinic:	$s_{11}, s_{22}, s_{33}, s_{15}, s_{35}$	$s_{44} + 2s_{23}, s_{66} + 2s_{13}, s_{66} + 2s_{12}, s_{25} + s_{44}$
III	Orthorhombic:	s_{11}, s_{22}, s_{33}	$s_{44} + 2s_{23}, s_{55} + 2s_{13}, s_{66} + 2s_{12}$
IV (a)	Tetragonal:	s_{11}, s_{33}, s_{16}	$s_{44} + 2s_{13}, s_{66} + 2s_{12}$
IV (b)	Tetragonal:	s_{11}, s_{33}	$s_{44} + 2s_{13}, s_{66} + 2s_{12}$
V (a)	Trigonal:	$s_{11}, s_{33}, s_{14}, s_{25}$	$s_{44} + 2s_{13}$
V (b)	Trigonal:	s_{11}, s_{33}, s_{14}	$s_{44} + 2s_{13}$
VI	Hexagonal:	s_{11}, s_{33}	$s_{44} + 2s_{13}$
VII	Isometric:	s_{11}	$s_{44} + 2s_{12}$

For both the trigonal and hexagonal systems, when the plane perpendicular to the 3- and 6-fold symmetry axis behaves isotropically, the combination $s_{66} + 2s_{12}$ is equal to $2s_{11}$. In order to separate the combinations given above and to determine the compliances s_{12} and s_{66} , for the trigonal and hexagonal systems, it is necessary to use some other mode of motion. Measurements limited to the extensional mode of bars are in no case sufficient to determine all elastic constants.

Most combinations of elastic compliances obtained from a length-extensional mode of bars can be separated using a pure contour-shear mode or an extensional mode I of square plates. Besides the triclinic system, which will not be considered here, the only exceptions are s_{55} of the monoclinic system, s_{66} of the tetragonal system [IV(a)], and s_{44} of the trigonal system [V(a)] (see Chart I). In these cases, it is necessary to use coupled contour modes to determine these compliances. A list of the crystal systems, together with those compliances that can be determined from the contour-shear

mode or the contour-extensional mode I of square plates, is as follows.

II	Monoclinic:	s_{44}, s_{66}, s_{46}
III	Orthorhombic:	s_{44}, s_{55}, s_{66}
IV (a)	Tetragonal:	s_{44}
IV (b)	Tetragonal:	s_{44}, s_{66}
V (a)	Trigonal:	s_{66}
V (b)	Trigonal:	$s_{44}, s_{66}, (s_{14})$
VI	Hexagonal:	s_{44}
VII	Isometric:	s_{44}

The compliance shown in parentheses can also be derived directly from the length-extensional mode of bars, where the determination from contour modes acts as a check.

2.7.2 Elastic Compliances from other Modes: In many cases the shear compliances can also be determined from the overtone shear modes of bars. An example is $s_{55}^D = s_{44}^D$ for the hexagonal class C_{6v} , which can be obtained from an (xz) cut.

To determine s_{12}^E or Poisson's ratio $\sigma = -s_{12}^E/s_{11}^E$ of a trigonal or hexagonal crystal, the contour-extensional mode III of square z -cut plates, or the contour-extensional mode of a z -cut disk, can be used, in addition to the length-extensional mode of a bar, giving s_{11} . Examples are crystals of classes C_{3v} and C_{6v} . Another method is based on the use of contour mode III and mode IV of a square z -cut plate. From measurements of both these modes, s_{11}^E and s_{12}^E can be determined and, in particular, Poisson's ratio is obtained from the ratio of the two frequencies measured on the same sample. The ratio of the frequency constants $N_{IV}/N_{III} = F_{IV}/F_{III}$ as function of Poisson's ratio σ is given in Table III.

An alternative method for the separation of combinations of elastic compliances, obtained from length-extensional modes of bars, is the use of thickness-shear modes. Some of the elastic shear-stiffnesses can be determined from a thickness-shear mode, and from these stiffnesses, the corresponding shear compliances can be calculated. This results in the same compliances as were obtained for contour modes of square plates as listed in Section 2.7.1. The symmetry conditions for plates cut from material of various crystal systems excited in the thickness-shear mode are identical with those for the contour-shear mode of square plates.

The three thickness modes of an arbitrarily oriented plate usually can be excited by a field perpendicular or parallel to the surface of the plate. All the elastic stiffnesses can be determined independently from a sufficient number of differently oriented plates and by using both types of excitation.

2.8 Piezoelectric Constants

All the eighteen piezoelectric constants can be derived from measurements of piezoelectrically excited bars and plates, oriented the same as those used for the determination of the elastic constants. Generally, both the elastic and piezoelectric constants can be derived from measurements on the same set of specimens. The number of specimens needed depends on the symmetry class of the crystal. There are two significant variants of the resonance method for the determination of the piezoelectric constants.

2.8.1 Capacitance Ratio Method: The effective piezoelectric constant δ is related to the capacitance ratio r and the frequency constant N of a particular mode of a given specimen according to (7) by

$$\delta = \pm \frac{1}{N} \sqrt{\frac{\epsilon^m}{\rho\beta r}} \quad (10)$$

where ϵ^m is the effective dielectric constant of the plate for the mode excited.

The effective piezoelectric constant δ is equivalent to a piezoelectric strain constant d for extensional modes of bars and contour modes of plates. The effective piezoelectric constant δ for thickness modes is equivalent to e/c , where e and c are the corresponding effective piezoelectric stress constant and stiffness, respectively.

Two cases are to be distinguished: 1) length-extensional modes of bars and contour modes of plates; and 2) thickness modes of plates.

Case 1: In (10) ϵ^m must be related to the constant stress or "free" dielectric constant ϵ^T , which can be measured directly at low frequency (see Section 3).

The effective dielectric constant ϵ^m is generally related to the capacitance ratio r by the equation

$$\epsilon^m = \frac{pr\epsilon^T}{1 + pr\chi} \quad (11)$$

where p , introduced in (8), is a factor characteristic of the mode considered. The expressions for p for various modes can be found in Table II. The factor χ takes into account the influence of the other modes of the specimen excitable with the same electrode arrangement. For specimens with a single series of modes, as fulfilled; e.g., for the length-extensional mode of a bar, the contour-shear mode and the contour-extensional mode III of square plates, and the radial mode of a disk, $\chi \approx 1$.

For the contour-extensional mode I of a square plate where a second mode, the contour-extensional mode II¹ is close in frequency, χ is of the order 0.91. By substituting ϵ^m from (11) in (10), the piezoelectric constant δ can be determined from the measured values of N , ρ , r , and ϵ^T of a particular mode from the equation

$$\delta = \pm \frac{1}{N} \sqrt{\frac{p}{\rho\beta} \frac{\epsilon^T}{1 + pr\chi}} \quad (12)$$

Case 2: In the case of thickness modes, $\delta = e/c$. For thickness modes $\epsilon^m \approx \epsilon^S$, where ϵ^S is the clamped dielectric constant. If no other modes are excitable in the plate except a single series of thickness modes (fundamental and overtone), then ϵ^m can be related to ϵ^T by $\epsilon^m \approx \epsilon^S = \epsilon^T / (1 + 1/pr)$ and finally

$$e = \pm 4N \sqrt{\frac{\rho p}{\beta} \frac{\epsilon^T}{1 + pr}} \quad (13)$$

2.8.2 Motional Capacitance Method: From measurements of the motional capacitance constant Γ and from measurement of the frequency constant N of a particular mode of a given specimen, the approximate piezoelectric constant δ can be determined according to (6) by

$$\delta = \pm \frac{1}{N} \sqrt{\frac{\Gamma}{\rho\beta}} \quad (14)$$

As mentioned in Section 2.8.1, the piezoelectric constant δ is identical with a piezoelectric strain constant d , for length-extensional modes of bars and contour modes of plates, and is identical with e/c for thickness modes where e is the piezoelectric stress constant and c is the stiffness.

In the case of the thickness mode

$$e = \pm 4N \sqrt{\frac{\rho}{\beta} \Gamma} \quad (15)$$

2.8.3 Comparison of Capacitance-Ratio and Motional Capacitance Methods: The capacitance ratio depends on the shunt capacitance and, therefore, on the actual permittivity ϵ^m which is a function of the frequency spectrum of the specimen as a whole. According to the expressions for the elements of the equivalent electric circuit C_1 , L_1 , and R_1 , these quantities are independent of the dielectric permittivities. Consequently, when using the capacitance ratio method, the quantity ϵ^m must be eliminated from (10) by means of (11). The motional capacitance method is independent of the dielectric permittivities. This method is, therefore, more accurate in cases of specimens having no sym-

¹ Contour-extensional mode II of square plates, another anti-symmetric mode (see [8], [11]), is not considered here since no application for the determination of the constants is made.

TABLE V
MODES FOR OBTAINING THE PIEZOELECTRIC STRAIN CONSTANTS FOR VARIOUS CRYSTAL CLASSES

	I			II		III		IV					V			VI					VII
	C_1	C_2	C_6	D_1	C_{3v}	C_1	S_4	D_4	C_{4v}	D_{2d}	C_4	D_2	C_{3v}	C_6	C_{3h}	D_6	C_{6v}	D_{3h}	T, T_d		
d_{11}	—	—	—	—	—	—	—	—	—	—	A	A, B	—	—	A, B	—	—	A, B	—		
d_{12}	A	—	A	—	—	—	—	—	—	—	— d_{11}	— d_{11}	—	—	— d_{11}	—	—	— d_{11}	—		
d_{13}	A	—	A	—	—	—	—	—	—	—	—	—	—	—	—	—	—	—	—		
d_{14}	A	A, B	—	A, B	—	A, B	A, B	A, B	—	A, B	A	A, B	—	A, B	—	A, B	—	A, B	A, B		
d_{15}	—	E	—	—	E	E	A, B	—	E	—	E	E	E	—	—	E	—	—	—		
d_{16}	—	—	—	—	—	—	—	—	—	—	— $2d_{11}$	— $2d_{11}$	—	— $2d_{11}$	—	—	—	—	—		
d_{21}	A	A	—	—	—	—	—	—	—	—	— d_{11}	—	— d_{11}	—	— d_{11}	—	—	—	—		
d_{22}	—	E	—	—	—	—	—	—	—	—	A	—	A	—	A, B	—	—	—	—		
d_{23}	A	A	—	—	—	—	—	—	—	—	—	—	—	—	—	—	—	—	—		
d_{24}	A	A	—	A, B	—	— d_{11}	d_{11}	d_{11}	d_{11}	d_{11}	d_{11}	d_{11}	d_{11}	d_{11}	—	—	d_{11}	—	d_{11}		
d_{25}	—	—	—	—	—	—	—	—	—	—	— d_{11}	— d_{11}	—	— d_{11}	—	— d_{11}	—	— d_{11}	—		
d_{31}	A	—	A	—	A	A, D	—	—	A, D	—	A, D	—	A, D	—	—	—	A, D	—	—		
d_{32}	A	—	A	—	A	A	— d_{11}	—	A	—	d_{11}	—	d_{11}	—	—	—	d_{11}	—	—		
d_{33}	—	E	—	—	E	E	—	—	E	—	E	—	E	—	—	—	E	—	—		
d_{34}	—	—	—	—	—	—	—	—	—	—	—	—	—	—	—	—	—	—	—		
d_{35}	—	E	—	—	—	—	—	—	—	—	—	—	—	—	—	—	—	—	—		
d_{36}	A	A, B	—	A	—	—	A	—	—	—	—	—	—	—	—	—	—	—	d_{11}		
$d_{11}-d_{12}$	A	—	A	—	—	—	—	—	—	—	$3d_{11}$	—	—	—	—	—	—	—	—		
$d_{11}-d_{13}$	A	—	A	—	—	—	—	—	—	—	d_{11}	—	—	—	—	—	—	—	—		
$d_{11}-d_{14}$	A	A	—	—	—	—	—	—	—	—	d_{11}	—	d_{11}	—	—	—	—	—	—		
$d_{11}-d_{15}$	A	A	—	—	—	—	—	—	—	—	$3d_{11}$	—	$3d_{11}$	—	—	—	—	—	—		
$d_{11}-d_{16}$	A	—	A	—	A	A	—	—	A	—	A	—	A	—	—	—	A	—	—		
$d_{12}-d_{13}$	A	—	A	—	A	$d_{11}-d_{11}$	—	—	$d_{11}-d_{11}$	—	$d_{11}-d_{11}$	—	$d_{11}-d_{11}$	—	—	—	$d_{11}-d_{11}$	—	—		
$d_{14}-d_{15}$	—	B	—	—	—	—	—	—	—	—	—	—	—	—	—	—	—	—	—		
$d_{24}-d_{15}$	—	—	—	—	B	—	—	—	—	—	—	—	—	—	—	—	—	—	—		

Piezoelectric coefficients in place of mode symbols are identical to the piezoelectric coefficients in the first column.
 Key: A=length-extensional mode of bars.
 B=contour-shear mode or contour-extensional mode I of square plates.
 D=contour-extensional mode III of square plates or contour-extensional modes of disks.
 E=computed from piezoelectric stress constant obtained in thickness modes.

metry relations with respect to the natural crystallographic axes, where a more complicated frequency spectrum occurs.

The actual dielectric constant ϵ^m can be determined, however, from both types of measurements according to the equation

$$\epsilon^m = \Gamma\gamma \tag{16}$$

which follows from (6) and (7). The dielectric constant ϵ^m can also be calculated [11].

2.8.4 Piezoelectric Strain Constants: Most of the piezoelectric strain constants can be determined from measurements on bars and square plates oriented in the same manner as used for determination of elastic compliances and excited in the same modes.

By using a sufficient number of independently oriented bars cut from asymmetric material (class C_1) excited in extensional mode by means of electrodes on their major surfaces, it is possible to determine nine piezoelectric strain constants

$$d_{12}, d_{13}, d_{14}, d_{21}, d_{23}, d_{25}, d_{31}, d_{32}, d_{36}$$

and six combinations of the other nine constants

$$d_{26}-d_{11}, d_{35}-d_{11}, d_{34}-d_{22}, d_{16}-d_{22}, d_{15}-d_{33}, d_{24}-d_{33}.$$

The number of piezoelectric strain constants for other classes decreases with increasing symmetry. The following crystal classes are free of combinations: $D_2, S_4, D_4, D_{2d}, D_3, C_{3h}, D_6, D_{3h}, T, T_d$. For these classes all piezoelectric strain constants can be determined independently from length-extensional modes of bars. Table V lists the modes of motion which may be used to obtain

the piezoelectric strain constants for the various crystal classes.

There are two methods of splitting the combinations of the piezoelectric strain constants obtained from the length-extensional mode of bars. One of these is based on measurements on plates vibrating in a thickness-shear mode, excited by a field parallel to the thickness. This results in the piezoelectric stress constants e from which the corresponding strain constants d can be calculated. Considering certain individual crystal classes, these piezoelectric stress constants are

$$C_2: e_{34}, e_{16}, \quad C_{2v}: e_{15}, e_{24}, \quad C_4, C_{4v}, C_6, C_{6v}: e_{15}.$$

The relation between these e and the d are given by

$$C_2: \quad d_{14} = e_{14}S_{44}^E + e_{16}S_{46}^E, \quad d_{16} = e_{14}S_{46}^E + e_{16}S_{66}^E, \\ d_{34} = e_{34}S_{44}^E + e_{36}S_{46}^E, \quad d_{36} = e_{34}S_{46}^E + e_{36}S_{66}^E \\ C_{2v}: \quad d_{15} = e_{15}S_{55}^E, \quad d_{24} = e_{24}S_{44}^E \\ C_4, C_{4v}, C_6, C_{6v}: \quad d_{15} = e_{15}S_{44}^E.$$

Another method for the separation of the combinations of the piezoelectric strain constants is based on the use of the overtone contour-shear mode of bars.

Both these methods usually result in a rather low degree of accuracy for the values obtained. The value for β given in Table II for the thickness modes is based on the assumption that the elastic displacement in the plane of the plate is uniform. Actually, the elastic displacement is not uniform, thus a correction for β is required. A general theory for the distribution of the displacement does not exist. The overtone contour-shear

mode of bars usually gives small values for $1/r$ or for the capacitance constant Γ , in comparison with the values for fundamental modes, resulting again in a low accuracy.

3. DIELECTRIC CONSTANTS

The several dielectric constants are evaluated from measurements of the capacitance of large plates provided with electrodes adhering to the major surfaces. These measurements are made at a frequency which is substantially lower than any of the resonance frequencies of the crystal plate and yield the dielectric constants at constant stress or "free" dielectric constants ϵ^T . In a crystal of the triclinic system there are 6 "free" dielectric constants, all of which can be evaluated by measuring a number of selected orientations.

From measurements of 3 plates cut perpendicular to the X , Y , and Z axes, the three main dielectric constants

$$\epsilon_{11}^T, \epsilon_{22}^T, \epsilon_{33}^T$$

can be obtained directly. The other three dielectric constants

$$\epsilon_{12}^T, \epsilon_{13}^T, \epsilon_{23}^T$$

can be found by measuring 3 plates, rotated about the X , Y , and Z axes, and solving 3 equations.

At frequencies very high compared to the principal natural frequencies of the plate, the dielectric constant approaches a steady value corresponding to the constant strain or "clamped" dielectric constant ϵ^S . Capacitance measurements similar to those described above, but at very high frequencies, result in all 6 values of ϵ_{ij}^S .

An inspection of Chart I for the different crystal systems shows that in most cases fewer than 6 orientations are required; for example, a single determination suffices for crystals belonging to the isometric system since only one value of the dielectric constant is involved.

The relations between the dielectric constants at constant strain and constant stress which follow from (2) and (3) (see also [1]) are given by

$$\epsilon_{ij}^S = \epsilon_{ij}^T - \sum_p^6 d_{jp} e_{ip}$$

where d_{jp} and e_{ip} are piezoelectric strain and stress constants, respectively. For nonrationalized units, the factor 4π is to be inserted before the summation sign.

A standard capacitance bridge is suitable for measuring the capacitance at low frequencies.

4. ELECTROMECHANICAL COUPLING FACTOR (k)

The use of the electromechanical coupling factor has become more prevalent since the 1949 IRE Standards was issued. This is especially true in the field of ferroelectric ceramics. The appropriate static coupling factor involves the material properties, and is closely related

to the capacitance ratio for various modes of motion. The numerical values of the electromechanical coupling factor are usually derived from measurements of the capacitance ratio (see Section 4.6).

Special applications of the electromechanical coupling factor, which are related to the measurements of the elastic, piezoelectric, and dielectric constants of some crystal classes of high symmetry, are considered briefly here.

The piezoelectric equations of state (see Section 1) can be derived from energy equations. For example the energy equations corresponding to (1) are [14]

$$\begin{aligned} \frac{1}{2} \sum_p S_p T_p &= \frac{1}{2} \sum_{pq} s_{pq}^E T_p T_q + \frac{1}{2} \sum_{pj} d_{jp} T_p E_j \\ &= U_1 + U_{12} \\ \frac{1}{2} \sum_i D_i E_i &= \frac{1}{2} \sum_{iq} d_{iq} E_i T_q + \frac{1}{2} \sum_{ij} \epsilon_{ij}^T E_i E_j \\ &= U_{12} + U_2. \end{aligned} \tag{17}$$

U_1 represents the elastic energy density, U_2 the electrical energy density, and U_{12} the piezoelectric energy density. Similar energy equations, corresponding to (3) and to the other two sets of equations of state, hold. These are not detailed in Section 1. The electromechanical coupling factor of the volume element associated with (17) can be defined as

$$k = \sqrt{\frac{U_{12}^2}{U_1 U_2}}. \tag{18}$$

The coupling factor, as defined by (18), is the square root of the ratio of the mutual elasto-dielectric energy density squared to the product of the stored elastic and dielectric energy densities. This definition applies to any specified elasto-dielectric state of a volume element of a material. The partial energy densities U are unique; they may, however, be expressed variously in terms of the elements of different submatrices.

Lumped piezoelectric coupling factors associated with finite electromechanical systems under known stress or strain, and known electric field or dielectric displacement distributions, are obtained in terms of volume integrals over the component energy densities. Under static conditions, where these distributions are uniform, the resulting coupling factors are identical with those of a volume element. For motional conditions, where the kinetic energy density not dielectrically coupled is an essential component, the associated motional coupling factors are dependent on the modes of motion of the specimen.

Under special conditions, such as crystallographic symmetry, expressions for the energy densities in terms of matrix components may be greatly simplified. In particular, where only certain parts of the energy density

components are of interest, simple expressions for the associated partial static coupling factors are obtained. Some examples are considered in the following sections.

4.1 One-Dimensional Coupling Factor

Assuming that only the stress component T_1 is not zero, while $T_2 \cdots T_6$ are zero, the expression for the static electromechanical coupling factor reduces to

$$k = k_{31} = \sqrt{\frac{d_{31}^2}{\epsilon_{33}^T s_{11}^E}}. \quad (19)$$

The subscripts 3 and 1 indicate the directions of the electric field and the mechanical displacement, respectively. The corresponding motional stress system is that for the length-extensional mode of bars.

4.2 Planar-Extensional Coupling Factor

The piezoelectric equations (1) for a Z plane is specialized for the tetragonal classes C_3 , C_{3v} and the hexagonal classes C_6 , C_{6v} , where $s_{11} = s_{22}$, $s_{66} = 2(s_{11} - s_{12})$, $s_{16} = s_{26} = 0$, and $d_{31} = d_{32}$. Assuming the symmetrical stress system $T_1 = T_2$, $T_3 \cdots T_6 = 0$, (1) becomes

$$\begin{aligned} S_1 + S_2 &= 2(s_{11}^E + s_{12}^E)T_1 + 2d_{31}E_3 \\ D_3 &= 2d_{31}T_1 + \epsilon_{33}^E E_3 \end{aligned} \quad (20)$$

or introducing the planar strain $S_1 + S_2 = S_p^2$ and setting $T_1 = T_2 = T_p$

$$\begin{aligned} S_p &= s_p^E T_p + d_p E_3 \\ D_3 &= d_p T_p + \epsilon_{33}^T E_3 \end{aligned} \quad (21)$$

where the planar elastic compliance s_p and the planar piezoelectric strain constant d_p are defined as

$$\begin{aligned} s_p^E &= \left. \frac{\partial S_p}{\partial T_p} \right|_{E_3} = 2(s_{11}^E + s_{12}^E) \\ d &= \left. \frac{\partial S_p}{\partial E_3} \right|_T = \left. \frac{\partial D_3}{\partial T_p} \right|_{E_3} = 2d_{31}. \end{aligned} \quad (21a)$$

The static planar coupling factor k_p becomes

$$k = k_p = \sqrt{\frac{d_p^2}{\epsilon_{33}^T s_p^E}} = \sqrt{\frac{2d_{31}^2}{\epsilon_{33}^T (s_{11}^E + s_{12}^E)}}. \quad (22)$$

The corresponding motional stress system is that for contour-extensional mode III and the radial mode of disks.

4.3 Planar-Shear Coupling Factor

It is assumed that the Z plane is parallel to a 2-, 4-, or 6-fold symmetry axis and that $s_{16} = s_{26} = 0$, $d_{36} \neq 0$,

² In this section, the subscript p indicates planar.

$d_{31} = d_{32} = 0$, and the stress component T_6 only is not zero. Then (1) or (2) reduce to

$$\begin{aligned} S_6 &= s_{66}^E T_6 + d_{36} E_3 \\ D_3 &= d_{36} T_6 + \epsilon_{33}^T E_3. \end{aligned} \quad (23)$$

From this equation, the static planar shear coupling factor becomes

$$k = \sqrt{\frac{d_{36}^2}{\epsilon_{33}^T s_{66}^E}}. \quad (24)$$

The corresponding motional stress system is that of the contour-shear mode.

When, under the same symmetry conditions for the plate, the two stresses, $T_1' = -T_2'$, are inclined at an angle of 45° to the symmetry axis, the coupling factor has the same form as (24). The corresponding motional stress system is that for the contour-extensional mode I of square plates.

4.4 Hydrostatic Coupling Factor

Another important stress system is the hydrostatic stress $T_1 = T_2 = T_3 = T_h$. In this case the linear piezoelectric equations (1) becomes, for crystals of the classes C_3 , C_{3v} , C_6 , and C_{6v} ,

$$\begin{aligned} S_1 + S_2 + S_3 &= [2(s_{11}^E + s_{12}^E) + 4s_{13}^E + s_{33}^E]T_1 \\ &\quad + (2d_{31} + d_{33})E_3 \\ D_3 &= (2d_{31} + d_{33})T_1 + \epsilon_{33}^T E_3 \end{aligned} \quad (25)$$

or, introducing the hydrostatic strain $S_1 + S_2 + S_3 = S_h^3$ and the hydrostatic piezoelectric strain constant d_h

$$\begin{aligned} S_h &= s_h^E T_h + d_h E_3 \\ D_3 &= d_h T_h + \epsilon_{33}^T E_3 \end{aligned} \quad (26)$$

where the hydrostatic elastic compliance and the hydrostatic piezoelectric strain constant are defined as follows

$$\begin{aligned} s_h^E &= \left. \frac{\partial S_h}{\partial T_h} \right|_{E_3} = 2(s_{11}^E + s_{12}^E) + 4s_{13}^E + s_{33}^E \\ &= \text{volume compressibility} \\ d_h &= \left. \frac{\partial S_h}{\partial E_3} \right|_{T_h} = \left. \frac{\partial D_3}{\partial T_h} \right|_{E_3} = 2d_{31} + d_{33}. \end{aligned} \quad (27)$$

The hydrostatic coupling coefficient is then defined as

$$\begin{aligned} k_h &= \sqrt{\frac{d_h^2}{\epsilon_{33}^T s_h^E}} \\ &= \sqrt{\frac{(2d_{31} + d_{33})^2}{\epsilon_{33}^T [2(s_{11}^E + s_{12}^E) + 4s_{13}^E + s_{33}^E]}}. \end{aligned} \quad (28)$$

³ In this section, the subscript h indicates hydrostatic.

TABLE VI
TYPICAL VALUES FOR MATERIAL CONSTANTS
AND MODE PARAMETERS

Material	ADP	Quartz	
Mode	Contour- Extensional I	Contour- Shear	
Specimen	Square Plate	Square Plate	Units
Orientation	(<i>zxt</i>) 45°	(<i>yxz</i>) 38°	
<i>N</i>	1298	3080	m sec ⁻¹
<i>Γ</i>	9.351	0.118	10 ⁻¹² Fm ⁻¹
<i>r</i>	13.4	350	
<i>ρ</i>	1.803	2.654	10 ⁹ m ⁻⁴ N sec ²
<i>ε^T</i>	135	41.5	10 ⁻¹² Fm ⁻¹
<i>ε^m</i>	125	41.3	10 ⁻¹² Fm ⁻¹
<i>k</i>	0.324	0.0711	
<i>s^E(1/<i>q</i>)</i>	<i>s</i> ₆₆ /2 = 82.3	<i>s</i> ₅₅ ' = 15.09	10 ⁻¹² m ² N ⁻¹
<i>d(δ)</i>	<i>d</i> ₃₆ /2 = 24.2	<i>d</i> ₂₆ ' = 1.78	10 ⁻¹² CN ⁻¹
<i>F</i>	1	1.2331	
<i>β</i>	5.2562	1.480	
<i>p</i>	0.657	0.563	

4.5 Coupling Factor for a Single Strain System

Assuming that only a single shear strain *T*₄ is finite in an infinitely extended *Z* plate, while all other strain components are zero, the piezoelectric equations (3) reduce to

$$T_4 = c_{44}^E S_4 - e_{34} E_3$$

$$D_3 = e_{34} S_4 + \epsilon_{33}^S E_3. \tag{29}$$

The static coupling factor derived from this equation is

$$\frac{k}{\sqrt{1-k^2}} = \sqrt{\frac{e_{34}^2}{\epsilon_{33}^S c_{44}^E}}. \tag{30}$$

A corresponding strain system is that for a thickness-shear mode of an infinite *Z* plate.

4.6 Relationship Between the Static Coupling Factor and the Capacitance Ratio for Various Modes of Motion

The static coupling factor *k* for a given stress or strain system is related to the capacitance ratio *r* of a mode having a similar stress or strain system, by the equation

$$k = \frac{1}{\sqrt{1 + pr\chi}} \tag{31}$$

which is similar to (8). The factor *χ* is already defined in (11) and usually is very close to unity with the exception of the extensional mode I of square plates.

In cases where *χ* ≈ 1, the dielectric constants *ε^m* and *ε^T* for a given mode are related by the coupling factor *k* by

$$\epsilon^m = \epsilon^T(1 - k^2) \tag{32}$$

which follows from (11) and (31).

TABLE VII
QUANTITIES, SYMBOLS, AND UNITS USED IN THESE STANDARDS

Quantity	Symbol	Units (mks)
Stress	<i>T</i>	Nm ⁻²
Strain	<i>S</i>	—
Electric field	<i>E</i>	Vm ⁻¹
Electric displacement	<i>D</i>	Cm ⁻²
Elastic compliance	<i>s</i> (1/ <i>q</i>)	m ² N ⁻¹
Elastic stiffness	<i>c</i> (<i>q</i>)	Nm ⁻²
Piezoelectric strain constant	<i>d</i> (<i>δ</i>)	CN ⁻¹ or mV ⁻¹
Piezoelectric stress constant	<i>e</i> (<i>δ</i> · <i>c</i>)	Cm ⁻² or Nm ⁻¹ V ⁻¹
Dielectric constant	<i>ε</i>	Fm ⁻¹
Density	<i>ρ</i>	m ⁻⁴ N sec ²
Linear dimension	<i>h</i> (<i>t</i> , <i>l</i> , <i>w</i>)	m
Frequency	<i>f</i>	sec ⁻¹
Frequency constant	<i>N</i>	m sec ⁻¹
Capacitance	<i>C</i>	F
Motional capacitance constant	<i>Γ</i>	Fm ⁻¹
Shunt capacitance constant	<i>Γ</i> ₀	Fm ⁻¹
Capacitance ratio	<i>r</i>	—
Coupling factor	<i>k</i>	—

The quantities *κ*, *F*, *β*, *p*, are numerical factors.

Eq. (31) is used to determine the static coupling factor from the measured capacitance ratio *r* for a given mode.

5. TYPICAL VALUES FOR MATERIAL CONSTANTS AND MODE PARAMETERS

Typical values for the material constants and for the mode parameters of two piezoelectric crystals are given in Table VI. Ammonium dihydrogen phosphate and quartz have been chosen as materials. The modes considered are contour-extensional mode I and contour-shear mode of square plates.

6. UNITS

In the 1949 IRE Standards, it was recommended that numerical values of all the quantities involved in the piezoelectric relations be given in rationalized mks units. All equations given in the present standard are written in rationalized units valid for either mks units or cgs esu. The quantities used herein, together with their mks units, are listed in Table VII. The conversion factors from cgs electrostatic to mks rationalized units for most of these quantities can be found in the 1949 IRE Standards.

REFERENCES

- [1] "IRE Standards on piezoelectric crystals, 1949," PROC. IRE, vol. 37, pp. 1378-1395; December, 1949.
- [2] "IRE Standards on piezoelectric crystals, 1957," PROC. IRE, vol. 45, pp. 353-358; March, 1957.
- [3] W. Voigt, "Lehrbuch der Kristallphysik," B. G. Teubner, Leipzig, Germany, 2nd ed.; 1928.
- [4] W. G. Cady, "Piezoelectricity," McGraw-Hill Book Co., Inc., New York, N. Y.; 1946.
- [5] W. P. Mason, "Piezoelectric Crystals and Their Application to Ultrasonics," D. Van Nostrand Co., Inc., New York, N. Y.; 1950.

- [6] K. S. Van Dyke and E. S. Creeger, "Piezoelectric Crystal Studies and Measurements," First Quart. Prog. Rep. (February 1 to April 30, 1953) of Wesleyan University, U. S. Army Signal Corps Contract No. DA-36-039 SC-42587; June, 1953.
- [7] W. P. Mason and H. Jaffe, "Methods of measuring piezoelectric, elastic, and dielectric coefficients of crystals and ceramics," *Proc. IRE*, vol. 42, pp. 921-930; June, 1954. "Correction," vol. 45, p. 160; February, 1957.
- [8] R. Bechmann, "Contour modes of square plates excited piezoelectrically and determination of elastic and piezoelectric coefficients," *Proc. Phys. Soc. (London)*, vol. B64, pp. 323-337; April, 1951.
- [9] H. G. Baerwald and C. Libove, "Breathing Vibrations of Planarly Isotropic Square Plates," Clevite Research Center, Cleveland, Ohio, Contract No. Nonr-1055(00), Tech. Rep. No. 8; December 12, 1955.
- [10] R. Bechmann, "Elastic, piezoelectric and dielectric constants of polarized barium titanate ceramics and some applications of the piezoelectric equations," *J. Acoust. Soc. Amer.*, vol. 28, pp. 347-350; May, 1956.
- [11] R. Bechmann, "Contour modes of plates excited piezoelectrically and determination of elastic and piezoelectric coefficients," 1954 IRE CONVENTION RECORD, vol. 2, pt. 6; pp. 77-85.
- [12] H. G. Baerwald, "Electrical Admittance of a Circular Ferroelectric Disc," Clevite Research Center, Cleveland, Ohio, Contract No. Nonr-1055(00), Tech. Rep. No. 3; January 19, 1955.
- [13] R. D. Mindlin, "Thickness-shear and flexural vibrations of crystal plates," *J. Appl. Phys.*, vol. 22, pp. 316-323; March, 1952.
- [14] R. Bechmann, "Some applications of the linear piezoelectric equations of state," IRE TRANS. ON ULTRASONICS ENGINEERING, vol. 3, pp. 43-62; May, 1955.
- [15] R. Bechmann and S. Ayers, "Piezoelectricity," General Post Office Selected Eng. Reps., Her Majesty's Stationery Office, London, Eng., Rep. No. 4, "The Theory of Dynamical Determination of Elastic and Piezoelectric Constants," pp. 73-92; 1957



CORRECTION

Prof. R. N. Bracewell, author of "Radio Interferometry of Discrete Sources" and "Restoration in the Presence of Errors," which appeared on pages 97 and 106, respectively, of the January, 1958, issue of PROCEEDINGS, has informed the editors that these two papers were incorrectly credited. The work reported was carried out entirely at Stanford University, Stanford, Calif., and supported throughout by the Air Force Office of Scientific Research, Contract AF 18(603)-53.

Correspondence

Bridge Method of Measuring Noise in Low-Noise Devices at Radio Frequencies*

The system to be described was used for accurately measuring the noise of junction diodes biased in the forward direction. In this application, the author succeeded in measuring noise resistances of the order of several hundred ohms with an over-all error of less than 5 per cent. The method is quite general and may be applied with equal success to noise measurement of any low-noise device at radio frequencies. The difficulties usually encountered result from the effects of the measuring amplifier's noise and input impedance, and the dependence of the amplifier's gain upon input load due to stray coupling feedback.

A block diagram of the author's equipment is shown in Fig. 1. To the right of the noise bridge the circuitry is conventional.

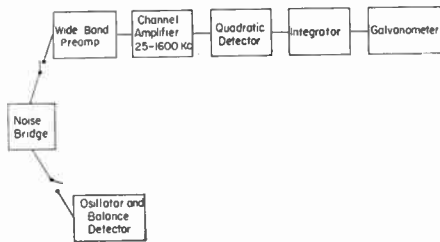


Fig. 1—Block diagram of noise measuring equipment.

The noise is first amplified by a wide-band, low-noise preamplifier which starts with three 6CB6's in parallel and has a noise resistance of about 300 ohms. This feeds a narrow pass-band amplifier possessing 7 channels selectable in octave steps from 25 kc to 1600 kc. The output of the channel amplifier is then detected by a square-law circuit, integrated, and displayed on a sensitive galvanometer.

The noise bridge is shown in detail in Fig. 2. One notes that the junction diode being measured is placed in one arm of a comparison bridge. The adjacent arm consists of a variable conductance and susceptance, G_x and B_x .

With the input of the preamplifier grounded, admittance balance is obtained by exciting the bridge at the desired frequency and adjusting G_x and B_x for balance detector null. The signal generator and balance detector are then removed from the circuit.

Next, the two lower bridge arms are adjusted for equal mean-square noise voltages, e_1^2 and e_2^2 . This is accomplished by passing current I_1 through noise diode 1 if the junction exhibits greater than thermal noise or I_2 through noise diode 2 if the junction noise is less than thermal. When the galvanome-

ter reads the same with the input selector in either position 1 or 2, the bridge is balanced for noise.

With the bridge balanced for both admittance and noise voltage, it follows that the mean-square short circuit noise currents are equal as well since the total bridge arm admittances, including preamplifier input admittance, are the same at the time of balance. If one represents the noise of the junction diode in terms of its equivalent saturated diode current, I_s , defined by

$$\bar{i}^2 = 2eI_s\Delta \quad (1)$$

one can equate the noise current generators in adjacent bridge arms. This yields

$$2eI_1\Delta f + 4kTG_x\Delta f = 2eI_2\Delta f + 2eI_s\Delta f. \quad (2)$$

Solving for I_s

$$I_s = (I_1 - I_2) + (2kT/e)G_x. \quad (3)$$

To find the noise ratio, or ratio of noise power to thermal noise power, one divides (3) by $(2kT/e)G_x$.

$$n = 1 + (e/2kT)(1/G_x)(I_1 - I_2). \quad (4)$$

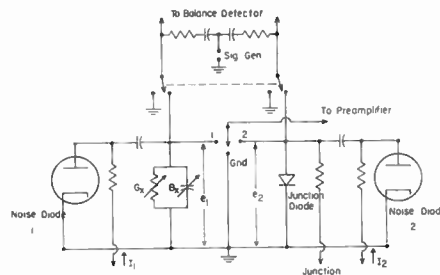


Fig. 2—Noise bridge circuit.

The advantages of the bridge method are many. Eqs. (3) and (4) give the noise parameters in terms of easily measured quantities which may be read simultaneously. Since only equality of noise readings is required, the exact characteristic of the detector circuit is relatively unimportant. Stray coupling feedback does not change the amplifier's gain during measurement because the input load remains the same with the input selector in either position. Finally, although the preamplifier's noise and input admittance affect the precision of the noise balance, they cancel out of the final result. The possible error from these sources can be easily estimated by observing the variation in I_1 or I_2 required to cause a detectable noise unbalance.

The author wishes to thank prof. A. van der Ziel for many valuable discussions of the problem.

KEITH S. CHAMPLIN
Dept. of Elec. Eng.
University of Minnesota
Minneapolis, Minn.

A Reactance Theorem for Antennas*

In connection with the paper of Dr. Levis¹ I should like to remark that the concept of the frequency derivative of the input reactance of an antenna is suitable for practical computations as well and may be used² for the determination of the bandwidth properties of linear arrays.

The Q is defined there, as follows:

$$Q = \frac{1}{2} \text{Im} \left\{ \frac{\omega}{P} \frac{dP}{d\omega} \right\}_{\omega=\omega_N}$$

where ω_N is the resonant frequency and P , the radiated power.

Applying this definition to linear arrays it was found that the Q of a linear array is the product of three factors.

$$Q = AQ_0Q_e$$

where A depends on the directional properties of the individual element, Q_e is the quality of the element itself, and $Q_0 \geq 1$ is a function of the geometrical arrangement and current distribution of the linear array.

L. SOLYMAR
Standard Telecommun. Labs., Ltd.
Enfield, Middlesex, England

* Received by the IRE, November 8, 1957.

¹ C. A. Levis, "A reactance theorem for antennas," *Proc. IRE*, vol. 45, pp. 1128-1134; August, 1957.

² M. Uzsoky and L. Solymer, "Theory of superdirective linear arrays," *Acta Phys. Acad. Sci. Hung.*, vol. 6, pp. 185-205; 1956.

Extension of Boolean Algebra for Analysis of Mixed-Switch Diode Circuits*

Conventional Boolean algebra may be extended by means of suitable operators to provide applications to the reduction of switching functions for combinatorial circuits composed of both switches and diodes.

It is often expedient to use diodes in combination with ordinary switches in order to further reduce the number of literals in a circuit. The following is a possible reduction technique for diode-switch combinations.

We introduce two elements J and K with following properties:

$$J + J = J, \quad J \times J = J, \quad K + K = K, \quad K \times K = K$$

$$J + K = 1, \quad J \times K = 0,$$

$$J + 1 = K + 1 = 1, \quad J \times 0 = K \times 0 = 0$$

$$J' = K, \quad K' = J$$

where J and K commute, associate, and distribute with all other elements, and 1, 0, ', +, and \times have their usual meaning. (1 de-

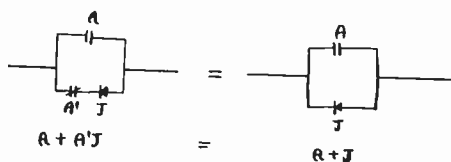
* Received by the IRE, November 5, 1957.

Received by the IRE, November 4, 1957. Work supported by Signal Corps Contract.

notes a closed contact, 0 an open contact, ' means negation, + parallel, and X, series connection.) The elements *J* and *K* are elements of a Boolean algebra and may be treated as such, subject to the additional rules of operation given above. Two separate elements *J* and *K* are used in order to preserve the symmetry of the algebra.

To each diode in a circuit ascribe the operator *J* or *K*, depending upon the direction of current flow in each given circuit path (*J* in one direction *K* in the other). It is arbitrary which orientation is used as long as one is consistent within a given circuit. *J* and *K* may be used as elements of a Boolean algebra (*i.e.*, as diodes in a circuit) or as operators upon circuit elements or circuits.

Example:



$$\begin{aligned}
 A + A'J &= A(J + K) + A'J = AJ + A'J + AK \\
 &= J(A + A') + AK = J + AK \\
 &= J(A + 1) + AK = JA + J + AK \\
 &= J + A(J + K) = J + A.
 \end{aligned}$$

B. BEIZER
136-33 68th Drive
Flushing, N. Y.

The Switching Time of the Cryotron*

Recently a new type of flip-flop, based on superconductivity, has been developed by Buck¹ and further studied by Slade and McMahon.² Its properties are superior in many respects to known elements; however, its low switching time might be a limiting factor in some applications. In the search for higher speed operation, the assumption¹ was made that the switching time is given by the *L/R* time constant of the circuit. In the course of investigation of a similar flip-flop based on the magnetoresistive effect,³ it was found^{4,5} that practically the switching time might differ by orders of magnitude from the *L/R* time constant. It was there-

fore considered worthwhile to study the cryotron case from a similar point of view.

The cryotron circuit is shown in Fig. 1. All the resistors *R_i* are superconductors, and their resistance is zero unless a current flows in the appropriate coil. All the coils and connecting leads have zero resistance. It is seen that when *i₃* = *i₄* = 0, there are two stable states, namely *i₁* = *I*, *i₂* = 0, *R₁* = 0, *R₂* ≠ 0 or *i₁* = 0, *i₂* = *I*, *R₁* ≠ 0, *R₂* = 0. A pulse of *i₃* or *i₄* serves to switch over the element from one stable state to the other.

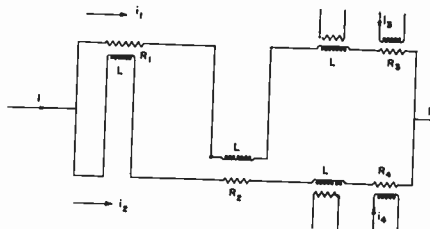


Fig. 1.

Now, suppose the element is initially in the state *i₁* = *I* and an *i₃* pulse is applied. This pulse is assumed to step *R₃* to its highest value *R_∞* in zero time. Kirchhoff's equations for this case are

$$\begin{aligned}
 i_1 + i_2 &= I \\
 i_1 R_1(i_2) + 2L \frac{di_1}{dt} + i_1 R_\infty &= i_2 R_2(i_1) + 2L \frac{di_2}{dt}. \quad (1)
 \end{aligned}$$

Substituting the notations

$$\begin{aligned}
 y &= i_1/I; \quad x = i_2/I; \quad \tau = 4L/R; \\
 T &= t/\tau; \quad r = R/R_\infty. \quad (2)
 \end{aligned}$$

in (1) one obtains

$$\begin{aligned}
 yr(1-y) + \frac{1}{2} dy/dT + y &= (1-y)r(y) - \frac{1}{2} dy/dT. \quad (3)
 \end{aligned}$$

Hence, the switching time from the stable state discussed to the vicinity of the other one is given by

$$T = - \int_1^{0.1} \frac{dy}{yr(1-y) + y - (1-y)r(y)}. \quad (4)$$

The choice of 0.1 as the upper limit of integration is done according to the usual convention in the definition of pulse rise time.⁶

Inserting in (4) for *r(y)* values taken from Fig. 2 of Slade and McMahon,² with the assumption *I* = 1 amp, numerical integration implied a switching time of 7½ *L/R*. In order to test the significance of this value, further calculation was done with the assumption that *r* has the form shown in Fig. 2. For simplicity it is assumed that one uses the smallest possible current, *i.e.*, *y₁* = 1, which is also reasonable.

Using this form for *r* in (4) and carrying out the necessary integrations, one finds that in the whole region 0.1 ≤ *y₀* ≤ 0.9, the time in terms of *L/R* varies between 7.4 and 9.2, with the minimum in the vicinity of *y₀* = 0.3. However, it should be pointed out

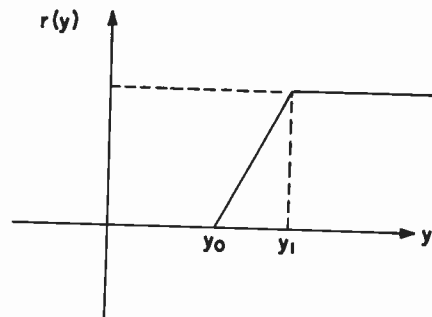


Fig. 2.

that the switching time calculated to the 0.1 level obviously will give a larger value than the *L/R* time constant, so that the use of *L/R* is justified for a rough estimate.

A. AHARONI
E. H. FREI
S. SHTRIKMAN
Department of Electronics
Weizmann Institute of Science
Rehovoth, Israel

A History of Some Foundations of Modern Radio-Electronic Technology*

I was especially interested to see mentioned in the above article¹ the experiments carried out in 1919 in the United States to establish radio transmission to underwater craft. Similar successful experiments were conducted by me in Russia for the Russian Navy between 1915 and 1916.

When World War I started, I was the Director and Technical Manager of the Russian Wireless Telegraph Company, and from the first day of the war was involved in different radio developments connected with the war requirements. Among other problems the Russian Navy requested that a method should be found to transmit signals to submerged submarines. Extensive tests were carried out in 1915 and 1916; they showed that quite strong signals could be received when the submarine was submerged to the depth of the order of between 15 and 20 feet. The antenna used was a closed frame built up with a highly insulated cable entering the submarine from one side and connected to the steel body on the other end. The cable and the submarine body in this way formed one frame, and, to obtain the biggest possible active service from this frame, the cable was suspended from the highest point of the conning tower.

The receiver was connected between the cable input and the body of the submarine. The receiver had one thermionic tube with positive feedback to compensate for the losses in the antenna when submerged in salt

* Received by the IRE, November 7, 1957.
¹ D. A. Buck, "The cryotron—a superconductive computer component," *Proc. IRE*, vol. 44, pp. 482-493; April, 1956.
² A. E. Slade and H. O. McMahon, "A cryotron catalog memory system," *Proc. of the East. Joint Computer Conference*, (to be published).
³ A. Aharoni, E. H. Frei, and G. Horowitz, "New active circuit element using the magnetoresistive effect," *J. Appl. Phys.*, vol. 26, pp. 1411-1415; December, 1955.
⁴ A. Aharoni, "The time-constant of a certain nonlinear network," *Bull. Res. Council Israel*, vol. 6A, pp. 144-145; January, 1957.
⁵ A. Aharoni, "Magnetoresistive memory," Ph.D. dissertation, Hebrew University, Jerusalem (in Hebrew); 1957.

⁶ See, for example, F. E. Terman and J. M. Pettit, "Electronic Measurements," McGraw-Hill Book Co., Inc., New York, N. Y., pp. 258-259, 2nd ed.; 1952.

* Received by the IRE, November 4, 1957.
¹ J. H. Hammond, Jr., and E. S. Purington, *Proc. IRE*, vol. 45, pp. 1191-1208; September 1957.

water. Different wavelengths were used, the best results being obtained with wavelengths between 5 and 12 thousand meters. Signals from the high power (300-kw spark transmitter) station at Zarskoe Selo near Petrograd were received by a submarine (700-1000 tons) at a western end of the Baltic Sea.

As a result of this experiment, a program was discussed with the Russian Navy to start in the Spring of 1917. Experiments in the Black Sea were to be carried out first with radio controlled motor boats and later to a radio controlled torpedo. This project did not materialize due to the Revolution in 1917.

S. M. AISENSTEIN
Consultant to the

English Electric Group of Companies
Chelmsford, Essex, England

Aperture Correction for Instrumentation Systems*

This note is an abstract of the writer's dissertation, which bears the same title.¹ The purpose of the study was to investigate a problem in electrical instrumentation: the compensation by a network for an averaging effect common to a large variety of sensing devices; *i.e.*, devices that convert a signal in one form of energy into a signal in another form of energy. A well-known example is an instrumentation system that converts spot-by-spot light intensity in a picture into a continuous electrical signal by aperture scanning. Hence the distortion involved is known as the aperture effect. For scanning at a uniform rate by a rectangular aperture, the transfer function relating the output and the input of the device in terms of the complex frequency p is $f(p) = h(1 - e^{-ap})/p$, where h expresses the sensitivity and a is the time the scanner takes to scan a distance equal to the length of its aperture. The rectangular aperture and its step-function response are shown in Fig. 1.

The circuits described in the dissertation represent a new approach to the problem of compensation. The transfer functions of the circuits suggested are inverse to those of the apertures, except for small departures introduced to ensure stability or caused by losses in delay lines. The common property of all these circuits is that they incorporate a delay device in the feedback loop of an active element or a delay line mismatched at both ends. The impulse responses possess some repetitive character. The corrective network for the rectangular aperture and its step-function response are shown in Fig. 2. The step-function response of a system consisting of a rectangular aperture in series with its corrective network is shown in Fig. 3. The system as shown does not have dc response. The dc response can be provided by incorporating a simple RC integrating

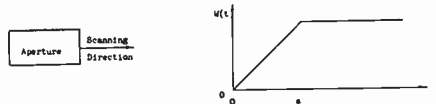


Fig. 1—The simplest form of a rectangular aperture and its step-function response.

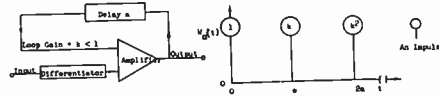


Fig. 2—The corrective network for a rectangular aperture and its step-function response $W_c(t)$. The response consists ideally of a series of impulses of decreasing amplitude.

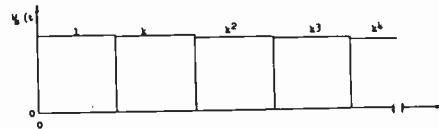


Fig. 3—The ideal step-function response $W_c(t)$ of a system consisting of a rectangular aperture in series with its corrective network.

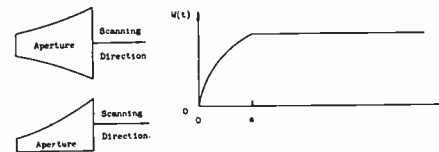


Fig. 4—Two forms of an exponential aperture and its step-function response $W(t)$.

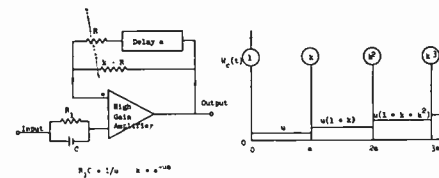


Fig. 5—The corrective network for an exponential aperture and its step-function response $W_c(t)$. The network here is shown in more detail, whereas the network of Fig. 2 was drawn schematically.

network parallel to the corrective network of Fig. 2.

The suggested method of achieving compensation seems to be of greatest importance when the smallest technically feasible aperture does not offer the required systematic accuracy. Even if the length of the aperture is greater than $2\pi/\omega_s$, where ω_s is the limiting frequency of the input spectrum, the corrective network can recover most of the original information from the distorted signal available at the output of the aperture.

Moreover, the compensation discussed will be found very useful in the case where the input spectrum is spread over the frequency band $0 < \omega < \omega_s$ and where high accuracy is required up to the limiting frequency ω_s . In such a case, a system consisting of only a sensing device cannot offer an acceptable solution, because the noise-to-signal ratio is large when the aperture is small enough not to cause a large distortion. In a system consisting of an aperture, an amplifier, and a corrective network, the aperture size can be chosen in such a way as to minimize the noise-to-signal ratio. The

length of such an aperture depends on the nature of noise and on the noise-minimization criterion, but it generally will be found ranging from $0.75\pi/\omega_s$ to $1.35\pi/\omega_s$. The amplifier after the aperture serves to lift the signal level well above the level of additional noise introduced in the corrective network. The compensation in the corrective network itself then provides the systematic accuracy required.

The compensating method offers special advantages when some preferred forms of the aperture, such as the birectangular or exponential, can be used. The transfer function of the exponential aperture has the form $h(1 - e^{-au}e^{-ap})/(p+u)$, where $u > 0$. This transfer function does not have any zeros on the $i\omega$ -axis nor in the right half-plane. Thus the exact inverse transfer function corresponds to a stable network. In this respect the exponential aperture differs from the other apertures discussed, which all exhibit zeros of the transfer function on the $i\omega$ -axis. The exponential aperture and its step-function response are shown in Fig. 4. The appropriate corrective network and its step-function response are shown in Fig. 5.

As part of this investigation, differentiation by a capacitor-resistor network and differentiation by a delay line are analyzed and compared. A prerequisite for carrying out the comparison is established; the origin of time of impulse responses in both cases is chosen in such a way as to eliminate the first error term in the transfer-function expansion in powers of ω .

The indebtedness of the writer to G. Hok, L. L. Rauch, and E. G. Gilbert is gratefully acknowledged.

JOSEPH OTTERMAN
Eng. Res. Inst.
University of Michigan
Ann Arbor, Mich.

Transistor Cutoff Frequency Measurement*

The alpha cutoff frequency of a transistor is normally defined as that frequency at which the short-circuit current gain in grounded base has fallen to 3 db below its low-frequency value. In consequence of the definition it is usual to measure by feeding the signal to the emitter. The writer believes it is not widely known that considerable advantage may be gained by avoiding the obvious and carrying out the measurement of alpha cutoff frequency by feeding the signal to the base.

Consideration of the simplified equivalent circuit of Fig. 1 shows that any measurement of cutoff frequency involves the collector capacitance and base resistance. If, as is often the case, an intrinsic cutoff frequency is required, the effects of $C_{b'e}$ and $r_{bb'}$ must be removed by means of a correction factor.

* Received by the IRE, November 8, 1957.

* Received by the IRE, November 28, 1957.
¹ J. Otterman, doctoral dissertation, Dept. of Elec. Eng., University of Michigan, Ann Arbor, Mich., May, 1955.

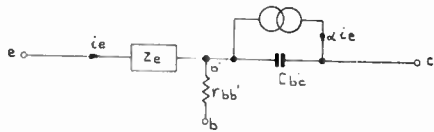


Fig. 1.

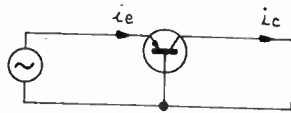


Fig. 2.

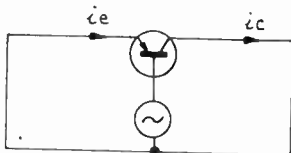


Fig. 3.

For the grounded base measurement (Fig. 2) the intrinsic and measured frequencies are related by the first-order expression

$$f_i = f_m(1 + 2\omega C_{bc}r_{bb'})$$

When measuring in grounded emitter, as in Fig. 3, the corresponding first-order expression is

$$f_i = f_m$$

so that an error of $200\omega C_{bc}r_{bb'}$ per cent has been removed. (The error is of the order of 10 per cent at 10 mc for $C_{bc} = 10\mu\mu f$, $r_{bb'} = 100\Omega$).

Thus the advantage of operating with the emitter grounded rather than the base is that a value nearer to that for the intrinsic cutoff frequency of the transistor is obtained.

L. G. CRIPPS
Mullard Res. Labs.
Surrey, England

Spectral Analysis*

I would like to make a comment on Grierson's paper¹ concerning the spectral analysis of whistlers and Nelson's reply.²

The scheme of using a plurality of contiguous filters has often been employed in applications similar to Grierson's. Its principal drawback is the expense of constructing a large number of filters and then devising a read-out for the plurality of outputs.

I would like to draw attention to another scheme not so extravagant in quantity of apparatus and yet capable of producing a

spectral analysis similar to that described by both Grierson and Nelson. The method is subject to certain limitations which will be apparent in the following description, but these are not serious enough to prevent a widespread use of this method in the aircraft and missile industries.

The scheme basically consists of making the transient response repetitive. The transient wavelet is recorded on magnetic tape which is then made into a loop and reproduced over and over again. By using a heterodyne type wave analyzer, wherein a single narrow-band filter is used, it will be possible to move the position of the filter in the spectrum by altering the frequency of the heterodyne oscillator. If the frequency of the heterodyne oscillator is progressively and continuously moved from one end of the spectrum to the other, a scanning of the spectrum by the filter results. A recording of the output of the wave analyzer produces an amplitude plot with frequency as the independent variable.

Each plot is equivalent to a fixed point in the time domain and a three-dimensional model of time-amplitude-frequency can be constructed quite easily. A similar display can be made by placing a number of amplitude-frequency plots in a time-family relationship. Such a parametric representation has been proposed by the Technical Products Company to the Rocket Engine Test Center at Edwards Air Force Base, where a similar problem exists. Equipment capable of producing such plots is now available.

ROBERT C. MOODY
Technical Products Co.
Los Angeles, Calif.

Satellite Doppler Measurements*

Beginning on October 5, 1957, frequency measurements of the signals transmitted from the Soviet Satellite No. 1 were made daily by the Frequency Control Branch of the U. S. Army Signal Engineering Laboratories. As an example of the information obtained, Fig. 1 through Fig. 3 show plots of frequency vs time for the near approaches of October 6, 11, and 19. Information contained in these graphs can be used to determine satellite velocity and slant range of nearest approach to a good approximation, as well as other quantities associated with the satellite.

The velocity of the satellite is determined from the Doppler equation

$$\frac{f}{f_0} = \frac{C + v_0}{C - v_1}$$

where

- f = frequency before the Doppler shift,
- f_0 = frequency of Doppler zero,
- C = velocity of light,
- v_0 = velocity of observer (assumed zero),
- v_1 = velocity of vehicle.

* Received by the IRE, November 27, 1957.

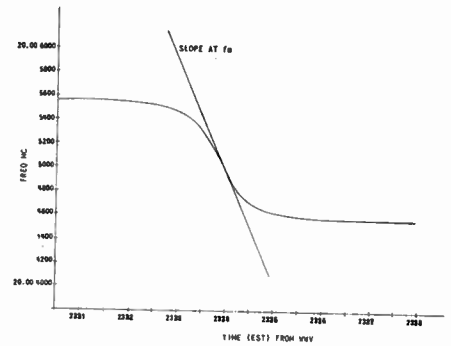


Fig. 1—Frequency Control Branch, October 6, 1957, 20 mc.

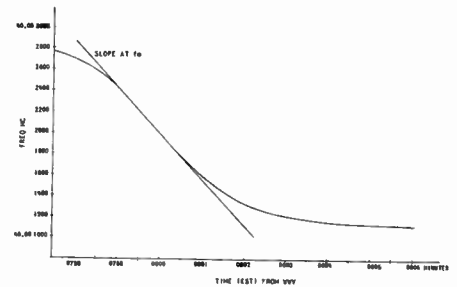


Fig. 2—Frequency Control Branch, October 11, 1957, 40 mc.

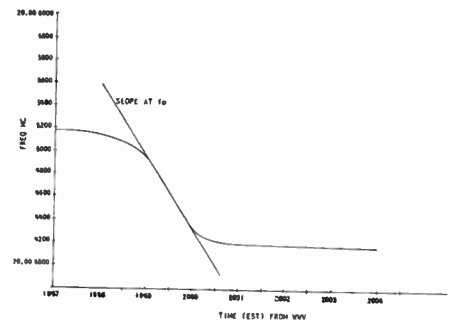


Fig. 3—Frequency Control Branch, October 19, 1957, 20 mc.

Using the information from Fig. 3, the velocity of the satellite was calculated to be 4.84 miles per second. For this orbit the distance of closest approach was calculated to be 232.9 miles using the following formula

$$d = \frac{f_0 v_1^2}{C df/dt}$$

where

- v_1 = velocity of vehicle,
- C = velocity of light,
- df/dt = slope of curve at f_0 ,
- d = distance.

A block diagram of the system used to obtain the frequency information is shown in Fig. 4. The unknown satellite frequency, f_s , is mixed in a receiver with a signal, f_a , of known frequency measurable to an accuracy of 1×10^8 . The difference between f_s and f_a , an audio frequency, is fed, after filtering, to one set of plates of an oscilloscope. The frequency of a variable audio oscillator is in-

* Received by the IRE, November 25, 1957.
¹ J. K. Grierson, "A technique for the rapid analysis of whistlers," Proc. IRE, vol. 45, pp. 806-811, June, 1957.
² R. R. Nelson, "Spectrum analyzer for whistlers," Proc. IRE, vol. 45, p. 1543; November, 1957.

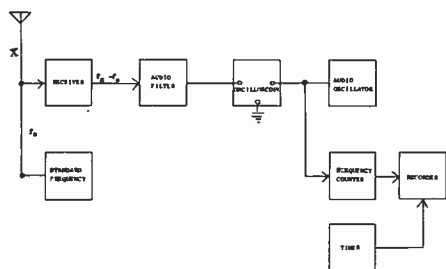


Fig. 4—Doppler shift measurement system.

jected into the other set of plates. The frequency of the audio oscillator was measured to an accuracy of ± 1 cycle by the frequency counter and automatically recorded. Since the frequencies fed into the oscilloscope are equal, when a Lissajou circle appears on the scope, the frequency of the unknown signal is determined by adding the frequency of the standard and the frequency of the audio oscillator. The audio oscillator was tuned manually to keep the Lissajou circle on the scope and frequency measurement was taken by manual triggering of the frequency counter whenever a circle was obtained on the scope. The frequency of the audio oscillator and the time, based on WWV, were automatically recorded. During the one second counting period of the frequency counter, the audio oscillator was not changed. This method gives a frequency accuracy of one ± 1 cps and a time accuracy of ± 0.5 second.

The indirect method used to measure the frequency difference between the satellite and standard frequencies was chosen instead of a direct frequency measurement for two reasons: 1) since during the first few days of the satellite transmission the signal was pulsed, 0.3 second on, 0.3 second off, it would be necessary to use the 0.1-second gate on the counter instead of the 1-second gate and the resulting accuracy of frequency measurement would be decreased; 2) a clean signal is needed for direct measurement, while with the method used a frequency measurement can be made even though a considerable amount of noise is present with the signal. This is true since the Lissajou figure is recognizable when the signal-to-noise ratio is small.

This work will be reported on at a later date in greater detail.

M. BERNSTEIN
G. H. GOUGOULIS
O. P. LAYDEN
W. T. SCOTT
H. D. TANZMAN
U. S. Army Signal Eng. Labs.
Fort Monmouth, N. J.

Invention and Insight*

A sharp distinction should be made between the production of innovations or inventions and the conception of new insights into physical or mathematical theory. The former can perhaps be described in terms of

the combinations of simple ideas and their relationships, and can conceivably be engendered in the project team environment. The latter is more precious and elusive and is generally scared out of existence by the peculiar emotional relationships which exists between people. Neither can claim a hierarchical precedence over the other since they go hand in hand, but it is clear that theory remains more fundamental and requires a greater reach of the imagination.

An important new insight or scientific theory is obviously not easily conceived. Many superior minds are engaged in thinking long and imaginatively, trying to cohere the disparate phenomena—especially at a time like the present when discovery outstrips explanation. Yet whenever a new theory is born, it is usually simple and often obvious. Why is the simple and obvious so difficult to see, why are beautiful insights at first rejected as bizarre or impossible when they are finally accepted as true or useful?

The reason is that the juxtaposition required is usually foreign to other people, the new insight is strange or trivial because the prevailing orientation of people's minds prevents any possible immediate alignment or understanding. An almost other-worldly viewpoint is necessary, which is perhaps one of the reasons that the oriental mind is proving singularly fruitful in proposing insights which the occidental mind cannot immediately see. The different cultural background is important and leads to the conclusion that children should be encouraged to live in worlds of their own, at least insofar as they theorize, allowing the freedom of mind which permits fresh, startling insights.

Because of the fact that the imaginative jumps required for a new insight may be very strange to another person it generally must be sequestered in one mind. The strangeness of assumptions, the sheer incomprehensibility of imagination when revealed can be a factor which prevents its realization in any usable form. How many brilliant ideas have escaped realization because they were ridiculed prematurely? If it were possible for theorists to leave behind inhibition and criticism like two boys playing a game, entering completely into the imagination of the other, then perhaps some kind of collaboration could result. This could conceivably take place between unspoiled youths or inspired people of long acquaintance, but it is questionable that any such rapport can be reached artificially. When it comes to the production of innovations or inventions, creative collaboration is probably possible, but because of the frailties of the human mind the more imaginative and therefore fruitful ideas are usually one person's province until final and complete.

The action of the mind when it comes to abstracting or theorizing is scarcely understood. Seemingly unrelated thoughts or sometimes silly ideas are felt by a person as sketches or analogies which have a related form or useful connection to the ideas at hand. These leaps of the mind either from an abstraction to the problem or vice versa are how the mind theorizes. And the greater the ability to summon up the skeletons of the unconscious, plus the ability to strip down to pure form, the more imaginative the leap. A certain amount of chance is required too—

a chance encounter which includes the particular generative idea or facts providing the logical links. Perhaps unconscious drive towards areas which can give the required clues plays another important part in the formulation of a new idea. Because people of each generation are usually provided with many common elements it is not unheard of that two or more identical theories are independently formulated. And at the same time people of a common culture have similar limitations which confine their imaginations.

It is clear that a uniform culture which does not tolerate differences soon reaches a barrier of imagination. Paradoxically a new barbaric element is required for growth itself. And similarly a person must allow a little barbaric thought to creep in, thought which will at first seem foreign or even stupid but which is the essence of growth. The only way to encourage this growth in a society is to permit somehow a radical turn of mind to flourish. All talk about incentives, desire for originality, free flow of ideas, etc., are useless if the limitation of uniformity prevents a person from purposeful dreaming and if there is no example other than the norm. Of what value is incentive to people who all have the same incentive? Of what value are ideas flowing freely between people with the same ideas, who cannot even tolerate a certain fancy in themselves?

The only climate conducive to creativity is one which tolerates and encourages differences, not only differences of opinion, but differences of viewpoint and character. A society must leave people alone and trust that they will have the stimulation and desire to grow and to create. It is naive to assume that outside direction is necessary for growth, as it is naive to continue to direct a child after he has a certain independence of thought: one can only sit back and watch the workings. The greatest hamper for anyone is the benign inquiry which takes the modern form, "How are you doing?"

ROBERT E. MUELLER
Caldwell-Clements Manual Corp.
New York, N. Y.

Germanium *N-P-I-N* Junction Transistor Triodes*

The results of recent development work at this laboratory indicate that 1) feasible device techniques are available for the preparation of acceptor diffused *P* regions in germanium, and 2) *n-p-i-n* diffused base devices may be fabricated using these techniques. Diffusion experiments of acceptors in germanium were performed using both sealed tube and open tube single and double stage flow methods. The diffusants investigated included zinc, boron, aluminum, gold, and indium. Surface concentrations were maintained in a useful diffused base device range through the use of diluted diffusion

* Received by the IRE, December 5, 1957.

* Received by the IRE, November, 18, 1957.

TABLE I
GERMANIUM N-P-I-N TRANSISTOR TRIODE ELECTRICAL DATA

Unit	BV_{cbo} (v)	BV_{ebo} (v)	Alpha	r_b' (ohms)	C_{ob} ($\mu\mu\text{f}$)	f_{ob} (mc)	$I_{cbo}(V_{cb}=20\text{ v})$ (μa)
1	>110	6	0.95	40	2.0	53	2
2	100	5	0.99	37	1.6	51	12
3	>110	2	0.93	24	4.2	51	4
4	>110	6	0.98	20	4.6	51	10
5	80	6	0.97	24	2.9	50	1
6	>110	9	0.99	49	1.8	58	1
7	>110	8	0.99	22	2.4	60	6
8	>110	10	0.98	43	1.6	60	9
9	40	9	0.99	41	1.5	59	2
10	>110	9	0.99	32	1.8	57	2
11	80	10	0.99	38	2.1	58	3
12	>110	9	0.99	44	1.7	58	2

sources. The typical diffusion temperature and time for the transistor structure to be described was 900°C for 8 hours.

A combined alloyed junction diffused base intrinsic collector design was used similar to that described by Kestenbaum and Ditrick¹ for their *p-n-p* structure. The optimum design geometry was not determined; dimensions were chosen for ease of fabrication and proof of structural (not optimum electrical) feasibility. The electrical data given in Table I above were observed ($I_c=4$ ma, $V_{cb}=10$ v). High-frequency power gain, as measured in a tuned input and output neutralized amplifier stage, was typically 25 db at 12.5 mc and 10 db at 45 mc.

The main problem involved in the fabrication of these units is background donor diffusion. The donor concentration in the diffusion arrangement must be limited to a value such that the subsequent acceptor diffusion predominates in both level of concentration and depth of diffusion in the germanium substrate (in this case, *P* intrinsic germanium).

D. M. UNGER

A. AVAKIAN

Sylvania Elec. Products, Inc.
Woburn, Mass.

¹ A. L. Kestenbaum and N. H. Ditrick, "Design, construction, and high-frequency performance of drift transistors," *RCA Rev.*, vol. 18, pp. 12-23; March, 1957.

High-Frequency Magnetic Permeability Measurements Using Toroidal Coils*

The problem of measuring the high-frequency initial permeability of a magnetic material by comparing the inductance of a coil wound on a toroidal specimen of the material with the inductance of an identical air core coil has recently been discussed by Schwartz.¹ A program designed to evaluate the accuracy of permeability measurements using the above technique was also completed at the National Bureau of Standards a short time ago. Although the NBS data are

reported in detail elsewhere,² a short note is in order summarizing the results obtained in relation to the conclusions reached by Schwartz.

The determination of the effective permeability of a material using coils wound on toroidal samples is based on

$$\mu = \frac{L_m}{L_s} \quad (1)$$

where L_m is the measured inductance of the coil with the sample and L_s is the calculated inductance of an equivalent air core coil assuming a thin uniform current sheet. An alternate method of evaluating L_s has been to measure the inductance of a coil identical to the magnetic sample coil but wound on a polystyrene core. Either method of evaluating (1) may lead to errors in the measurement of the permeability of the material. Various corrections^{3,4} for (1) have been proposed in the literature in an effort to account for these errors. A further source of error which was suggested by Schwartz on the basis of a study of plexiglass cores with a small number of turns lies in the contribution of the so-called "circumferential inductance" to the total measured inductance of a coil.

The NBS program was in general concerned with a study of coils having a sufficiently large number of turns to make the "circumferential inductance" negligible compared to the total inductance of the coils. The errors resulting from neglecting leakage flux and from assumptions as to the location of effective current sheets were investigated experimentally as a function of permeability, core dimensions, wire spacing, and wire size. The majority of the measurements were made by winding toroids on polystyrene cores with rectangular cross section.

It was observed that errors can exist in permeability measurements using (1) even when a large number of turns are involved. Presumably the "circumferential inductance" correction referred to by Schwartz would become small compared to the total inductance as the number of turns goes up. It apparently could account at least for some of the errors associated with a small number of windings. The NBS study showed

² B. Kostyshyn and P. H. Haas, "Discussion of current-sheet approximations in reference to high-frequency magnetic measurements," *J. Res. NBS*, vol. 52, pp. 279-287; June, 1954.

³ V. E. Legg, "Magnetic measurements at low flux densities using the a.c. bridge," *Bell Sys. Tech. J.*, vol. 15, pp. 39-62; January, 1936.

⁴ E. B. Rosa and F. W. Grover, "Formulas and Tables for the Calculation of Mutual and Self-Inductance," *Bull. of the Bureau of Standards*, Sci. Paper No. 169, (Revised), p. 125; 1912.

that the error in permeability measurements on coils with a large number of turns is associated with the violation of the assumption that the current sheet is adjacent to the toroidal sample. It was observed that as the number of turns was decreased, the error associated with leakage fields beyond the confines of the coil also began to play an important part in the over-all error in the measurements. It was also shown that within limits at least approximate corrections for leakage fields and location of current sheets relative to the toroid could be made using the correction terms referred to in the literature above.

These conclusions refer to the first method mentioned above for evaluating L_m/L_s (*i.e.*, compare the measured value of L_m to the calculated value of L_s with the appropriate corrections). Regarding the second method of evaluating (1) in which the measured value of L_m is compared to the measured value of inductance of an identical coil wound on a polystyrene core, it should be noted that the NBS results showed that values of μ lower than the true permeability of the material will always be obtained. Furthermore, the absolute error using this second method will be larger for a higher permeability material. This error is of course in addition to the error obtained due to the difficulty of winding a coil on a polystyrene core which is exactly like the coil wound on the magnetic sample.

R. D. HARRINGTON

R. C. POWELL

National Bureau of Standards
Boulder, Colo.

Passive Repeater Using Double Flat Reflectors*

In the above paper, Yang,¹ the possibilities and theoretical performance of a passive repeater system using double flat reflectors are discussed and a typical example is worked out to show the feasibility of a microwave radio link using passive repeaters.

May we call your attention to a paper² published in Italy dealing with the same problem, where the same results are obtained though in a more general form. We feel the more general form might be of some use to those interested in the subject.

A comparison of the various methods usually adopted³⁻⁵ for the calculation of the path attenuation of a system, including an antenna and a single passive repeater close to it, enabled us to conclude that the method given by Jakes³ for an elliptic pass-

* Received by the IRE, November 21, 1957.

¹ R. F. H. Yang, 1957 IRE NATIONAL CONVENTION RECORD, pt. 1, pp. 36-41.

² F. Cappuccini and F. Gasparini, "Sull'uso dei ripetitori passivi nei ponti radio a microonda," *L'Eletronicca*, vol. 43, pp. 296-302; June, 1956.

³ W. C. Jakes, Jr., "A theoretical study of an antenna-reflector problem," *Proc. IRE*, vol. 41, pp. 272-274; February, 1953.

⁴ D. R. Crosby, "Theoretical gain of flat microwave reflectors," 1954 IRE CONVENTION RECORD, pt. 1, pp. 71-75.

⁵ R. E. Greenquist and A. J. Orlando, "An analysis of passive reflector antenna systems," *Proc. IRE*, vol. 42, pp. 1173-1178; July, 1954.

* Received by the IRE, December 6, 1957.
¹ R. F. Schwartz, "Calculation of inductance of toroids with rectangular cross section and few turns," *Proc. IRE*, vol. 45, pp. 1416-1417; October, 1957.

ive repeater with circular projected area seems to be the most complete and comprehensive. In our paper² the path attenuation is given for a system in which two rectangular passive repeaters are closely spaced, but are at a sufficiently large distance from the terminal antennas to permit the incoming field to be dealt with as a uniform plane wave. The field intensity E_1 at the aperture of the receiving antenna at distance R_2 from the reflector A_b is given, with the same notations of the above paper,¹ as:

$$\bar{E}_1 = -\bar{E}_0 \frac{d \cdot \exp \left[-i \frac{2\pi}{\lambda} (d + R_2) \right]}{R_2} \left[\left(\int_{(a'-a'')/\sqrt{2\lambda d}}^{(a'+a'')/\sqrt{2\lambda d}} C(t) dt - i \int_{(a'-a'')/\sqrt{2\lambda d}}^{(a'+a'')/\sqrt{2\lambda d}} S(t) dt \right) \right. \\ \left. \left(\int_{(b'-b'')/\sqrt{2\lambda d}}^{(b'+b'')/\sqrt{2\lambda d}} C(t) dt - i \int_{(b'-b'')/\sqrt{2\lambda d}}^{(b'+b'')/\sqrt{2\lambda d}} S(t) dt \right) \right]. \quad (1)$$

tion obtained from the Jakes' curves, in the manner explained before, shows that the errors are not greater than 1.5 db.

To conclude, it may be of some interest to mention that multichannel microwave radio links using double flat passive repeaters are, in fact, quite common in Italy on difficult mountainous paths where they give satisfactory performances. Fig. 1 shows a typical example of a multichannel radio link in the 6000-mc band made by TELETTRA Laboratories, Milan, Italy. The total length

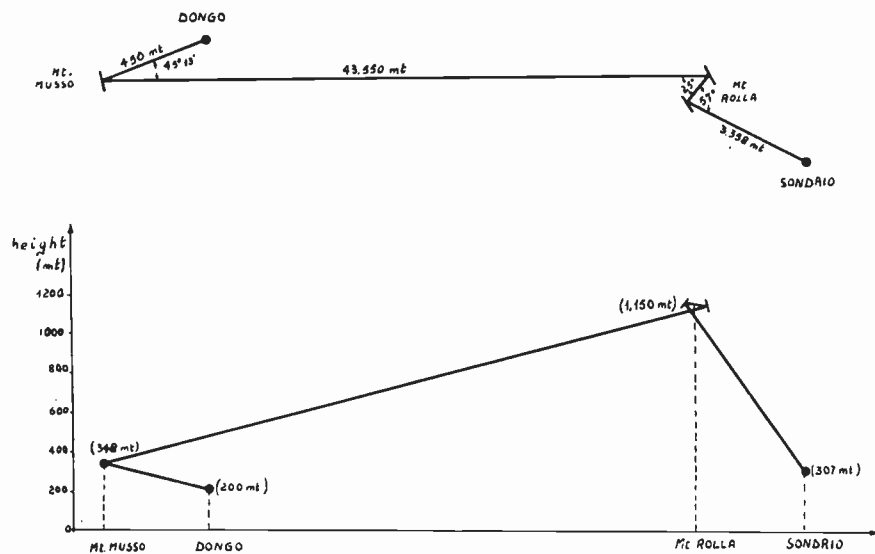


Fig. 1.

The transverse dimensions of the projected reflecting surfaces are, respectively, $a', a''; b', b''$.

As one can easily see, the formula written in the Appendix of Yang's paper¹ is readily obtained from the preceding formula as a particular case putting $a' = a''; b' = b''$.

The basic hypothesis (*i.e.*, uniform plane wave arriving at the first reflector) is such that the problem becomes the same as for an antenna with uniform aperture illumination and a closely spaced repeater. Therefore, one can make use of the curves given by Jakes, provided that the graphs are entered with the diameter of circles having an area equal to that of the repeaters' projected surfaces. Some error is unavoidable for two reasons: 1) Jakes' calculations are based on a 10-db parabolic illumination taper of the antenna aperture; 2) other conditions being unchanged, a decrease of the distance antenna-to-repeater or repeater-to-repeater increases the importance of the surface shape over the surface area. The errors are, however, small enough in most practical cases. A comparison between the path attenuation, calculated with (1) and the path attenua-

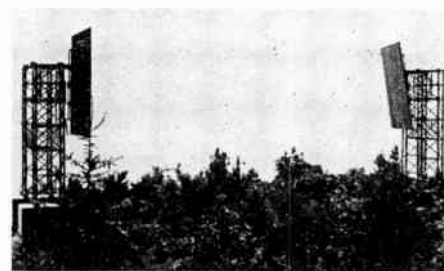


Fig. 2.

of the path from Dongo (Lake of Como) to Sondrio is 47.378 km and develops mostly on high lands as shown by the altimetry in Fig. 1. The passive repeaters are flat rectangular surfaces being a single 6x5 meters repeater over Mount Musso and two 9x7.5 meters repeaters over Mount Rolla. Fig. 2 is a picture of the Mount Rolla repeater.

F. CAPPUCCINI
F. GASPARINI
Elec. Eng. Inst.
University of Padua
Padua, Italy

Observations of Magneto-Ionic Duct Propagation Using Man-Made Signals of Very Low Frequency*

INTRODUCTION

Echoes of radio signals from station NSS on 15.5 kc in Annapolis, Md. (50°N geomagnetic latitude), with delays up to nearly one second have been detected at Cape Horn, South America (45°S). These observations provide the first controlled test of the Eckersley-Storey theory of "whistler" propagation in which energy is guided from one hemisphere to the other, following the lines of force of the earth's magnetic field.

Whistlers are electromagnetic signals, usually of descending audio frequency, and were shown by Eckersley¹ to result from the dispersion of lightning energy. Storey advanced the hypothesis, supported by considerable experimental data, that the path of propagation extends between the hemispheres through the outer ionosphere, following lines of force of the earth's magnetic field.² Subsequent observations at spaced stations supported his predictions regarding the area concentration of energy and the locations of the end points of the path.³⁻⁵ The basic idea was expanded and strengthened by the discovery and explanation of the "nose" whistler.⁶ Whistler paths, which we shall call "magneto-ionic ducts," extend as far as 20,000 miles above the surface of the earth. The group velocity along these ducts is of the order of ten per cent of that in free space, which accounts for the long delays observed.

The controlled experiment opens up new possibilities for long distance communication at very low frequencies. It presents a new factor which must be considered in the design and operation of world-wide frequency standards and navigation systems. The technique provides a powerful new tool for the systematic study of the outer ionosphere, a little understood but extremely important link between the sun and the earth. The purpose of this note is to give a brief report on the first results from this experiment. Additional data will be published when the analysis is complete.

APPARATUS

Most of the observations were made using quarter-second pulses transmitted from NSS every two seconds for a 15-minute

* Received by the IRE, November 20, 1957. This experiment was supported primarily by the Office of Naval Res. (Contract Nonr (225)-27, with help from the Air Force Office of Sci. Res., Contract AF 19 (603)-126, and a National Science Foundation grant for IGY Project 6.10/20.

¹ T. L. Eckersley, "Musical atmospherics," *Nature*, vol. 135, pp. 104-105; January 19, 1935.

² L. R. O. Storey, *Phil. Trans. Roy. Soc. A.*, vol. 246, pp. 113-141; July 9, 1953.

³ J. H. Crary, R. A. Helliwell, and R. F. Chase, "Stanford-Seattle whistler observations," *J. Geophys. Res.*, vol. 61, pp. 35-44; March, 1956.

⁴ J. R. Koster and L. R. O. Storey, "An attempt to observe whistling atmospherics near the magnetic equator," *Nature*, vol. 175, pp. 36-37; January 1, 1955.

⁵ M. G. Morgan and H. E. Dinger, "Observations of whistling atmospherics at geomagnetically conjugate points," *Nature*, vol. 177, pp. 29-30; January 7, 1956.

⁶ M. G. Morgan, and G. McK. Allcock, *Nature*, vol. 177, pp. 29-31; January 7, 1956.

⁷ R. A. Helliwell, J. H. Crary, J. H. Pope, and R. L. Smith, "The 'Nose' whistler, a new high latitude phenomenon," *J. Geophys. Res.*, vol. 61, pp. 139-142; March, 1956.

period each night. The radiated power was about 50 kw. Most of the successful runs were begun at 0535 GMT, shortly after local midnight.

The optimum receiving location was presumed to be the opposite end (called the "conjugate" point) of the field line originating at the transmitter's location at Annapolis. Its estimated location lies in practically inaccessible waters about 1000 miles southwest of the Straits of Magellan. The area of the Straits was chosen for the receiving tests and was a compromise between accessibility and proximity to the calculated point of arrival of the magneto-ionic duct signal. This location lies at the edge of the "effective" area of a whistler as calculated by Storey, and therefore the signal was expected to be of marginal strength.

The particular local receiving sites were selected for minimum man-made noise. The first site was an oil prospecting camp at the east end of the Straits of Magellan. No echoes were observed at that location⁷ although whistler reception was good. Next an attempt was made to set up a receiving station eighty miles southwest of Cape Horn on the rugged and barren *Islas Diego Ramirez*, which is 250 miles closer to the conjugate point. Bad weather prevented landing at that location and the station was returned to a lighthouse about 100 miles northwest of Cape Horn. It was there that NSS echoes were first observed. There were no power lines in the area and no man-made interference was detected. Equipment was powered from 12-v storage batteries which were charged by wind generators. Ample energy was abstracted from the almost continuous high winds which are characteristic of the area.

The receiving equipment for NSS consisted of a three-turn thirty-foot-high triangular loop antenna balanced and resonated with series capacitor, a low-noise four-stage trf receiver of 100-cps bandwidth, and an Ampex Model 601 tape recorder. The receiver noise level was equivalent to an rms field intensity of 0.01 μv per m. The loop was calibrated by coupling a known voltage in series with one of the loop leads, using a transformer. Conversion of signals to 1500 cycles facilitated aural observation and recording. A crossed-loop goniometer system for changing the null direction was set up towards the end of the experiment, to check on the direction of arrival of the echoes. Whistlers were recorded with the same equipment, except that a broadband receiver was substituted for the NSS receiver.

RESULTS

The direct signal (propagation between earth and E layer) was received with good strength, the measured nighttime rms field intensity being about 150 μv per meter. During the first three weeks of operation at Cape Horn, observations were made at 0835 GMT, and weak echoes were first heard on January 15th. On January 25th, the listening period was shifted to 0535 GMT, a time of lower background noise, and better echoes were observed. The delay was estimated

⁷ Subsequent analysis of the tape recordings revealed echoes, which will be described in a later paper

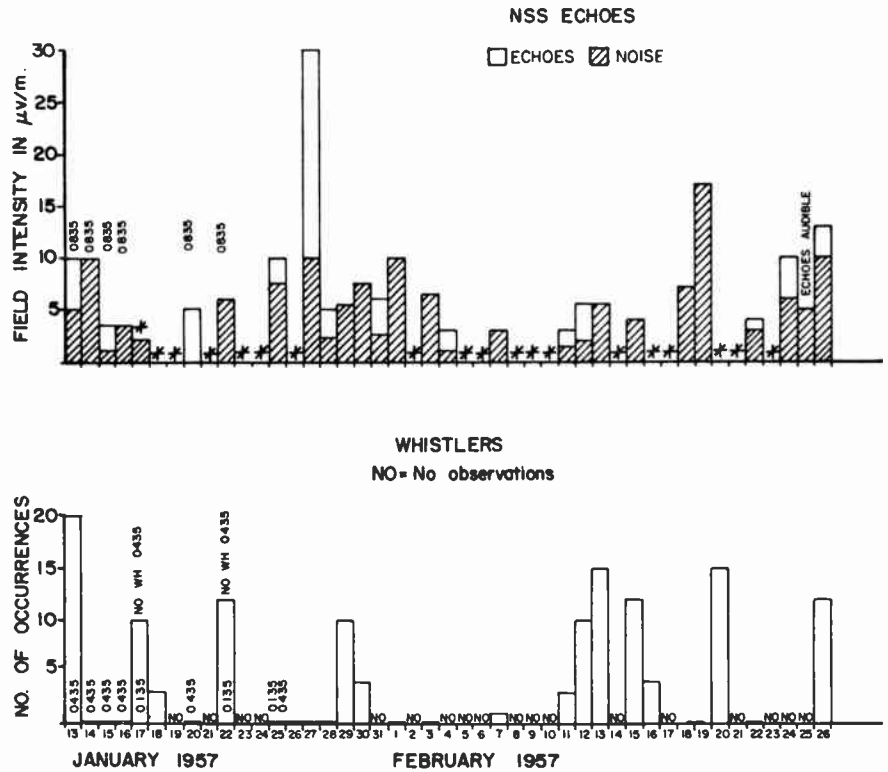


Fig. 1—Strengths of NSS echoes and occurrence frequency of whistlers during January and February, 1957.

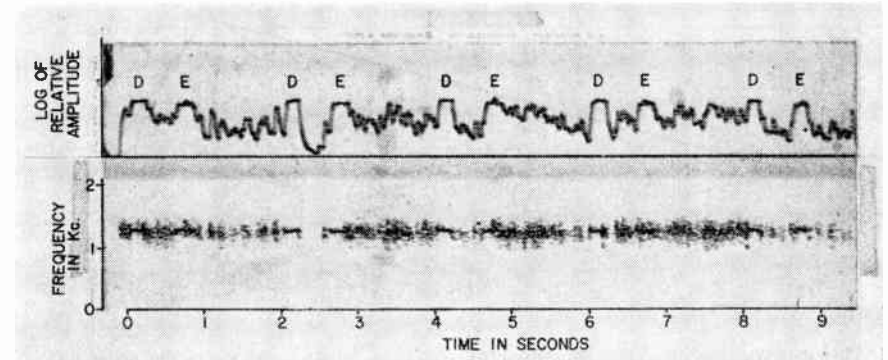


Fig. 2—Direct (D) and echo (E) signals from NSS on January 27, 1957. Upper graph shows relative amplitude; lower graph shows spectrum of same signals.

aurally to be about two-thirds of a second; the intensity was roughly 30 db below the direct wave. From a later A-scan presentation of the tape-recorded signals, estimates were made of the rms signal strength and background noise for each period of recording. These data are plotted in Fig. 1.⁸ There seems to be some evidence for an inverse correlation between the whistler rate and the occurrence of NSS echoes. This rather surprising result might be explained in terms of a north-south shift in the end points of the relevant paths of propagation. This explanation supposes that the whistlers origi-

⁸ On many days, marked by an asterisk on Fig. 1, ordinary text was being transmitted and echoes often were detected. The earliest of such observations, discovered on the tapes only recently, was made on November 21, 1956. Although quantitative measurements of the delays are not yet available, it was found that detectable echoes were present on at least 80 per cent of the days of observation. On certain other days no observations were made.

nate at points considerably south of the NSS transmitter, possibly in the thunderstorm area of the Caribbean. When the path from that area terminates at Cape Horn, the path from NSS would be expected to terminate farther south and the echoes would not be heard. Conversely, when the NSS path terminates near Cape Horn, the whistlers arrive too far north to be heard. In this connection, the observations on January 27, 1957, are particularly noteworthy since the echo intensity increased greatly, reaching field intensity peaks which were only 10 db below the direct signals, but again no whistlers were heard. Both NSS echo and whistler occurrence were compared with the magnetic-K index, but no relationship could be detected. However, there are too few data to say conclusively that there is no correlation.

NSS echo delays were readily measured

with the aid of A-scan recordings made from the magnetic tapes. A section of the January 27th record is shown in Fig. 2. The upper part is a plot of the log of relative field strength, and the lower part shows the spectrum of the recorded signal, both as functions of time.⁹ A single echo follows each direct pulse with a delay of 0.61 second. To this must be added 0.03 second for the calculated travel time of the direct wave, giving a total delay of 0.64 second. On other nights different delays were observed, ranging from 0.3 to 0.9 second. During some periods, two separate echoes could clearly be distinguished by ear, with spacings up to 0.4 second. Sometimes the echo intensity dropped off gradually, with the echo lasting perhaps half a second. These results indicate the presence of multiple paths of propagation whose properties change markedly from night to night. Multiple whistlers, apparently arising from a single source, were also observed with a similar range of delays at 15.5 kc.

One of the most unexpected results from this experiment was the observation of marked and systematic fading of the echoes. Fig. 3 shows a plot of the relative amplitude of each NSS echo recorded during the run of January 27th. The fading period is about 50 seconds, and the ratio of maximum-to-minimum strength is roughly ten-to-one.

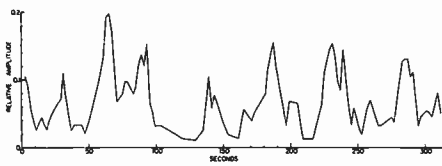


Fig. 3—Relative amplitude of NSS echoes on January 27, 1957.

The significant point is that the fading is fairly regular and deep, suggesting the beating of two components of nearly equal amplitude. These might be similar in origin to the split components described above, except for a reduced spacing. This phenomenon may be associated with the so-called whistler "pair." The time separation of the members of a whistler pair is typically of the order of 0.1 second at 15.5 kc; therefore, the components would overlap in this experiment, since the pulse length was 0.25 second. The necessary relative phase change in the two paths might be produced by irregularities drifting through the regular ionospheric layers or by differential changes in the more remote magneto-ionic duct paths.

The cause of echo splitting and the multiple components of whistlers remains uncertain. A double echo might be caused by the normal pattern of a short vertical antenna which concentrates the energy in a ring around the source. Although this mechanism may operate, it does not explain more than two components, a condition often encountered in whistler spectra. It seems necessary to look further for the explanation.

⁹ This record was made with a Sonograph equipped with an amplitude display unit. The tape was played at four times normal speed.

One possibility is that the transmission coefficient of E region varies from place to place as a result of patchiness, such as sporadic E. Its effect would be to permit reception of only those rays which could pass through the E region at both ends of the path. Another possibility is that the magneto-ionic ducts are, in fact, paths along which the ionization is enhanced—in effect, field-aligned columns of ionization stretching all or part of the way between the hemispheres. Further data on this problem might be obtained by correlating the temporal and spatial variations in E region reflection properties with multiple magneto-ionic duct signals.

As a check on the fundamental difference between the modes of propagation of the direct signal and the echoes, the ground wave was nulled using a crossed-loop goniometer. It was possible to reduce the amplitude of the direct wave by at least 30 db, without reducing the echo intensity more than a few db at the most. This is additional evidence that the echo is propagated in an entirely different manner from that of the direct wave. It is consistent with a downcoming wave of circular polarization as predicted by whistler theory.

CONCLUSION

A unique mode of very-low-frequency radio transmission, called magneto-ionic duct propagation, has been demonstrated. Its close similarity to whistler propagation provides new evidence in support of the Eckersley-Storey theory of whistlers.

The large variations in echo time delay from day to day must be caused by changes in the medium of propagation, since the locations of both transmitter or receiver were fixed.

The frequent observation of NSS echoes when no whistlers could be heard shows that the absence of whistlers is probably due to a lack of suitable lightning sources at the proper location, and not to poor propagation conditions in the magneto-ionic duct. There is strong evidence that the magneto-ionic duct path may be open nearly all of the time.

The systematic fading and the splitting of echoes suggest the presence of multiple paths of propagation of variable relative phase.

The observed echo intensities, which were 10 to 30 db below the direct wave, together with the fact that the receiver appears to have been located near the edge of the "effective" area, suggest that echo strengths comparable to or greater than the direct wave may be found near the conjugate point. Under these conditions, the new mode would be an important factor in vlf communication. Depending on the way in which it is used, it could be either an advantage or a disadvantage.

Because of their long and variable delays, magneto-ionic duct signals can be expected to interfere seriously with the operation of phase-sensitive navigation systems at very-low frequency. A world-wide frequency standard in this range would likewise be adversely affected in the region of the effective area.

The new technique has important ad-

vantages over whistlers for the study of the outer ionosphere. Unlike the lightning source, the vlf transmitter can be turned on at will and its location and radiation properties are readily determined. Data obtained in this way should yield new facts about the structure of the outermost regions of the ionosphere, including the strength and form of the earth's magnetic field at great distances from the earth. These data in turn are expected to be of help in advancing our understanding of magnetic storms and auroras. The experiment could be usefully extended by receiving the signal in a satellite and telemetering phase and amplitude information back to earth. In this way, the properties of the path between transmitter and satellite could be separated from that of the total path. Since a satellite occupies many different locations in a short period of time, it should be possible to measure the effective beamwidth, the transmission loss, and the distribution of irregularities.

ACKNOWLEDGMENT

We are indebted to Commander Neely of the Naval Communications Division, Chief of Naval Operations, for providing the special NSS transmissions.

The excellent cooperation of the Chileans in setting up the receiving station is gratefully acknowledged. Particular thanks are due the Chilean Navy which provided certain essential facilities and transportation south of Punta Arenas. Persons who contributed valuable assistance are General Ramon Canas y Montalva, Chairman of the Executive Committee for the International Geophysical Year; Tte. Coronel Alberto Stegmaier, Chief of the Army Radio Service of Chile; Dr. Cinna Lomnitz, Seismological Institute, University of Chile; Oscar Schneider, Director of Exploration for the National Petroleum Agency (Empresa Nacional del Petroleos); Claude Hardy, Punta Arenas.

Important messages were handled by Amateur Radio and we are indebted to the Telecommunications Section of the General Directorate of Electric Services of Chile for granting a license for station CE8BT. Special thanks are due Alfred M. Faries, W600U, Menlo Park, Calif., who handled most of the traffic.

R. A. HELLIWELL
E. GEHRELS
Radio Propagation Lab.
Stanford University
Stanford, Calif.

Tuning a Probe in a Slotted Line*

It is a usual practice to tune a slotted line probe by first locating a position of the maximum detected energy and then tune the probe at this very position. This will

* Received by the IRE, December 5, 1957.

usually lead to an imperfect tuning and thus distort the detected standing wave pattern. This note presents a correct method of tuning with a simple analytic explanation.

A slotted line or guide system can be schematically represented by the equivalent circuit shown in Fig. 1, in which the equivalent constant current generator has an internal impedance G_G and the load is represented by G_L , both normalized with respect to Y_0 , the characteristic admittance of the line, while the complex parts of both the generator and the load admittances have been included in the lengths x_G and x_L , respectively. The probe admittance is represented by G_p and B_p in parallel.

The power P_s absorbed by the probe can be easily calculated with the assumption of a perfect matching between the generator and the line; i.e., $G_G = 1$,

$$P_s = \frac{i_0 G_p (1 + G_L^2 \tan^2 \theta)^2}{[1 + G_L + G_p + G_L(1 + G_L + G_p G_L) \tan^2 \theta]^2 + [B_p + (1 - G_L^2) \tan \theta + B_p G_L^2 \tan^2 \theta]^2} \quad (1)$$

where $\theta = 2\pi x_L / \lambda_g$.

In order to analyze the behavior of the probe, it is convenient to consider separately the following two cases, i.e., $G_L = 0$ and $G_L \neq 0$. In case of $G_L = 0$, (1) may be reduced to

$$P_s = \frac{i_0 G_p}{(1 + G_p)^2 + (B_p + \tan \theta)^2} \quad (2)$$

and the nulls of P_s correspond to the condition $\tan \theta = \infty$, which is a condition independent of B_p , or independent of the probe tuning. On the other hand, the maxima occur at $\tan \theta = -B_p$. Hence whenever B_p is different from zero, the detected maxima of the standing wave are shifted with respect to the maxima of the true standing wave pattern as shown in Fig. 2. The relative positions shift from the left to the right as B_p varies from positive to negative.

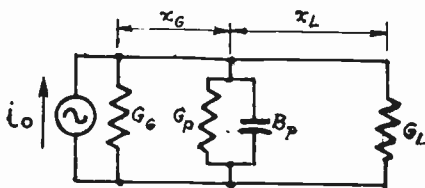


Fig. 1.

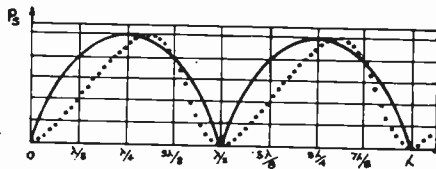


Fig. 2.

In the case where G_L is different from zero, the probe susceptance B_p will affect the positions of the maxima and the minima of

the detected pattern. This leads to the conclusion that the only unaffected points of the detected pattern due to the probe susceptance are those points corresponding to the nulls under short-circuit condition.

From the above analysis, it will be obvious to see why errors are introduced into such standing wave measurements when the probe is tuned according to the usual practice by starting with an arbitrary condition of the probe, i.e., with an unknown B_p , to locate a point of maximum detected energy. Then the probe is finally tuned at this point for maximum reading.

The maximum point thus determined is actually not the true maximum of the standing wave pattern in the line, due to a shift resulting from an initial nonvanishing value of B_p , as has been shown. This kind of tuning actually corresponds to a condition of maxi-

mum value of P_s of (2) and will not lead, in general, to the condition $B_p = 0$ which is required for a proper tuning, simply as a consequence of the fact that $\tan \theta \neq 0$ at the point the tuning is performed.

Therefore, a more adequate procedure for probe tuning includes: first, a location of the proper point for correct tuning which is the point of the true maximum, and second, tuning properly performed at that point. This procedure may consist of the following steps:

- 1) Always use a short-circuit termination ($G_L = 0$).
- 2) Locate two consecutive nulls.
- 3) Move the probe to the center point between the two nulls ($\tan \theta = 0$).
- 4) Tune the probe for a maximum output ($B_p = 0$).

This technique has been used successfully in this laboratory for microwave measurements.

JOSE I. CAICOYA
Instituto Tecnológico de Aeronautica
Sao Jose dos Campos
Sao Paulo, Brazil

Cutoff Phenomena in Transversely Magnetized Ferrites*

Suhl and Walker¹ have made an extensive study of the cutoff phenomena in a longitudinally magnetized ferrite-filled circular waveguide and the results have been summarized by Kales.² They have shown

that there are three kinds of cutoffs. The first is similar to the cutoff which occurs if the circular waveguide is filled with a homogeneous, isotropic medium. The second and third types of cutoff were shown to occur when $\mu^2 - K^2 = 0$ and $\mu = 0$, respectively. The author³ had also made some cutoff studies for circular waveguides partially filled with ferrite.

In the case of a transversely magnetized ferrite, it appears that similarly interesting results occur. Furthermore, the mathematics are sufficiently simpler than the circular waveguide case to permit easy calculation of the cutoff frequencies. By plotting the cutoff frequencies as a function of the dc magnetic field for various ferrite and waveguide geometries, a better understanding of the phenomena can be achieved. Therefore, we present here some theoretical results and interpretations of the cutoff phenomena in transversely magnetized ferrites. Experimentally determined cutoff frequencies are also presented to substantiate the behavior predicted by theory.

Consider the problem of a rectangular waveguide loaded with a ferrite slab magnetized transverse to the direction of propagation as shown in Fig. 1. By solving the boundary value problem, the transcendental equation involving the propagation constant β can be shown to be⁴

$$\frac{k_a^2}{\rho^2} \cos k_a(L - \delta) + \frac{k_a k_m}{\rho} \cot(k_m \delta) \sin k_a(L - \delta) = \frac{-j\beta k_a}{\rho \theta} \sin k_a(L - \delta) \quad (1)$$

where

$$\rho = \frac{\mu \mu_0}{\mu^2 - K^2} = \frac{1 + \chi_{xx}}{(1 + \chi_{xx})^2 + \chi_{xy}^2}$$

$$\theta = \frac{\mu}{-jK} = \frac{1 + \chi_{xx}}{\chi_{xy}}$$

$$k_m^2 = \omega^2 \epsilon_0 \mu_0 \frac{1}{\rho} - \beta^2$$

$$k_a^2 = \omega^2 \epsilon_0 \mu_0 - \beta^2 \quad (2)$$

and

$$\chi_{xx} = \frac{4\pi M_s \gamma (\gamma H_i)}{(\gamma H_i)^2 - \omega^2}$$

$$\chi_{xy} = -\frac{j\omega \gamma 4\pi M_s}{(\gamma H_i)^2 - \omega^2} \quad (3)$$

$4\pi M_s$ is the saturation magnetization of the ferrite and $\gamma = 2.8$ mc/oersted. ω is the wave frequency while H_i is the dc field in the ferrite medium. The cutoff frequencies ω_c corresponding to $\beta = 0$ can be readily determined as a function of H_i by setting $\beta = 0$ in (1) and (2) and combining to yield:

$$-\sqrt{\frac{\epsilon_0}{\rho \epsilon}} = \frac{\cot \left[\omega_c \sqrt{\mu_0 \epsilon} \sqrt{\frac{1}{\rho}} \delta \right]}{\cot \left[\omega_c \sqrt{\mu_0 \epsilon_0} (L - \delta) \right]} \quad (4)$$

* Received by the IRE, December 20, 1957.

¹ H. Suhl and L. R. Walker, "Topics in guided-wave propagation through gyromagnetic media—Part I. The completely filled cylindrical guide," *Bell Sys. Tech. J.*, vol. 33, pp 579-659; May, 1954.

² M. L. Kales, "Topics in guided-wave propagation in magnetized ferrites," *Proc. IRE*, vol. 44, pp 1404-1405; October, 1956.

³ R. F. Soohoo, "Higher-Order Mode Propagation in Ferrite Devices and Wide-Band Tunable Ferrite Microwave Filters," presented at the Annual PGMTT Meeting, New York, N. Y., May, 1957.

⁴ B. Lax, K. J. Button and L. M. Roth, "Ferrite phase shifters in rectangular waveguide," *J. Appl. Phys.*, vol. 25, pp 1413-1421; November, 1954.

¹ For a more detailed discussion, see C. G. Montgomery, "Technique of Microwave Measurements," M.I.T. Rad. Lab. Series, McGraw-Hill Book Co., Inc., New York, N. Y., vol. 11, pp. 483-485.

For an infinite ferrite medium $k_m=0$ and (2) gives

$$\beta = \omega \sqrt{\mu_0 \epsilon} \sqrt{\frac{1}{\rho}} \quad (5)$$

If $1/\rho$, the equivalent permeability, is negative, $\sqrt{1/\rho}$ and therefore β is imaginary and the fields would vary as (y being the direction of propagation):

$$\exp - \omega \sqrt{\mu_0 \epsilon} \sqrt{\frac{1}{|\rho|}} y \quad (6)$$

signifying reactive attenuation or cutoff. Now, $1/\rho$ goes from positive to negative at the point where $\mu^2 - K^2 = 0$. Utilizing definitions (2) and (3), we have:

$$\omega_{co} = \gamma(H_i + 4\pi M_s) \quad (7)$$

It also goes from negative infinity to positive infinity at resonance, *i.e.*, when $\mu=0$. Again, (2) and (3) give:

$$\omega_{cr} = \gamma \sqrt{H_i(H_i + 4\pi M_s)} \quad (8)$$

For a particular field H_i , (7) and (8) yield two frequencies ω_{co} and ω_{cr} between which $1/\rho$ is negative. Thus, these frequencies can be considered as the cutoff frequencies of the magnetized infinite ferrite medium. Repeating this procedure for another value of field, cutoff frequency vs internal field characteristics can be obtained. The result for a particular ferrite is shown in Fig. 2.

For a waveguide totally filled with ferrite, *i.e.*, $L = \delta$, (4) shows that

$$\omega_c \sqrt{\mu_0 \epsilon} \sqrt{\frac{1}{\rho}} L = n\pi \quad (9)$$

where $n=1$ for the TE₁₀ mode. Combining (2), (3), and (9), we obtain a quadratic equation in ω_c^2 :

$$\begin{aligned} (\omega_c^2)^2 - \left[\gamma^2(H_i + 4\pi M_s)^2 + \left(\frac{\pi}{L\sqrt{\mu_0 \epsilon}} \right)^2 \right] (\omega_c^2) \\ + [\gamma^2 H_i(H_i + 4\pi M_s)] \left(\frac{\pi}{L\sqrt{\mu_0 \epsilon}} \right)^2 = 0. \end{aligned} \quad (10)$$

Eq. (10) has been plotted for a regular X-band waveguide totally filled with ferrite, also in Fig. 2. The distinguishing feature of the curves compared to that of the infinite medium is the appearance of a finite cutoff frequency at zero field and another branch of the $\beta=0$ curve above resonance field (below resonance frequency) attributed to the quadratic nature of (10). The cutoff frequency is seen to approach that at zero field as H_i takes on very large values. This is as it should be since $1/\rho$ approaches 1 as H_i approaches infinity. Since the field required for resonance is independent of the sample shape, provided that one considers only the internal field H_i , the $\mu=0$ line represents one of the cutoff curves which is a characteristic of the medium only. A little reflection will show that the shaded portion represents the forbidden region (no propagation possible) in the totally filled guide. From Fig. 2, it is seen that there is a range of very small frequencies at small H_i values, (*i.e.*, the frequencies between the $\mu=0$ curve and the above resonance field branch of the $\beta=0$ curve) which could propagate. Indeed, a

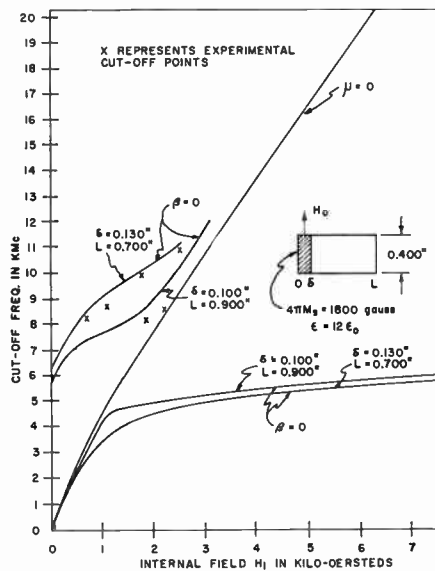


Fig. 1—Cutoff frequency vs internal field characteristics for a rectangular waveguide partially filled with ferrite.

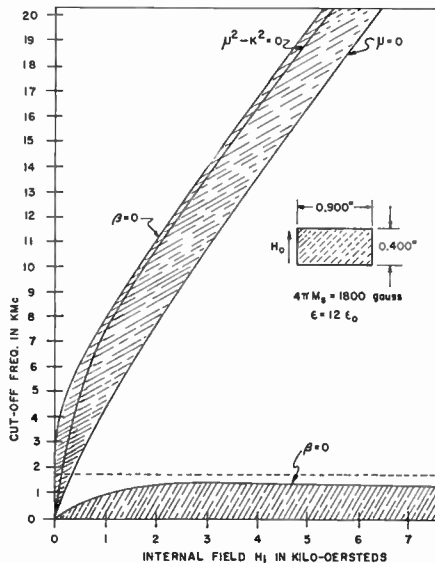


Fig. 2—Cutoff frequency vs internal field characteristics for a rectangular waveguide totally filled with ferrite.

little reasoning would show that it is possible to propagate microwaves in an extremely small ferrite-filled waveguide for appropriate field values. This is not too surprising as $1/\rho$ is positive infinite just on the high side of resonance, making the guide appear electrically very large there.

If the ferrite medium does not completely fill the waveguide, then the cutoff behavior would be expected to differ from that predicted by (9) above. Intuitively, one would expect that if the slab thickness δ is very small, one would not be able to cut off the partially loaded waveguide even if the ferrite is biased so that $1/\rho$ is negative. Quantitatively, for any particular slab thickness δ and guide size L , the transcendental equation (4) can be solved for ω_c , at a particular field H_i , by plotting both sides of the equation vs frequency. The first intersection of

the two curves would give the cutoff frequency ω_c of the TE₁₀ mode. This has been done for two separate cases, one with $\delta=0.100$ inch and $L=0.900$ inch and one with $\delta=0.130$ inch and $L=0.700$ inch. It is seen that the behavior agrees with the qualitative speculations above.

Experiments have been performed to check the cutoff behavior predicted by (4). The experimentally determined cutoff frequencies for a partially loaded guide are plotted in Fig. 1 for comparison with the theoretical values. The demagnetization factors were assumed to be those of a sample whose cross section is an elongated ellipse; the saturation magnetization is in the direction of the major axis. This assumption is reasonably good as there are tapers in the ferrite slab at each end to improve matching of the loaded and unloaded sections. Note that H_0 in Figs. 1 and 2 is the applied dc field which is related to the internal field H_i through the demagnetization factors.

The experimental cutoff frequencies agree reasonably well with the theoretical values, as shown in Fig. 1. The electric field inside the ferrite-loaded waveguide at cutoff was monitored and was found to decay exponentially and rapidly with distance in the direction of propagation with no maxima or minima observed even with a short at the output end of the device. This supports the contention that the phenomenon is predominately a cutoff one. Indeed, a BWO swept source was used to observe the cutoff phenomena over the whole X band. When the applied field was zero, the transmission was almost complete with hardly any reflections over the band. As the field was increased, the transmission decreased to zero, while the reflection increased to a high value, first at 8.2 kmc and then moved gradually up on the frequency scale. At some value of field, the nearly complete reflection was observed over the whole X band. When the field was further increased, the low-frequency end began to transmit again and transmission could be observed over the whole band if the field was increased still further. This agrees with the predictions of Fig. 1. Thus, the band rejection characteristic due to the changing ferrite permeability with applied field is definitely established. Indeed, a tunable cutoff filter was made using this phenomenon.³

We have considered a lossless ferrite in our theoretical treatment. Experimentally, it was found that loss changes the cutoff picture somewhat. First of all, the cutoff and ferromagnetic resonance are no longer infinitely sharp when loss is included. Therefore, in the region where the $\beta=0$ curve is close to the resonance or $\mu=0$ curve (Fig. 1) it would not be easy to observe the cutoff phenomena because of finite ferrite line width. This is the case for the $\delta=0.100$ inch, $L=0.900$ inch configuration at frequencies above 9 kmc. In the $\delta=0.130$ inch, $L=0.700$ inch case, however, because the $\beta=0$ and $\mu=0$ curves are widely separated in the 8.2- to 12.4-kmc region, the cutoff phenomena could be distinctly observed over the entire X band.

RONALD F. SOOHOO
Cascade Research
Monogram Precision Industries, Inc.
Los Gatos, Calif.

Contributors

Elie J. Baghdady, for a biography and photograph, please see page 305 of the February, 1958, issue of PROCEEDINGS.



Lynn A. Beattie was born in Detroit, Mich., on August 21, 1945. He received the B.S. degrees in electrical engineering and mathematics in 1951,



L. A. BEATTIE

the M.S. in electrical engineering in 1952, the A.M. in mathematics in 1955, and the Ph.D. in electrical engineering in 1957, all from the University of Michigan, Ann Arbor, Mich.

From 1951-1957, Dr. Beattie was employed by the electronic defense group of the University of Michigan, finally serving this organization in the capacity of task engineer. Presently, Dr. Beattie is with the teaching faculty of the University of Idaho, Moscow, Idaho.

Dr. Beattie is a member of Eta Kappa Nu and Sigma Xi.



Anthony C. Brown (M'55) was born on September 27, 1932, in London, England. He received the B.Sc. degree in electrical engineering from the University of London in May, 1955, which was followed by microwave research work at The Polytechnic, Regent Street, London. He then joined the Microwave Division of EMI Electronics Limited, Feltham, Middlesex, England, where he has been engaged in the



A. C. BROWN

research and development of ferrite and other microwave components.

Mr. Brown is also a graduate of the Institution of Electrical Engineers.



Roy S. Cole was born in London, England, on February 16, 1932. He was educated at University College, London, where he received the B.Sc. degree in physics in 1954.



R. S. COLE

In 1956, he received the Full Technological Certificate in Telecommunications from the City and Guilds of London Institute. At present he is engaged in the research and development of ferrite and

other microwave components in the Microwave Division of EMI Electronics Limited, Feltham, Middlesex, England. He is also engaged in post graduate research work at Birkbeck College, London.

Mr. Cole is a graduate of the Institute of Physics.



Winfield J. Giguere (M'57) was born in Claremont, N. H., on June 20, 1930. He received the B.S.E.E. degree from the University of New Hampshire, Durham, N. H., in 1954, and soon after joined the technical staff of Bell Telephone Laboratories, Murray Hill, N. J.



W. J. GIGUERE

His first work was in engineering and development of carrier systems, microwave networks, and methods for diode measurement. More recently Mr. Giguere has been concerned with transistorized radio equipment and radio transmission.

Mr. Giguere, who was winner of a Westinghouse Achievement Scholarship, was a student officer of the American Institution of Electrical Engineers and Tau Beta Pi and is also a member of Phi Kappa Phi.



William N. Honeyman was born on September 20, 1934, in Cumberland, England. He received the B.Sc. degree in physics from the University of Durham in 1954, and the full Technological Certificate in Telecommunications from the City and Guilds of London Institute in 1956.



W. N. HONEYMAN

At present he is engaged in research and development in ferrites and other microwave components at the Microwave Division of EMI Electronics Limited, Feltham, Middlesex, England.



Dietrich A. Jenny (A'47-M'55) was born on August 15, 1920, in Switzerland. He studied at the University of Zurich and the Swiss Federal Institute of Technology from 1939 to 1946, and received the Diploma in Physics (M.S.) in 1946, and the degree of Doctor of Natural Science (Ph.D.) in 1951, from the Department of Mathematics and Physics.

He joined RCA Laboratories in Princeton, N. J., in 1947, where he worked on his doctoral dissertation in the field of secondary electron emission. Dr. Jenny was also en-

gaged in research on thermionic emission, electron optics, color television kinescopes, and other electron tube problems. Since 1952, he has been active in the field of solid state research, particularly semiconductor physics and devices where he specialized in compound semiconductor work. He is a cotranslator of the book "Electronic Semiconductors" by E. Spenke.

Dr. Jenny is a member of the American Physical Society and Sigma Xi.



D. A. JENNY



William H. Louisell was born in Mobile, Ala., on August 22, 1924. He received the degrees of B.S. in physics in 1948, the M.S. in physics in 1949, and the Ph.D. in physics in 1953, all from the University of Michigan. He has been a member of the technical staff at Bell Telephone Laboratories, Murray Hill, N. J. since 1953.



W. H. LOUISELL

Dr. Louisell has been concerned with the study of a new microwave coupling principle and the application of ferrites to traveling-wave tubes.

He is a member of the American Physical Society, Phi Eta Sigma, Phi Kappa Phi, Sigma Xi, and Gamma Alpha.



C. F. Quate (S'43-A'50-M'55) was born in Baker, Nev., on December 7, 1924. He received the B.S. degree in electrical engineering from the University of Utah in 1944 and the Ph.D. degree from Stanford University in 1950. He has been a member of the technical staff in the research department of the Bell Telephone Laboratories, Murray Hill, N. J., since 1949.



C. F. QUATE

Dr. Quate has been engaged in research on electron dynamics which is the study of vacuum tubes in the microwave frequency region.

Dr. Quate is a member of Tau Beta Pi and Sigma Xi.



Hideo Seki (A'52-SM'57) was born in Yamagata, Japan, on October 13, 1905. He attended the Tokyo Institute of Technology

and was graduated in 1932, with the degree of Kogakushi. In 1943, he received the Ph.D. degree from the same institute for a dissertation on "The Study of Noise in Radio Receivers."

He studied at Massachusetts Institute of Technology, Cambridge, Mass., in 1952.

From 1926 until 1929, he was an assistant technician of the first section of the Electrical Research Lab. of Tokyo, in the study of piezoelectric

oscillators. In 1932, he was employed by the International Telecommunications Company, engaged in the design of transoceanic radio receivers and in research work on communications systems. In 1947, he became chief of the Communication Research Section of the Sixth Division of the Railway Technical Lab., remaining with them until 1949, when he was employed as a staff official of the engineering and monitoring division of the Radio Regulatory Administrative Office. From 1952 until 1953, he was chief of the Second Division of the Radio Research Laboratories of the Ministry of Postal Service. From 1953 to the present time he has been with the research division of Iwasaki Tsushinki Co., where he is engaged in the development of new electronic products. During 1947-1949, he was also a professor at the University of Electro-Communication and from 1951-1953, lectured at Tokyo Institute of Technology.

Dr. Seki is a lecturer at the University of Electro-Communication, Ministry of Education of the Japanese Government; a member of the Commission V, Japanese URSI and consultative member of the Commissions IV and VI; member of the first, second, and third Consultative Commissions of Radio Engineering, Radio Regulatory Office, Ministry of Postal Service; Chairman of the Information Theory Commission, Institute of Electrical Communication Engi-



H. SEKI

neers of Japan; and Chairman of the Speech Analysis and Synthesis Commission, Acoustical Society of Japan.



Harry Suhl was born on October 18, 1922, in Leipzig, Germany. He received the B.Sc. degree from the University of Wales in 1943,

and the Ph.D. degree in theoretical physics from Oriol College, Oxford, in 1948.

From 1943 to 1946, he worked on radar at the Admiralty Signal Establishment. In 1948, he joined Bell Telephone Laboratories, where he has worked on electron-dynamics, physical properties of germanium,



H. SUHL

electromagnetic wave propagation, and ferromagnetic resonance. He is currently concerned with solid-state theory.

Dr. Suhl is a member of the American Institute of Physics and a Fellow of the American Physical Society.



Ping K. Tien (S'49-A'51-M'56) was born in Chekiang, China, on August 2, 1919. He received the B.S.E.E. degree from the National Central University of China in 1942, and the M.S. and Ph.D. degrees from Stanford University in 1948 and 1951.



P. K. TIEN

then research associate at Stanford University.

Since 1952, Dr. Tien has been a member of the technical staff of the Bell Telephone Laboratories, Murray Hill, N. J., where he has worked on electron dynamics, electromagnetic wave propagation, microwave tubes, and ferrite devices.

He is a member of Sigma Xi.



Louis Weinberg (M'52-SM'56) was born on July 15, 1919, in Brooklyn, N. Y. He received the B.A. degree from Brooklyn College in 1941, the M.S. degree in engineering sciences and applied physics from Harvard University in 1947, and the Sc.D. degree in electrical engineering from the Massachusetts Institute of Technology in 1951.



L. WEINBERG

From 1942 to 1943, Dr. Weinberg worked for the Office of the Chief Signal Officer. He left to join the Army Air Force, where he remained until 1946, serving as a radar and electronics officer, and as technical advisor to the American Embassy at the Hague, Netherlands. From 1947 to 1951, he was an instructor in the Department of Electrical Engineering at M.I.T. Since 1951, he has worked for the Hughes Research and Development Laboratories, Culver City, Calif., where he is at present a Senior Staff Engineer and head of a group working on networks and statistical communications.

From 1952-1954, he was a lecturer in engineering at the University of California, Los Angeles; in 1955-1956 he was a visiting associate professor of electrical engineering at the University of Southern California. Dr. Weinberg is now a visiting professor of electrical engineering at the California Institute of Technology.

Dr. Weinberg is a member of Propylaea and Sigma Xi.



Scanning the Transactions

Interplanetary communication, until very recently a subject discussed only in science fiction circles, is now a matter of serious engineering speculation and planning. The first venture to the moon and beyond will no doubt be made by unmanned instrumented space-research vehicles. A two-way radio system will be needed for a guidance and communication link between the Earth and the vehicle. A recent study indicates that for controlled flights around the moon a system of this sort would require a 2 kw transmitter on the vehicle and a 200 kw transmitter on the Earth. This equipment is within our present capabilities. To reach Mars, this system would have to be boosted to a formidable 6 megawatts on the vehicle and 600 megawatts at the Earth station.

For manned space flights the radio requirements would be less severe because humans will perform many of the control and observational functions that would have to be radioed to and from an unmanned vehicle. Reducing the amount of information to be sent in a given time serves to increase the communication range. It has been estimated that with present-day techniques we could provide manned space craft with navigational and communication coverage over the entire solar system by using point-to-point beamed transmissions. Omnidirectional transmissions, on the other hand, would not presently serve us even to the nearest planet, but by 1975 it can be expected that technical advances will extend this range out to Jupiter.

Any discussion of space flight brings with it some novel proposals. For example it is possible that once a space vehicle reaches cruising speed and begins coasting, its antenna problem could be solved by simply ejecting a very large collapsible directional antenna. The antenna would coast along beside the ship and could be pointed toward home base to achieve long range communication with limited power. The fact that the vacuum in space exceeds anything we can presently realize on Earth prompts another interesting thought. Will we build tubes without envelopes to make use of this characteristic?

The foregoing seems to indicate that interplanetary radio communication will decidedly prove to be feasible. Indeed we have already taken the first small electromagnetic step into space by bouncing AM voice signals off the Moon and detecting them on Earth,¹ a round trip of half a million miles. What about *interstellar* communication? The nearest star is about 24 trillion miles away. Even if we could achieve this tremendous range some day, one wonders if we would want to. If we sent a message to someone on that star, say next Tuesday, we would have to wait 8 years before we had a reply. (H. E. Prew, "Space exploration—a new challenge to the electronics industry," IRE TRANS. ON MILITARY ELECTRONICS December, 1957. P. A. Castruccio, "Communications and navigation techniques of interplanetary travel," IRE TRANS. ON AERONAUTICAL AND NAVIGATIONAL ELECTRONICS, December, 1957.)

Waveguides filled with ionized gas offer interesting potentialities that have not been explored yet to any great extent or even recognized by engineers in general. It has been found that at microwave frequencies a wave traveling through a waveguide filled with an inert gas like neon in the presence of a magnetic field will encounter rotational and resonance effects much like those produced by ferrites, but without the frequency limitations associated with ferrites. Hence, the gas-filled waveguide may find application in some situations similar to those in which ferrites are now used. It has also

been noted recently² that at frequencies of the order of a few megacycles a waveguide filled with ionized gas exhibits unexpected pass bands below the usual waveguide pass band. We can probably expect to see this aspect of gaseous electronics take on new importance in the near future. (L. Goldstein, "Nonreciprocal electromagnetic wave propagation in ionized gaseous media," IRE TRANS. ON MICROWAVE THEORY AND TECHNIQUES, January, 1958.)

Satellite tracking has been a problem that has engaged nearly everyone's attention of late. The PROCEEDINGS alone has published 7 letters on this subject in just the last 5 months. As hundreds of amateurs and scientists all over the world strained to spot the tiny elusive moons, our sister publication, the IRE STUDENT QUARTERLY, quietly proffered its own ingenious solution to the spotting problem in the February issue, as shown below.



Reprinted from IRE STUDENT QUARTERLY

Electronic heart-sound recording techniques are becoming an important tool in the study of the heart and its abnormalities. Such recordings are particularly useful in providing a record of the timing of normal and abnormal sounds. They are usually made in conjunction with electrocardiograms and recordings of pulse and respiration to provide additional information concerning the heart. A spectral analysis of the sounds can be performed to give still further information regarding the character of the sounds. One interesting technique, developed just in the past four years, involves threading a catheter through a vein and into the heart to obtain sound recordings from within the heart itself. A miniature barium titanate transducer has recently been developed as an acoustic pickup device for the heart end of the catheter and has been used successfully on a number of patients. Making several recordings at different locations in the heart has proved a decided aid in localizing and diagnosing certain types of heart ailments. Thus an acoustic device first developed for undersea warfare is now being used to preserve life rather than to destroy it. (Symposium on Heart Sound Reproduction and Recording, IRE TRANS. ON MEDICAL ELECTRONICS, December, 1957).

¹ J. H. Trexler, "Lunar radio echoes," PROC. IRE, vol. 46, pp. 286-292; January, 1958.

² L. D. Smullin and P. Chorney, "Properties of ion filled waveguides," PROC. IRE, vol. 46, pp. 360-361; January, 1958.

Technical institutes should be expanded ten times in the next decade, while other forms of higher education are being doubled, if we are to get truly efficient utilization of our scientists and engineers. To support this viewpoint a prominent educator states that whether we realize it or not, 50 to 75 per cent of the work being done in the engineering departments of manufacturing plants today can be done as well, if not better, by engineering technicians who graduate from two-year technical institutes. The present technicians-to-engineers ratio of 0.7 to 1 should, and probably will, be increased to 2.8 to 1. If this tremendous expansion comes about, by 1970 we will see more than 600,000 students enrolled in two-year technical institutes as compared with 400,000 in four-year engineering colleges. Whether or not the particular numbers cited above prove to be the right ones, there can be no doubt that the technical institute will play a far more prominent and vital role in the future technical welfare of our society. In this connection it is significant that the IRE just last year extended to its student members in technical institutes most of the privileges and benefits enjoyed by college student members. (H. R. Beatty, "The role of the technical institute in the next decade," IRE TRANS. ON EDUCATION, March, 1958.)

The recent declassification of Doppler navigation systems has resulted in a special issue of the TRANSACTIONS on this subject. These papers make abundantly clear the revolutionary effect that Doppler techniques are having on air navigation. Formerly, uncertainties in aircraft velocity and drift measurements limited navigational accuracy to such an extent that frequent external fixes were necessary to avoid the accumulation of large errors. The use of Doppler systems to determine ground speed and drift has improved the accuracy of the dead reckoning method to the point that it will soon be the most accurate source of navigational data available on many flights. Moreover, this makes the aircraft entirely independent of external navigation aids except on very long flights.

The complete system consists of three basic components: (1) a Doppler velocity measuring system, (2) a heading reference, such as a magnetic or gyrocompass, and (3) a navigational computer. Velocity is measured by the frequency shift observed in the return signal of a radar aimed at an angle toward the ground. Two beams must be used to determine both forward speed and drift angle. However, three and sometimes four beams are often used for greater accuracy and also to measure the rate of climb or descent.

Great strides have been made in reducing the weight and increasing the accuracy of the velocity measuring gear. Equipments weighing less than 100 pounds are now being produced and accuracies to within less than one per cent seem assured. It is probable that these systems will see broad use in the air transport industry, and to a lesser extent even in light private planes, in the next very few years. As a footnote to history, it might be mentioned that the application of the Doppler effect to electromagnetic waves was first demonstrated in 1938 by the Naval Research Laboratory and that the early efforts of NRL to develop an airborne Doppler velocity measuring system were under the direction of John P. Hagen, now the director of Project Vanguard. (IRE TRANS. ON AERONAUTICAL AND NAVIGATIONAL ELECTRONICS, December, 1957).

Luminescent and photoelectric materials research is becoming one of the most active areas today in the solid-state field. Although the results of this research are now only beginning to be applied, many radically new devices are already being considered involving light at either the input or output end. Even in the older field of phosphors important progress is currently being made in making transparent phosphor films for cathode-ray tube screens. It is expected that transparent films will do much to improve the brightness, resolution and contrast of television pictures. Transparent phosphors have

also been proposed for use in the recently developed "thin" or "flat" cathode-ray tubes. The tube could then be mounted in the windshield of an aircraft to present radar information to the pilot without blocking his view.

Electroluminescent materials (*i.e.*, solids that use electric fields or currents, rather than electron bombardment, to generate light) have become of great interest recently, both as a potential method of illumination and of displaying images. The latter application, when perfected, will make possible very large display devices only a fraction of an inch thick, and may in time revolutionize the television receiver.

Considerable progress has also been made in the past two years in cadmium sulfide, a semiconductor whose conductivity increases greatly when exposed to light. Cadmium sulfide has been proposed for solar batteries and photorectifiers, but its widest field of application will probably come in combination with electroluminescent materials. The list of present and proposed photoconductor-electroluminescent devices includes light amplifiers, solid-state power amplifiers, radiation (infrared, ultraviolet and X-ray) amplifiers and image converters, and a variety of control and computer devices. (H. F. Ivey, "Recent advances in luminescence," IRE TRANS. ON COMPONENT PARTS, December, 1957; L. L. Antes, "Progress in cadmium sulfide," *loc. cit.*).

Spherical surface-wave antennas provide a novel type of radiator with an unconventional shape. The propagation of surface waves over dielectric-clad surfaces has been the subject of considerable investigation since their discovery in 1950. Until recently, these investigations have centered on the guiding properties rather than the radiation characteristics of these surfaces. The applications of surface waves have therefore been principally in connection with transmission lines. It now appears that a dielectric-coated spherical cap, using surface waves, makes an excellent beacon antenna for aircraft, ground and shipboard installations where a low silhouette is desirable. (R. E. Plummer, "Surface-wave beacon antennas," IRE TRANS. ON ANTENNAS AND PROPAGATION, January, 1958).

Receiver loudspeaker systems seem to have come a full circle in their development. The earliest broadcast receivers were equipped first with earphones and then with separate loudspeakers. Four decades later finds us returning to earphones for pocket receivers and separate loudspeaker installations for hi-fi systems. The first major innovation came in the early 1920's when the loudspeaker was placed inside the same cabinet with the receiver, a development in which, incidentally, the IRE Editor Emeritus played a leading role. The next step did not come until just a few years ago when hi-fi sets were introduced with two loudspeakers in the cabinet, each reproducing a part of the frequency spectrum. The next major step now seems to be separating the loudspeaker entirely from the receiver housing and, at the same time, multiplying the number of speakers. In this arrangement two low-range speakers (below 420 cps) are housed together in a separate corner cabinet, while two high-range speakers are located some distance apart from each other and from the listener in such a way as to diffuse the sound in a manner more closely resembling concert hall conditions. (G. J. Bleeksmas and J. J. Schurink, "A loudspeaker installation for high-fidelity reproduction in the home," IRE TRANS. ON AUDIO, September-October, 1957.)

Checking transistor circuits with a computer may lead to substantial reductions in the time required to design such circuits for switching applications. Certain combinations of transistor characteristics are known to be most detrimental to the proper performance of transistor switching circuits. These combinations are relatively hard to find in new transistors, and usually occur only after the device has been in operation for thousands of hours. A method of simulation has been developed which permits the designer, using a computer,

to observe in 15 to 20 minutes how a circuit containing up to ten transistors will operate at the end of the life of the transistors. The method is not a substitute for the preliminary design of circuits, but rather for the final bench setup, allowing the designer to obtain more accurate performance data and to shorten his over-all design time. (R. J. Domenico, "Simulation of transistor switching circuits on the IBM 704," IRE TRANS. ON ELECTRONIC COMPUTERS, December, 1957).

Synchronous and exalted-carrier detection techniques which are no strangers to other types of communications systems, are now being experimented with as a possible means of improving television reception in fringe areas. The synchronous detector lessens the problem of detecting a weak signal in noise by using the noisy received carrier to generate in the receiver a new and stronger noise-free carrier that is

locked in frequency and phase to it. This requires special receiver circuitry. In a conventional receiver a smaller degree of improvement can be obtained by shaping the IF response so as to emphasize (exalt) the received carrier with respect to its sidebands, achieving a noise-free effect approaching that of a synchronous detector. It still remains to be seen what price must be paid for these improvements in performance in terms of added receiver complexity and cost, and whether it will be worth it. With the radio astronomy issue of PROCEEDINGS still a fresh memory it might be noted in passing that the major external source of TV receiver noise is the radio emissions from the Milky Way and distant galaxies. (J. Avins, T. Brady, and F. Smith, "Synchronous and exalted-carrier detection in television receivers," IRE TRANS. ON BROADCAST AND TELEVISION RECEIVERS, February, 1958.)

Books

Stereophonic Sound by N. H. Crowhurst

Published (1957) by John F. Rider, Inc., 116 W. 14th St., N. Y. 11, N. Y. 115 pages+3 index pages +x pages. 61 figures. 5½×8½. \$2.25.

This instructive booklet is aimed at the technician and the advanced high-fidelity enthusiast who wishes to learn about stereophonic sound. The first chapter calls to the reader's attention the multitude of stereophonic listening experiences in everyday life and relates them to a simplified theory of hearing. The second chapter simply explains the generation and propagation of sound from one and more sources. The remainder of the book describes the various types of systems for recording and reproducing stereophonic sound in the home, the studio, and the theatre. The aims of the book are well met and it is recommended as "first course" for those who have not had previous technical experience with stereophony, or those who wish to learn about the latest thinking in this field.

B. B. BAUER
CBS Labs.
New York 22, N. Y.

Progress in Semiconductors, Volume Two, ed. by A. F. Gibson, P. Aigrain and R. E. Burgess

Published (1957) by John Wiley & Sons, Inc., 440 Fourth Ave., N. Y. 16, N. Y. 277 pages+2 index pages+vii pages. Illus. 9½×6½. \$10.50.

This second volume in the series entitled *Progress in Semiconductors* contains eight papers:

I. Semiconductor Alloys.

This paper by F. Herman, M. Glicksman and R. H. Parmenter reviews recent work on crystalline semiconductors whose atomic structure is characterized by a substantial degree of disorder. These materials are categorized as: lightly doped ordered crystals; crystals with missing or extra host atoms; heavily doped ordered crystals; mixed crys-

tals; crystals with random stacking; and crystals with randomly arranged host atoms. Many examples are cited to illustrate each of these categories. Methods for estimating one-electron energy levels are discussed. A review of methods for determining vibrational spectra of disordered crystals is included. Intrinsic and extrinsic optical properties of these systems are discussed. A final section is devoted to a discussion of the effects of alloying on the transport of charge and heat. Much use is made of the virtual crystal approximation throughout the entire paper. While this paper is highly condensed, reviewing seventy-eight papers from original literature in twenty-eight pages, it nevertheless summarizes the state of the art in a very satisfactory way.

II. Properties of III-V Compound Semiconductors.

F. A. Cunnell and E. W. Saker review the properties of nine compounds formed by combinations from the two groups of three, aluminum, gallium and indium, and phosphorus, arsenic and antimony. These compounds, all of which display the same diamond-like crystal structure as the Group IV elements, offer possibilities in the development of diodes and transistors suitable for high temperature operation. This follows from the property that the energy gap increases relatively more than the melting point, leading to a series of semiconductors with lower melting points for a given energy gap than the Group IV semiconductors. This group of materials covers a range of energy gaps from 0.17eV for InSb to several eV for AlP. Methods employed in the preparation of these materials are discussed together with techniques for purifying the components and compounds.

Although no detailed calculations have been carried out for the energy band scheme of any of the III-V compounds, speculations as to the possible general features of these energy bands based on qualitative argu-

ments and existing knowledge of the band structures of germanium and silicon are presented.

General properties of III-V compounds reviewed include: carrier effective masses; energy gaps and degeneracy; dependence of Hall constant and magnetoresistance effect on magnetic field strength; electron lattice mobility; low temperature measurements and impurity band conduction; carrier lifetime; and infrared absorption. Among the materials surveyed, the information is most extensive on the properties of indium antimonide although it is very sketchy even in the case of this compound.

This paper closes with a section reviewing known applications of the III-V compounds. The paper is an excellent summary of the state of the art. 86 papers from original literature in the field are reviewed.

III. Radiation Effects in Semiconductors.

J. H. Crawford, Jr., and J. W. Cleland review in this paper the results of fast particle bombardment experiments on a number of semiconducting systems. It is established that the dominant effect of this bombardment is the creation of lattice defects with their associated localized energy states. A brief discussion covers the mechanisms by which defects are created during bombardment, techniques for measuring the displacement energy, and the rate of defect formation during bombardment.

Apparent differences in the behavior of germanium and silicon under the influence of bombardment are discussed. Models which have been suggested to account for the complex energy level structures of irradiated semiconductors are reviewed.

Experimental indications of defect states are summarized for germanium, silicon, indium antimonide, and gallium antimonide. Effects of annealing of bombardment producing defects in germanium, silicon, and gallium antimonide are presented and discussed.

This paper concludes with a section discussing the effects of radiation on mobility, optical absorption, spectral dependence of photoconductivity, minority carrier phenomena, and magnetic susceptibility. The paper is relatively comprehensive, containing 68 references to original literature. It summarizes well the present state of this area pointing out weaknesses in existing theories.

IV. Lifetime of Free Electrons and Holes in Solids.

A. Rose outlines a method of analysis for computing lifetimes of free carriers in solids which is uniformly applicable to a wide range of problems. He considers the distribution of energy states which may be occupied by a carrier before it is captured by an opposite carrier, the population of these states, the capture cross-sections, the effects of thermal and kinetic processes, and defines lifetimes. The analysis is then applied in discussing the lifetimes when excited densities predominate and when thermal carrier densities predominate. A final brief section discusses the transition from semiconductors to insulators. This chapter is concise and well written, summarizing the subject in an interesting way.

V. The Production of High-Quality Germanium Single Crystals.

I. G. Cressell and J. A. Powell survey the available methods of crystal growth, discussing in particular the horizontal zone melt technique as applied to the production of germanium single crystals ranging in resistivity from the intrinsic resistivity to that normally used for transistors. Crystal imperfections including foreign atoms, dislocations, and vacant lattice sites and interstitial atoms are briefly discussed. This is followed by a section on crystal growth from the melt covering conditions which must be satisfied in growing single crystal germanium; the older vertical pulling methods, and the horizontal zone melt method. A separate section is incorporated further detailing the single crystal zone melt process. In addition to discussing this technique in detail, an apparatus developed for horizontal zone melt crystal growing is described and discussed.

A section is devoted to a discussion of resistivity variations, lifetime of minority carriers, and crystalline perfection. These factors determine the quality of the crystals grown.

The paper contains several photographs of etched crystals and reviews 65 papers from original literature. It is an excellent summary of the art.

VI. Impurities in Germanium.

W. C. Dunlap starts by reviewing the general properties resulting from the introduction of impurities into germanium. These include a discussion of segregation coefficients, solubility, diffusion coefficients, electrical effectiveness, ionization energy, impurity scattering, transport properties, photoconductivity, optical absorption, recombination and trapping, intrinsic properties, and interference effects of one impurity upon another. He next reviews methods for analyzing impurities in germanium including the use of radioactive tracers,

neutron activation analysis, mass spectrometry, chemical analysis and optical spectrography.

The next section reviews the work of Pfann, Burton, Hall, Thurmond, Struthers, Hodgkinson, Longine, Greene, and others on the segregation and solubility of impurities and rate growing. The following section discusses impurity diffusion and heat treatment. The author has done much work in this area. In addition to general considerations, he specifically reviews work in which copper and lithium are the impurities in germanium.

In his review of the electrical effects of impurities in germanium, Dunlap starts with the Bethe hydrogen model for impurity action. He reviews the experimentally determined ionization energies for Group III-V elements. The theory of Wannier orbitals for impurities in germanium is outlined. General methods for studying multiple levels are reviewed and this is followed by a review of Group II, double acceptor, elements and Group I, triple acceptor elements. Amphoteric (may be either donor or acceptor) impurity action in gold doped germanium is discussed. The other elements producing deep states in germanium are reviewed. A variety of applications of deep states in germanium studies are presented and discussed. Effects of neutral impurities in germanium such as carbon, silicon and tin are discussed.

This excellent paper closes with three brief sections on photoconductivity and absorption, recombination and trapping, and impurity interaction effects. 98 papers from original literature are reviewed.

Dunlap, in contrast with most authors who emphasize Group III and Group V impurities in germanium, attempts to discuss impurities on a broader basis seeking a more general understanding of the effects of impurities.

VII. High Electric Field Effects in Semiconductors.

This theoretical paper by J. B. Gunn starts with a derivation of mobility changes in a high electric field. The treatment is an elementary version of that given by Shockley and Conwell. This is followed by derivations and discussions of avalanche ionization, avalanche breakdown in a $p-n$ junction, avalanche injection and avalanche at a current constriction. Finally, Gunn reviews experimental results covering small quadratic changes in mobility, major variations of mobility, avalanche ionization and $p-n$ junction breakdown, light emission from an avalanche, avalanche injection, and the resistance of a current constriction.

This is one of the more interesting papers, reviewing less understood and newer properties of semiconductors. Many of the ideas discussed in this paper suggest new applications of semiconductors. 35 papers from original literature are reviewed.

VIII. Theories of Electroluminescence.

This paper by D. Curie reviews three types of phenomena: pure or intrinsic electroluminescence (Destriau effect); carrier injection electroluminescence; electrophotoluminescence (Gudden-Pohl effect) and other effects.

Under pure or intrinsic electroluminescence of phosphors are discussed the mechanism of electroluminescence, the excitation process, the kinetics of electroluminescence, the supply of electrons to the conduction band, the acceleration process, some conditions for good sensitivity, and electroluminescence of organic substances. Carrier-injection electroluminescence covers low field phenomena and field emission luminescence phenomena. Under electrophotoluminescence and other effects are the Gudden-Pohl effect, the quenching effect of electric fields on photoluminescence and the enhancing effect.

In this interesting review, covering 82 papers from the original literature, Curie has given an up-to-date summary of the work in progress in electroluminescence.

In summary, Volume II, *Progress in Semiconductors* is a welcome addition to the growing list of books emphasizing the importance and summarizing the results of recent work in solid state physics.

L. T. DEVORE
Stewart-Warner Electronics
Chicago 51, Ill.

The Ionosphere by Karl Rawer

Published (1957) by Frederic Ungar Publishing Co., 105 E. 24 St., N. Y. 10, N. Y. 190 pages+8 bibliography pages+4 index pages. 72 figures, 9 1/2 x 6 1/2. \$7.50.

The subject of the upper atmosphere in general and of the ionosphere in particular has long outgrown the state where it is only of interest to a few specialists in the field and undoubtedly will gain even more importance in the approaching space age. Nevertheless it is surprising to find only few systematic presentations in textbook form covering the entire subject. Rawer's book has been published to fill this gap. It describes in systematic form the regular and irregular behavior of the various ionospheric layers as deduced from echo soundings; it deals with the physical processes thought to be responsible for these layers and their variations; it explains how radio waves propagation is affected by the ionosphere and it outlines the various methods used by the prediction services for radio communication. Related subjects like the neutral upper atmosphere, aurora, airglow, geomagnetism, and meteors are treated to some extent.

The book is useful first of all for the reader who has little overall knowledge of the ionospheric literature and who is interested and willing to familiarize himself with the ionosphere as a new field whether he be a physicist, radio engineer, or radio amateur. But even the specialist will find this book handy for quick references and he will appreciate many details not easy to find in the literature. The book should not be looked at as a competition to S. K. Mitra's *The Upper Atmosphere* which is still a standard work on the subject. It is much smaller in volume, even smaller than the chapter on ionosphere in Mitra's book, and in general it is written in a much more condensed form touching some of the secondary problems only briefly. It, however, places more emphasis on the problems encountered in radio communication where the author is able to contribute his special experience. Although the original

German text shows up in the style the translation is done skillfully. The few mistakes I have found in the book are of very minor importance. All in all I think the book is a worthwhile investment for anyone seriously interested in the ionosphere.

WOLFGANG PFISTER
Air Force Cambridge
Research Center
Bedford, Mass.

Digital Computer Components and Circuits by R. K. Richards

Published (1957) by D. Van Nostrand Co., Inc., 257 Fourth Ave., N. Y. 10, N. Y. 503 pages + 7 index pages + vii pages. Illus. 9 1/2 x 6 1/4. \$10.75.

This is a companion book to Dr. Richards' previous work, *Arithmetic Operations in Digital Computers*, in which he emphasized the organization, logical design, and arithmetic operations involved in digital computers. This new book complements the first by providing information about the circuits and components which can be used to reduce these concepts to working machines.

In this new volume the author brings together into a systematic framework much of the information on digital computer circuits and components which has hitherto been widely scattered in various conference reports, journals, and papers. The broad coverage can perhaps best be illustrated by listing the chapter titles: 1. History and Introduction; 2. Diode Switching Circuits; 3. Vacuum Tube, Systems of Circuit Logic; 4. Transistor Systems of Circuit Logic; 5. Magnetic Core Systems of Circuit Logic; 6. Large Capacity Storage: Non-Magnetic Devices; 7. Storage on a Magnetic Surface; 8. Magnetic Core Storage; 9. Circuits and Tubes for Decimal Counting; 10. Miscellaneous Components and Circuits; and 11. Analog-to-Digital and Digital-to-Analog Converters.

The author emphasizes concepts and design philosophies rather than design details and the coverage is, therefore, almost entirely qualitative. As he notes in the preface, this appears to be desirable since the details of designs rapidly tend to become obsolete in this fast moving art. The reader is assumed to be familiar with electronic fundamentals but no detailed computer background or knowledge of the information contained in the first book is required. The book is intended primarily for use as a reference book for the specialist and as a means for the newcomer to the field to rapidly "get on board."

In general, the selection and organization of the material is excellent. The explanations are lucid and complete. Undoubtedly, some specialists will disagree with Dr. Richards on his selection of material and on the amount of space allocated to the various circuit techniques, but this is unavoidable in a book of this type. Although adequate bibliographies are included with each chapter, the reviewer feels that the value of the volume as a reference book would have been enhanced by a more thorough use of references to the bibliographies within the text material.

To the reviewer's knowledge, this is by far the most complete coverage of this subject in a single book up to the present time.

For this reason it should prove quite useful. It is highly recommended for engineers involved in digital computer circuit design.

W. B. CAGLE
Bell Telephone Labs.
Whippany, N. J.

Elektronenröhren by M. J. O. Strutt

Published (1957) by Springer-Verlag, Reich-
peitschauer 20, Berlin W. 35, Germany. 362 pages + 22
pages of bibliography + 7 index pages + xv pages.
456 figures. 7 x 10. 58.50 DM.

This German book reflects the prodigious work and the international background of its author who went to school in Java, studied in Munich, obtained his doctor's degree at Delft at the age of twenty-three, was department head at the Philips Laboratories in Eindhoven, has more than one hundred patents (sixty of them U.S.A. patents) and six books on multigrid tubes, uhf and vhf receivers, amplifiers, transistors, and special functions to his credit, and is now full professor at the Institute of Technology in Zurich.

Electron tubes, in the most general sense of the word, diodes, triodes, multigrid tubes, rectifier tubes, semiconductor diodes, transistors, photocells and photomultipliers, cathode ray tubes, storage tubes and TV pick-up tubes are the subject of this book. It is divided into three parts: electrophysics and technical fundamentals (105 pages, 119 figures); electron control with electromagnetic fields (179 pages, 234 figures); and data and properties of typical electron tubes (78 pages, 103 figures). The bibliography lists 654 references, including 119 publications by the author.

The first chapter describes basic properties of electrons, mass and charge, wave nature, and high-velocity phenomena. Chapter 2 is concerned with solid state physics, such as electrons and holes in metals, semiconductors, and insulators, electron emission, photoelectric effects, and emission of secondary electrons. Electromagnetic fields in high-vacuum tubes, and interelectrode capacitances are the subject of the third chapter. A chapter on conducting and insulating materials and on manufacturing techniques for electron tubes concludes the first part of the book.

The four chapters of the second part discuss (1) static characteristics of high-vacuum, gas-filled, and semiconductor diodes, (2) static and dynamic characteristics and properties of triodes and multigrid tubes and four-pole representation of tubes, (3) electron optics, including magnetic and electric lenses, and (4) tube noise.

Descriptions of various commercially available electron tubes for receiving and transmitting of radio and TV signals, and cathode ray tubes for a multitude of TV applications are given in the four chapters of the third part. Microwave tubes, such as klystrons, magnetrons, and travelling wave tubes are not covered.

The first three chapters provide excellent background material for the understanding of the physics of electron tubes and justify the subtitle of the book: *Volume III of a Text-book on Wireless Communications*. Reading on, one finds that the presentation becomes more and more advanced and that a

thorough knowledge of electromagnetic theory is needed to understand the second part which presents an advanced and modern treatment of the theory of electron flow in diodes and triodes based on the equation of motion of electrons and on Poisson's equation for plane and cylindrical boundaries. The author derives normalized tube characteristics which are independent of specific geometries or supply voltages. Of particular interest for the specialist are comparisons of theoretical and experimental tube data which show the possibilities and limitations of an analytical approach to tube design. A careful and detailed analysis expresses tube and transistor noise in terms of the equivalent noise resistance and noise figure. Here, as everywhere, the presentation benefits greatly from the author's thorough knowledge of the American literature in this field.

The last part is a short handbook of electron tubes (always excluding microwave tubes) with concise descriptions and extensive data of German and American tubes and transistors.

The book as a whole is essentially a modern and up-to-date encyclopedia of electron tubes with a wealth of factual information. Unfortunately, readability has at times been sacrificed to conciseness and completeness to the extent that much information is crowded into the captions of over 400 figures, which average a paragraph of fine-print legend. Furthermore, it is quite difficult to find source information on a particular statement because references to the bibliography are collected at the end of each section. These are the shortcomings of a book which otherwise represents a major contribution to the literature on electron tubes.

The particular value of the book lies in its completeness and in its analytical approach to electron tube phenomena. The book should be most helpful to specialists in electron tube research and development and to engineers and physicists who want to gain a deeper insight into the complex phenomena governing the control of electron flow in a vacuum or gas-filled tube. However students in electronics and communications may find this book quite advanced and fairly difficult to read.

W. H. VON AULOCK
Bell Tel. Labs.
Whippany, N. J.

Notes on Analog-Digital Conversion Techniques ed. by A. K. Susskind

Published (1957) by The Technology Press, M.I.T., Cambridge 39, Mass. 410 pages + viii pages. Illus. 9 x 6. \$10.00.

This text treats the field of analog-digital conversion techniques in three parts. In the first part, systems aspects of digital information processing that influence the specifications for analog-to-digital and digital-to-analog conversion devices are considered. To set the stage for this part of the discussion, the uses of digital information processing equipment requiring such converters are placed in three categories; namely, (a) data reduction systems, (b) programmed control systems, (c) control systems containing a digital computer. Following this, the implication of such matters as sampling, quan-

tizing, and codes (or digital number representations) on systems aspects are discussed.

In the second part of the text, the engineering analysis and evaluation of a variety of conversion devices is presented. After considering basic digital circuit building blocks, conversion or coding and decoding techniques and devices for electrical signals are presented. These devices are placed in several categories, such as coding and decoding, by intermediate conversion to a time interval, incremental phase shift decoders, decoding networks, comparison coders, coders using cascaded weighting stages, and coding tubes. The theory of operation of each of these categories is presented with several specific types of converters in each category being reviewed. In each instance the critical components in so far as converter accuracy capability is concerned are pinpointed and elaborated upon.

Coding and decoding techniques for translational and angular motion are then presented. These are placed in categories such as coding by intermediate conversion to voltage or time analog, incremental pattern devices, and coded pattern (disc coders, etc.) devices. Again the critical elements are singled out and analyzed.

The third part of the text is devoted to a case study based on development work done at the Servomechanism Laboratory of the M.I.T. Department of Electrical Engineering. Numerous practical aspects are, of course, presented here, and an opportunity for the further "jelling" of some of the techniques and concepts presented earlier is afforded to the reader new to the field.

As the authors have pointed out, the presentation in this text is aimed primarily at readers who have been away from formal academic work for some time and who have little previous knowledge of the field. Therefore, some background information is included, and an effort was made to develop methods of presentation which require a minimum of sophistication. The choice of subject matter was based primarily on what, in the opinion of the authors, was considered to be of greatest interest to the practicing engineers.

This text presents a well integrated treatment of the subject. Within the space limitations under which they were working, the coverage of the subject is reasonably comprehensive. This book may be regarded as a welcome addition to the growing body of literature in the field of computer control systems engineering, and is recommended for the bookshelf of workers in this field.

C. T. LEONDES
University of California
Los Angeles, Calif.

Scientific and Technical Translating and Other Aspects of the Language Problem by UNESCO

Published (1957) by the United Nations Educational, Scientific and Cultural Organization, N. Y., N. Y. 251 pages+24 pages of appendix+6 index pages+vi pages. Illus. 9½×6¼. \$4.00.

This volume is the third of the UNESCO series, *Documentation and Terminology of Science*. The two earlier volumes are valuable bibliographies of scientific and technical dictionaries and glossaries. Of this book it can be said: to paraphrase a well-known

expression, that it is too much and too late—too much, because most of it resembles a draft more than a finished work; too late, because major portions of it were written in 1953 if not earlier and they are thoroughly out of date.

The procedure adopted for the preparation of this book is referred to in the preface as a "successful experiment." This consisted of sending preliminary papers "drafted by the Secretariat" to three national editors, one in Italy, one in France, and one in the U. K. The editors circulated the preliminary papers in their own countries to people known to be interested in translating, then embodied the comments into reports. These reports were combined and sent out in mimeographed form "not only to most of the original contributors but also to additional persons in other countries." At this time copies reached the United States and were distributed, thanks to the energetic interposition of Mrs. Helen Brownson of the National Science Foundation. Of 219 persons listed in an appendix as having collaborated, 27 are from the United States, none from Russia.

The Secretariat and Dr. J. E. Holmstrom, who was apparently the editor although it is nowhere so stated, should be given credit for trying to please everyone. Conflicting views are quoted. Equal space is given to comments from recognized experts and to incompetents—it was apparently assumed that because a man had a reputation as a translator his comments on the teaching of foreign languages should have equal prominence with those from experienced teachers. Only rarely does the editor take a position in summarizing.

There are good sections in the book. Chapter I, "Quantitative Appraisal of the Problem," brings together the best statistical picture I have seen of the effect of Babel on scientific communication. The following conclusions are worth quoting: "... at least 50 per cent of scientific literature is in languages which more than half the world's scientists cannot read. Nearly two-thirds of engineering literature appears in English, but more than two-thirds of the world's professional engineers cannot read English and a still larger proportion of English-reading engineers cannot read scientific literature in other languages. In other words, leaving qualitative differences aside, the greater part of what is published is inaccessible to most of those who could otherwise benefit from it." When figures on the ability of scientists to read foreign languages are tabulated "the result is a little startling, for they imply that many more Russians than Germans can read scientific German, that twice as many Russians as Frenchmen can read scientific French, and that scientists able to read English total two-fifths as many in the U.S.S.R. as in the United States and the British Commonwealth put together." A diagram used as a frontispiece summarizes these statistics so effectively that it would be worth reproducing here.

The best chapter is the last, "Terminology and Lexicography," not merely because the reviewer, like a canoeist following a stream through a bog, was tired of the meanderings, the repetitions, the contradictions, and the apparent lack of forward

motion, but because one quickly feels that in this chapter Dr. Holmstrom is in familiar territory. This is a topic on which he has written and will write more, yet it is a little surprising that this chapter should have been included when a section on consecutive and simultaneous interpreting methods for international conferences had to be omitted in order to "keep the length of the report within limits." Typical is the fact that "Appendix 3, Bibliography of Books for Technical Language Study," complete with Universal Decimal Classification numbers, contains 50 per cent out-of-print items, if a check of the U. S. publications under the headings, French for English Readers and German for English Readers, is representative.

In short, we have here a mass of comments, opinions, and facts, all the materials for writing a good book two or three years ago.

W. N. LOCKE
Mass. Inst. of Technology
Cambridge 39, Mass.

RECENT BOOKS

- Brown, A. I., and Marco, S. M., *Introduction to Heat Transfer*, 3rd ed. McGraw-Hill Book Co., Inc., 330 W. 42 St. N. Y. 36, N. Y. \$6.75.
- Burstein, Herman, and Pollak, H. C., *Elements of Tape Recorder Circuits*. Greenback Library, Inc., 154 W. 14 St., N. Y. 11, N. Y. \$2.90, soft cover; \$5.00, hard cover.
- Ceramic Fabrication Processes*, ed. by W. D. Kingery. The Technology Press and John Wiley & Sons, Inc., 440 Fourth Ave., N. Y. 16, N. Y. \$9.50.
- Control Engineering Manual*, ed. by B. K. Ledgerwood and staff of Control Engineering. McGraw-Hill Book Co., Inc., 330 W. 42 St., N. Y. 36, N. Y. \$7.50.
- Corcoran, G. F., and Reed, H. R., *Introductory Electrical Engineering*. John Wiley & Sons, Inc., 440 Fourth Ave., N. Y. 16, N. Y. \$7.95.
- Elsevier's Dictionary of Electronics and Waveguides*. Compiled by W. E. Clason. In six languages: English/American, Dutch, French, German, Italian and Spanish. D. Van Nostrand Co., Inc., 120 Alexander St., Princeton, N. J. \$17.50.
- Information Theory Third London Symposium—1955*, ed. by Colin Cherry. Academic Press, Inc., 111 Fifth Ave., N. Y. 3, N. Y. \$11.50.
- Lang, D. G., *Marine Radar*. Pitman Publishing Corp., 2 W. 45 St., N. Y. 36, N. Y. \$4.75.
- Millman, Jacob, and Taub, Herbert, *Pulse and Digital Circuits*. McGraw-Hill Book Co., Inc., 330 W. 42 St., N. Y. 36, N. Y. \$12.50.
- Pinney, Edmund, *Ordinary Difference-Differential Equations*. Univ. of Calif. Press, Berkeley 4, Calif. \$5.00.
- Progress in Semiconductors—Volume One*, ed. by A. F. Gibson, P. Aigrain and R. E. Burgess. John Wiley & Sons, Inc., 440 Fourth Ave., N. Y. 16, N. Y. \$8.00.
- 1956 National Symposium on Vacuum Technology Transactions*, ed. by E. S. Perry and J. H. Durant. Pergamon Press, 122 E. 55 St., N. Y. 22, N. Y., \$12.50.

Abstracts of IRE Transactions

The following issues of "Transactions" have recently been published, and are now available from the Institute of Radio Engineers, Inc., 1 East 79th Street, New York 21, N. Y. at the following prices. The contents of each issue and, where available, abstracts of technical papers are given below.

Sponsoring Group	Publication	Group Members	IRE Members	Non-Members*
Aeronautical & Navigational Electronics	Vol. ANE-4, No. 4	\$1.95	\$2.90	\$5.85
Antennas & Propagation	Vol. AP-6, No. 1	3.85	5.80	11.55
Audio	Vol. AU-5, No. 5	0.70	1.05	2.10
Broadcast & TV Receivers	Vol. BTR-4, No. 1	0.80	1.20	2.40
Component Parts	Vol. CP-4, No. 4	1.60	2.40	4.80
Education	Vol. E-1, No. 1	1.10	1.65	3.30
Electronic Computers	Vol. EC-6, No. 4	1.20	1.80	3.60
Medical Electronics	PGME-9	1.60	2.40	4.80
Microwave Theory & Techniques	Vol. MTT-6, No. 1	2.65	3.95	7.95
Military Electronics	Vol. MIL-1, No. 2	0.55	0.85	1.65
Telemetry & Remote Control	Vol. TRC-3, No. 3	0.80	1.20	2.40

* Public libraries and colleges may purchase copies at IRE Member rates.

Aeronautical & Navigational Electronics

VOL. ANE-4, NO. 4,
DECEMBER, 1957

Albert A. Nims (p. 152)

Report on the Fourth Annual East Coast Conference on Aeronautical and Navigational Electronics (p. 153)

Notes from the Guest Editor—J. L. Dennis (p. 154)

The Design of Airborne Doppler Velocity Measuring Systems—F. B. Berger (p. 157)

The nature of Doppler velocity measurement is reviewed briefly. This is followed by a discussion of the basic requirements for obtaining a usable signal for practical systems, which include achieving requisite coherence, fulfilling certain signal-to-noise criteria, and maintaining known functional relationships between measured Doppler frequencies and aircraft velocity. Then, those factors peculiar to over-water operation of Doppler systems are discussed.

Techniques suitable for the design of systems that fulfill the various existing theoretical and practical requirements are considered. The various interrelated design considerations are grouped into five main categories: 1) choice of the number of beams to employ, 2) antenna stabilization, 3) type of antenna, 4) transmission-reception techniques, and 5) Doppler frequency measurement techniques. A summary of design considerations and the choices made in the cases of systems now declassified are contained in Tables I and III-VI.

Principles and Performance Analysis of Doppler Navigation Systems—W. R. Fried (p. 176)

The fundamental concepts of a Doppler navigation system are described. The theory of

operation, design considerations, performance characteristics, and limitations of a Doppler radar are discussed along with the basic principles and major characteristics of navigational computers and heading references. The over-all performance characteristics of a Doppler navigation system and their dependence on the various characteristics of its major components are analyzed. It is shown that the over-all system accuracy of a Doppler system is a function of the accuracies of all three major components of the system—the Doppler radar, the computer, and the heading reference. Thus, over-all system accuracy is shown to be no better than that of its weakest link. In most current systems, it is the heading reference error which swamps other errors in the system.

The performance capabilities of typical modern Doppler navigation systems are outlined. Such systems are shown to provide information on ground speed, drift angle, present position, and course and distance to destination. Complete Doppler navigation systems have been or are being built which will produce maximum (95 per cent probability) position errors of less than 1.5 per cent of distance traveled over land and average sea state (neglecting unknown water motion effects). The maximum position error over water of any sea state is likely to be less than 2 per cent of distance traveled. Over-all position errors in per cent of distance traveled tend to decrease with distance. Typical modern Doppler navigation systems, including computer and heading reference, should weigh less than 200 pounds, and will be in production well before 1959.

Current research and development effort on Doppler systems is concentrated along the lines of increased system accuracy, particularly over water, increased heading reference accuracy, decreased size and weight, and maximum system reliability.

Basic Design Considerations—Automatic Navigator AN/APN-67—M. A. Condie (p. 197)

Some of the considerations involved in the design of the Automatic Navigator, AN/APN-67, are presented along with a description and photographs of the equipment design selected. Characteristics of the Doppler signal are also described. The microwave part of the system utilizes two continuous-wave pencil beams generated by a klystron transmitter and a single fixed mounted, space duplexed antenna with offset antenna feeds. The Doppler data are stabilized by use of computing elements and vertical reference data. Advantages of this design relative to other alternatives are pointed out.

The AN/APN-81 Doppler Navigation System—F. A. McMahon (p. 202)

The AN/APN-81 is a self-contained Doppler navigation system which accurately determines ground speed and drift angle independently of ground aids. This paper explains the techniques employed in the measurement of ground speed and drift angle. The beam pattern is described and major system parameters are given. In block diagram form, the functions of the transmitter and receiver, the frequency tracker, and the wind computer are explained. Accuracies of measurement and some specific applications of the equipment are given.

The AN/ASN-9: A Compact, Minimum-Weight DR Navigational Computer—J. J. Insalaco and F. M. Kirr (p. 212)

This paper describes the AN/ASN-9—a miniaturized, dead-reckoning navigational computer. The design premises which allow its size reduction are explained; problem solution equations are given; and system functional diagrams are presented. Some of the techniques employed in achieving its small size are described, as are certain areas of its application.

Communications and Navigation Techniques of Interplanetary Travel—P. A. Casuccio (p. 216)

Radio and radar techniques will aid future space travelers in at least three major fields: navigation, communications, and collision warning. In space the basic limitation to any navigational or communications system is the achievable range. Present-day techniques are capable of providing point-to-point beamed coverage of the entire solar system, but they are inadequate for omnidirectional coverage even to the nearest planet. Sufficient advances in the state of the art by 1975 are foreseen to insure omnidirectional coverage within the orbit of Jupiter. Communications to the nearest stars appear impossible even with anticipated 1975 techniques, and radar warning systems against meteors appear impractical.

Correspondence (p. 224)

Abstracts of Papers Presented at the 1957 National Conference on Aeronautical Electronics (p. 225)

PGANE News (p. 227)

Contributors (p. 229)

Index to IRE Transactions on Aeronautical and Navigational Electronics—Volume ANE-4, 1957 (follows p. 230)

Antennas & Propagation

VOL. AP-6, NO. 1, JANUARY,
1958

News and Views (p. 1)

Contributions—An Analytic Study of Scattering by Thin Dielectric Rings—L. L. Philipson (p. 3)

An analysis of the scattering effect of a thin dielectric ring on an electromagnetic field is developed under two assumptions: the incident field is the free space field of the source, and the scattered field tends asymptotically to zero as the radial thickness of the ring approaches zero. When an integral equation of Barrar and Dolph, derived directly from Maxwell's equations, is employed, a formal expansion of the field in powers of the thickness is obtained, and then it is proved that the linear approximation obtained from it is indeed asymptotically equal to the total field. The sufficiency of this approximation is justified by experimental evidence. The far-zone pattern function of the ring is next obtained, and the resulting formulas are applied to the situation where the incident field is generated by a dipole antenna coaxial with the ring for which experimental comparisons are possible.

Theoretical Investigation of the Radiation Characteristics of a Quasi-Flush Mounted Cardioid-Pattern Antenna—H. E. Shanks (p. 8)

This paper determines the radiation characteristics of a semi-flush-mounted cardioid-pattern antenna on a theoretical basis. The antenna is similar to one described by Clapp in a report of the Electronic Research Laboratory of the University of California.

By judicious use of image theory in a radial transmission line formed by extending the antenna surfaces to infinity, the approximate fields of the principal polarization in the antenna are determined. If these fields are terminated in the aperture by a magnetic current sheet, the exterior radiation fields are obtained by integration over the aperture, according to the well-known equivalence theorem. Experimental patterns are given for comparison.

On the Propagation of Surface Waves Over an Infinite Grounded Ferrite Slab—R. L. Pease (p. 13)

A theoretical study is made of the propagation of surface waves along an infinite plane conductor coated with a layer of ferrite material subjected to a constant external magnetic field. For three directions of the external field, the electric and magnetic fields are computed for the separate media, and the relations between them arising from boundary conditions are expressed as transcendental equations. In the limiting case of small ferrite layer thickness (because of the loss problem of greatest physical interest), the fields and propagation constants may be expressed as simple closed forms.

Polarization Fading Over an Oblique Incidence Path—D. A. Hedlund and L. C. Edwards (p. 21)

This paper discusses the results of an investigation of polarization fading conducted over a one-hop F2 layer path from eastern Massachusetts approximately 1000 miles westward. Continuous recordings of pulse transmissions were made to study the instantaneous variations in amplitude of the vertically and horizontally polarized components of the received signal.

Results are presented which show a strong dependence between the amplitudes of the two components. Deep fades on one component were found to be accompanied by maxima of the other. A possible interpretation is presented which involves interference between the magneto-ionic components and leads to some interesting conclusions regarding their characteristics. Results are also included to illustrate the variations in these signal levels as the MUF is approached.

A Two-Dimensional Slotted Array—G. C. McCormick (p. 26)

A two-dimensional slotted array of which the radiating surface is one face of a parallel-plate region is discussed. This configuration differs from others previously reported in that a higher mode is utilized in the parallel-plate

region. The array is equivalent thereby to a number of slotted waveguides parallel to each other. The stability of the desired mode requires that the array amplitude be uniform laterally; however, it may have an arbitrary taper longitudinally. The radiation field of the array is discussed with particular regard to the generation of second-order beams. The performance of several such arrays is described.

Shunt and Notch-Fed HF Aircraft Antennas—R. L. Tanner (p. 35)

In the hf range radiation from aircraft must be accomplished by exciting radiating currents on the airframe itself. One method of exciting such currents is by shunts or notches which electrically penetrate the airframe.

The strength of coupling of such devices is analyzed and shown to be proportional to the square of the normal mode current which they interrupt.

A theory is developed and substantiated by experimental data, which enables the prediction of the impedance characteristics of such antennas. It is shown that these antennas are most effective when located in a region of high current concentration, and that the current concentration which occurs in the fillet area of swept-wing aircraft makes this area particularly favorable for their installation.

Shunt and notch antennas, when they can be used, have a number of structural advantages over cap-type antennas, and certain electrical advantages also. They require no special lightning protection and eliminate the need for special isolating devices. In general, they are capable of handling higher powers before encountering high-altitude voltage breakdown.

On the Fresnel Approximation—R. B. Barrar and C. H. Wilcox (p. 43)

The purpose of this paper is to show the power of the Sommerfeld expansion in computing Fresnel and near fields of antennas, a matter which has become of increasing importance in high resolution antennas. A connection is shown between the Fresnel and Fraunhofer approximations for radiation fields which is derived by using Sommerfeld's expansion of the field in inverse powers of radial distance. This expansion permits an estimate of the error incurred in using the Fresnel approximation. Higher-order corrections to the phase and amplitude portion of the Fresnel approximation are also exhibited. By way of illustrating the power of the Sommerfeld expansion of the fields in the Fresnel (intermediate) region of a radiation source, numerical calculations of amplitude, phase, and power patterns have been made for a finite line source of length D with an equiphase cosine-on-a-pedestal current distribution. It is found that the first five terms of the series are sufficient to obtain accurate results when $r \geq D^2/2\lambda$, as compared with the Fraunhofer approximation which is usually considered valid for $r \geq 2D^2/\lambda$. Non-Fraunhofer zone effects on the power pattern and phase front are discussed as a function of distance r and the type of current distribution.

The Approximate Parameters of Slot Lines and Their Complement—G. H. Owyang and T. T. Wu (p. 49)

An approximate attenuation coefficient due to ohmic loss is derived for both parallel slots and parallel strip lines. The capacitance per unit length, as well as the inductance per unit length of the lines are also obtained. The properties of a transmission line immersed in a lossless dielectric are thus completely determined. The attenuation coefficient due to lossy dielectric may be approximated by similar procedure.

Propagation of Electromagnetic Pulses Around the Earth—B. R. Levy and J. B. Keller (p. 56)

The propagation of electromagnetic pulses around the earth is investigated analytically. The pulses are assumed to be produced by a

vertical electric or magnetic dipole. The earth is treated as a homogeneous sphere of either finite or infinite conductivity and the atmosphere is assumed to be homogeneous. It is found that very short pulses become longer the further they propagate, in addition to diminishing in amplitude. The duration of a pulse which is initially a delta-function increases as θ^2 , where θ is the angle between source and receiver. The results are represented as products of several factors, which we call the amplitude factor, the pulse-shape factor, the time-dependent height-gain factors for the source and receiver, and the conductivity factor. Graphs of these factors and of the pulse shape for several cases are given.

Scattering of Electromagnetic Waves in Beyond-the-Horizon Radio Transmission—D. I. Paul (p. 61)

A formula is developed for the cross section in electromagnetic wave propagation beyond the horizon. The theory assumes that the propagation is the result of scattering by ellipsoidal shaped inhomogeneities in the atmosphere causing variations in the dielectric constant. The method of derivation is straightforward and gives a clear physical picture of the nature of the process. Simplifications concerning the geometric shape, size, and distribution of these inhomogeneities yield 1) the semi-empirical formula of Norton and 2) the formula derived by Gordon for large sized inhomogeneities. Thus, the physical implications contained in these formulas are clearly demonstrated.

Radio Echoes from Auroral Ionization Detected at Relatively Low Geomagnetic Latitudes—R. L. Leadabrand and A. M. Peterson (p. 65)

High-frequency radio echoes from ionization associated with the Aurora Borealis have been identified at Stanford University (geomagnetic latitude 43.75°). The echoes occur at ranges between 1400 km and 4700 km corresponding to reflection from ionization in the zone of maximum auroral occurrence located far to the north of Stanford. The formation of the ionization is attributed to the bombardment of the upper atmosphere by high-speed charged particles emitted from the sun. The echoes have great amplitudes with duration times between one second and one hour. Their appearance and disappearance is quite similar to the behavior of visual auroras; the occurrence of the echoes has been found to be related to geomagnetic disturbances. The heights of reflection appear to be between 100 km and 1200 km above the surface of the earth. The paths which the auroral signals travel over the relatively enormous distance from Stanford to the auroral zone (and back) are greatly influenced by the presence of the normal ionospheric layers. The echoes have been observed at ranges and bearings which indicate reflection from ionization at points along the auroral zone all the way from eastern Canada to Alaska.

The Geometry of Auroral Communications—R. L. Leadabrand and I. Yabroff (p. 80)

As early as 1939, radio amateurs found auroral ionization useful for communication purposes. Such ionization makes hf and vhf propagation possible over paths as great as several hundred kilometers when other more normal ionospheric propagation modes do not exist. The geometry of reflection is investigated for a variety of transmitter locations based upon the assumption of specular reflection from columnar ionization aligned with the earth's magnetic field lines. The results of the investigations outline the region of useful auroral ionization and the regions on the earth within which the auroral propagation is possible. The probability has been determined of obtaining propagation from a particular transmitter location to any receiver location within the region of propagation. These geometrical studies allow the communicator to predict the most

useful transmitter and receiver locations in utilizing auroral ionization for communication purposes. The studies also may suggest methods of minimizing the effects of auroral propagation when it is considered a detrimental propagating mode, for example, when it results in undesirable multipath effects.

A Statistical Model for Forward Scattering of Waves Off a Rough Surface—L. M. Spetner (p. 88)

Using methods of physical optics, a statistical description of the scattering of waves off a rough surface is obtained. The rough surface is assumed to consist of a large number of independent point scatterers which fluctuate randomly in vertical position and also disappear and appear at random. The surface is divided into cells so that no more than one scatterer can occupy a cell, and the events in any two different cells are independent of each other. The average scattered signal, the mean square fluctuation, and the time covariance of the fluctuating portion of the signal are computed in terms of the mean-square scatterer height, the grazing angle, the radiation wavelength, the decay time for disappearance of scatterers, the time autocorrelation of a scatterer height, and the *a priori* probability of finding a given cell occupied by a scatterer.

A Method for Evaluating Antennas—Judd Blass (p. 95)

An ideal figure of merit for a communications antenna is derived. This figure of merit is a measure of the time required to transmit a given message to an isotropic receiving antenna from a transmitter which uses the antenna under evaluation.

Wide-Angle Scanning with Microwave Double-Layer Pillboxes—Walter Rotman (p. 96)

The double-layer pillbox is a microwave parallel-plate system in which the image space and the object space relative to a two-dimensional internal reflector are electrically separated by a metal septum. The double-layer prevents the shadowing effects and impedance mismatch that result in a single-layer pillbox when energy from the reflector reenters the primary feed. It also allows correction of the optical aberrations of the system in the image space, the object space, or both.

The pillbox with semicircular reflector has wide-angle scanning properties. Its inherent spherical aberration can be reduced by such elements as dielectric lenses, geodesic contours, quasi point-source feeds, and auxiliary reflectors. These techniques have been applied to the construction of pillboxes whose wide-angle scanning properties and improved radiation characteristics substantiate the theory.

Surface-Wave Beacon Antennas—R. E. Plummer (p. 105)

Experimental results with center-fed corrugated and dielectric-clad spherical-cap antennas are presented and compared with the theory. The spherical surface waves supported by these structures give rise to radiation field patterns which are omnidirectional in the azimuth plane and which can be shaped in the elevation plane over a considerable range. The corrugated sphere provides vertical polarization while the dielectric sphere can support either polarization. The spherical caps are shown to have a natural application as low-drag beacon antennas when the surface geometries and sphere radii are appropriately adjusted.

Mechanical and Electrical Tolerances for Two-Dimensional Scanning Antenna Arrays—R. S. Elliott (p. 114)

An analysis is presented of the effect on radiation pattern of random errors in the construction of a two-dimensional scanning array. Translational and rotational errors in the positions of all elements are assumed together with errors in the electrical excitations themselves. Translational errors are found to cause the dominant effect. A formula connecting side

lobe level and errors is derived and representative curves are shown. For a given tolerance, pattern deterioration is found to decrease as the array is enlarged. For the same tolerance, pattern deterioration is less for a planar array of size L^2 than it is for a linear array of length L . Side lobe increase due to random errors does not depend on scan angle.

Fundamental Relations in the Design of a VLF Transmitting Antenna—H. A. Wheeler (p. 120)

For a VLF flat-top antenna much smaller than the radian sphere (a sphere whose radius is one radianlength), the effective height, effective area, and effective volume are defined. The required power factor of radiation proportionately determines the effective volume. For a specified power to be radiated, the effective height inversely determines the current and the effective area inversely determines the voltage. For a limited electric gradient on the overhead wires, the current requires a proportionate area of conductor surface. A corresponding total length of wire in the flat top is adequate if disposed for uniform distribution of charge and if spread out to realize the required effective area. These objectives are obtained more readily by some configurations, such as long parallel wires or concentric circles of wire. This study has been made for the U. S. Navy's high-power transmitter to be located in Maine, the first to radiate 1 megawatt continuously at 15 kc.

Fundamental Limitations of a Small VLF Antenna for Submarines—H. A. Wheeler (p. 123)

A submarine requires a small VLF antenna for reception while submerged. Since the propagation in sea water is nearly vertical (downward from the surface), the only operative types are horizontal dipoles, electric and magnetic. The electric dipole is coupled by conduction and the magnetic dipole by induction in a loop. The former has no resonance and nearly unlimited bandwidth, but fails when not submerged. The latter, by resonance, is able to present much greater interception area and available power. The magnetic interception area is determined by the size of the radome and by the radianlength or skin depth in sea water (2 meters at 15 kc). The radiation power factor, which is essential to bandwidth and efficiency, is influenced also by the size of the inductor and by the magnetic permeability of an iron core. Simple formulas illustrate these relations for the idealized spherical shape of radome, coil and core. Omnidirectivity in azimuth requires crossed coils in a two-phase circuit.

The Prolate Spheroidal Antenna: Current and Impedance—C. P. Wells (p. 125)

This paper studies the near field of the prolate spheroidal antenna. By expanding the components of the electromagnetic field in terms of the spheroidal functions, we determine the current distribution over the antenna and the impedance at the gap. We consider both center and off-center gaps for $kL=1, 1.49, 2, 3, 4$, where $k=2\pi/\lambda$, L is the semifocal length of the spheroid, and λ is the wavelength. The radiation resistance is calculated from the far field and found to be in excellent agreement with the resistance at the gap calculated from the near field.

An Application of Paragometrical Optics to the Design of a Microwave Mirror—L. Ronchi and G. Toraldo Di Francia (p. 129)

A microwave device is described which collimates the radiation from a point feed into a parallel beam. The instrument operates by both reflection and diffraction. The offense against the sine condition is corrected perfectly, so that no monochromatic aberration is present for a moderate field even at very high apertures. The expressions of the aberrations are worked out and a graph is given where one can read the maximum values of the aperture and field for a given tolerance. It seems that the device described may be useful for

radio astronomy and for rapid scanning.

End-Fire Echo Area of Long Thin Bodies—Leon Peters, Jr. (p. 133)

The echo area resulting from traveling waves excited on the surface of long, thin bodies is considered. A means of predicting this echo area on the basis of antenna theory is derived. Computed and measured values are compared for a long wire, an ogive, and a shorted polyrod.

Back-Scattering Cross Section of a Center-Loaded Cylindrical Antenna—Yueh-Ying Hu (p. 140)

A solution of the broadside back-scattering cross section, σ , of a center-loaded cylindrical antenna with any load impedance, Z_L , is obtained by a variational method through a four-terminal network approach. A simple formula for σ , in terms of Z_L and the parameters Z_{11} , Z_{12} , and Z_{22} associated with the antenna has been derived. The impedances Z_{11} , Z_{12} , and Z_{22} are independent of the load and they are determined by using the variational principle. Numerical results of the first order approximation are presented, and they are in good agreement with some measured results available in the literature.

Electromagnetic Diffraction by Dielectric Strips—D. C. Stickler (p. 148)

In this paper the scattering of a plane wave by a rectangular dielectric strip is calculated by approximating polarization currents in the strip. One advantage of the technique applied here is that no variational calculations are needed. Results of experimental investigation show good agreement with the predicted pattern.

Communication—A Line Source with Variable Polarization—J. N. Hines and J. Upson (p. 152)

Contributors (p. 154)

Audio

VOL. AU-5, NO. 5, SEPTEMBER-OCTOBER, 1957

PGA News (p. 113)

Principles of Loudspeaker Design and Operation—Joseph Chernof (p. 117)

The electrical and physical parameters which are of interest in loudspeaker design are discussed. The analysis of loudspeaker action on the basis of its analogy to a vibrating rigid disk is presented. The limitations of such an analysis are indicated. Electromechanical analogies are used to formulate an equivalent electromechanical circuit from which loudspeaker performance factors can be derived. Design criteria for commercial and "hi-fi" units are developed. Means of improving loudspeaker performance, particularly at low audio frequencies, are discussed.

A Loudspeaker Installation for High-Fidelity Reproduction in the Home—G. J. Bleekma and J. J. Schurink (p. 127)

For more than a quarter of a century the normal broadcast receiver has been equipped with a single loudspeaker fitted inside the cabinet. The introduction of sets with two separate speakers, each reproducing part of the frequency spectrum on the Philips "Bi-Ampli" principle, dates only from the last few years.

The installation described goes a big step further, the loudspeakers being entirely separated from the amplifying part; two low-note speakers are housed together in a special cabinet and two high-note speakers separately in their own boxes. The quality of reproduction has been remarkably improved in this way, which appears to full advantage with FM reception and the playback of gramophone records or tape recordings.

A Transistorized Decade Amplifier for Low-Level Audio-Frequency Applications—A. B. Bereskin (p. 138)

The amplifier described in this paper has an input resistance of approximately 400,000 ohms in the audio-frequency range. The output noise level is equivalent to 5 μ v at the input terminals with a response that is down 3 db at 5 cycles and at 100 kc. The amplifier has been designed in a self-contained package, the size of a frozen orange juice can, suitable for plugging into the standard banana plug terminals of a sensitive vacuum tube voltmeter. The design may be modified, with considerable reduction in volume, to incorporate the amplifier in a small package with a low signal source.

Contributors (p. 142)

Broadcast & TV Receivers

VOL. BTR-4, No. 1,
FEBRUARY, 1958

Meet Our New Chairman (p. 1)

Notice (p. 2)

Minutes of the Meeting of the Administrative Committee of the IRE Professional Group on Broadcast and Television Receivers (p. 3)

Design Considerations of a Developmental UHF Tuner Using an RF Amplifier—J. B. Quirk (p. 5)

In the development of a product it is desirable to obtain information concerning both its ultimate capabilities and its performance when incorporated in a practical unit. The development of a uhf tuner incorporating an rf amplifier was a project calculated to yield data concerning the practical application of a ceramic triode.

Calendar of Coming Events (p. 11)

Methods for Determining Amplitude-Modulation Rejection Performance of Frequency-Modulation Detectors—R. J. Schultz (p. 13)

This bulletin considers the problem of measuring AM rejection performance of FM detector systems. The requirements imposed on signal generating equipment and the methods of measurement used for determination of AM rejection are discussed. Four measuring methods are described: (1) center-frequency method, (2) oscilloscope method, (3) band-elimination filter method and (4) high-pass filter method. The oscilloscope method has been found most useful for design and the high-pass filter method the most useful meter method.

Synchronous and Exalted-Carrier Detection in Television Receivers—J. Avins, T. Brady and F. Smith (p. 15)

This paper describes the fringe-signal picture performance that can be obtained by generating a noise-free carrier in a television receiver. Quantitative data are given on the improvement possible with ideal synchronous detection. This improvement is shown to vary significantly depending upon whether the basis of reference chosen is (1) the normal IF response curve with the carrier 6 db down from the flat top or (2) a peaked response with the carrier at the peak. Both with synchronous and exalted-carrier detection, a further improvement in signal-to-noise ratio can be obtained by reducing the post-detection high-frequency video response. An experimental approach is followed because of the difficulty of analytically weighting the unequal contribution of various parts of the noise spectrum to the subjective degradation of the picture.

Deflection Distortions Contributed by the Principal Field of a Ring Deflection Yoke—R. B. Gethmann (p. 24)

In this paper equations for the magnetic field of the ring yoke are obtained as solutions of the Laplace differential equation. The paths of axial and para-axial rays through this field are then calculated for the principal field of the ring yoke. Three types of distortions are shown to be contributed by this field.

A special 110 degree tube having a very thin neck in the vicinity of the deflection yoke which permits translation of the deflection yoke with respect to the electron beam was used to obtain experimental verification of the computed distortions.

1957 Awards of the PGBTR (p. 35)

Component Parts

VOL. CP-4, No. 4,
DECEMBER, 1957

Information for Authors (p. 103)

PGCP Chapter Officers—1957-1958 (p.104)

Survey of Square-Loop Magnetic Materials—V. E. Legg (p. 106)

The magnetic and electrical properties of available square-loop materials are discussed for applications in cores for magnetic amplifiers, pulse modulators, and memory and switching coils. Among materials having high magnetic induction, oriented 50-50 nickel-iron is outstanding. Its pre-eminence for magnetic amplifier applications can be challenged only by new alloys such as Supermendur. Materials having lower saturation find application in varied fields; e.g., 4-79 Mo-permalloy in fast switching coils, and ferrites in memory arrays.

Electrical Properties of Epoxy Resins—C. F. Pitt, B. P. Barth, and B. E. Godard (p. 110)

Power factor, loss factor, dielectric constant, volume resistivity, surface resistance, and dielectric strength of epoxies, varying in viscosity and reactivity and cured with several types of hardeners, have been determined and form the basis for this report.

The effect of cure, temperature, and frequency on electrical properties also is presented. The importance of proper selection of resin, hardener, and resin/hardener ratio for optimum properties is emphasized. In most illustrations, the ratio of epoxy/hardener is used that exhibits optimum heat distortion. The heat distortion point of an epoxy system is shown to provide a good indication of the effect of temperature on power factor and dielectric constant.

Brief reference is made to a number of field applications of epoxy electrical insulation.

Recent Advances in Luminescence (Cathodoluminescence and Electroluminescence)—H. F. Ivey (p. 114)

Recent developments are reviewed in the field of cathodoluminescence and electroluminescence. Emphasis is placed on the applications of luminescence to electronics, although some attention also is given to simplified explanations of the phenomena involved. Included are discussions of transparent phosphor films for "flat" cathode-ray tubes and other purposes, solid-state image display devices, and solid-state radiation converters and amplifiers.

Progress in Cadmium Sulfide—L. L. Antes (p. 129)

Considerable progress has been made during the last two years in both the understanding and application of cadmium sulfide, which is an outstanding photoconductor material. Improved crystal growing techniques have resulted in large single crystals with more perfect crystal structure and higher purity. Further improvements in purity are sought by zone refining of cadmium and sulfur. Ultrasonic cutting methods have been applied successfully to shaping the crystals. High-temperature, high-pressure equipment has been used to grow crystals from the melt. P-type CdS crystals have been produced by heavy copper doping. Thin film techniques have been advanced. Surface volume studies of photoconductors have been made, which clarify certain surface deteriorations. Methods of producing ohmic and barrier electrodes have been

improved. All of these fundamental studies have contributed to an improvement in the efficiency, stability, and uniformity of elements used in devices such as photocells, gamma detectors, solar generators, and photorecifiers.

Lightweight Ceramic Materials as High-Frequency Dielectrics—J. L. Pentecost and P. E. Ritt (p. 133)

To eliminate some of the weight problems usually associated with ceramic dielectrics, lightweight (porous) ceramic materials have been developed which show excellent electrical properties at temperatures up to 800°C and a high strength-to-weight ratio. These materials generally are characterized by low-dielectric constant values, low loss, and a flat temperature vs dielectric constant relation.

Some suggested uses for lightweight ceramic materials are fillers for microwave devices, microwave lenses for high temperature use, and low-loss high-temperature insulators.

Two types of dielectric materials are discussed: 1) a Wollastonite foam, and 2) a 90 per cent aluminum oxide foam. The transverse strength of these foam materials was found to be approximately 400-450 psi, and this strength could be more than doubled in thin sections, by the application of dense ceramic coatings to the foam material.

The thermal expansion of these lightweight materials was 5-6 microinches per inch per °C, and the thermal conductivity was 5 to 7 × 10⁻⁴ cal/cm sec °C.

The dielectric constant of these foam materials was found to follow closely the Gladstone Dale relation:

$$\frac{\sqrt{K} - 1}{\rho} = C$$

where K = dielectric constant, ρ = bulk density, and C = constant for material; or by rearranging:

$$K = (1 + C\rho)^2.$$

The loss tangent of these materials generally was less than 0.002.

The forming of these foam materials is simple and requires only common metal working tools.

The availability of these materials in commercial quantities awaits the demand of the electronic applications, since the production techniques which have been developed are adequate for many types of materials.

Correction (p. 135)

Correspondence (p. 135)

Contributors (p. 137)

Index to IRE Transactions on Component Parts—Volume CP-4, 1957 (follows p. 138)

Education

VOL. E-1, No. 1, MARCH, 1958

An Editorial (p. 1)

College Recruiting—1958 (p. 2)

Job opportunities for engineering college graduates for 1958 is discussed. The survey includes information from a number of east coast electronic industries. In nearly every case, a reduction in the number of new employees is indicated. A lowering of the salary scale is not anticipated. Employers will emphasize quality. It is pointed out that the opportunities for employment may make a sudden reversal from the trend indicated due to a change in national defense planning. The data presented would support the view that the engineering college graduate for 1958 would not be sought after with the vigor of the past few years.

IRE Student Members (p. 3)

IRE Professional Group on Education—J. D. Ryder (p. 4)

The Crisis in Education—A. V. Loughren (p. 6)

This article concentrates on the problems throughout the educational system, but particularly in the fields of the sciences and engineering, created by the loss of faculty members to industry and the difficulty of attracting qualified replacements, and discusses some ideas for correcting them. Included in a discussion of incentives and rewards of a teaching career is a table showing the years of education and experience required for comparable positions in industry and teaching, as well as average salaries for these positions in a medium-sized corporation. There is also a suggestion of how a change in the tax laws would benefit the fund-raising campaigns of schools and universities.

The Vanishing Science and Engineering Teacher—A. W. Straiton (p. 8)

The extreme shortage in recent years of engineers and scientists with advanced degrees has caused a severe depletion of younger university teachers in these fields. The simultaneous increase in the number of technical students in universities has put an added load on the remaining faculty. While the larger student population promises to provide warm bodies to fill technical positions, there is a great danger that the quality of the product will deteriorate.

The Case for a Two-Year Graduate Degree—B. C. Boulton (p. 10)

In response to the need of industry, several of the leading engineering colleges are granting a Professional degree after two years of graduate work instead of the one year normally required for a Master's degree. The technical difficulty and complexity of industry's development programs tax unduly the training given for a Master's degree. More depth and breadth in such subjects as mathematics, advanced mechanics, thermodynamics, and electronics are required. Many capable men would be willing to devote two years to graduate work who are unwilling to spend the time necessary for a Ph.D. degree and hence content themselves with a Master's degree, thus handicapping themselves and industry.

Beyond Space and Time—J. A. Hannah (p. 12)

Outstanding national achievements to the development of which higher education has contributed substantially are cited, among them being 1) attainment of a high standard of living based on scientific and technological accomplishments, 2) a high degree of social mobility, and 3) a high degree of political stability. Difficulties confronting colleges and universities in meeting greatly increased demands are examined in the light of developments which have deprived them of the priority of support they once enjoyed. It is contended that higher education must be adequately supported at whatever cost if immediate and future demands are to be satisfied.

Incentives Leading Industry into Cooperation with Education—L. C. Van Atta (p. 16)

The success of an industrial enterprise is largely determined by the quality of its technical and management personnel and its long-range research program. Industry depends upon education to supply creative people and new ideas. Education depends upon the community to which industry is perhaps the most important element, to voice its educational needs and to provide support. The personnel and equipment of industrial laboratories can be used both in the company and in the schools to stimulate teachers and students and to acquaint them with the content and requirements of modern industrial technology. Financial aid from industry can support new educational projects pending budgetary acceptance.

The Role of the Technical Institute in the Next Decade—H. R. Beatty (p. 20)

During the next ten years, technical institute education in the United States should be

expanded ten times while other forms of higher education are doubled. Only in this way will we be able to get efficient utilization of our scientists and engineers. The many developments in science and technology that will take place in the next decade will call for a greatly expanded technical manpower team, and the largest potential source of supply is the manpower pool composed of individuals with aptitudes that qualify them to become engineering technicians.

We can produce twice as many engineering technicians as engineers for the invested educational dollar, for the engineering technician is graduated in two years while the engineer needs four years.

Through better acceptance of the engineering technician by industry and the engineering profession, this much needed expansion is bound to be realized.

Technicians as an Aid to Engineers—N. V. Petrou (p. 26)

The word "technician" embraces a broad spectrum of skilled workers. This paper is concerned with a few specialized groups who are defined in detail for further study. The examination includes their background and training, the organization for administration and supervision of their work, where they come from, and what their opportunities presently seem to be.

The paper describes certain factors which determine how many technicians may be utilized effectively and the experienced trends of one organization. It concludes with a short discussion of the use of the title "engineer" and the problem of technician job stability.

Contributors (p. 31)

Electronic Computers

VOL. EC-6, No. 4,

DECEMBER, 1957

The Synthesis and Analysis of Digital Systems by Boolean Matrices—J. O. Campeau (p. 231)

In this paper methods are described by which Boolean matrices can be used to synthesize digital systems. The matrices offer a means by which the design of such systems can be systematized much in the same way as do matrix methods when applied to electrical circuit design. They also present a means by which the problems of optimum logical design and programming can be approached.

Simulation of Transistor Switching Circuits on the IBM 704—R. J. Domenico (p. 242)

When the configuration of a circuit and the equivalent representations of the transistors are known, a computer program can be written to yield the performance of the circuit and the mean values of the circuit parameters. Non-linearity of the transistors is accounted for by piece-wise linearization of an equivalent circuit. Rules of interconnection have been devised to combine this procedure efficiently with the manipulation of the matrix equations that define the linear external circuitry. The general method can be extended to combinations of basic circuits.

An Optimum Character Recognition System Using Decision Functions—C. K. Chow (p. 247)

The character recognition problem, usually resulting from characters being corrupted by printing deterioration and/or inherent noise of the devices, is considered from the viewpoint of statistical decision theory. The optimization consists of minimizing the expected risk for a weight function which is preassigned to measure the consequences of system decisions. As an alternative, minimization of the error rate for a given rejection rate is used as the criterion. The optimum recognition is thus obtained.

The optimum system consists of a conditional-probability densities computer; character channels, one for each character; a rejection channel; and a comparison network. Its precise structure and ultimate performance depend essentially upon the signals and noise structure.

Explicit examples for an additive Gaussian noise and a "cosine" noise are presented. Finally, an error-free recognition system and a possible criterion to measure the character style and deterioration are presented.

An Analysis of Certain Errors in Electronic Differential Analyzers—I—Bandwidth Limitations—P. C. Dow, Jr. (p. 255)

When a differential analyzer or analog computer is set up to solve a given equation, certain errors are introduced into the solution because the components of the computer are not perfect. Stated another way, the computer produces the solution to an equation, called the "machine equation," which differs from the given equation. In this paper the computer imperfections considered are 1) operational amplifier frequency response, 2) capacitor leakage resistance, and 3) stray capacitance in summing and integrating amplifier circuits. It is shown that when the given equation is a system of one or more linear differential equations with constant coefficients, the machine equation can be expressed approximately as an equation of the same degree as the given equation and with constant coefficients which are functions of the coefficients of the given equation and of the computer imperfections.

Synthesis of Vector Networks—R. E. Horn and V. G. Fauque (p. 261)

The convenience of vector notation in formulating physical geometrical problems results principally because the significance of the problem can be isolated from the analysis used in its solution. When analog computer techniques are employed in problems of this nature, the advantages of the vector methods frequently are lost because the computer inherently is more adaptable to solving problems described in the algebraic field of real numbers rather than in a vector space, and vector equations must be reduced to their scalar counterparts before a network for solving the equations may be synthesized. To facilitate treatment of problems of this type, a method is presented for synthesizing networks directly from the vector notation. This method will simplify synthesis and analysis of the networks by drawing a closer analogy between the mathematics and the electronics.

The application of transformations and operators represents two areas in which the pertinent aspects of the method can be illustrated. This is accomplished by presenting first the basic mathematical background, followed by the network aspects of the problem, and finally, by the illustrative examples. The more extensive problems usually encountered, for example, in airborne fire-control systems, then may be synthesized by proper application of the elementary "vector networks."

Switching Functions of Three Variables—D. W. Davies (p. 265)

A switching function is a function of variables which take only the values 0 and 1, and which takes only these values itself. There are 256 different switching functions of three variables, but only 218 of these really depend on all three variables.

A switching function of three variables can be expressed in terms of switching functions of two variables. For example

$$F_1\{F_2[A, F_3(B, C)], F_4(B, C)\}$$

can be shown to represent any function of A, B, and C if $F_1F_2F_3$ and F_4 are suitably chosen switching functions.

The problem solved is: for each switching function of three variables, what is the least

number of switching functions of two variables required to express it?

This problem leads to a discussion of the symmetry of switching functions. Expressions which, like the one above, can represent any switching function of three variables are investigated. Expressions which, by permutation of variables, can represent any switching function of three variables are also determined.

The investigation is done by means of "logical diagrams," which give a better intuitive understanding than the functional expressions.

Analysis of Sequential Machines—D. D. Aufenkamp and F. E. Hohn (p. 276)

This paper begins with Mealy's model of a sequential machine and introduces a "connection matrix" which describes the machine completely. The "equivalence" of states of such a machine may be analyzed systematically by an iterative technique, the validity of which is rigorously established. Once equivalence is completely analyzed, it is a simple matter to write the connection matrix for the simplest equivalent machine. The process is not difficult to execute, even in complex cases, and could be programmed for a computer.

Correspondence (p. 285)

Contributors (p. 288)

PGEC News (p. 289)

Reviews of Current Literature (p. 291)

Index to IRE Transactions on Electronic Computers—Volume EC-6, 1957 (follows p. 308)

Medical Electronics

PGME-9, DECEMBER, 1957

(Symposium on Present Status of Heart Sound Production and Recording)

History and Present Status of Phonocardiography—H. B. Sprague (p. 2)

Phonocardiography originated in an attempt to time the occurrence of heart sounds in the cardiac cycle in relation to the mechanical activity of the heart, as recorded in the apex beat or in arterial pulsations.

The method evolved from an era when the observer manually inserted a signal in a pulse tracing at the time he heard the sounds. Later, this was done by mechanical synchronous record, then by an electric signal produced by a telephone pickup which stimulated a frog muscle to contract, then by direct recording through a capillary electrometer, or string galvanometer, and finally by electron tube amplification. Low-inertia capsule and mirror with photographic recording were also used, as well as other ingenious variations.

Present day phonocardiography has developed mainly through improved instrumentation with low-noise level amplifiers and satisfactory filters. Spectral phonocardiography is the most important advance.

The value of phonocardiography in clinical work lies in its ability to record for objective analysis the transient sounds and murmurs to which the hearing mechanism of different observers adds or subtracts subjective variants. It has been most useful in timing and explaining heart sounds having abnormal components—split sounds, atrial sounds, opening snaps, and gallop rhythms. It is also valuable in the study of certain murmurs, particularly in mitral disease and congenital heart disease. It has contributed to teaching and has been a useful diagnostic aid prior to cardiac surgery.

Physiological Auscultatory Correlations: Heart Sounds and Pressure Pulses—D. G. Greene (p. 4)

Our knowledge of the cause of sounds arising in the heart has depended on indirect evidence of events of the cardiac cycle in man and direct observations made in other animals. The accessibility of the human heart for study in this era of cardiac surgery now permits the direct observation made in animals to be repeated in

man and the indirect correlations to be confirmed.

Discussion of Session I-A (p. 6)

Does Cavitation Contribute to Cardiovascular Sounds?—S. A. Talbot and S. H. Boyer (p. 8)

The Genesis of Musical Murmurs—V. A. McKusick (p. 11)

Transients in Heart Sounds and Murmurs—Simon Rodbard (p. 12)

A new approach to the analysis of heart sounds and murmurs has been developed. These acoustic phenomena are considered to be generated by a series of transient sounds which, because of the long persistence of the low-frequency components of the sounds, tend ordinarily to fuse into a single sound. The separate events such as valve closures which produce discrete clicks therefore tend to fuse, and time discrimination of these important events is lost. An apparatus which filters out the low frequencies has been developed. The remaining high-frequency, short duration waves can thereby be displayed as a series of separate events, each representing closure or opening of a valve. Several records obtained with this system are shown, and the potential value of this mode of analysis is discussed.

Discussed of Session I-B (p. 15)

Quantitative Auscultation of Heart Sounds with Internal Calibration—E. Lepschkin and D. Larcou (p. 16)

Absolute vs Acoustic Standardization in Electrosthethography and the Need for Studying Cardiac Vibrations as Transients—F. L. Dunn (p. 17)

The marked variations in the audiograms of the individuals and the wide variation in frequency response of different flexible stethoscopes preclude the possibility of any widespread system of standardization. Phonocardiography has well recognized teaching and clinical value but is limited in usefulness as a clinical tool. Electrosthethography eliminates the use of auditory recordings and is a direct measure of vibrations and can be easily calibrated in absolute, *i. e.*, cgs units. The patterns produced have a gross resemblance to phonocardiographic patterns but provide measurable frequency and amplitude data.

The many factors which affect heart vibrations together with the numerous types of artefacts that can occur suggest the electrosthethograms should not be studied according to the techniques developed from electrocardiography but should be done with long records, multifrequency channels, and calibrated amplifiers. This method is further improved by studying the vibrations as transients on a cv scope with locked sweep and provisions for recording of selected single cycles.

Newer Studies of Selective Phonocardiography Including a New Method for the Identification of the Frequency Range of Extra Sounds—A. A. Luisada, C. Aravanis, O. M. Haring, C. K. Liu, and C. Friedland (p. 19)

Problems dealing with the registration of either apical or basal diastolic murmurs of poor magnitude are discussed. Current methods of phonocardiography are reviewed.

Eight normal subjects and thirty abnormal cases were studied by means of a variable band-pass filter with additional amplification. The various frequencies of the cardiac murmurs were analyzed. A band between 60 and 110 vibrations per second was found adequate for magnifying and recording murmurs caused by mitral stenosis. A band between 150 and 200 was found adequate for magnifying and recording murmurs caused by aortic defects or mitral insufficiency.

A routine method of study of cardiac murmurs, called "selective phonocardiography," is outlined. It is based on the use of the two above bands in addition to "stethoscopic" phonocardiograms. Incorporation of filters in

the case of the phonocardiograph is recommended.

A new method of study of the frequency of extra sounds is described. Preliminary observations are reported.

A new technique of intracardiac(ic) phonocardiography during routine catheterization is described. Preliminary studies in animals are reported.

Discussion of Session II-A (p. 22)

Part I—Phonocatheters: Their Design and Application—J. D. Wallace, J. R. Brown, Jr., D. H. Lewis, and G. W. Deitz (p. 25)

A miniature cylindrical barium titanate tubular element has been designed as an acoustic pickup and placed at the distal end of a specially designed catheter. The catheter is, in fact, an extension of the general design technique used to evolve underwater sound transducers used in antisubmarine warfare. Catheters have been designed in both single- and double-lumen types, with provisions in the latter case for the usual practice of heart catheterization simultaneously with the phono work. Details of the response of the catheters and performance of the experimental system used are given. Sound spectrograms which plot time as the abscissa, frequency as the ordinate, and amplitude as the density have been made, as well as conventional photographic recording galvanometer records. Preliminary experimentation was carried out in dogs where both left and right catheterizations are cited.

Part II—Intracardiac Phonocardiography—D. H. Lewis, G. W. Deitz, J. D. Wallace, and J. R. Brown, Jr. (p. 31)

Using specially designed catheters and amplifying equipment, studies of intracardiac sounds have been carried out in man at the time of cardiac catheterization. The catheters, either single- or double-lumen, are passed into the lesser circulation under fluorescent guidance. The first and second heart sounds are heard in the heart and in the great vessels leading to and from the heart. The first sound is loudest in the ventricle and the second sound is loudest in the pulmonary artery. In some cases a third heart sound has been detected. In all cases with atrial contractions, a fourth sound is detected and is loudest in the atrium. With atrial fibrillation no fourth sound is heard.

Even when no murmurs are heard on the chest or in the heart, there is routinely a mid-systolic murmur in the pulmonary artery. In the presence of disease, abnormal murmurs are heard inside the heart. In certain types of congenital heart disease the localization of the murmur is of help in the diagnosis. Records are shown to illustrate that this technique is capable of localizing heart sounds and murmurs to an extent not heretofore obtainable.

High-Sensitivity Capacitance Pickup for Heart Sounds and Murmurs—D. Groom and Y. T. Sihvonen (p. 35)

Exploration of heart murmur frequencies requires a pickup and associated electronics having great sensitivity and a wide range. Such a system, employing a capacitance principle, has been applied to reproduction of sounds from the precordium. The pickup is of the direct contact type, is relatively insensitive to extraneous noise, and is capable of recording murmurs of extremely low intensity.

Evaluation of the Spectral Phonocardiographic Analysis—G. N. Webb and T. T. Chen (p. 41)

Heart sounds can be divided into three classes: short duration pulses (first and second heart sounds); broad-band long duration noise (murmur); and long duration sounds having distinct harmonic pattern (musical murmurs). The characteristics of the analysis of these classes are illustrated, and the timing, duration, and filtering artifacts are discussed. A comparison between phase and amplitude filtering is given. Application of this research instru-

ment to clinical size and cost is considered.

Instrumentation Problems in a High-Frequency Heart Sound Analyzer—Wilson Greatbatch (p. 44)

It is accepted generally in medical practice that the low-frequency vibrations (up to 600 cps) of heart sounds and murmurs contain virtually all the available information. Newer concepts have been proposed that these signals actually consist of irregularly occurring transients which comprise the important information regarding heart action. These transients can be analyzed by recording the frequencies above 1000 cps. The level of these signals is subaudible and in some cases is below the noise level of the usual electronic amplifier.

A preliminary model of such a heart sound analyzer which has been built and tested reveals the existence of vibrations in the range mentioned with amplitudes less than 1 per cent of those in the lower frequency ranges. Instrumentation aspects of this are discussed. Limitations imposed by lack of suitable microphones are mentioned and specifications for such a microphone are suggested. Available variable cutoff frequency filters have the inherent capability of introducing artifactual signals not present in the original heart sound. A specially designed filter, free of such artifact, is described.

Discussion of Session II-B (p. 48)

Evening Panel Discussion (p. 49)

Standardization of Phonocardiography—Edgar Mannheim (p. 54)

Standardization of Phonocardiography: Efforts in the Netherlands—D. H. Bekkering and J. Weber (p. 55)

Microwave Theory & Techniques

VOL. MTT-6, NO. 1, JANUARY, 1958

Clarence Lester Hogan (p. 2)

The Pace of Modern Technology (p. 3)

Foreword (p. 4)

The Status of Microwave Applications of Ferrites and Semiconductors—Benjamin Lax (p. 5)

The recent developments in the field of ferrite devices are reviewed. Emphasis is placed on the extension of nonreciprocal devices to lower microwave frequencies and high powers. The design considerations and achievements of broad banding also are covered. Fundamental principles leading to the applications of nonlinear properties of ferrites are described briefly. Preliminary experimental accomplishments in the construction of frequency doublers, mixers, and ferromagnetic resonance amplifiers are summarized. The possible role of the new ferrimagnetic garnet material is indicated. Although no significant new semiconductor devices have been developed at microwave frequencies, possibilities are considered for doing this with use of cyclotron resonance and spin resonance phenomena and their related properties in semiconductors.

Nonreciprocal Electromagnetic Wave Propagation in Ionized Gaseous Media—L. Goldstein (p. 19)

The nonreciprocal propagation of electromagnetic waves in ionized gaseous media is discussed, and experimental observations are reported in this paper. The classical Faraday experiment in the optics of anisotropic media has suggested an analogous phenomenon at microwave frequencies. The anisotropic behavior of the free electron gas which is immersed in a magnetic field and subjected to an incident electromagnetic wave is determined. Guided microwave experiments were performed which confirm the theoretical predictions of nonreciprocal wave propagation in such ionized gases.

The Three-Level Solid-State Maser—H. E. D. Scovil (p. 29)

This article gives an introduction to amplification by solid-state maser techniques. Emphasis is placed on the three-level solid-state maser. The relevant physical properties of paramagnetic salts are discussed. The basis of the three-level excitation method is reviewed. Some design considerations are given. The design and performance characteristics of a particular device are mentioned.

Nonmechanical Beam Steering by Scattering from Ferrites—M. S. Wheeler (p. 38)

A small aperture radiating circularly polarized energy is loaded with a spherical ferrite to produce an electronic beam directing system. The ferrite is immersed in a static magnetic field which is in general at an oblique angle with the undeflected direction of radiation. It is shown that radiation is principally in the direction of the magnetic field when the polarization is in the negative sense. From symmetry this allows beam deflection with two degrees of freedom.

To consider an application for such a device, it is proposed that this deflection system be used in conical scan. A mechanization is shown which solves the problem in principle, but it is not competitive with present mechanical scanners from the point of view of side lobes, etc.

A Ferrite Boundary-Value Problem in a Rectangular Waveguide—C. B. Sharpe and D. S. Heim (p. 42)

A solution is obtained for the electric field at the air-ferrite interface ($z=0$) in a rectangular waveguide filled with ferrite in the semi-infinite half ($z>0$) and magnetized in the direction of the electric field. The field is expressed in terms of a Neumann series obtained by iteration of a singular integral equation which satisfies the boundary conditions at the interface. The equivalent circuit for the junction is also presented.

Some Techniques of Microwave Generation and Amplification Using Electron Spin States in Solids—D. I. Bolef and P. F. Chester (p. 47)

Possible modes of operation of two-level solid state masers utilizing the techniques of population inversion used in nuclear magnetic resonance are described. Methods of continuous operation of two-level masers and their usefulness as microwave generators are discussed.

A Microwave Ferrite Frequency Separator—Harold Rapaport (p. 53)

When multiple filter groups are interconnected for operation out of a single source, interaction effects between filters can occur. Frequently, unless special precautions are taken, the filters may interact to such an extent that severe deterioration in performance may result. Introduction of the gyrator by Tellegen and the subsequent microwave realization of the circulator by Hogan, Rowen, and others provide new possibilities for design of channel-branching circuits and frequency-spectrum partition arrays.

The nature of the frequency separation problem is reviewed, and the application of the ferrite circulator to effect channel branching is considered in detail. Several specific multi-channel systems comprising various circulator filter and one-way line filter arrays are presented and their relative merits examined.

A 4-port (3-channel) experimental prototype separator system consisting of a Faraday rotation type of circulator and maximally flat band-pass waveguide filters is described. A quantitative theory of operation of the prototype is developed. Experimental data and performance curves are given. These data show close agreement with results predicted by the theory.

Ferrite-Loaded, Circularly Polarized Microwave Cavity Filters—W. L. Whirry and C. E. Nelson (p. 59)

Circularly polarized cavities have made possible a group of compact, high- Q , microwave waveguide filters having useful directional properties. When these cavity filters are ferrite loaded, frequency sensitive circulators result and magnetic tuning becomes possible. This paper presents several new three- and four-port ferrite-loaded filters, some with 3-db waveguide couplers, which can be used as tunable band-pass filters, tunable band-rejection filters, or as passive, selective duplexers. As duplexers, they can be operated at a fixed frequency or can be magnetically tuned over a one to five per cent frequency range at X band depending upon the allowable loss. Experimental loss, bandwidth, isolation, and tuning data are presented. Temperature stability and power handling capacity are also discussed.

Resonant Properties of Nonreciprocal Ring Circuits—F. J. Tischer (p. 66)

The ring circuit investigated consists of a resonant ring guide coupled to a main guide. The properties can be described by the equations for the waves in the ring guide resulting from excitation in the main guide. The influence of nonreciprocity on the properties is investigated under conditions of varying coupling. The representation of the ring waves by the poles and zeros is chosen to permit interpretation of the results under the large variety of operational conditions with respect to coupling and nonreciprocity. The application for measuring the material constants of ferrites is discussed.

Exact Solution for a Gyromagnetic Sample and Measurements on a Ferrite—H. E. Bussey and L. A. Steinert (p. 72)

An outline of an exact solution for a gyromagnetic rod centered in a right circular cylindrical cavity resonator is given. This solution is applied in evaluating dielectric and tensor-magnetic measurements on a well-known ferrite. Complex frequencies and constitutive parameters are introduced and the solution is expanded in series to obtain a convenient calculational scheme. Comparisons are made of exact and perturbation calculations of results from a small and a large sample. The effect of insufficient symmetry of the cavity is discussed and the condition for sufficient symmetry is given. The g value of electrons was 2.02.

Resonance Measurements on Nickel-Cobalt Ferrites as a Function of Temperature and on Nickel Ferrite-Aluminates—J. E. Pippin and C. L. Hogan (p. 77)

The variation of line width (ΔH) and effective g factor (g_{eff}) with cobalt content and with temperature is studied in a series of ferrites of composition $Ni_{1-\alpha}Co_{\alpha}Mn_{0.02}Fe_{1.9}O_{4\pm}$. Here α lies between 0 and 0.09; temperatures range from 20°C to 240°C. A minimum in ΔH is observed at $\alpha=0.027$; g_{eff} decreases with increasing α . The temperature dependence of each is qualitatively that which would be expected on the basis of the temperature dependence of the anisotropy of the mixed ferrite. Above room temperature ΔH and g_{eff} increase or decrease, depending on the cobalt content. It is also shown that the shape of the resonance line is determined by the sign of the anisotropy constant. For negative K_1 the line is steeper on the low-field side of resonance—for positive K_1 it is steeper on the high-field side.

Resonance data are presented on several nickel-cobalt ferrite-aluminates, of composition $Ni_{1-\alpha}Co_{\alpha}Mn_{0.02}Fe_{2-t}Al_tO_{4\pm}$, with α varying from 0 to 0.025 for $t=0.3, 0.4, 0.5, \text{ and } 0.6$. The reduction of ΔH and g_{eff} expected from anisotropy considerations is observed.

Ferrimagnetic Resonance in Some Polycrystalline Rare Earth Garnets—G. P. Rodrigue, J. E. Pippin, W. P. Wolf, and C. L. Hogan (p. 83)

Ferrimagnetic resonance measurements have been carried out on a series of polycrystalline garnets of composition $5Fe_2O_3 \cdot 3M_2O_3$

with $M=Y$, Sm, Gd, Dy, Ho, Er, and Yb. These measurements were made over a temperature range from 20°C to the Curie points (approximately 280°C). The variations of line widths and effective g values over this temperature range are reported. Y, Yb, and Sm garnets have g values of approximately 2.0 at room temperature while those of Dy, Ho, and Er are appreciably less than 2.0. High-density yttrium garnet has a line width of approximately 50 oersteds at room temperature; line widths of other members of this series were found to vary from 400 to greater than 3000 oersteds. The effective g value and line width of the gadolinium garnet tend to very high values as its compensation point (17°C) is approached. The narrow line width of the yttrium garnet is found to depend strongly on the density of the sample. When the density decreases from 96 per cent to approximately 92 per cent of the theoretical value, the line width increases from 50 to about 150 oersteds. Several technical applications in which these materials might be particularly advantageous are discussed briefly.

Reciprocal Ferrite Devices in TEM Mode Transmission Lines—D. Fleri and B. J. Duncan (p. 91)

Several new reciprocal ferrite devices have been designed in TEM mode transmission lines to operate over both narrow and extremely broad bandwidths in the low-microwave frequency region. These include variable attenuators, an amplitude modulator, and a traveling-wave tube equalizer. Each component utilizes the attenuation associated with gyromagnetic resonance in low saturation magnetization ferrites. The techniques used to overcome the matching problems inherent in TEM mode transmission lines when ferrite loaded, and the design considerations pertinent to each component, are treated in detail. Parameters affecting characteristics of each device are discussed, and final design and operating characteristics of components are presented.

Measurement of Ferrite Isolation at 1300 MC—G. S. Heller and G. W. Catuna (p. 97)

Optimum geometry for ferrite isolators at low microwave frequencies in rectangular waveguide is discussed and measurements are presented which show the feasibility of constructing a practical isolator at 1300 mc using commercially available ferrites.

Further data for a narrower line-width ferrite are presented. The high-reverse to forward-loss ratios obtained are in accord with predictions from perturbation theory.

An Electronic Scan Using a Ferrite Aperture Luneberg Lens System—D. B. Medved (p. 101)

Beam displacements up to $\pm 30^\circ$ have been observed in the radiation patterns from various ferrite-loaded waveguide apertures in transverse magnetic fields. The apertures are used as feeds for Luneberg lenses, and electrical lobing of narrow pencil beams is accomplished. The proposed use of a square waveguide ferrite-filled feed for a sequential lobing system is described.

Round Table Discussion on Design Limitations of Microwave Ferrite Devices (p. 104)

Correspondence (p. 111)

PGMTT News (p. 113)

Contributors (p. 115)

Membership Roster of the IRE Professional Group on Microwave Theory and Techniques as of November 5, 1957 (p. 121)

Military Electronics

VOL. MIL-1, No. 2, DECEMBER, 1957

Announcement of M. Barry Carlton Award (p. 33)

Editorial (p. 34)

A Message from the National Chairman (p. 35)

Instrument Landing at Sea—F. Akers and F. G. Kear (p. 36)

The paper is a narrative account of two years of intensive effort by the Navy and civilian engineers which, after many trying periods, achieved success on July 30, 1935, when a completely hooded instrument landing was made aboard the aircraft carrier, *USS Langley*, 100 miles at sea off San Diego, Calif.

In the summer of 1933, when the aircraft carrier emerged as the future striking power of our Navy, Rear Admiral Ernest King, Chief of the Bureau of Aeronautics (later Fleet Admiral King), was hunting for every means to improve the capability of our carriers. One of the most important was their ability to operate in all types of weather. As a result of his examination of the Bureau of Standards' development work on an instrument landing system, he negotiated a contract with the Washington Institute of Technology to apply the basic principles and modify this system for aircraft carrier operations. The Washington Institute of Technology was formed specifically for the purpose of developing this system under the presidency of Sidney Mashbir. The development engineers were Gomer Davies and Dr. Frank G. Kear. Lieutenant Frank Akers, U. S. Navy (now Rear Admiral), was designated the project officer and flight test pilot for this effort. The small field at College Park, Md., was chosen as the location for the tests.

Throughout the fall and winter of 1933 and 1934, the equipment was built and many test flights made. A satisfactory installation was completed so that by May, 1934, completely hooded instrument landings were being made regularly at the College Park Airport.

Satisfied with the success of the ground installation, Admiral King decided to have the equipment installed aboard our first aircraft carrier, the *USS Langley*. The structural work was done at the Norfolk Naval Shipyard at Portsmouth, Va. The *Langley* sailed back with the fleet to the Pacific Ocean. The equipment installation was completed by the fall of 1934 and flight tests began. Many unexpected problems were encountered, particularly in regard to the glide path and localizer. These resulted in some rather major modifications, but eventually they were solved and an entirely satisfactory system was completed which resulted in the successful landing at sea by Lt. Akers on July 30, 1935.

Space Exploration—The New Challenge to the Electronics Industry—H. E. Prew (p. 43)

The electronics industry today faces its greatest challenge, the development of a system to control remotely a space-research vehicle. It must prepare man's path into space.

A two-way radio data link will be one specific goal. This link should transfer data between Earth and vehicle to provide guidance and observation data, and to permit control of vehicle trajectory and instrumentation through an Earth-to-vehicle control loop. The system should operate out to Mars, a distance of 50 million miles, under extremes of temperature and radiation far above present standards, and with self-contained power sources.

A radar-beacon data link providing guidance through a simple inertial autopilot would appear to be a reasonable approach, based upon extensions to presently-developed techniques. Operating with Earth-based, 500-mc radars resembling present transhorizon communications equipment, a vehicle beacon of 2-kw output power would permit vehicle orbiting of the Moon; 6-megw would be required to reach Mars. The respective Earth transmitters would require 200-kw and 600-megw power output.

Present remote-control equipment will not meet all the above needs; significant advances must be made before man can venture with confidence into space.

New Look at Submarines—C. B. Momsen (p. 49)

Contributors (p. 52)

Telemetry & Remote Control

VOL. TRC-3, No. 3,
DECEMBER, 1957

The Chairman's Message—C. H. Doersam, Jr. (p. 1)

A Theoretical Study of Errors in Radio Interferometer Type Measurements Attributable to Inhomogeneities of the Medium—G. J. Simmons (p. 2)

The effects of the variation of the index of refraction of the earth's atmosphere on the angular information yielded by radio interferometers for terrestrial and near-terrestrial sources are investigated, and a second-order correction is derived. Numerical values are not given since, in general, they require the use of high-speed computers to integrate the error term over the index of refraction profile; however, for various special "models," this need can be circumvented. One such case, the "flat-earth free-space" model is treated, both to serve as a check on the mathematical derivations, since it can be solved directly, and to give some idea of the size of the expected error.

Correction (p. 5)

Telemetering Receiving System at the Air Force Missile Test Center—H. A. Roloff (p. 6)

The receiving system used at the Missile Test Range in Florida and the West Indies is described. An over-all picture of the radio-telemetering ground receiving equipment is offered including the antennas, rf distribution facilities, and demodulation equipment. Several units of this system have been developed expressly for use at the Air Force Missile Test Center (AFMTC). The requirements leading to the design, along with the performance capabilities and operational utilization of the equipment are discussed. Some significant test results are outlined, and the current methods of testing the receiving system is presented.

Correction (p. 9)

Problems in Aircraft Telemetering—E. F. Shanahan (p. 10)

The development of aircraft telemetering at the Martin Company, Baltimore, Md. is described and the basic differences between aircraft telemetering as opposed to missile telemetering are discussed.

Some outstanding problems, findings, and solutions are indicated.

Telemetry Standards for Guided Missiles—(IRIG Document No. 103-56)—Prepared by Inter-Range Telemetry Working Group, Inter-Range Instrumentation Group, Air Force Missile Test Center, Holloman Air Development Center, Naval Air Missile Test Center, Naval Ordnance Missile Test Facility, Naval Ordnance Test Station, and White Sands Proving Ground (p. 13). (Not an official IRE Standard.)

Magnetic Recorder/Reproducer Standards—(IRIG Document No. 101-57)—Prepared by Inter-Range Instrumentation Group, Air Force Missile Test Center, Holloman Air Development Center, Naval Air Missile Test Center, Naval Ordnance Missile Test Facility, Naval Ordnance Test Station, White Sands Proving Ground (p. 19). (Not an official IRE Standard.)

Abstracts and References

Compiled by the Radio Research Organization of the Department of Scientific and Industrial Research, London, England, and Published by Arrangement with that Department and the *Electronic and Radio Engineer*, incorporating *Wireless Engineer*, London, England

NOTE: The Institute of Radio Engineers does not have available copies of the publications mentioned in these pages, nor does it have reprints of the articles abstracted. Correspondence regarding these articles and requests for their procurement should be addressed to the individual publications, not to the IRE.

Acoustics and Audio Frequencies.....	805
Antennas and Transmission Lines.....	806
Automatic Computers.....	807
Circuits and Circuit Elements.....	807
General Physics.....	809
Geophysical and Extraterrestrial Phenomena.....	810
Location and Aids to Navigation.....	811
Materials and Subsidiary Techniques..	811
Mathematics.....	813
Measurements and Test Gear.....	814
Other Applications of Radio and Electronics.....	814
Propagation of Waves.....	814
Reception.....	815
Stations and Communication Systems..	815
Subsidiary Apparatus.....	816
Television and Phototelegraphy.....	817
Transmission.....	817
Tubes and Thermionics.....	817
Miscellaneous.....	818

The Index to the Abstracts and References published in the PROC. IRE from February, 1956 through January, 1957 is published by the PROC. IRE, May, 1957, Part II. It is also published by *Electronic and Radio Engineer*, incorporating *Wireless Engineer*, and included in the March, 1957 issue of that journal. Included with the Index is a selected list of journals scanned for abstracting with publishers' addresses.

The number in heavy type at the upper left of each Abstract is its Universal Decimal Classification number and is not to be confused with the Decimal Classification used by the United States National Bureau of Standards. The number in heavy type at the top right is the serial number of the Abstract. DC numbers marked with a dagger (†) must be regarded as provisional.

U.D.C. NUMBERS

Extensions and changes in U.D.C. numbers published in P.E. Notes, up to and including P.E. Note 609, will be introduced in Abstracts and References where applicable, notably the subdivisions of 621.372.8 waveguides published in P.E. Note 594. U.D.C. publications are obtainable from The International Federation for Documentation, Willem Witsenplein 6, The Hague, Netherlands, or from The British Standards Institution, 2 Park Street, London, W.1, England.

JOURNAL REFERENCES

References to Russian publications will henceforth be based on the Russian title which will be abbreviated on the principles of The World List of Scientific Periodicals. The main changes are as follows:

Dokl. Ak. Nauk S.S.S.R. (formerly *C.R. Acad. Sci. U.R.S.S.*),
Izv. Ak. Nauk S.S.S.R. (formerly *Bull. Acad. Sci. U.R.S.S.*).

ACOUSTICS AND AUDIO FREQUENCIES

534.22-14-8:546.212 657
The Measurement of the Velocity of Sound in Doubly Distilled Water Containing Differing Amounts of Gas and at Various Temperatures—H. Markgraf. (*Hochfreq. u. Elektroak.*, vol. 65, pp. 169-173; March, 1957.)

534.23:621.396.677.3 658
Arrays with Constant-Beam Width over a Wide Frequency Range—D. G. Tucker. (*Nature, London*, vol. 180, pp. 496-497; September 7, 1957.) A linear array of omnidirec-

tional transducers is considered. Directivity is achieved in all planes containing the line of the array by the synthesis of directional patterns from elementary $(\sin x)/x$ patterns using delay lines to produce these patterns at various angles of deflection from the normal. See also 336 of 1958 (Berman and Clay).

534.232 659
The Directivity and Impedance of Artificially Compensated Cylindrical Acoustic Transducers—M. Federici. (*Ricerca Sci.*, vol. 27, pp. 1826-1838; June, 1957.) Sound radiation from a source consisting of cylindrical elements vibrating radially with variable phase is investigated (see also 3469 of 1955). By suitably arranging and phasing a number of transducer elements sound can be beamed in the direction of the cylinder axis. The characteristics of this type of source are calculated. The acoustic impedance of a cylinder of infinite length is expressed as the ratio of two Hankel functions of the first order.

534.844:681.84.087.7 660
Reverberation Chambers for Broadcasting and Recording Studios—M. Rettinger. (*J. Audio Eng. Soc.*, vol. 5, pp. 18-22; January, 1957.) The design and construction of reverberation chambers are considered.

534.861:534.784 661
Acoustic Conditions for Broadcast Transmission of Speech—L. Malecki. (*Nachr. Tech.*, vol. 7, pp. 267-273; June, 1957.) The conditions in a transmission channel which are necessary for the correct reproduction of the acoustic structure of speech are determined, and the influence of acoustic conditions at the microphone on transmission quality are investigated. The importance of allowing for differences in language characteristics is considered.

621.395.623.7 662
Mechanical Crossover Characteristics in Dual-Diaphragm Loudspeakers—A. B. Cohen. (*J. Audio Eng. Soc.*, vol. 5, pp. 11-17; January, 1957.) The role of diaphragm shape and material in controlling mechanical crossover characteristics is discussed. Frequency response curves which show the effect of an auxiliary diaphragm are given for conical and curvilinear diaphragms.

621.395.623.7:537.523.3 663
The Corona-Wind Loudspeaker—G. Shirley. (*J. Audio Eng. Soc.*, vol. 5, pp. 23-31; January, 1957.) An experimental model is described and illustrated, and problems arising in the construction of a practical loudspeaker,

with particular reference to commercial production, are discussed. See also 659 of 1956 (Tombs) and Tombs *et al.*, *Electronics*, vol. 30, pp. 198, 200; July 1, 1957.)

621.395.625.3 664
Tape Storage Problems—F. Radocy. (*J. Audio Eng. Soc.*, vol. 5, pp. 32-35; January, 1957.) The reduction of adverse effects in storing magnetic recording tapes is discussed.

ANTENNAS AND TRANSMISSION LINES

621.315.212:621.372.54.001.2 665
The Design of T-Stub Lines—P. Vielhauer. (*Nachr. Tech.*, vol. 7, pp. 241-243; June, 1957.) The dimensions of a T-stub line for use in vestigial-sideband filters are calculated.

621.372.2 666
Synthesis of Lumped-Parameter Precision Delay Line—E. S. Kuh. (PROC. IRE, vol. 45, pp. 1632-1642; December, 1957.) The two parts of the problem of designing delay lines are a) to provide the required time delay and bandwidth with the least complicated network and b) to have a good time response. The network obtained is a tandem connection of a low-pass ladder and an all-pass bridge structure.

621.372.2:621.372.43 667
A New Wide-Band Balun—W. K. Roberts. (PROC. IRE, vol. 45, pp. 1628-1631; December, 1957.) This balun has low loss and excellent impedance characteristics over a 3:1-frequency band, without any adjustments. The bandwidth increase is obtained by the use of a $\lambda/4$ transmission-line section which is placed inside one of the balanced arms.

621.372.8:621.372.2 668
A Method for Calculating Propagation Constants in Waveguides with Imperfectly Conducting Walls—L. N. Loshakov. (*Radiotekhnika, Moscow*, vol. 11, pp. 8-11; September, 1956.) An approximate method and a numerical example of its application are given. See also 1273 of 1957.

621.372.831 669
Designing Tapered Waveguide Transitions—B. J. Migliaro. (*Electronics*, vol. 30, pp. 183-185; November 1, 1957.) "A procedure for designing well-matched transitions between different waveguides where the guide wavelength varies along the taper. Simple graphical method employs data presented here for double-ridge-to-rectangular transitions. Procedure may also be used for rectangular-to-rectangular or ridge-to-ridge tapered transitions with corresponding accuracy."

- 621.372.85 670
Some Waveguides with Discontinuous Structure—M. Jouguet. (*C.R. Acad. Sci., Paris*, vol. 245, pp. 297–298; July 17th, 1957.) The propagation of em waves in a waveguide having thin insulating sheets at right angles to and parallel with its axis is considered for negligible and appreciable dielectric losses.
- 621.396.67:621.372.43:621.397.62 671
A Diplexer Two-Set Coupler—M. Harris. (*Radio TV News*, vol. 58, pp. 69, 176; September, 1957.) This is a network for supplying two television receivers from a common antenna and is the electrical equivalent of two $\lambda/4$ transmission lines.
- 621.396.67.029.62:621.3.015.1 672
V.H.F. Voltage Distribution in Communal Antenna Installations—A. Fiebranz. (*Nachr. Tech. Z.*, vol. 10, pp. 349–356; July, 1957.) Approximation formulas, curves, and details of other aids are given to assist in the installation of distribution systems for blocks of flats, etc.
- 621.396.677:523.16:523.72 673
Tests on a Model of an Antenna for Use in Radio Astronomy—G. C. Corazza and G. Francini. (*Ricerca Sci.*, vol. 27, pp. 1777–1786; June, 1957.) Radiation diagrams were obtained for a 1:15 scale model of an array of helical antennas for solar observations at 200 mc. Tests on the model were made at 3 kmc; the equipment is briefly described.
- 621.396.677.029.63:621.397.62 674
Television Antennas for Bands IV and V—F. R. W. Strafford. (*Wireless World*, vol. 64, pp. 11–13; January, 1958.) The requirements of television antennas suitable for these frequency bands are discussed and attention is drawn, with the aid of performance figures taken at 654 mc, to the advantages of the corner reflector with "bow-tie" dipole.
- 621.396.677.3:534.23 675
Arrays with Constant Beam Width over a Wide Frequency Range—(See 658.)
- 621.396.677.71:621.397.61 676
The Antenna of the Television Transmitter Feldberg/Schwarzwald—H. Mack. (*Nachr. Tech. Z.*, vol. 10, pp. 356–361; July, 1957.) Design and construction details of a two-section slotted-cylinder antenna structure about 105 feet high, on top of a 135-foot tower.
- 621.396.677.73 677
Ridge Vane Antenna Provides Constant Beam Width—W. A. Scanga. (*Electronics*, vol. 30, pp. 196, 198; November 1, 1957.) A pair of vanes, extending from the open end of a ridge waveguide, act as an end-fire antenna which has good wide-band properties.
- 621.396.677.8:551.578 678
The Effect of Atmospheric Precipitation on the Electrical Properties of Wire-Mesh Surfaces—V. K. Paramonov. (*Radiotekhnika, Moscow*, vol. 11, pp. 12–20; September, 1956.) The effect of icing on the reflecting properties of mesh surfaces is considered. Formulas are derived for determining the coefficient of transmission through a mesh, the conductors of which are covered with a uniform layer of ice. Experimental results are given, confirming the correctness of the method proposed.
- AUTOMATIC COMPUTERS**
- 681.142 679
A Multipurpose Electronic Switch for Analogue Computer Simulation and Autocorrelation Applications—N. D. Diamantides. (*IRE TRANS.*, vol. EC-5, pp. 197–202; December, 1956. Abstract, *Proc. IRE*, vol. 45, p. 574; April, 1957.)
- 681.142 680
An Error Analysis of Electronic Analogue Computers—V. A. Marsocci. (*IRE TRANS.*, vol. EC-5, pp. 207–212; December, 1956. Abstract, *Proc. IRE*, vol. 45, p. 574; April, 1957.)
- 681.142 681
A Wide-Band Multiplier using Crystal Diodes—M. E. Fisher. (*Electronic Eng.*, vol. 29, pp. 580–585; December, 1957.) The principle of quarter-square multiplication is used, the squaring being performed by networks of biased Ge diodes in the feedback paths of standard computing amplifiers. These networks have phase shifts of less than 1° at 50 kc and the errors of the multiplier are less than 0.3 per cent of maximum output.
- 681.142 682
A New Storage Element Suitable for Large-Sized Memory Arrays—the Twistor—A. H. Bobeck. (*Bell Sys. Tech. J.*, vol. 36, pp. 1319–1340; November, 1957.) Use is made of the Wiedemann effect whereby a torsion applied to a magnetic wire shifts the preferred direction of magnetization into a helical path. Three modes are suggested in using the effect for storage cells: a) the coincidence of circular and longitudinal magnetic fields inserts information into the wire as a polarized helical magnetization; b) operation similar to the coincident-current toroid with the wire acting as its own sensing winding; c) the wire is not twisted but the screw-sense of the flux path is related to the current polarities. Equations relating to the switching performance of a twistor are derived and a description of an experimental 320-bit array is given.
- 681.142 683
The IBM 705 EDPM Memory System—R. E. Merwin. (*IRE TRANS.*, vol. EC-5, pp. 219–223; December, 1956. Abstract, *Proc. IRE*, vol. 45, p. 574; April, 1957.)
- 681.142:537.227 684
A New Type of Ferroelectric Shift Register—J. R. Anderson. (*IRE TRANS.*, vol. EC-5, pp. 184–191; December, 1956. Abstract, *Proc. IRE*, vol. 45, p. 574; April, 1957.)
- 681.142:538.221 685
Ferroresonant Circuits for Digital Computers—C. B. Newport and D. A. Bell. (*J. Brit. IRE*, vol. 17, pp. 619–630; November, 1957.) An analysis of bistability in ferroresonant circuits, and the practical application to high-frequency operation (present limit 1 mc). Circuits are shown for a shift register, 3-stage binary counter, and 2-input logical adder.
- 681.142:621.314.7 686
Logic Circuits for a Transistor Digital Computer—G. W. Booth and T. P. Bothwell. (*IRE TRANS.*, vol. EC-5, pp. 132–138; September, 1956. Abstract, *Proc. IRE*, vol. 45, p. 255; February, 1957.)
- 681.142:621.314.7 687
Junction-Transistor Switching Circuits for High-Speed Digital Computer Applications—G. J. Prom and R. L. Crosby. (*IRE TRANS.*, vol. EC-5, pp. 192–196; December, 1956. Abstract, *Proc. IRE*, vol. 45, p. 574; April, 1957.)
- 681.142:621.317.729 688
An Electrolytic Tank as an Analogue Computing Machine for Factorizing High-Degree Polynomials—S. K. Ip. (*Quart. J. Mech. Appl. Math.*, vol. 10, pp. 369–384; August, 1957.) By means of simple measurements all the roots of a polynomial as high as the sixteenth degree can be located to within about 4 per cent.
- 681.142:621.373.43 689
Pulse Generator and High-Speed Memory Circuit—Z. Bay and N. T. Grisamore. (*IRE TRANS.*, vol. EC-5, pp. 213–218; December, 1956. Abstract, *Proc. IRE*, vol. 45, p. 574; April, 1957.)
- 681.142:621.398 690
A Simple Shaft Digitizer and Store—A. Tiffany. (*Electronic Eng.*, vol. 29, pp. 568–574; December, 1957.) A shaft position encoder of simple construction for analog-to-digital conversion is described.
- CIRCUITS AND CIRCUIT ELEMENTS**
- 621.318.57:621.318.134 691
Some Applications of Square-Loop Ferrite Cores to Telecommunication Switching—W. Six and R. A. Koolhof. (*Philips Telecommun. Rev.*, vol. 18, pp. 105–124; September, 1957.) Slightly abridged version of paper published in *Proc. IEE*, Pt. B, vol. 104, pp. 491–501; July, 1957.)
- 621.318.57:621.385.83 692
High-Speed Gating Circuit using the E8OT Beam-Deflection Tube—L. Sperling and R. W. Tackett. (*IRE TRANS.*, vol. ED-4, pp. 59–63; January, 1957. Abstract, *Proc. IRE*, vol. 45, p. 897; June, 1957.)
- 621.372:621.3.018.41 693
The Approximation of Special Frequency Laws by means of Tables of Frequency Functions—H. Dobesch. (*Hochfreq. u. Elektroak.*, vol. 65, pp. 159–164; March, 1957.) An approximation method facilitating the synthesis of two-pole and quadripole networks is described.
- 621.372.2:512.831 694
Admittance, Impedance and Scattering Matrices—C. G. Corazza and F. Serracchioli. (*Note Recensioni Notiz.*, vol. 6, pp. 336–342; May/June, 1957.) The concepts and their interrelation are defined.
- 621.372.4/.5:621.317.729.1 695
Analysis and Synthesis of Electrical Circuits by means of an Electrolyte Tank—M. L. D'Attri and U. Pellegrini. (*Note Recensioni Notiz.*, vol. 6, pp. 305–326; May/June, 1957.) Experimental procedure for solving network problems is described.
- 621.372.412:549.514.51 696
Effects of X-Ray Irradiation on the Frequency/Temperature Behaviour of AT-Cut Quartz Resonators—A. R. Chi. (*Phys. Rev.*, vol. 107, pp. 1524–1529; September 15, 1957.) Results for resonators fabricated from natural quartz, synthetic quartz grown on several different cuts of seed plates, and synthetic quartz containing Al or Ge impurity, are reported.
- 621.372.412.088.33:621.317.3 697
Tolerances of Quartz Crystals for Filters and their Measurement—C. Kurth and R. Miozynski. (*Nachr. Tech.*, vol. 7, pp. 244–249; June, 1957.) Methods for measuring series resonance and crystal inductance are indicated.
- 621.372.5:621.375.13 698
Negative Impedances and Gytrators—J. Gensel. (*Nachr. Tech.*, vol. 7, pp. 249–256; June, 1957.) Survey of characteristics and classification of the various types of impedance inverter and gyrator. Their realization in the form of transistor circuits is discussed. See; e.g., 2867 of 1955 (Bogert).
- 621.372.5.016.35 699
Stability Criteria for Linear Systems and Realizability Criteria for RC Networks—A. T. Fuller. (*Proc. Camb. Phil. Soc.*, vol. 53, pt. 4, pp. 878–896; October, 1957.) A new set of stability criteria in linear systems is derived; about half of the Hurwitz criteria can be neglected when certain of the coefficients of the

characteristic equation are positive. The conditions for realizability of RC networks are closely related to the stability and aperiodic criteria and are given in the form of polynomial coefficients.

621.372.54 700

Basic Properties and Characteristics of a Synchronous Filter—N. K. Ignat'ev. (*Radiotekhnika, Moscow*, vol. 11, pp. 59–71; September, 1956.) The operation of integrating devices used for improving signal/noise ratio is discussed. A simple circuit with a long open-circuited line as store is analyzed.

621.372.54 701

The Development of a New Method of Circuit Analysis in Ladder Networks—L. F. Coker. (*Commun. & Electronics*, no. 30, pp. 158–160; May, 1957.) The method outlined is applied to networks consisting of tandem-connected L sections. Calculations are simpler than in conventional methods.

621.372.54 702

Explicit Formulas for Tschebyscheff and Butterworth Ladder Networks—L. Weinberg. (*J. Appl. Phys.*, vol. 28, pp. 1155–1160; October, 1957.) A new set of simple formulas has been found for the element values in a Tschebyscheff or Butterworth ladder network, which apply when the degree of the denominator of the transfer function is odd and the reflection coefficient has zeros alternating in the left and right half-planes.

621.372.54+621.373.5]:621.314.7 703

RC Filters and Oscillators using Junction Transistors—N. Sohrabji. (*Electronic Eng.*, vol. 29, pp. 606–608; December, 1957.)

621.372.54:621.376.3:621.3.018.78 704

The Distortion of Frequency-Modulated Oscillations caused by RC Networks. General Remarks on Distortion Factors of Filters not Accurately Tuned to the Carrier, which have a Skew-Symmetric Phase Characteristic and a Mirror-Symmetric Amplitude Characteristic—E. G. Woschni. (*Hochfreq. u. Elektroak.*, vol. 65, pp. 165–169; March, 1957.)

621.372.54:621.396.621 705

Mutual Correlation of Fluctuation-Type Interference at the Output of Frequency Filters—M. V. Maksimov. (*Radiotekhnika, Moscow*, vol. 11, pp. 28–38; September, 1956.) The method is discussed of determining the interference correlation function for two filters forming the loads of a two-frequency-channel receiving system with or without detector.

621.373.029.6:538.569.4 706

Proposal for a Solid-State Radio-Frequency Maser—J. Itoh. (*J. Phys. Soc. Japan*, vol. 12, p. 1053; September, 1957.) A brief comment on conditions which are necessary to construct a maser using Zeeman levels of the pure quadrupole spectrum.

621.373.029.64:538.569.4 707

Characteristics of the Beam-Type Maser: Part 1—K. Shimoda. (*J. Phys. Soc. Japan*, vol. 12, pp. 1006–1016; September, 1957.) Velocity distribution of molecules in a beam-type maser is analyzed by an approximate method. The average velocity of the molecules is much less than the most probable velocity when the power level and focusing voltage are low. The relations between amplitude, focuser voltage, and frequency agree well with experimental results to be detailed in Part 2.

621.373.029.64:538.569.4 708

Solid-State Oscillator for Microwave Frequencies—(*Engineer, London*, vol. 203, p. 389; March 8, 1957.) An experimental solid-state device using gadolinium ethyl sulphate, an

ionically bound paramagnetic salt, as the active element is described. See 2108 of 1957 (Scovil *et al.*)

621.373.4:537.525 709

The Influence of a High-Frequency Gas Discharge on the Frequency of a Self-Excited Short-Wave Oscillator Stage—E. Häusler. (*Z. angew. Phys.*, vol. 9, pp. 60–66; February, 1957.) Continuing earlier investigations [381 of 1955 (Häusler and Koch)] further tests were made with a 20–50 mc oscillator under various conditions of discharge, coupling, and magnetic field. Characteristic curves indicating a linear relation between frequency and anode voltage are obtainable. The interpretation of the observations is discussed.

621.373.42 710

Polyphase Oscillators—A. S. Gladwin. (*Electronic Radio Eng.*, vol. 35, pp. 16–24; January, 1958.) The frequency stability and freedom from harmonics is greater for single-phase than for symmetrical polyphase oscillators.

621.373.42 711

Phase Generator has Resistive Shifter—G. E. Pihl. (*Electronics*, vol. 30, pp. 175–177; November 1, 1957.) The generator operates over a frequency range 20 cps–20 kc and supplies a pair of sinusoidal voltages with an accurately known phase relation that is continuously adjustable over 360°.

621.373.42 712

Designing Oscillators for Greater Stability—S. N. Witt, Jr. (*Electronics*, vol. 30, pp. 180–182; November 1, 1957.) Methods of improving the frequency stability of an oscillator which can be divided into an amplifier and a feedback network are described and examples are given.

621.373.421 713

Simultaneous Pulled Oscillations in a Triode Oscillator Incorporating Two Oscillatory Circuits—Abd El-Samie Mostafa. (*Commun. & Electronics*, no. 30, pp. 120–127; May, 1957.) Simultaneous oscillation at two frequencies is possible and owing to mutual pulling both frequency and amplitude modulation occur. A physical explanation of the pulling of a nonlinear oscillator by an external input signal is given. See also 398 of 1958 (Feist).

621.373.43 714

Second-Order Nonlinear Systems—L. Sideriades. (*J. Phys. Radium*, vol. 18, pp. 304–311; May, 1957.) In these systems, where time is not explicitly shown, the four-space is split into a displacement subspace and a velocity subspace, the two being related by a hypercone in a 1-1 transformation. Singularities of integral curves and certain shock phenomena are discussed, and the analysis is applied to two types of multivibrator. See also 1369 of 1957.

621.373.43:681.142 715

Pulse Generator and High-Speed Memory Circuit—Bay and Grisamore. (See 689.)

621.373.431.1 716

Cathode-Coupled Flip-Flop—T. G. Clark. (*Wireless World*, vol. 64, pp. 24–27; January, 1958.) A reliable design procedure.

621.373.431.1 717

Analysis of Cathode-Coupled Free-Running Multivibrator—D. C. Sarkar. (*Indian J. Phys.*, vol. 31, pp. 431–439; August, 1957.) A quantitative equivalent-circuit analysis valid for frequencies where the interelectrode capacities can be neglected, gives results in good agreement with experiment.

621.373.431.1:621.318.57 718

High-Speed Flip-Flops for the Millimicrosecond Region—Z. Bay and N. T. Grisamore.

(IRE TRANS., vol. EC-5, pp. 121–125; September, 1956. Abstract, PROC. IRE, vol. 45, p. 254; February, 1957.)

621.373.431.1:621.318.57:621.314.7 719

Transient Analysis of Second-Order Flip-Flops—L. M. Vallese. (*Commun. & Electronics*, no. 30, pp. 161–166; May, 1957.) A mathematical analysis of the trigger sensitivity and switching speed of flip-flop circuits whose action can be represented by a second-order differential equation. The method is applied to a point-contact emitter-input transistor flip-flop.

621.373.5:621.317.361.089.68 720

A Sawtooth Crystal Calibrator—E. L. Campbell. (*QST*, vol. 41, pp. 22–24; July, 1957.) Circuit and construction details of a sawtooth generator triggered from a 100-kc crystal and giving detectable harmonics up to 50 mc.

621.373.52 721

Feedback Coupling in Circuits with Crystal Triodes—Va. K. Trokhimenko. (*Radiotekhnika, Moscow*, vol. 11, pp. 46–53; September, 1956.) Circuit design methods are described and the formulas derived are tabulated.

621.374.32 722

Binary-Decimal Counter Operates at 10 Mc/s—D. E. Cottrell. (*Electronics*, vol. 30, pp. 186–189; November 1, 1957.) A design of counter which produces one output pulse for every ten input pulses is described. It uses logical "and" gates in a feedback loop.

621.374.32:621.3.083.8 723

Statistical Fluctuations and Optimum Transfer Functions of a Counting Rate Meter—H. Maier-Leibnitz. (*Z. angew. Phys.*, vol. 9, pp. 57–60; February, 1957.) Equations are derived to obtain the optimum response conditions and suitable circuits are described.

621.375.2:621.317.733 724

An Amplifier for A.C. Bridges—A. H. Allan, J. R. Gabriel, and B. H. Robinson. (*Electronic Eng.*, vol. 29, pp. 597–599; December, 1957.) "The requirements of an amplifier for ac bridges working to an accuracy of one part in ten thousand or better, from power frequencies to audio frequencies, are discussed. An amplifier to meet, in part, these requirements is described, and figures are given for its performance."

621.375.2.029.63 725

A U.H.F. Wide-Band Amplifier—J. Kason. (*Electronic Eng.*, vol. 29, pp. 600–602; December, 1957.) Description of the design of a 500-mc amplifier with bandwidth about 40 mc for program distribution.

621.375.23 726

A Feedback Circuit Equivalence—A. W. Keen. (*Electronic Radio Eng.*, vol. 35, pp. 8–12; January, 1958.) Transfer-network representations and their transformations are used to show that the feedback in a bootstrap amplifier with shunt feedback may be considered either positive or negative without inconsistency.

621.375.3 727

Dynamic Core Behaviour and Magnetic-Amplifier Performance—L. A. Finzi and D. L. Critchlow. (*Commun. & Electronics*, no. 30, pp. 229–240; May, 1957.) Discrepancies between theoretical analyses and measurements of magnetic-amplifier performance are attributed to excessively simplified representations of core behavior. Experimentally acquired knowledge of core flux characteristics is used to predict the operation of amplifier systems.

- 621.375.4:621.3.018.756 728
Reduction of the Distortion of Pulse Fronts in Transistor Video Amplifiers—T. M. Agakhanyan. (*Radiotekhnika, Moscow*, vol. 11, pp. 54–58; September, 1956.) Methods are described for reducing the distortion of leading edges caused by diffusion and other effects in the transistor base region. Compensating circuits are analyzed and phase and amplitude response curves are given.
- 621.375.4:621.314.7 729
Compensation for Changes in Base to Emitter Voltage with Temperature—P. Tharma. (*Mullard Tech. Commun.*, vol. 3, pp. 106–109; May, 1957.) An economical method of compensating power-transistor circuits consists in including in the emitter circuit metallic resistors having small positive temperature coefficients.
- 621.375.4.024 730
D.C. Amplifier using Transistors and a Silicon Bridge Modulator—K. Holford. (*Mullard Tech. Commun.*, vol. 3, pp. 126–137; June, 1957.) Matched Si junction diodes are used in a bridge modulator to convert the input to ac, which is then amplified by transistors and detected. The design is suitable for measuring dc inputs of 2 mv and 0.2 μ a or more.
- 621.375.427 731
Transistor Class-B Push-Pull Stages—L. H. Light. (*Mullard Tech. Commun.*, vol. 3, pp. 98–101; May, 1957.) The relative merits of single-ended and symmetrical output stages are discussed. In general the single-ended circuit offers considerable advantages.
- 621.375.427 732
Feedback Arrangements in Transformerless Push-Pull Output Stages—L. H. Light. (*Mullard Tech. Commun.*, vol. 3, pp. 102–105; May, 1957.) Different methods of applying negative feedback to single-ended and symmetrical class-B circuits (731 above) are discussed.
- 621.375.9:538.569.4:621.396.822 733
Measurement of Noise in a Maser Amplifier—L. E. Alsop, J. A. Giordmaine, C. H. Townes, and T. C. Wang. (*Phys. Rev.*, vol. 107, pp. 1450–1451; September 1, 1957.) Measurements on an NH_3 -beam maser whose cavity and input and output loads were cooled to near liquid-nitrogen temperature, yielded a noise figure of -2.0 db based on room temperature, as compared with a theoretical figure of -2.3 db.
- 621.375.9:538.569.4.029.6 734
Computation of Noise Figure for Quantum-Mechanical Amplifiers—M. W. P. Strandberg. (*Phys. Rev.*, vol. 107, pp. 1483–1484; September 15, 1957.) An expression is derived in terms of the physical quantities of the electromagnetic structure and of the paramagnetic salt used.
- 621.375.9:538.569.4.029.6 735
Theory of a Three-Level Maser—Javan. (See 764.)
- 621.375.9:538.569.4.029.6 736
Gain Bandwidth and Noise in Maser Amplifiers—A. E. Siegman. (*Proc. IRE*, vol. 45, pp. 1737–1738; December, 1957.) A theoretical study reveals that the optimum gain-bandwidth product of the two-port maser is only half that of the circulator maser for the same basic cavity. The optimum noise figure is the same if some bandwidth is sacrificed in the two-port maser. Practical considerations may, however, make the latter competitive.
- 621.375.9:538.569.4.029.6:621.396.822 737
Experimental Determination of the Noise Figure of an Ammonia Maser—J. P. Gordon and L. D. White. (*Phys. Rev.*, vol. 107, pp. 1728–1729; September 15, 1957.) An outline of the technique of measurement is given.
- GENERAL PHYSICS**
- 530.145:533.15 738
Modified WKB Approximation for Bothe's Differential Equation in Diffusion Theory—H. Joos and P. L. Ferreira. (*Anais acad. brasil. cienc.*, vol. 29, pp. 9–22; March 31, 1957. In English.)
- 533.6.011 739
Equipartition of Energy and Local Isotropy in Turbulent Flows—M. S. Uberoi. (*J. Appl. Phys.*, vol. 28, pp. 1165–1170; October, 1957.) Homogeneous turbulence was produced experimentally and experiments showed that the turbulence became isotropic at a faster rate than equipartition of energy occurred. Other experiments where approximately isotropic turbulence was subjected to deformation indicated that even at high Reynolds number the deformation in a shear flow can cause anisotropy. The connection of the investigation with turbulent flows in general is discussed.
- 535.215 740
Barrier-Layer Photo-e.m.f. of Photoelectric Elements with Dyestuffs—I. A. Karpovich and A. T. Vartanyan. (*Dokl. Akad. Nauk S.S.S.R.*, vol. 117, pp. 57–60; November 1, 1957.) Tests were made on photo elements consisting of dyestuffs deposited on a quartz plate clamped between semitransparent electrodes of Pt, Au, or Rh. Three different types of assembly were transversely illuminated; in most cases a positive photo emf was obtained.
- 537.122 741
On the Nature of the Electron—J. L. Salpeter. (*Proc. IRE, Austral.*, vol. 18, pp. 183–193; June, 1957. *Proc. IRE*, vol. 45, pp. 1588–1598; December, 1957.) "In this paper the concept of the electron as a fundamental particle of modern physics is discussed in relation to Pauli's exclusion principle, wave mechanics, the uncertainty principle, and relativity."
- 537.222.6 742
The Charge Density near a Sharp Point on a Conductor—R. Cade. (*Proc. Camb. Phil. Soc.*, vol. 53, pt. 4, pp. 870–877; October, 1957.) The idea that surface charge tends to infinity at convex sharp points on conductors and to zero at concave points is investigated on electrostatic principles. It is found that the problem has not been solved; a new attempt is made using potential-theory methods from which a fairly general solution is obtained.
- 537.311.33:538.6 743
Evaluation of Transport Integrals for Mixed Scattering and Application to Galvanomagnetic Effect—A. C. Beer, J. A. Armstrong, and I. N. Greenberg. (*Phys. Rev.*, vol. 107, pp. 1506–1513; September 15, 1957.) The Johnson-Whitesall evaluations of the conductivity integrals for mixed scattering have been extended to allow their application to the high-mobility semiconductors. Applications in the analysis of Hall effect, Corbino magnetoresistance, and thermomagnetic phenomena as functions of magnetic field are illustrated.
- 537.312.62:530.145.6 744
Interaction between Waves and Electrons, with some Remarks on Superconductivity—L. Brillouin. (*J. Phys. Radium*, vol. 18, pp. 331–336; May, 1957.) Discussion of interactions occurring between elastic waves and free electrons in metal, particularly below the Debye temperature.
- 537.52 745
Silent Electric Discharge at Low Frequency in Air, using Insulating Electrodes—D. P. Jatar and H. D. Sharma. (*C.R. Acad. Sci., Paris*, vol. 245, pp. 414–416; July 22, 1957.) Note on the Joshi effect and the variation of discharge current as a function of applied voltage, using beeswax electrodes in dry air irradiated by light.
- 537.525:537.222 746
Three-Dimensional Potential Well—H. B. Williams. (*Phys. Rev.*, vol. 107, pp. 1451–1452; September 1, 1957.) The possibility of generating potential wells having depths of the order of thousands of electron volts is discussed.
- 537.525:621.3.011.3 747
Variation of Inductance by Dielectrics, in particular Plasmas—R. Seitner. (*Z. angew. Phys.*, vol. 9, pp. 66–68; February, 1957.) A qualitative interpretation of the frequency changes in oscillatory circuits which are coupled to electrodeless gas discharges. See; e.g., 709 above.
- 537.533 748
Analysis of MultiveLOCITY Electron Beams by the Density-Function Method—A. E. Siegman. (*J. Appl. Phys.*, vol. 28, pp. 1132–1138; October, 1957.) Mathematical techniques useful in the solution and interpretation of the density-function equations as applied to multiveLOCITY electron-beam problems are presented with some conclusions about the non-conservative nature of signal or noise propagation along a multiveLOCITY beam. The paper serves as a background for a detailed calculation of noise propagation through the gun region of an electron beam (749 below).
- 537.533:621.396.822 749
Density-Function Calculations of Noise Propagation on an Accelerated MultiveLOCITY Electron Beam—A. E. Siegman, D. A. Watkins, and Hsung-Cheng Hsieh. (*J. Appl. Phys.*, vol. 28, pp. 1138–1148; October, 1957.) The propagation of noise fluctuations through the low-voltage multiveLOCITY region immediately in front of the potential minimum of a diode or electron beam has been computed. Despite the absence of any conventional loss elements, two noise parameters or measures of the noise fluctuations when the beam is passed through a multiveLOCITY region are significantly different at the output from those at the input. Changes are such as to lower significantly the minimum noise figure of a microwave tube.
- 537.533.74 750
The Elastic Scattering of Electrons—R. Zouckermann. (*J. Phys. Radium*, vol. 18, pp. 133–137; February, 1957.) An examination of basic theory, in particular the Rutherford formula, with reference to experimental results.
- 537.533.8 751
Theory of Secondary Electron Emission by High-Speed Ions—E. J. Sternglass. (*Phys. Rev.*, vol. 108, pp. 1–12; October 1, 1957.) A new theoretical treatment shows that the yield of secondaries is proportional to the rate of energy loss of the incident particles and is independent of work function, conductivity, and other bulk properties of the metal. The theory explains the experimental observations and its application to general problems of electron escape and capture is discussed.
- 537.533.8 752
Estimate of the Time Constant of Secondary Emission—A. van der Ziel. (*J. Appl. Phys.*, vol. 28, pp. 1216–1217; October, 1957.) Energy considerations allow a simple estimate to be made of the time constant of secondary emission.
- 537.56 753
Ionization by Positive Ions—H. B. Gilbody and J. B. Hasted. (*Proc. Roy. Soc. A.*, vol. 240,

pp. 382-395; June 11, 1957.) A method of measuring the ionization cross section of atoms is described in which electrons are collected from single collisions of an ion beam passing through a gas at low pressures. Measurements are given for twenty-three cases over energy ranges approximately 5-40 kev and 100 ev-3 kev.

537.56:538.69 754

Plasma Oscillations in a Steady Magnetic Field: Circularly Polarized Electromagnetic Modes—T. Pradhan. (*Phys. Rev.*, vol. 107, pp. 1222-1227; September 1, 1957.) The propagation of em waves in the direction of the field is considered. By taking account of the thermal motion of electrons, results are derived which differ markedly from those of the Appleton-Hartree electromagneto-ionic theory near the cyclotron resonance frequency.

538.11 755

Notes on the Ground State of Antiferromagnetism—O. Nagai. (*J. Phys. Soc., Japan*, vol. 12, pp. 978; August, 1957.) The conclusions reached by earlier investigators are compared with those which result from the spin-wave theory [see; e.g., 726 of 1956 (Marshall)]. The discrepancies are briefly discussed.

538.3 756

General Solutions of Equations of a Classical Nonconservative Electromagnetism—P. Gautier. (*C.R. Acad. Sci., Paris*, vol. 245, pp. 45-47; July 1, 1957.)

538.312 757

Electromagnetic Potentials in a Heterogeneous Nonconducting Medium—A. Nisbet. (*Proc. Roy. Soc. A*, vol. 240, pp. 375-381; June 11, 1957.) For em fields in a stationary nonconducting medium (isotropic or anisotropic), the dielectric constant and permeability of which are given point functions, the general theory of representations in terms of scalar and vector potentials and of Hertzian potentials is developed.

538.566:538.221 758

Tensor Theory of Gyromagnetic Power—Y. Le Corre. (*J. Phys. Radium*, vol. 18, pp. 312-317; May, 1957.) General linear relations for nonabsorbing media are derived. The influence of symmetry upon tensor equations and the effect of magnetic anisotropy on em wave propagation is examined.

538.566:621.384.622 759

Electromagnetic Waves in Nearly Periodic Structures—E. Wild. (*Quart. J. Mech. Appl. Math.*, vol. 10, pt. 3, pp. 322-341; August, 1957.) "The theory of simple harmonic electromagnetic waves in a nearly periodic structure of the type used in linear accelerators is discussed by an expansion in a series of appropriately defined transmission modes of the field in a unit cell of the structure. The possibility of the expansion being assumed, it is shown that the coefficients can be expressed as integrals of the field over the input or output apertures of the unit cell. The modification to the corresponding solution in the strictly periodic structure can be calculated by perturbation theory. In the first approximation the structure can be represented by a series of four-terminal networks, and the voltages and currents in these can be defined in such a way that the relevant parameters vary smoothly in the neighborhood of resonance."

538.569.4:538.2:53.082.5 760

Optical Detection of Magnetic Resonance in Alkali Metal Vapour—W. E. Bell and A. L. Bloom. (*Phys. Rev.*, vol. 107, pp. 1559-1565; September 15, 1957.) The apparatus is described, together with experimental conditions under which signals have been observed. A

possible application of the technique is the measurement of weak magnetic fields.

538.569.4:538.22 761

Heterodyne Detection of Free Precession in Nuclear Magnetic Resonance—H. Benoit and R. Klein. (*C.R. Acad. Sci., Paris*, vol. 245, pp. 155-157; July 8, 1957.) Details of a method applied to proton resonance in solutions.

538.569.4:538.22 762

Narrowing Effect of Dipole Forces on Inhomogeneously Broadened Lines—S. Geschwind and A. M. Clogston. (*Phys. Rev.*, vol. 108, pp. 49-53; October 1, 1957.) Observations of the effect in Mn ferrite and yttrium iron garnet are described. The theory for cases in which the spatial period of the inhomogeneity is large compared to atomic distances and is either short or comparable to sample size is discussed, and its applications are considered.

538.569.4:621.372.826:537.226 763

Dielectric Rod Waveguide Cells for Microwave Spectroscopy—E. B. Brackett, P. H. Kasai, and R. J. Myers. (*Rev. Sci. Instr.*, vol. 28, pp. 699-702; September, 1957.) The calculation of the distribution of microwave power around a quartz rod excited in the dipole mode enabled rod sizes to be selected for cells covering the range 17-60 kmc. Teflon windows were found to be satisfactory. See also 3843 of 1957 (Costain).

538.569.4.029.6:621.375.9 764

Theory of a Three-Level Maser—A. Javan. (*Phys. Rev.*, vol. 107, pp. 1579-1589; September 15, 1957.) A complete theory is discussed for a gaseous system with an extension to paramagnetic solids.

GEOPHYSICAL AND EXTRATERRESTRIAL PHENOMENA

523.16 765

An Attempt to Detect Linearly Polarized Radio Emission from the Galaxy—J. M. Thomson. (*Nature, London*, vol. 180, pp. 495-496; September 7, 1957.) A 7.5-m paraboloidal reflector was used at a frequency of 159.5 mc with receiver bandwidth 4 mc. Plots of position angle of the plane of polarization against time are given for regions near 05 h and 18 h and show that its variation is in the direction to be expected from the ionospheric data.

523.16 766

Relative Intensities of the Four Principal R.F. Sources Observed at a Wavelength of 22 cm; Note on R.F. Source Sagittarius A—G. Westerhout. (*C.R. Acad. Sci., Paris*, vol. 245, pp. 35-38; July 1, 1957.) Some 55 rf sources have been located during observations of the Milky Way region made by means of the new 25-m radio telescope at Dwingeloo, The Netherlands. Special studies have been made of five of these in Cass A, Cygn A, Taur A, Virg A, and Sgr A, and the equivalent temperatures have been determined.

523.16:523.72 767

The Effects of Incomplete Resolution on Surface Distributions Derived from Strip-Scanning Observations, with Particular Reference to an Application in Radio Astronomy—S. F. Smerd and J. P. Wild. (*Phil. Mag.*, vol. 2, pp. 119-130; January, 1957.) The limitations of one-dimensional scanning methods for measuring surface distribution, particularly that of radio brightness over the sun's disk, are discussed. See; e.g., 2607 of 1955 (O'Brien and Tandberg-Hanssen).

523.16:523.72:621.396.677 768

Tests on a Model of an Aerial for Use in Radio Astronomy—Corazza and Francini. (See 673.)

523.16:523.841.11 769

Radio Emission from the Remnants of the Supernovae of 1572 and 1604—J. E. Baldwin and D. O. Edge. (*Observatory*, vol. 77, pp. 139-143; August, 1957.) Measurements at 1.9 m λ are compared with previous radio and optical observations [see, e.g., 2708 of 1956 (Mills, et al.)].

523.165 770

The Cosmic Radiation and Solar-Terrestrial Relationships—J. A. Simpson. (*Ann. Geophys.*, vol. 11, pp. 305-329; July-September, 1955. In English.) Paper presented at the Assembly of the Union Géodésique et Géophysique Internationale, Rome, September, 1954, reviewing the properties of cosmic radiation and its association with solar and geophysical processes, and including a description of experimental methods developed to study low-energy cosmic-ray particles.

523.5 771

The Incidence of Meteor Particles upon the Earth—A. A. Weiss. (*Aust. J. Phys.*, vol. 10, pp. 397-411; September, 1957.) Radio echo rates for both shower and sporadic meteors, measured at Adelaide with 27-mc cw equipment, are applied to the calculation of the incident flux of meteors above limiting brightnesses in the region $M_R < +7.5$. Dependence of ionizing probability on velocity is discussed, and the fluxes and densities agree reasonably well with independent evaluations from visual meteor rates.

523.53 772

A Prediction of a Meteor Orbital Period—E. G. Bowen. (*Observatory*, vol. 77, pp. 99-102; June, 1957.) The probable orbital period of a meteor shower, observed on December 5-6, 1956, is predicted from examination of snow-fall records in Japan, assuming the suggested correlation between precipitation and occurrence of meteor showers to be real.

550.385 773

Analysis of the Sinusoidal Variation of Magnetic Declination of 11th April 1954—K. Burkhart and E. Selzer. (*Ann. Geophys.*, vol. 11, pp. 353-368; July-September, 1955.) Analysis of magnetograms of 14 European stations suggests the development of a counter-clockwise vortex-like perturbation in the ionosphere bordering on the southern limits of the auroral zone and lasting less than 2 h.

551.5:621.396.96 774

Radar in the Rain—(*Electronic Radio Eng.* vol. 35, pp. 13-15; January, 1958.) An outline of radar investigations into cloud structure.

551.508.822 775

Radiosonde Trials at Payerne, 1956—A. H. Hooper. (*Meteor. Mag., London*, vol. 86, pp. 33-36; plates; February, 1957.) Report of trials in Switzerland in May and June, 1956 in which 14 types of radiosonde from various countries were compared.

551.510 776

Investigation of the Upper Layers of the Atmosphere—V. V. Mikhnevich and I. A. Khvostikov. (*Izv. Akad. Nauk S.S.S.R., Ser. Geofiz.*, no. 11, pp. 1393-1409; November, 1957.) Measurement of composition, pressure, density, and temperature, up to a height of 90 miles, were made by means of containers which collected samples of air after being automatically released from rockets. Experimental data are tabulated and some results obtained in the U.S.A. and U.S.S.R. compared. Seventy-eight references.

551.510.535 777

Ionospheric Drifts at Brisbane—M. J. Burke and I. S. Jenkinson. (*Aust. J. Phys.*, vol.

10, pp. 378-386; September, 1957.) Measurements over a 2-year period show that speeds are less than those observed at higher latitudes. The E-region 12-h and 8-h solar harmonics show large seasonal phase changes in the northward component; the phase for the 12-h northward component in summer is in fair agreement with higher latitudes. The F-region 12-h harmonic seasonal change is greater in the eastward than in the northward component.

550.510.535 778
Measurement of Ionospheric Winds—P. Lejay. (*C.R. Acad. Sci., Paris*, vol. 245, pp. 253-257; July 17, 1957.) Experiments made at Domont, France, by the three-receiver method are described. The electron displacements deduced from observations correspond to some extent with those necessary to account for the daily variations in the earth's magnetic field.

551.510.535:551.593.9 779
Some Possible Relations between the Nightglow and the Ionosphere—P. St. Amand. (*Ann. Géophys.*, vol. 11, pp. 450-460; October-December, 1955. In English.) "Ionospheric data from Stanford, Calif., are compared with nightglow data from Cactus Peak, Calif. The nocturnal variation of the brightness of the green line, 5 577, of [OI] is found to be similar to the variation of height of the F region. The nocturnal variation of the brightness of the red lines 6 300-6 364 of [OI] is found to be similar to that of the electron density of the F region. The possibility that the red lines are produced by radiation following dissociative recombination of electrons with O_2^+ ions is discussed." Paper presented at the Assembly of the Union Géodésique et Géophysique Internationale, Rome, September, 1954.

551.510.535:621.396.11 780
The Reflection Coefficient of Ionospheric Layers—G. Pillet. (*C.R. Acad. Sci., Paris*, vol. 245, pp. 335-338; July 17, 1957.) Experiments made at 2.1 and 3.4 mc show that the reflection coefficient which is nearly unity for the F layer falls to a very low value for the E layer and that loss of energy due to reflection from the latter is of the same order as the nondeviative absorption.

551.510.535:621.396.11.029.62 781
The Scattering of Radio Waves of Very High Frequency in the Ionosphere—Ionescu. (See 890.)

551.594.22:621.396.969 782
Radar Echoes from Inter-stroke Processes in Lightning—F. J. Hewitt. (*Proc. Phys. Soc.*, vol. 70, pp. 961-979; October 1, 1957.) Radar echoes at 50 cm λ were used to investigate interstroke lightning processes. The most intense activity of junction streamers is between heights of 4-7 km; these junction streamers may sometimes grow in height up to 10 km although their activity decreases with height; the lowest level at which they occur remains constant throughout flashes and their horizontal extent is about $1\frac{1}{2}$ to 2 km. Echoes from these junctions always decrease before the onset of a flash.

551.594.5 783
Theory of the Auroral Spectrum—D. R. Bates. (*Ann. Géophys.*, vol. 11, pp. 253-278; July-September, 1955. In English.) Paper presented at the Assembly of the Union Géodésique et Géophysique Internationale, Rome, September, 1954. The main luminescence observed is due to a) inelastic collisions made by the incident particles and by the ejected electrons, b) degradation of the ultraviolet radiation emitted and scattering of solar radiation, c) thermal processes such as dissociative recombination. Eighty-one references.

551.594.5:551.593.9 784
The Work of Soviet Scientists on the Luminescence of the Night Sky and Aurorae—B. A. Bagaryatski. (*Izv. Akad. Nauk S.S.S.R.*, Ser. geofiz., no. 11, pp. 1410-1417; November, 1957.) A review of the research carried out in the last 30 years with particular reference to the IGY, in a network of stations all over the U.S.S.R. One-hundred-eighteen references.

551.594.6 785
A Method for Interpreting the Dispersion Curves of Whistlers—L. R. O. Storey. (*Can. J. Phys.*, vol. 35, pp. 1107-1122; September, 1957.) An analytical solution to the problem of determining the dispersion of a whistler from a known electron density in the outer atmosphere is formulated. The results are then applied to the inverse problem of deducing the variation in electron density from the dispersion curve. A numerical example is given.

551.594.6:621.396.663 786
Calibration of Narrow-Sector Radiogoniometers for Atmospheric—Carbenay. (See 788.)

LOCATION AND AIDS TO NAVIGATION

534.88-14 787
Underwater Acoustic Echo-Ranging—J. W. R. Griffiths and A. W. Pryor. (*Electronic Radio Eng.*, vol. 35, pp. 29-32; January, 1958.) Measurements having shown the reverberation power spectrum to be similar to that of the emitted pulse, the effects of pulse duration and receiver bandwidth on reverberation level and peak-signal reverberation ratio are examined theoretically. The pulse should be as short as possible and the product bandwidth \times pulse duration should be approximately unity.

621.396.663:551.594.6 788
Calibration of Narrow-Sector Radiogoniometers for Atmospheric—F. Carbenay. (*C.R. Acad. Sci., Paris*, vol. 245, pp. 298-300; July 17, 1957.) An extension of the method of calibrating omnidirectional recording receivers with reference to signal flux and effective antenna height. See 1451 of 1957, 1651 of 1951, and back references.

621.396.933:621.395.625.3 789
Multiple-Track Tape Recorders in Air Traffic Control—K. Heideleuf. (*Nachr. Tech. Z.*, vol. 10, pp. 344-348; July, 1957.) Description of German 14-track equipment.

621.396.96:551.5 790
Radar in the Rain—(See 774.)

621.396.96:621.316.726.078 791
Transistorized A.F.C. uses Triangular Search Sweep—H. H. Hoge and D. L. Spotten. (*Electronics*, vol. 30, pp. 178-179; November 1, 1957.) Circuit details of a radar afc system.

MATERIALS AND SUBSIDIARY TECHNIQUES

533.5 792
Generalities about Outgassing at Room Temperature—R. Geller. (*Le Vide*, vol. 12, p. 194; May/June, 1957. In French and English.)

533.5 793
Outgassing at Room Temperature of Materials under Vacuum—R. Barré, R. Geller, and G. Mongodin. (*Le Vide*, vol. 12, pp. 195-201; May/June, 1957. In French and English.) Work done in connection with the construction of the synchrotron at Saclay is described. The over-all outgassing of a standard vacuum installation may be calculated on the hypothesis that most metals used are comparable to steel. Characteristics obtained for rubber are shown.

533.5:621.385.032.213.13 794
Practical Experiences with a Vacuum-Tight Sealing Mechanism for the Repeated Use of Activated Oxide Cathodes—H. Fetz and K. Schiefer. (*Z. angew. Phys.*, vol. 9, pp. 13-14; January, 1957.) The equipment described is used in investigations of cathode sputtering processes. The life of the cathode is prolonged by protecting the cathode from contact with the oxygen of the atmosphere every time the sputtering vessel is opened. An interpretation is given of experimental results observed in tests of a BaO cathode.

533.5:621.389 795
Mass Spectrometer for Leak Detection operating with a Mixture containing a Small Percentage of Helium—H. Warmoltz and H.A.M. de Grefte. (*Le Vide*, vol. 12, pp. 202-207; May/June, 1957.)

535.215:546.32-1 796
The External Photoelectric Effect of the Alkali Metals: Part 1—H. Thomas. (*Z. Phys.*, vol. 147, pp. 395-418; January 12, 1957.) The dependence of the photoelectric effect on the thickness of the metal film, and the range of photoelectrons in K are investigated. Measurements indicate a bulk effect in the wavelength range 289-578 μ . A satisfactory interpretation of results is obtained on the basis of plasma theory. Forty-seven references.

535.215:546.32-1 797
The External Photoelectric Effect of the Alkali Metals: Part 2—H. Mayer and H. Thomas. (*Z. Phys.*, vol. 147, pp. 419-441; January 12, 1957.) The spectral distribution of the quantum yield was investigated for thin films and heavier deposits of K. Experimental results can be satisfactorily interpreted by theory based on a photoelectric bulk effect which is also applicable to the spectral distribution obtained with solid K. Forty-seven references. Part 1: 796 above.

535.215:546.32-1 798
The External Photoelectric Effect of Alkali Metals: Part 3—S. Methfessel. (*Z. Phys.*, vol. 147, pp. 442-464; January 12, 1957.) The energy distribution of photoelectrons emitted from K and Cs films of various thicknesses was measured. The photoeffect is found to be mainly a bulk effect. Thirty-eight references. Part 2: 797 above.

535.215+535.376]:546.472.21 799
Anisotropy in Electroluminescence and Conductivity of Single Crystals of ZnS—A. Lempicki, D. R. Frankl, and V. A. Brophy. (*Phys. Rev.*, vol. 107, pp. 1238-1239; September 1, 1957.) The marked anisotropy observed is considered to arise from stacking faults in the direction of the c axis.

535.215:546.59 800
Images of Strained Metal Samples, obtained with a Photoemission Microscope—R. Bernard, C. Guillaud, and R. Goutte. (*J. Phys. Radium*, vol. 18, pp. 327-330; May, 1957.) The crystalline structure of pulled gold samples after etching by ionic bombardment were examined. Areas of maximum strain showed an increased brightness which could be due to a local increase of photoelectric emission.

535.215:546.682.19:621.383.4 801
Photoelectric Effects in InAs at Room Temperature—C. Hilsun. (*Proc. Phys. Soc. B*, vol. 70, pp. 1011-1012; October 1, 1957.) A note of the photoconductive and photoelectromagnetic effects in InAs, showing the spectral sensitivity of a photocell constructed by etching.

535.215:546.816.231 802
Optical Sensitization of Photoconductors of the Lead Salt Group—V. Schwetsoff. (*C. R.*

- Acad. Sci., Paris*, vol. 245, pp. 149–152; July 8, 1957.) A residual increase of conductivity σ and variation of relative sensitivity $\Delta\sigma/\sigma$, are observed after subjecting photoconductors at low temperature (77°K) to visible light. The effect is confirmed for PbS, PbSe, and PbTe.
- 535.37** 803
Sulphur Vacancy Emission in ZnS Phosphors—N. T. Melamed. (*Phys. Rev.*, vol. 107, p. 1727; September 15, 1957.) An emission band centred on 3950 Å is attributed to sulphur vacancies rather than interstitial silver activator.
- 535.37** 804
The Luminescence of Alkali Vanadates—H. Gobrecht and G. Heinsohn. (*Z. Phys.*, vol. 147, pp. 350–360; January 10, 1957.) Results of an experimental investigation of four different vanadates are compared and an interpretation of the luminescence mechanism is given.
- 537.226/.227** 805
Dielectric and Thermal Study of Tri-glycine Sulphate and Tri-glycine Fluoberyllate—S. Hoshino, T. Mitsui, F. Jona, and R. Pepinsky. (*Phys. Rev.*, vol. 107, pp. 1255–1258; September 1, 1957.) The dielectric constants ϵ_0 show a pronounced anomaly at the Curie temperatures of 48°C and 70°C for the sulphate and the fluoberyllate respectively. The dielectric constants ϵ_a and ϵ_e are practically temperature-independent. Measurements of the specific heat as a function of temperature yield values of entropy change $\Delta S = 0.48$ and 1.17 cal/mole degree, respectively.
- 537.226/.227:546.431.824–31** 806
Preparation of Thin Single Crystals of Barium Titanate—J. T. Last. (*Rev. Sci. Instr.*, vol. 28, pp. 720–721; September, 1957.) Single crystal samples as thin as 1.5 μ were prepared using phosphoric acid as an etchant and Teflon-silicone tape as a support.
- 537.226/.227:546.431.824–31** 807
Domain Effects in Polycrystalline Barium Titanate—E. C. Subbarao, M. C. McQuarrie, and W. R. Buessem. (*J. Appl. Phys.*, vol. 28, pp. 1194–1200; October, 1957.) The indirect observation of domain changes under electrical and mechanical stresses was undertaken principally by means of X-ray reflections and dimensional changes. Observations were made of the changes as a function of time.
- 537.226/.227:546.431.824–31** 808
Effect of Iron-Group Ions on the Dielectric Properties of BaTiO₃ Ceramics—T. Sakudo. (*J. Phys. Soc., Japan*, vol. 12, p. 1050; September, 1957.) The Curie point of these ceramics falls with the addition of Fe or Ni ions but is hardly affected by Mn or Co. For Cu, the Curie point rises; this is briefly discussed.
- 537.226.2** 809
The Existence Domain of Complex Dielectric Constant of Binary Mixture—F. Irie. (*Ann. Phys., Lpz.*, vol. 19, pp. 31–40; November 15, 1956. In English.) Extension of existing theory and notes on its applications.
- 537.226.2/.3:[543.261+547.262** 810
The Dielectric Properties of Methyl and Ethyl Alcohols in the Wavelength Range 3 cm–52 cm—E. H. Grant. (*Proc. Phys. Soc.*, vol. 70, pp. 937–944; October 1, 1957.) The dielectric behavior of both alcohols can be described in terms of a principal dispersion region at cm λ , together with a subsidiary dispersion region occurring at mm λ .
- 537.227** 811
Ferroelectricity in Glycine Silver Nitrate—R. Pepinsky, Y. Okaya, D. P. Eastman, and T. Mitsui. (*Phys. Rev.*, vol. 107, pp. 1538–1539; September 15, 1957.) Ferroelectricity is observed below –55°C. At –195°C the spontaneous polarization is 0.55 $\times 10^{-6}$ C/cm² and the coercive field is 740 v/cm. There are no dielectric anomalies between 4°K and –55°C.
- 537.227** 812
Ferroelectricity of Dicalcium Strontium Propionate—B. T. Matthias and J. P. Remeika. (*Phys. Rev.*, vol. 107, p. 1727; September 15, 1957.) Preliminary results are reported.
- 537.311.31:538.63** 813
Magnetoresistance in Metals—D. K. C. MacDonald. (*Phil. Mag.*, vol. 2, pp. 97–104; January, 1957.) Report of experimental measurements on plate-shaped specimens of Na and Rb, and on a cylindrical specimen of Na.
- 537.311.31:538.63** 814
New Type of Oscillatory Magnetoresistance in Metals—J. Babiskin and P. G. Sebenmann. (*Phys. Rev.*, vol. 107, pp. 1249–1254; September 1, 1957.) The magnetoresistive properties of a thin sodium wire have been studied at 1°K in transverse magnetic fields up to 60 000 G. The oscillations observed were not of the de Haas-van Alphen type: they are interpreted as being caused by surface scattering.
- 537.311.33** 815
Theory of Impurity-Centre Electrons: Part 2—Nonradiative Transitions—G. Helm. (*Ann. Phys., Lpz.*, vol. 19, pp. 41–54; November 15, 1956.) Further application of the method given in Part 1 (3770 of 1956).
- 537.311.33** 816
The Effect of Free Electrons on Lattice Conduction at High Temperatures—R. Stratton. (*Phil. Mag.*, vol. 2, pp. 422–424; March, 1957.) Phonon-electron scattering is considered for the range above the Debye characteristic temperature θ . See 2017 of 1956 (Ziman) for lattice temperatures below θ .
- 537.311.33** 817
Variation of Mobility with Electric Field in Nondegenerate Semiconductors—M. S. Sodha. (*Phys. Rev.*, vol. 107, pp. 1266–1271; September 1, 1957.) By assuming a Maxwellian distribution of electron velocities at normal temperatures, in a semiconductor having low impurity concentration, it is shown that the net zero field mobility decreases monotonically with decreasing “impurity” mobility.
- 537.311.33** 818
Semiconductor Compounds Open New Horizons—A. Coblenz. (*Electronics*, vol. 30, pp. 144–149; November 1, 1957.) In this survey inorganic and organic semiconducting compounds are distinguished from conventional semiconductors, and their characteristics, unusual properties and applications are discussed. Tabulated data on a large number of compounds are given.
- 537.311.33** 819
Thermo-compression Bonding—(*Bell Lab. Record*, vol. 35, p. 336; September, 1957.) A combination of heat and pressure is used to provide a firm bond between various soft metals and clean single-crystal semiconductor surfaces.
- 537.311.33** 820
Cleaning Semiconductor Components—(*Bell Lab. Record*, vol. 35, p. 337; September, 1957.) A continuous water-washing system is described for removing water-soluble materials that remain after etching, and for monitoring the effectiveness of the washing procedure.
- 537.311.33:538.63** 821
Magnetoresistance of Holes in Germanium and Silicon with Warped Energy Surfaces—J. G. Mavroides and B. Lax. (*Phys. Rev.*, vol. 107, pp. 1530–1534; September 15, 1957.) Experimental directional magnetoresistance effects and the variation of magnetoresistance with magnetic field are interpreted in terms of calculated values of the magnetoresistance coefficients.
- 537.311.33:546.23:535.3** 822
Absorption of Light in Se Near the Band Edge—W. J. Choyke and L. Patrick. (*Phys. Rev.*, vol. 108, pp. 25–28; October 1, 1957.) Photovoltaic measurements, at temperatures 80°K–440°K with photons of energy 1.6 eV–2.0 eV, show that the transitions are indirect at the band edge, requiring the absorption or emission of a phonon. The energy gap for hexagonal Se is deduced and the band edges for hexagonal and amorphous Se are compared.
- 537.311.33:546.24** 823
Growth of Tellurium Single Crystals by the Czochralski Method—T. J. Davies. (*J. Appl. Phys.*, vol. 28, pp. 1217–1218; October, 1957.)
- 537.311.33:546.28** 824
Threshold Energy for Electron-Hole Pair Production by Electrons in Silicon—A. G. Chynoweth and K. G. McKay. (*Phys. Rev.*, vol. 108, pp. 29–34; October 1, 1957.) Measurements of the reverse bias necessary for the onset of multiplication in silicon *p-n* junctions of various widths lead to a value of 2.25 ± 0.10 eV for the threshold energy for electron-hole pair production by energetic electrons. An apparent slight variation of threshold energy with crystallographic direction is noted and the ionization rate is found to be greater for electrons than for holes. The maximum phonon drag opposing the acceleration of an electron up to the threshold energy by a parabolic field distribution is equivalent to a field of 5.2 $\times 10^4$ v/cm.
- 537.311.33:546.281.26** 825
Intrinsic Electrical Conductivity in Silicon Carbide—J. H. Racette. (*Phys. Rev.*, vol. 107, pp. 1542–1544; September 15, 1957.) Measurements on *n*-type hexagonal single crystals are described. The band gap at absolute zero is 3.1 ± 0.2 eV on the assumption of an intrinsic conductivity variation of the form $\sigma = \text{constant} \times \exp(-\Delta E/2kT)$.
- 537.311.33:546.289** 826
Processes of Preparation of Germanium Single Crystals—T. Niimi, H. Baba, N. Ogawa, K. Furusho, and C. Tadachi. (*Rep. Elec. Commun. Lab., Japan*, vol. 5, pp. 5–9; May, 1957.) Accepted production methods are outlined and some special techniques are described which have been developed to solve problems in the processes of reduction, zone melting, and preparation of single crystals.
- 537.311.33:546.289** 827
Free Bonds on the Clean Surfaces of Germanium Single Crystals—A. Kobayashi and S. Kawaji. (*J. Phys. Soc. Japan*, vol. 12, p. 1054; September, 1957.) Field effect patterns have been observed on clean and oxidized surfaces. The density of the fast states is estimated at 1.7 $\times 10^{13}$ cm⁻² eV for a clean surface and 2.4 $\times 10^{13}$ cm⁻² eV for an oxidized surface.
- 537.311.33:546.289** 828
Detection of Both Vacancies and Interstitials in Deformed Germanium—J. N. Hobstetter and P. Breidt, Jr. (*J. Appl. Phys.*, vol. 28, pp. 1214–1215; October, 1957.) Experimental evidence supporting the view that interstitials, as well as vacancies, form during deformation of Ge was developed from studies of the effect of small compressions on the electrical conductivity of specimens of various initial conductivities.

- 537.311.33:546.289:534.2-8 829
Acousto-electric Effect in *n*-Type Germanium—W. Sasaki and E. Yoshida. (*J. Phys. Soc. Japan*, vol. 12, p. 979; August, 1957.) The flow of acoustic energy through a Ge crystal has been measured over a range of ultrasonic frequencies. The results confirm the prediction made by Parmenter (2281 of 1953) concerning the interaction of electrons and acoustic waves. See also 1039 of 1957 (Weinreich).
- 537.311.33:546.289:539.16 830
Effect of Irradiation on the Hole Lifetime of *N*-Type Germanium—O. L. Curtis, Jr., J. W. Cleland, J. H. Crawford, Jr., and J. C. Pigg. (*J. Appl. Phys.*, vol. 28, pp. 1161-1165; October, 1957.) The minority-carrier lifetime in *n*-type Ge is extremely sensitive to irradiation by fast neutrons and γ rays. The simple dependence of recombination rate on irradiation received, permits prediction of the expected decrease in lifetime in a known radiation field. For the same change in carrier concentration, change in lifetime is much smaller when produced by γ radiation than by fast neutrons
- 537.311.33:546.431-31 831
Fundamental Absorption of Barium Oxide from its Reflectivity Spectrum—F. C. Jahoda. (*Phys. Rev.*, vol. 107, pp. 1261-1265; September 1, 1957.) Results compare favorably with those obtained previously by Zollweg (2024 of 1955) from transmission measurements with thin films.
- 537.311.33:546.682.19:535.3 832
Optical Absorption in *p*-Type Indium Arsenide—F. Stern and R. M. Talley. (*Phys. Rev.*, vol. 108, pp. 158-159; October 1, 1957.) An absorption peak, observed on the long-wavelength side of the intrinsic absorption edge, is attributed to transitions between the light- and heavy-hole bands and a smaller peak at 0.055 eV to lattice absorption.
- 537.311.33:546.682.86:537.312.9 833
Piezoresistive Effect in Indium Antimonide—F. P. Burns and A. A. Fleischer. (*Phys. Rev.*, vol. 107, pp. 1281-1282; September 1, 1957.) "Room-temperature measurements on the variation of resistivity of pure InSb with hydrostatic and uniaxial stress were made to determine the piezoresistive and elastoresistive coefficients of pure InSb. The results are consistent with a spherical conduction-band model."
- 537.311.33:546.817.221:621.314.7 834
Transistor Action on Natural Galena Surface after Heat Treatment with H₂S—J. N. Das and P. V. Khandekar. (*Z. Phys.*, vol. 147, pp. 271-276; January 10, 1957. In English.) Report of experiments on *n*-type galena crystals. Transistor action and photovoltaic effects were observed. See also 2560 of 1956 (Bhide *et al.*).
- 537.312.62 835
Superconducting Alkaline Earth Compounds—B. T. Matthias and E. Corenzwit. (*Phys. Rev.*, vol. 107, p. 1558; September 15, 1957.)
- 537.323 836
Friedel Theory of Thermoelectric Power Applied to Dilute Magnesium Alloys—E. I. Salkovitz, A. I. Schindler, and E. W. Kammer. (*Phys. Rev.*, vol. 107, pp. 1549-1552; September 15, 1957.)
- 537.324:539.23 837
Juxtaposition Thermocouples in the form of Thin Films—A. Aron. (*C. R. Acad. Sci., Paris*, vol. 245, pp. 48-50; July 1, 1957.) Report of measurements on thermocouple systems, one element of which is a film of Ag or Al on pyrex glass, and the other a film of Cu₂O, Te or antimony oxide deposited on an Al or Ag film.
- 537.582:546.883 838
Thermionic Emission from a Planar Tantalum Crystal—H. Shelton. (*Phys. Rev.*, vol. 107, pp. 1553-1557; September 15, 1957.) For a clean [211] surface the work function is 4.352 ± 0.01 eV and the emission constant A is $120 \text{ A/cm}^2 \text{ } ^\circ\text{K}^2$. Results for contaminated surfaces are also given.
- 538.22 839
The Magnetic Properties of Iron Selenide Single Crystals—K. Hirakawa. (*J. Phys. Soc., Japan*, vol. 12, pp. 929-938; August, 1957.) Large single crystals of Fe₇Se₈ and Fe₃Se₄ were prepared and their magnetic properties investigated below the Curie point. A change in the direction of easy magnetization occurs for the former but not for the latter crystal.
- 538.221 840
Magnetic Domain Patterns on Single-Crystal Iron Whiskers—R. V. Coleman and G. G. Scott. (*Phys. Rev.*, vol. 107, pp. 1276-1280; September 1, 1957.) These have been investigated using the Bitter powder technique. Whiskers with axes along the [111] and [100] directions have a very simple domain structure in the unmagnetized state.
- 538.221 841
The Investigation of the Magnetic Reversal Process in High-Coercivity Alnico by means of the Powder Pattern Technique—W. Andrä. (*Ann. Phys., Lpz.*, vol. 19, pp. 10-18; November 15, 1956.) Continuation of the work of Kussman and Wollenberger (3805 of 1956).
- 538.221 842
Remarks of Zener's Classical Theory of the Temperature Dependence of Magnetic Anisotropy Energy—R. Brenner. (*Phys. Rev.*, vol. 107, pp. 1539-1541; September 15, 1957.) The temperature dependence of the first anisotropy constant for Ni is calculated by averaging the local anisotropy over a Langevin function. Reasonably good agreement with the experimental curve is obtained for $T/\theta_c > 0.3$.
- 538.221 843
Anhyseretic Remanent Magnetization of Ferrimagnetics—F. Rimbart. (*C. R. Acad. Sci., Paris*, vol. 245, pp. 406-408; July 22, 1957.) Remanence characteristics of Fe₃O₄ and α -Fe₂O₃ samples subjected to a continuous field superimposed on a decreasing alternating field are shown.
- 538.221 844
Evidence for Subgrains in MnBi Crystals from Bitter Patterns—W. C. Ellis, H. J. Williams, and R. C. Sherwood. (*J. Appl. Phys.*, vol. 28, pp. 1215-1216; October, 1957.)
- 538.221:539.23:53.087.63 845
Magnetic Writing on Thin Films of MnBi—H. J. Williams, R. C. Sherwood, F. G. Foster, and E. M. Kelley. (*J. Appl. Phys.*, vol. 28, pp. 1181-1184; October, 1957.) The domain structure of thin films ($\sim 1000 \text{ \AA}$) of MnBi and their capability of storing information magnetically have been studied. Information can be read optically using the Faraday effect. The films have a uniaxial direction of easy magnetization normal to their surfaces and retain magnetization after saturation along this direction in spite of the large demagnetizing factor. High optical contrast between writing and background can be obtained.
- 538.221:[621.318.124+621.318.134 846
Magnetic Anisotropy of Cobalt Ferrite (Co₁₋₀₁Fe₂₋₀₀O₃₋₆₂) and Nickel Cobalt Ferrite (Ni_{0.72}Fe_{0.20}Co_{0.08}Fe₂O₄)—H. Shenker. (*Phys. Rev.*, vol. 107, pp. 1246-1249; September 1, 1957.) Measurements of the first magnetic anisotropy constant K_1 are described. The results are similar to those for metallic ferromagnetic materials for which the temperature variation of K_1 is expressed in the form $K_1(T)/K_1(0) = \exp(-aT^2)$.
- 538.221:621.318.134 847
Ferrimagnetic Resonance of Erbium Garnet at 9400 Mc/s—J. Paulevé. (*C. R. Acad. Sci., Paris*, vol. 245, pp. 408-411; July 22, 1947.) Experimental results were obtained for temperatures from 4°K to 530°K. The compensation temperature is 84°K. See also 3214 of 1957.
- 538.224:546.3-1'56'47 848
The Magnetic Susceptibility of α and β Brass—B. G. Childs and J. Penfold. (*Phil. Mag.*, vol. 2, pp. 389-403; March, 1957.) Measurements of magnetic susceptibility were made at 77° and 300°K on a series of Cu-Zn alloys. The results are discussed with reference to the theory proposed by Henry and Rogers (2824 of 1956).
- 538.632 849
Hall Effect in Titanium, Vanadium, Chromium and Manganese—S. Foner. (*Phys. Rev.*, vol. 107, pp. 1513-1516; September 15, 1957.) Measurements have been made at room temperature with fields up to 30 000 oersteds. The effect is linear with magnetic field and positive.
- 538.632:546.32-1:539.23 850
Hall Effect and Conductivity Measurements on Thin Films of Potassium—W. Cirkler. (*Z. Phys.*, vol. 147, pp. 481-498; January 12, 1957.) Measurements were made for a thickness range of 30-2000 Å. Experimental results are compared with those obtained theoretically.
- 549.514.5:539.185.9 851
Effect of Rapid Neutrons on some Physical Constants of Crystalline Quartz and Vitreous Silica—G. Mayer and J. Gigon. (*J. Phys. Radium*, vol. 18, pp. 109-114; February, 1957.)
- 621.315.612+621.318.124+621.318.134 852
Some New Electrical and Magnetic Ceramics—G. Campbell. (*J. Sci. Instr.*, vol. 34, pp. 337-348; September, 1957.) Well-known insulating and conducting ceramics are briefly discussed and the ferroelectric and ferromagnetic types are examined in some detail. Their applications are described including transducers, dielectric amplifiers, storage devices, and microwave components, and including future developments in "solid" circuits.
- 621.315.614.6:621.317.335.3.029.64 853
Dielectric Anisotropy of Paper at 3400 Mc/s. Influence of Humidity—R. Servant and J. Cazayus-Claverie. (*C. R. Acad. Sci., Paris*, vol. 245, pp. 509-511; July 29, 1957.) Extension of earlier measurements at 9 350 mc [3140 of 1956 (Servant and Gougeon)] gives similar results; strong birefringence accompanied by rectilinear dichroism.
- 621.357.53 854
Conductive and Resistive Coatings—R. J. Phair. (*Bell Lab. Rec.*, vol. 35, pp. 331-335; September 1957.) Details are given of the preparation of conductive layers by the use of resins and lacquers pigmented with metals or carbon. These are applied like paint to give thin resistive films in complex patterns.

MATHEMATICS

- 518.2 855
Mathematical Tables—a Bibliography—C. R. Sexton. (*Product Eng.*, vol. 28, pp. 183-194; July, 1957.) An annotated list of mainly American publications.

MEASUREMENTS AND TEST GEAR

- 529.786+621.3.018.41(083.74) 856
Standards of Time and Frequency—L. Essen. (*Research, London*, vol. 10, pp. 217–224; June, 1957.) The mean solar second is used for current purposes and is uniform to approximately ± 5 parts in 10^9 . A quartz clock used at the National Physical Laboratory since June, 1955 and calibrated by a caesium atomic standard to an accuracy within ± 1 part in 10^{10} provides a basis for monitoring msf standard-frequency transmissions. Astronomical standards will still be required for preserving the continuity of time measurements over long periods.
- 621.3.018.41(083.74):621.396.666 857
Fade-Cancelling Zero-Beat Indicator for Reception of Standard Radio Frequencies—R. J. Blume. (*Rev. Sci. Instr.*, vol. 28, pp. 703–708; September, 1957.) A simple circuit is described which enables a local secondary frequency standard to be set quickly to a definite zero beat with a received sw standard-frequency signal, without the usual uncertainty due to amplitude fading of the signal. The bandwidth of the device may be made much less than 1 cps.
- 621.3.089.6:061.6 858
Electronic Calibration Centre of the National Bureau of Standards—(*Engineer, London* vol. 203, pp. 852–853; May 31, 1957.) Description of the center under construction at Boulder, Colo., which will provide greatly expanded facilities for calibration services at all frequencies in general use.
- 621.317.2:621.373.42 859
Simplified General-Purpose Signal Generator—M. W. Kirby. (*Short Wave Mag.*, vol. 15, pp. 243–244; July, 1957.) A low-cost circuit using two tubes: one as a cathode-coupled oscillator, allowing wide frequency coverage by means of coil switching, the other as modulator
- 621.317.2:621.373.52:621.397.62 860
A Transistorized TV Bar Generator—T. G. Knight. (*Radio TV News*, vol. 58, pp. 48–49; September, 1957.) A self-contained television pattern generator for checking the linearity of deflection circuits. It operates over a range 48–64 mc.
- 621.317.3:621.314.7 861
Accurate Measurement of r_c and α_0 for Transistors—M. A. Melehy. (*Proc. IRE*, vol. 45, pp. 1739–1740; December, 1957.)
- 621.317.3:621.372.412.088.33 862
Tolerances of Quartz Crystals for Filters and their Measurement—Kurth and Miczynski. (See 697.)
- 621.317.335.3.029.63/.64 863
Method of Measurement to Determine the Complex Dielectric Constant at Wavelengths from 8 to 80 cm and Temperatures to -150°C —H. K. Ruppersberg. (*Z. angew. Phys.*, vol. 9, pp. 9–13; January, 1957.) The method described is one of input impedance measurement on a coaxial line filled with the liquid under test. Special arrangements are made to counter the effects of low temperature, including the use of a short-circuit plunger (1198 of 1957.) The method is particularly suitable for lossy materials; errors range from 1 to 5 per cent. A modification of another method [2160 of 1956 (Lueg and Ruppersberg)] is outlined which is suitable for solid disk-shaped specimens.
- 621.317.335.3.029.64 864
Measurement of the Complex Dielectric Constant of Very-High-Dielectric-Constant Materials at Microwave Frequencies—I. Brady. (*Commun. & Electronics*, no. 30, pp. 225–228; May, 1957.) Two methods of measurement are described, one for low-loss and the other for high-loss specimens. A short-circuited waveguide is used in both cases, but greater sensitivity is obtained than with conventional methods.
- 621.317.335.3.029.64:546.217 865
Microwave Refractometer Cavity Design—A. W. Adey. (*Can. J. Technol.*, vol. 34, pp. 519–521; March, 1957.) The operation of the instrument involves the comparison of the resonance frequency of a sealed reference cavity with that of a cavity exposed to the atmosphere. Limitations of the instrument due to the flushing time of the ventilated cavity are avoided in a design described in which 67 per cent of the end area is cut away without affecting the cavity Q. Operation is in the TE₀₁₁ mode at 9.1 kmc.
- 621.317.335.3.029.64/.65 866
Measurement of the Complex Dielectric Constant of Liquids at Centimetre and Millimetre Wavelengths—A. G. Mungall and J. Hart. (*Can. J. Phys.*, vol. 35, pp. 995–1003; September, 1957.) A free-space method is described for the measurement of absorption and reflection coefficients. Results obtained for methyl and ethyl alcohol at 13 and 9 mm λ agree with those previously quoted by other authors.
- 621.317.351:621.316.825 867
The Measurement of the Dynamic Characteristics of Thermistors—G. Barzilai. (*Note Recensioni Notiz.*, vol. 6, pp. 343–348; May/June, 1952.) Oscillograms of voltage and current are given which were obtained in tests made at frequencies between 0.02 and 5 cps. The method described, in which a double-beam cro is used, permits the direct observation of waveforms at the thermistor terminals.
- 621.317.39:531.74.07 868
Design, Performance and Application of the Vernier Resolver—G. Kronacher. (*Bell Sys. Tech. J.*, vol. 36, pp. 1487–1500; November, 1957.) Description of an angle transducer consisting of a variable-coupling transformer with the primary winding on a rotor and the secondary windings on a stator. Repeatability within ± 3 seconds of shaft rotation is possible.
- 621.317.39:534.154 869
Vibration Measurements—J. T. Broch. (*Electronic Eng.*, vol. 29, pp. 575–579; December, 1957.) Principles of the technique and a particular BaTiO₃ accelerometer are described.
- 621.317.616:621.373.4.029.3 870
Audio-Frequency Sweep Generator—R. Graham. (*Radio TV News*, vol. 58, pp. 63–65, 140; August, 1957.) The unit covers a range 30 cps–2 kc in one sweep, three times a second. A crystal-controlled oscillator beats with a variable-frequency oscillator controlled by a reactance tube and a 3-cps sawtooth waveform.
- 621.317.725.029.6 871
A Millivoltmeter for Ultra-high Frequencies—C. C. Eaglesfield. (*Electronic Eng.*, vol. 29, pp. 603–694; December, 1957.) The technique of measurement involves the use of a modulated vhf source, the detection of the signal by a crystal diode probe, and the subsequent amplification and measurement of the modulation.
- 621.317.729.1 872
Note on the Measurement of Gradient in the Electrolyte Tank—A. Lepschy, U. Pellegrini, and A. Ruberti. (*Note Recensioni Notiz.*, vol. 6, pp. 327–335; May/June, 1957.) The suitability of various types of probes for plotting gradients in electrolyte tanks is discussed. A four-electrode type appears preferable; test results obtained with it are given and a specially designed probe holder is described.
- 621.317.77 873
Extended-Angular-Range Direct-Reading Phase Meter—S. Bigelow and J. Wuorinen, Jr. (*Rev. Sci. Instr.*, vol. 28, pp. 713–717; September, 1957.) A direct-reading pulse-position comparison instrument is described which enables angles from 540° lagging to 540° leading to be measured to $\pm 1^\circ$ for input amplitudes from 0.1 to 100 v.

OTHER APPLICATIONS OF RADIO AND ELECTRONICS

526.2:621.396.9 874
Precise Measurement of Distance by Microwaves—R. Hammond. (*Instr. Practice*, vol. 11, pp. 828–831 and 942–945; August and September, 1957.) A description of the "Tellurimeter" giving results of a series of operational tests. See 3250 of 1957.

531.76.621.374.3 875
One-Tenth-Microsecond, Multichannel Chronograph—L. E. Bollinger. (*Aust. J. Instr. Tech.*, vol. 13, pp. 97–104; August, 1957.) Circuit details and description of an instrument for measuring the velocity of combustion waves, using optical or insulated probes and Schmitt trigger, oscillator, and scaling circuits.

534.23–8:620.179.1 876
Automatic Ultrasonic Inspection—H. W. Taylor. (*J. Brit. IRE*, vol. 17, pp. 649–661; November, 1957.) A description of flaw-detection equipment developed to replace earlier manual inspection.

621.384.613 877
The Development of Iron-Free Betatrons with an Operating Frequency of 2.5 and 8.0 kc/s—G. Hentze. (*Ann. Phys., Lpz.*, vol. 19, pp. 55–81; November 15, 1956.) Design details of a 2.5-kc and an 8-kc pulsed betatron incorporating air-cored inductors are given.

621.385.833 878
The Computation of Rotationally Symmetrical Potential Fields in Electron Lenses—F. Lenz. (*Ann. Phys., Lpz.*, vol. 19, pp. 82–88; November 15, 1956.) A modification of Regensstreif's theory (2500 of 1951) for the three-electrode lens is discussed and approximation methods are compared.

621.387.422 879
Boron Trifluoride Counters—J. J. Beauval, S. Dousson, and P. Prugne. (*Le Vide*, vol. 12, pp. 208–214; May/June, 1957.) A description of the techniques used at Saclay for detecting neutrons.

621.398:681.142 880
A Simple Shaft Digitizer and Store—Tiffany. (See 690.)

655.3.024:621–523.8 881
Colour Printing—(*Electronic Radio Eng.*, vol. 35, pp. 26–28; January, 1958.) Description of an electronic method of color correction applied in block-making.

PROPAGATION OF WAVES

621.396.11 882
A Note on the Propagation of the Transient Ground Wave—J. R. Wait. (*Can. J. Phys.*, vol. 35, pp. 1146–1151; September, 1957.) Formulas are derived showing how idealized pulses, represented by ramp, step, and pulse functions, are modified by propagation.

621.396.11:523.5 883
The Forward-Scattering of Radio Waves from Overdense Meteor Trails—C. O. Hines and P. A. Forsyth. (*Can. J. Phys.*, vol. 35, pp.

- 1033-1041; September, 1957.) An approximate formula has been obtained by using a simplified working model. The received power is found to vary as the square root of the initial line density of electrons and the transition between underdense and overdense trails occurs at the same value of charge density as in the backscatter case.
- 621.396.11:523.5:621.396.43 884
Some Airborne Measurements of V.H.F. Reflections from Meteor Trails—J. P. Casey and J. A. Holladay. (PROC. IRE, vol. 45, pp. 1735-1736; December, 1957.) The probability of simultaneous reception of meteor bursts at separated receivers was investigated using one fixed receiver and one installed in an aircraft.
- 621.396.11:523.72 885
On the Effect of Solar Ultra-radiation on Radio Propagation Conditions on 23rd February 1956—B. Beckmann, P. Dietrich, and H. Salow. (Nachr. Tech. Z., vol. 10, pp. 329-334; July, 1957.) Report of observations carried out under conditions favorable for assessing the effects of high-energy corpuscular radiation. Results of measurements obtained in various parts of the northern hemisphere are analyzed and discussed.
- 621.396.11:551.510.52 886
The Possible Transmission Band for Long-Range Tropospheric Propagation—V. N. Troitski. (Radiotekhnika, Moscow, vol. 11, pp. 3-7; September, 1956.) The distortion of transmission is considered on the assumption that the atmosphere is anisotropic and that the horizontal inhomogeneities of permittivity are smaller than the vertical inhomogeneities. Formulas are derived for determining the band for distortionless transmission. The effect of the directivity of antennas on the possible transmission band is analyzed. See also 1216 of 1957.
- 621.396.11:551.510.535 887
Brief Outline of Modern Concepts on the Propagation of Radio Waves in the Ionosphere—Ya. L. Al'pert. (Izv. Ak. Nauk S.S.S.R., Ser. geofiz., no. 11, pp. 1418-1430; November, 1957.) The influence on wave propagation of earth curvature and heterogeneity of surface is discussed. The effect of ionospheric inhomogeneity and propagation in the troposphere is considered. Fifty-six references.
- 621.396.11:551.510.535 888
Back-Scatter Sounding: an Aid to Radio Propagation Studies—A. F. Wilkins and E. D. R. Shearman. (J. Brit. IRE, vol. 17, pp. 601-616; November, 1957.) A comprehensive account of the radar technique for studying ionospheric propagation. Theoretical and practical aspects are treated. Results obtained at Slough at frequencies between 10 and 26 mc are discussed; seasonal variations of echo patterns, very-long-range scattering, and errors due to antenna beam width are included. The utility of the rotating-antenna system is stressed.
- 621.396.11.029.62 889
V.H.P. Propagation Measurements in the Rocky Mountain Region—R. S. Kirby, H. T. Dougherty, and P. L. McQuate. (IRE TRANS. vol. VC-6, pp. 13-19; July, 1956. Abstract, PROC. IRE, vol. 44, p. 1213; September, 1956.)
- 621.396.11.029.62:551.510.535 890
The Scattering of Radio Waves of Very High Frequency in the Ionosphere—T. V. Ionescu. (C.R. Acad. Sci., Paris, vol. 245, pp. 520-522; July 29, 1957.) Vhf transmission over distances greater than 1000 km [see 243 of 1956 (Bailey et al.)] can be explained on the basis of the large number of negative oxygen ions at heights between 50 and 90 km having natural periods of vibration similar to the wavelengths used.
- 621.396.11.029.62:551.510.535 891
N.B.S. Equatorial-Region V.H.F. Scatter Research Program for the I.G.Y.—K. Bowles and R. Cohen. (QST, vol. 41, pp. 11-15; August, 1957.) Scattering from elongated centers in the F region over a 2580-km path centered on the magnetic equator is to be attempted. Reception by amateurs at greater ranges is suggested.
- 621.396.11.029.62:621.396.82 892
The Occurrence of E_s and F₂ Skip in the 30-50 Mc/s Mobile Band—E. W. Allen. (IRE TRANS., vol. VC-6, pp. 39-42; July, 1956.) Possible interference in the 30-50-mc band allocated for mobile services is discussed, considering skip-distance/frequency curves and field strength data from earlier reports. For a typical 250-w base station with antenna 200 feet above ground, interference via the F₂ layer from a similar station 2200 miles away may reduce the median service radius from 60 to 12 miles. Interference via the E_s layer from a similar station 1000 miles away may reduce the radius to 36 miles.
- 621.396.11.029.64 893
On the Radio Wave Propagation in a Stratified Atmosphere: Part 2—R. Yamada. (J. Phys. Soc. Japan, vol. 12, pp. 1022-1030; September, 1957.) The field produced by a microwave antenna is calculated assuming that the refractive index varies with height according to a second-order expression. The solution gives a series of rays reflected 1, 2, 3, or more times from the ground; these rays explain the "duct" mode of propagation. A possible explanation is given for the deep fading associated with duct propagation. Part 1: 2088 of 1955.
- 621.396.11.029.64:621.3.018.7 894
Distortion in Tropospheric Scatter Propagation—H. Bremmer. (Philips Telecommun. Rev., vol. 18, pp. 137-154; September, 1957.) The Booker-Gordon theory is extended to transmitter currents that are not time-harmonic functions. The average intensity of the field scattered by a single "blob" is first derived and the summation of the field contributions due to the total scattering volume leads to a "convolution product." This is shown to depend on the Fourier spectrum of the "delay-time function" with which all distortion effects are connected. An approximate evaluation shows that the received field is equivalent to a small number of components with different amplitudes and delays. As a numerical example the distortion in FM frequency-division multiplex is found to depend on the relative amplitudes of the delayed signals.

RECEPTION

- 621.396.62:621.314.7 895
Midget Self-Contained Transistor Receiver—S. F. Weber. (R.S.G.B. Bull., vol. 33, pp. 66-58; August, 1957.) Circuit and construction details of a fixed-tuned medium-wave receiver incorporating a built-in ferrite rod antenna and a hearing-aid earpiece.
- 621.396.62:621.314.7 896
Transistorized Regenerative Receiver—(QST, vol. 41, pp. 36-37; July, 1957.) Circuit and constructional details of a two-transistor receiver suitable for the 80-, 40-, and 20-m bands.
- 621.396.62:629.11 897
Car Radio Receiver Design—J. C. Beckley. (Wireless World, vol. 64, pp. 36-40; January, 1958.) A hybrid circuit for 12-v operation with transistor output.
- 621.396.621.54 898
The Interceptor—C. W. Cragg. (R.S.G.B. Bull., vol. 33, pp. 56-60; August, 1957.) Circuit details of a simple double-superheterodyne communication receiver for the amateur.
- 621.3.018.41(083.74):621.396.666 899
Fade-Cancelling Zero-Beat Indicator for Reception of Standard Radio Frequencies—Blume. (See 857.)
- 621.396.823 900
Receiving Aerials and Industrial Interference—V. V. Roditi and M. S. Gartsenshtein. (Radiotekhnika, Moscow, vol. 11, pp. 21-27; September, 1956.) Methods are discussed for determining the effective height of indoor antennas and a coefficient of interference transfer as the main parameters determining the quality of radio reception in towns. Data are given on measurements of these quantities in some cities of the U.S.S.R., and the results obtained are analyzed statistically.

STATIONS AND COMMUNICATION SYSTEMS

- 621.376.56 901
What Use is Delta Modulation to the Transmission Engineer?—F. K. Bowers. (Commun. & Electronics, no. 30, pp. 142-147; May, 1957.) The signal/noise ratio and pulse rate of the delta modulation system are compared with those for pcm, and the coding and decoding arrangements are discussed. See also 3084 of 1955 (Zetterberg).
- 621.391 902
Information-Theory Impact on Modern Communications—P. Mertz. (Commun. & Electronics no. 32, pp. 431-437; September, 1957. Elec. Eng., New York, vol. 76, pp. 659-664 and 773-776; August and September, 1957.) The contributions made by Nyquist and Hartley and the concept of entropy are examined, and their influence on practical communications is outlined, with reference to facsimile, television, and telephony systems.
- 621.391 903
Non-binary Error Correction Codes—W. Ulrich. (Bell Sys. Tech. J., vol. 36, pp. 1341-1388; November, 1957.) A theoretical study of the problem of correcting information which has become distorted by transmission via a noisy channel. Codes are derived for correcting any single unrestricted error in a message of arbitrary length and for correcting a number of errors in messages of restricted length, for an arbitrary number of different signals.

- 621.391 904
Shortest-Connection Networks and some Generalizations—R. C. Prim. (Bell Sys. Tech. J., vol. 36, pp. 1389-1401; November, 1957.) A consideration of the problem of interconnecting a given set of terminals with the shortest possible network of direct links. Simple graphical and computational methods are described.

- 621.391:621.396.822 905
Conditions for the Equivalence of the Statistical Properties of Radio Communication Systems with a Large Number of Random Parameters—V. I. Siforov and Yu. B. Sindler. (Dokl. Ak. Nauk S.S.S.R., vol. 116, pp. 956-958; October 21, 1957.) Short analysis concerning signal/noise ratio in radio relay and radio-location systems. See also 1586 of 1957 (Sindler).

- 621.396.3:621.396.41:523.5 906
On the Influence of Meteor-Radiant Distributions in Meteor-Scatter Communication—M. L. Meeks and J. C. James. (Proc. IRE, vol. 45, pp. 1724-1733; December, 1957.) An idealized distribution in which the radiants lie near the ecliptic is analyzed and the results compared with previous calculations for a uniform radiant distribution. Some experimental data show evidence of a rather diffuse concentration of radiants near the ecliptic. A method for predicting the contributions of meteor showers to forward-scatter propagation is developed and applied to an example.
- 621.396.3:621.396.43 907
Storage Capacity in Burst-Type Communication Systems—L. L. Campbell. (Proc. IRE, vol. 45, pp. 1661-1666; December, 1957.) Mean rate of transfer of information is derived, in terms of storage capacity, for known probability distributions of signal duration and interval between signals.
- 621.396.3:621.396.43:523.5 908
The Principles of JANET—a Meteor-Burst Communication System—P. A. Forsyth, E. L. Vogan, D. R. Hansen, and C. O. Hines. (Proc. IRE, vol. 45, pp. 1642-1657; December, 1957.) Propagation characteristics and design considerations of the system are surveyed and preliminary operating experience is summarized.
- 621.396.3:621.396.43:523.5 909
Bandwidth Considerations in a JANET System—L. L. Campbell and C. O. Hines. (Proc. IRE, vol. 45, pp. 1658-1660; December, 1957.) "It is shown that the mean rate of transfer of information increases with bandwidth, for bandwidths in the range currently contemplated, in spite of the consequent decrease in the duty cycle. A system designed to maintain a constant signal/noise ratio by varying the bandwidth with received signal power is discussed, and its advantage over a fixed bandwidth system is calculated."
- 621.396.3:621.396.43:523.5 910
The Canadian JANET System—G. W. L. Davis, S. J. Gladys, G. R. Lang, L. M. Luke, and M. K. Taylor. (Proc. IRE, vol. 45, pp. 1666-1678; December, 1957.) The equipment is designed for use with double sideband AM vhf radio links having 3-kc bandwidths. Standard 60-wpm teletype machines are used, the instantaneous transmission rate (obtained automatically in both directions whenever a meteor reflection giving adequate signal/noise ratio is present) being 1300 wpm. The messages are initially stored in parallel on paper tape in standard 5-digit form. Over the radio link they appear as a ppm code having two pulse positions for each digit of the teletype code, together with a synchronizing tone. At the receiver the message is reconverted from ppm to pcm and stored in parallel on magnetic tape. The read-out mechanism, operating continuously at 60 wpm, removes the message from the store and converts it into a standard $7\frac{1}{2}$ -digit serial code to operate the printer. An average information rate of 60 wpm with an error rate of 0.09 per cent has been achieved when using 500-w transmitters with 5-element Yagi antennas, over a 600-mile path in Canada.
- 621.396.3:621.396.43:523.5 911
The Utility of Meteor Bursts for Intermittent Radio Communication—G. F. Montgomery and G. R. Sugar. (Proc. IRE, vol. 45, pp. 1684-1693; December, 1957.) Transmission experiments at vhf in a 100-kc band show that about half the signal bursts are distorted by multipath effects.
- 621.396.3:621.396.43:523.5 912
A Meteor-Burst System for Extended-Range V.H.F. Communications—W. R. Vincent, R. T. Wolfram, B. M. Sifford, W. E. Jaye, and A. M. Peterson. (Proc. IRE, vol. 45, pp. 1693-1700; December, 1957.) Describes equipment transmitting teletype or speech information over an 820-mile path. A frequency-shift system is used for teletype with a 2-kw transmitter and 3-element Yagi antennas, the information being sent at 600 wpm during bursts. SSB is used for speech, which is transmitted at five times normal rate in a band of 16.5 kc wide with a power of 1 kw. Magnetic-tape storage is used at the receiver in both cases.
- 621.396.3:621.396.43:523.5 913
Analysis of Oblique-Path Meteor-Propagation Data from the Communications Viewpoint—W. R. Vincent, R. T. Wolfram, B. M. Sifford, W. E. Jaye, and A. M. Peterson. (Proc. IRE, vol. 45, pp. 1701-1707; December, 1957.) Characteristics such as duration, interval between usable signals, antenna direction effects, diurnal rate and duty cycle, and rate of signal decay are presented.
- 621.396.3:621.396.43:523.5 914
An Investigation of Storage Capacity Required for a Meteor-Burst Communications System—R. A. Rach. (Proc. IRE, vol. 45, pp. 1707-1709; December, 1957.) A theoretical analysis of systems having storage either with or without simultaneous read-out.
- 621.396.3:621.396.43:523.5 915
On the Wavelength Dependence of the Information Capacity of Meteor-Burst Propagation—V. R. Eshleman. (Proc. IRE, vol. 45, pp. 1710-1714; December, 1957.) The wavelengths dependence of the information capacity of meteor-burst propagation is approximately $\lambda^{2.7}$, to be compared with $\lambda^{4.7}$ for the continuous forward-scatter. The advantages to which this leads are pointed out.
- 621.396.3:621.396.43:523.5:621.397.2 916
Experimental Facsimile Communication Utilizing Intermittent Meteor Ionization—W. H. Bliss, R. J. Wagner, Jr., and G. S. Wickizer. (Proc. IRE, vol. 45, pp. 1734-1735; December, 1957.) Preliminary results obtained over a 910-mile path at 40 mc gave encouraging results; one frame was transmitted per meteor burst.
- 621.396.3:621.396.43:621.396.812.3 917
Intermittent Communication with a Fluctuating Signal—G. F. Montgomery. (Proc. IRE, vol. 45, pp. 1678-1684; December, 1957.) Analysis of a Rayleigh distribution of signal amplitudes suggests that intermittent operation when the signal is high gives greater average transmission rates than with continuous operation for the same average message error. Binary FM and PM are considered.
- 621.396.41:621.318.57.01 918
A Network containing a Periodically Operated Switch Solved by Successive Approximations—C. A. Desoer. (Bell Sys. Tech. J., vol. 36, pp. 1403-1428; November, 1957.) The analysis of a basic system, such as is used in multiplex working, consisting of two reactive networks connected for a time τ with switching period T . The ratio τ/T is taken as 10^{-3} , considered to be as small as practicable. Examples are given of the application of the method which involves less work than the rigorous treatment of Bennett (IRE TRANS, vol. CT-2, pp. 17-22; March, 1955.)
- 621.396.41:621.396.65:621.372.55 919
Experimental Transversal Equalizer for TD-2 Radio Relay System—B. C. Bellows and R. S. Graham. (Bell Sys. Tech. J., vol. 36, pp. 1429-1450; November, 1957.) A correction system, based on the echo principle of a transversal filter, for correcting residual gain and delay distortions in television relay systems. Directional couplers are used for tapping and controlling the leading or lagging echo voltages, required for correction purposes, which are applied in the pass band 60-80 mc. Some details of the assembly and typical field trials are given.
- 621.396.43:523.5:621.396.96 920
Directional Characteristics of Meteor Propagation Derived from Radar Measurements—V. R. Eshleman and R. F. Mlodnosky. (Proc. IRE, vol. 45, pp. 1715-1723; December, 1957.) The geometrical correspondence between the radar and oblique-path detection of meteors is considered, and radar measurements of range and azimuth are used to determine the best directions in which to point the antenna beams on particular oblique paths for maximum duty cycle. For a N-S path the beams should be pointed west of the path at night and east of the path during the day. For an E-W path, north during the morning and south during the evening.
- 621.396.43:621.396.11:523.5 921
Some Airborne Measurements of V.H.F. Reflections from Meteor Trails—Casey and Holladay. (See 884.)
- 621.396.65:029.64 922
New Microwave Repeater System using a Single Travelling-Wave Tube as both Amplifier and Local Oscillator—H. Kurokawa, I. Someya, and M. Morita. (Proc. IRE, vol. 45, pp. 1604-1611; December, 1957.) This system uses a minimum number of vacuum tubes and requires no afc. Output power, frequency stability, and crosstalk are considered. See also 1212 of 1956 (Sawazaki and Honma).
- 621.396.931 923
A Narrow-Band Experimental F.M. Mobile Telephone System—W. A. Miller. (Commun. & Electronics, no. 30, pp. 98-100; May, 1957.) Trials on an experimental split-channel system transmitting on 35.52 mc and receiving on 43.52 mc show that it is feasible to reduce frequency deviation from 15 kc to 7.5 kc to double the number of channels available.

SUBSIDIARY APPARATUS

- 621.311.6:621.373.52 924
The Balanced Transistor D.C. Converter—J. Noordanus. (Philips Telecommun. Rev., vol. 18, pp. 125-136; September, 1957.) A theoretical analysis of operation is given.

- 621.314.63 925
Current/Capacitance Characteristics of Metal Rectifiers—Y. Moriguchi and A. Okazaki. (Proc. Phys. Soc., London, vol. 70, pp. 991-999; October 1, 1957.) Report of measurements and discussion of the reverse current/voltage and capacitance/voltage characteristics of metal rectifiers at room and liquid-air temperatures.

- 621.314.63:546.28 926
Silicon Rectifiers—E. Nitsche. (Elektron. Rundschau, vol. 11, pp. 197-199; July, 1957.) The characteristics are given of an experimental rectifier unit rated at 0.5 a and 650-v peak inverse voltage. It is hermetically sealed in a metal case of 7-mm diameter.

- 621.314.632.1:546.56-1 927
The Influence of the Copper Raw Material on the Properties of Copper-Oxide Rectifiers—F. Eckart and C. Fritzsche. (Ann. Phys., Lpz., vol. 19, pp. 19-30; November 15, 1956.) The characteristics of Cu_2O rectifiers were investigated as a function of manufacturing conditions and degree of purity of the copper used. Results are tabulated and show that rectifier

characteristics are considerably affected by the oxygen content of the copper.

TELEVISION AND PHOTOTELEGRAPHY

621.397.2:621.396.3:621.396.43:523.5 928
Experimental Facsimile Communication utilizing Intermittent Meteor Ionization—Bliss, Wagner, and Wickizer. (See 916.)

621.397.5:621.395.625.3 929
Status of Video Tape in Broadcasting—H. A. Chinn. (*J. Soc. Mot. Pict. Telev. Engrs.*, vol. 66, pp. 453-458; August, 1957.) Experiences in the use of magnetic tape recording for television and some effects produced by faults in the recording equipment or tape are described.

621.397.611.2 930
Wide-Screen Television—S. Rosin and M. Cawein. (*J. Soc. Mot. Pict. Telev. Engrs.*, vol. 66, pp. 404-406; July, 1957. Discussion, p. 406.) In the "scanscope" system described an aspect ratio of 8×3 instead of 4×3 is used. A special lens (see 931 below) compresses an 8×3 scene into 4×3 , which is photographed, transmitted, and expanded electronically in the monitor.

621.397.611.2:771.35 931
Anamorphic Lens System—S. Rosin. (*J. Soc. Mot. Pict. Telev. Engrs.*, vol. 66, pp. 407-409; July, 1957.) The optical design of the anamorphic "scanscope" lens is described and details of its application are given.

621.397.62:621.317.7:621.373.52 932
A Transistorized TV Bar Generator—Knight. (See 860.)

621.397.62:621.396.67:621.372.43 933
A Diplexer Two-Set Coupler—Harris. (See 671.)

621.397.62:621.396.677.029.63 934
Television Antennas for Bands IV and V—Strafford. (See 674.)

621.397.62.029.63 935
Reception on Band V—(*Wireless World*, vol. 64, pp. 7-10; January, 1958.) An introduction to uhf circuit techniques for reception on 650 mc.

621.397.62.029.63 936
Band V on a Turret Tuner—P. R. Stutz. (*Wireless World*, vol. 64, pp. 14-16; January, 1958.) Adaptation of an existing band I-band III television tuner for uhf.

621.397.621:621.385.832.032.2 937
Wobbled Scanning with a New C.R.T.—(*Radio TV News*, vol. 58, pp. 52-53; August, 1957.) Scanning lines are merged by applying a 2-mc oscillation to a split grid in the cr tube.

621.397.621.2:535.623:621.385.832 938
Low-Voltage Colour-Tube Gun Assembly with Periodic Focusing—P. H. Gleichauf and H. Hsu. (*IRE TRANS.*, vol. ED-4, pp. 63-69; January, 1957. Abstract, *PROC. IRE*, vol. 45, p. 897; June, 1957.)

621.397.7(71+73) 939
Television Station List—M. I. Schiller. (*Radio-Electronics*, vol. 28, pp. 82-83; January, 1957.) A list of U. S. and Canadian stations correct to December 1, 1956 giving call sign, location, and channel number.

TRANSMISSION

621.396.61:621.373.42 940
The Design and Construction of a Drive Unit for Amateur Use—N. Shires. (*R.S.G.B. Bull.*, vol. 33, pp. 61-65; August, 1957.) Constructional details of a unit providing a constant output level between 3.5 and 3.8 mc for A1, A2, A3, F1, or F3-type transmissions.

621.396.61:621.376.22 941
Controlled-Carrier Constant Modulation—(*Short Wave Mag.*, vol. 15, pp. 298-299; August, 1957.) A modulation system in which a rectified af voltage is used to modulate the screen grid of a transmitter power amplifier stage. A suggested circuit is shown.

621.396.61:621.376.222 942
Transmitter Cost Trimmed by Series Gate Modulator—R. H. Baer. (*Electronics*, vol. 30, pp. 167-169; November 1, 1957.) In this type of modulator power economy is obtained by varying the average carrier level in step with the modulation level.

TUBES AND THERMIONICS

621.314.63 943
A Theory of Voltage Breakdown of Cylindrical P-N Junctions, with Applications—H. L. Armstrong. (*IRE TRANS.* vol. ED-4, pp. 15-16; January, 1957. Abstract, *PROC. IRE*, vol. 45, p. 897; June, 1957.) See also 3681 of 1957 (Armstrong, et al.).

621.314.63:537.311.33 944
Impedance of Bulk Semiconductor in Junction Diode—T. Misawa. (*J. Phys. Soc. Japan*, vol. 12, pp. 882-890; August, 1957.) The small-signal impedance is shown to have an inductive component, using the low-level solution. This reactance is small compared with the resistive component but it becomes comparable to the junction impedance as the injection level rises.

621.314.63+621.314.7](083.74) 945
IRE Standards on Graphical Symbols for Semiconductor Devices, 1957—(*PROC. IRE*, vol. 45, pp. 1612-1617; December, 1957.) Standard 57 IRE 21.S3.

621.314.632:546.289 946
Minority-Carrier Current across Metal/Germanium Rectifying Contacts—G. Mesnard and A. Dolce. (*C.R. Acad. Sci., Paris*, vol. 245, pp. 42-44; July 1, 1957.) The minority-carrier current is calculated as a function of the applied voltage, taking account of variable lifetimes and surface recombination velocities calculated on the basis of recombination centers.

621.314.632:546.289 947
The Relative Contribution of Majority and Minority Carriers to the Current across Metal/Germanium Rectifying Contacts—G. Mesnard and A. Dolce. (*C.R. Acad. Sci., Paris*, vol. 245, pp. 152-155; July 8, 1957.) Electron and hole currents at the contact and at the limit of the space-charge zone are evaluated as a function of the applied emf. The results are applicable to emitter and collector point contacts of transistors.

621.314.632:621.314.7 948
Small-Signal Wave Effects in the Double-Base Diode—J. J. Suran. (*IRE TRANS.*, vol. ED-4, pp. 34-43; January, 1957. Abstract, *PROC. IRE*, vol. 45, p. 897; June, 1957.) See also 3562 of 1956.

621.314.7 949
Operation and Manufacture of Transistors—A. J. Oliphant. (*R.S.G.B. Bull.*, vol. 33, pp. 107-111; September, 1957.) The basic theory of semiconductors is outlined and its application to transistors is discussed. Manufacturing techniques in producing transistors are briefly described and their present limitations are reviewed.

621.314.7 950
Low-Injection-Level Behaviour and Base Width Measurement in Junction Transistors—D. Long. (*J. Appl. Phys.*, vol. 28, pp. 1219-1220; October, 1957.)

621.314.7 951
The Junction Transistor as a Charge-Controlled Device—J. J. Sparkes and R. Beaufoy. (*PROC. IRE*, vol. 45, pp. 1740-1742; December, 1957.) See 308 of 1958.

621.314.7:621.317.3 952
Accurate Measurement of r_c and a_o for Transistors—M. A. Melehy. (*PROC. IRE*, vol. 45, pp. 1739-1740; December, 1957.)

621.314.7:621.318.57 953
The Effect of Collector Capacity on the Transient Response of Junction Transistors—J. W. Easley. (*IRE TRANS.* vol. ED-4, pp. 6-14; January, 1957. Abstract, *PROC. IRE*, vol. 45, p. 897; June, 1957.) See also 4044 of 1957 (Macdonald).

621.314.7:621.372.57 954
Tandem Transistors with the Properties of Thermionic Valves—H. E. Hollmann. (*Hochfreq. u. Elektroak.*, vol. 65, pp. 149-159; March, 1957.) The relation of junction transistors to space-charge and transit-time tubes is defined in terms of duality. The tandem transistor is almost equivalent to a space-charge tube; some of its applications are discussed (see also 3001 of 1956).

621.314.7:621.385.4 955
The Tetrode Power Transistor—J. T. Maupin. (*IRE TRANS.*, vol. ED-4, pp. 1-5; January, 1957. Abstract, *PROC. IRE*, vol. 45, pp. 896-897; June, 1957.)

621.314.7.012.8 956
Equivalent Circuits for Junction Transistors—L. E. Jansson. (*Mullard Tech. Commun.*, vol. 3, pp. 151-160; June, 1957.) Elements representing each major process in a junction transistor are assembled to form a complete equivalent circuit, which is then converted to a conventional two-generator grounded-base T circuit; other commonly used equivalent circuits are ultimately derived from this.

621.314.7.012.8 957
Base-Width Modulation and the High-Frequency Equivalent Circuit of Junction Transistors—J. Zawels. (*IRE TRANS.*, vol. ED-4, pp. 17-22; January, 1957. Abstract, *PROC. IRE*, vol. 45, p. 897; June, 1957.)

621.383.4:456.682.86 958
Cooled Photoconductive Detectors using Indium Antimonide—D. W. Goodwin. (*J. Sci. Instr.*, vol. 34, pp. 367-368; September, 1957.) "Improvement in the sensitivity of InSb photoconductive cells which operate at room temperature can be achieved under certain conditions by cooling cells to temperatures below ambient. Details of the performance of such cooled cells are given."

621.383.42 959
Resensitization of Selenium Photocells at Low Temperatures by the Action of the Near-Infrared—G. Blet. (*J. Phys. Radium*, vol. 18, pp. 121-127; February, 1957.) See 607 of 1957.

621.383.42 960
Internal Resistance and Capacitance of Selenium Photocells at Low Temperatures—G. Blet (*J. Phys. Radium*, vol. 18, pp. 297-303; May, 1957). Forward and reverse conductances of normal and reactivated cells have been measured as a function of the applied potential difference in the range 0.001-5v and at 66°-300°K. Observed variations extended over a range of 1-10%. See also 1266 and 2951 of 1957.

621.385.029.6 961
Potential-Minimum Noise in the Microwave Diode—A. E. Siegman and D. A. Watkins. (*IRE TRANS.*, vol. ED-4, pp. 82-86;

- January, 1957. Abstract, PROC. IRE, vol. 45, pp. 897-898; June, 1957.)
- 621.385.029.6 962
Linear Beam-Tube Theory—C. C. Wang. (IRE TRANS., vol. ED-4, pp. 92-106; January, 1957. Abstract, PROC. IRE, vol. 45, p. 898; June 1957.)
- 621.385.029.6 963
Space-Charge Effects in Klystrons—W. E. Waters, Jr. (IRE TRANS., vol. ED-4, pp. 49-58; January, 1957. Abstract, PROC. IRE, vol. 45, p. 897; June, 1957.)
- 621.385.029.6 964
Cylindrical Reflex Klystron with Lecher System as Oscillatory Circuit—J. Koch. (*Z. angew. Phys.*, vol. 9, pp. 1-8; January, 1957.) The design and construction of a new type of klystron are described. Tests to determine the optimum arrangement of the control-electrode system are discussed. Measured values are in agreement with calculated parameters. A further development of this klystron providing facilities for wide-range frequency tuning appears feasible.
- 621.385.029.6 965
Some Special Magnetrons—(*Wireless World*, vol. 64, pp. 17-22; January, 1958.) A simple theory of operation and its application to voltage-tuned, minimum-voltage, and spatial-harmonic magnetrons, and to the problem of scaling.
- 621.385.029.6 966
Stability of a Cylindrical Electron Beam in Nonsinusoidal Periodic Magnetic Focusing Fields—D. C. Buck. (IRE TRANS., vol. ED-4, pp. 44-49; January, 1957. Abstract, PROC. IRE, vol. 45, p. 897; June, 1957.) See 2546 of 1954 (Mendel *et al.*).
- 621.385.029.6 967
Travelling-Wave-Tube Gain Fluctuations with Frequency—S. A. Cohen. (IRE TRANS., vol. ED-4, pp. 70-78; January, 1957. Abstract, PROC. IRE, vol. 45, p. 897; June, 1957.)
- 621.385.029.6 968
Development of a Medium-Power L-Band Travelling-Wave Amplifier—L. W. Holmboe and M. Ettenberg. (IRE TRANS., vol. ED-4, pp. 78-81; January, 1957. Abstract, PROC. IRE, vol. 45, p. 897; June, 1957.)
- 621.385.029.6 969
Electron Bunching and Energy Exchange in a Travelling-Wave Tube—S. E. Webber. (IRE TRANS., vol. ED-4, pp. 87-91; January, 1957. Abstract, PROC. IRE, vol. 45, p. 898; June, 1957.)
- 621.385.029.6 970
The Gain and Bandwidth Characteristics of Backward-Wave Amplifiers—M. R. Currie and D. C. Forster. (IRE TRANS., vol. ED-4, pp. 24-34; January, 1957. Abstract, PROC. IRE, vol. 45, p. 897; June, 1957.)
- 621.385.032.213.13 971
Donor Diffusion in Oxide Cathodes—R. W. Peterson. (*J. Appl. Phys.*, vol. 28, pp. 1176-1181; October, 1957.) "The activation of oxide cathodes by chemical impurities present in the base nickel is analyzed using classical diffusion theory and a model in which the concentration of donors in the oxide particles is controlled by alkaline earth metal adsorbed on the oxide particles. Strong surface adsorption of the alkaline earth metals on the oxide crystal surfaces is indicated."
- 621.385.032.265 972
Current and Velocity Fluctuations at the Anode of an Electron Gun—E. V. Kornelsen, R. F. C. Vessot, and G. A. Wootton. (*J. Appl. Phys.*, vol. 28, pp. 1213-1214; October, 1957.) Measurements of the high-frequency, noise-current fluctuations are reported.
- 621.385.1+621.314.7 973
Valves, Transistors and Efficiencies—(*Wireless World*, vol. 64, pp. 41-44; January, 1958.) A simple theoretical discussion of the efficiencies obtainable from tubes and transistors, used, for example, in af output stages and dc converters.
- 621.385.1:537.525.92 974
The Determination of Plane Space-Charge Fields as well as those of Circular and Spherical Symmetry by means of Simple Resistance Networks with Additional Current Sources—G. Čremošnik and M. J. O. Strutt. (*Z. angew. Math. Phys.*, vol. 8, pp. 329-360; September 25, 1957.) Theoretical consideration of the application of a network analog, with details of practical measurements. See also 3358 of 1957.
- 621.385.832:535.37 975
Luminescence Decrease of Phosphor Screens by Electron Burn—K. H. K. Rottgardt. (*Elec. Commun.*, vol. 34, pp. 130-135; June, 1957.) English version of 3420 of 1954.
- 621.385.832:621.396.963.3 976
Operation and Performance of the 6866 Display Storage Tube—E. M. Smith. (*RCA Rev.*, vol. 18, pp. 351-360; September, 1957.) Description of a storage tube for direct viewing with an exceptionally bright display of radar-type information for periods as long as a minute. Principles of operation, important design features, and performance characteristics are discussed.
- 621.385.832:621.397.62 977
A Thin Cathode-Ray Tube—W. R. Aiken. (PROC. IRE, vol. 45, pp. 1599-1604; December, 1957.) In this tube, only a few inches thick, the beam is injected parallel to one edge and caused to pass through two right-angle deflections; the first sends the beam into the region between the front and back tube surfaces, and the second turns it into the phosphor-coated front surface. See also 2484 of 1955 and 588 of 1954.
- 621.385.832:77 978
A Thin-Window Cathode-Ray Tube for High-Speed Printing with "Electrofax"—R. G. Olden. (*RCA Rev.*, vol. 18, pp. 343-350; September, 1957.) Constructional details are given and performance tests described; writing speeds of over 10,000 characters per second appear possible. See also 1132 of 1955 (Young and Greig).
- 621.385.832.032.2:621.397.61 979
Wobbled Scanning with a New C.R.T.—(See 937).
- 621.385.832.032.269.1 980
The Influence of Anode Voltage Penetration on the Performance of Cathode-Ray Tube Guns—W. F. Niklas. (*J. Telev. Soc.*, vol. 8, pp. 186-190; January/March, 1957.) Change of spot size with intensity modulation, caused by lens strength alteration and space-charge influences, is reduced by a gun of new design, whose mechanism and performance are discussed.
- 621.385.832.032.36:621.397.621.2:535.623 981
Bilayer Bichromatic Cathode Screen—C. Feldman. (*J. Opt. Soc. Amer.*, vol. 47, pp. 790-794; September, 1957.) Screens consisting of superimposed, thin transparent layers have been formed by vacuum deposition. A screen consisting of Al/CaWO₄-W (blue)/ZnS-Mn (yellow)/glass supported in a 4-inch cr tube is considered in detail. The laws of color mixture are found to be obeyed. The basic ideas of a multi-layer chromatic system are briefly discussed.
- 621.387 982
Deionization in Gas Triodes and Tetrodes—E. Knoop. (*Z. angew. Phys.*, vol. 9, pp. 126-132; March, 1957.) The effect of external operating conditions on the various parameters controlling deionization is investigated for a number of commercial-type gas-filled tubes. See also 1542 of 1953.
- 621.387 983
A Particular Characteristic of Gas Triodes under Relaxation Conditions—J. Lagasse, R. Lacoste, and G. Giralt. (*C. R. Acad. Sci., Paris*, vol. 245, pp. 412-414; July 22, 1957.) The minimum voltage across a thyatron in a relaxation oscillator can become very low and be almost zero for certain values of the time constant of the anode circuit.
- 621.387 984
Pulse Firing Time and Recovery Time of the 2D21 Thyatron—J. A. Olmstead and M. Roth. (*RCA Rev.*, vol. 18, pp. 272-284; June, 1957.)
- 621.387:621.318.57 985
A Novel Cold-Cathode Tube—D. W. Hill. (*A.T.E. J.*, vol. 13, pp. 147-150; April, 1957.) A current-operated cold-cathode tube for use in electronic telephone exchanges is described; it has a movable trigger electrode of magnetic material.
- 621.387:621.318.57 986
Applications of a New Type of Cold-Cathode Trigger Tube—K. F. Gimson and G. O. Crowther. (*Electronic Eng.*, vol. 29, pp. 462-468, 536-545, and 591-596; October-December, 1957.) Discussion of the general characteristics of trigger tubes and the design of the Type Z803U which has a highly stable ignition voltage. Its applications in timing, protection, and counting circuits and in self-extinguishing circuits, such as a relaxation oscillator, are described.
- 621.387:621.396.822.029.6 987
Gas-Discharge Noise Tubes in the Range of High Discharge Admittances—H. Schmitzer. (*Nachr. Tech. Z.*, vol. 10, pp. 236-240; May, 1957.) The range of noise generators can be extended to lower frequencies by coupling the gas discharge to a delay line. Parameters of the equivalent circuit are calculated and are confirmed by measurement. The calibration of hard-tube noise generators in the range 100-1000 mc by means of gas-discharge tubes is outlined.
- 621.387.032.212.3 988
Oxide-Coated Cathode for Cold-Cathode Discharge Tubes—T. Imai and N. Mizushima. (*Rep. Elec. Commun. Lab., Japan*, vol. 5, pp. 10-15; May, 1957.) The effect of glow discharge on the cathode is investigated and methods of preparing a suitable cathode surface for practical use are described.
- MISCELLANEOUS
- 538.56:621.37 989
The Technique of Ultra-short Electromagnetic Waves since Heinrich Hertz—F. W. Gundlach. (*Nachr. Tech. Z.*, vol. 10, pp. 317-328; July, 1957.) A review article with one-hundred references.
- 001.891:621.396 990
Radio Research 1956: The Report of the Radio Research Board and the Report of the Director of Radio Research. [Book Review]—Publishers: H.M. Stationery Office, London, 1957, 47 pp., 3s. (*Nature, London*, vol. 180, pp. 642-643; September 28, 1957.)